


ฤทธิ์ของเคอร์คิวมินในการยับยั้งไบโอฟิล์มของเชื้อ *Helicobacter pylori* :
บทบาทของยีนส์แฟลเจลลา และการวิเคราะห์เปรียบเทียบโปรตีนโอมิกส์



นางสาวปาหนัน ภัททิยธนี

วิทยานิพนธ์นี้เป็นส่วนหนึ่งของการศึกษาตามหลักสูตรปริญญาวิทยาศาสตรดุษฎีบัณฑิต

สาขาวิชาชีวเวชศาสตร์ (สหสาขาวิชา)

บัณฑิตวิทยาลัย จุฬาลงกรณ์มหาวิทยาลัย

ปีการศึกษา 2552

ลิขสิทธิ์ของจุฬาลงกรณ์มหาวิทยาลัย

ศูนย์วิทยานิพนธ์
จุฬาลงกรณ์มหาวิทยาลัย

INHIBITORY ACTIVITY OF CURCUMIN AGAINST *HELICOBACTER PYLORI*
BIOFILMS : THE ROLE OF FLAGELLAR GENES AND
COMPARATIVE PROTEOMICS ANALYSIS



Miss Panan Pattiyathanee

A Dissertation Submitted in Partial Fulfillment of the Requirements
for the Degree of Doctor of Philosophy Program in Biomedical Sciences
(Interdisciplinary Program)

Graduate School
Chulalongkorn University
Academic year 2009

Copyright of Chulalongkorn University

จุฬาลงกรณ์มหาวิทยาลัย
คณะวิทยาศาสตร์
ศูนย์วิจัยทางการแพทย์

Thesis Title **INHIBITORY ACTIVITY OF CURCUMIN AGAINST
HELICOBACTER PYLORI BIOFILMS : THE ROLE OF
FLAGELLAR GENES AND COMPARATIVE
PROTEOMICS ANALYSIS**

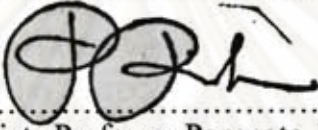
By **Miss Panan Pattiyathanee**

Field of Study **Biomedical Sciences**

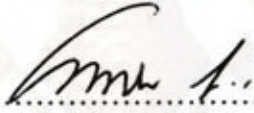
Thesis Advisor **Assistant Professor Nuntaree Chaichanawongsaroj, Ph.D.**

Thesis Co-advisor **Associate Professor Ratha-korn Vilaichone, M.D., Ph.D.**

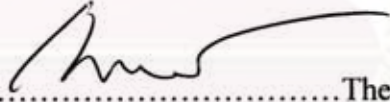
Accepted by the Graduate School, Chulalongkorn University in Partial
Fulfillment of the Requirements for the Doctoral Degree


.....Dean of the Graduate School
(Associate Professor Pornpote Piumsomboon, Ph.D.)

THESIS COMMITTEE



.....Chairman
(Assistant Professor Tewin Tencomnao, Ph.D.)

Nuntaree Chaichanawongsaroj
.....Thesis Advisor
(Assistant Professor Nuntaree Chaichanawongsaroj, Ph.D.)


.....Thesis Co-advisor
(Associate Professor Ratha-korn Vilaichone, MD., Ph.D.)

Siriporn Chuchawankul
.....Examiner
(Siriporn Chuchawankul, Ph.D.)

Rachaneeporn Tiyawisutsri
.....Examiner
(Rachaneeporn Tiyawisutsri, Ph.D.)


.....External Examiner
(Assistant Professor Pitak Santanirand, Ph.D.)

ปัทนันท์ ภัททิยธนี : ฤทธิ์ของเคอร์คิวมินในการยับยั้งไบโอฟิล์มของเชื้อ *HELICOBACTER PYLORI*: บทบาทของฮิสทีดามีนและการวิเคราะห์เปรียบเทียบโปรตีโอมิกส์ (INHIBITORY ACTIVITY OF CURCUMIN AGAINST *HELICOBACTER PYLORI* BIOFILMS : THE ROLE OF FLAGELLAR GENES AND COMPARATIVE PROTEOMICS ANALYSIS.) อ. ที่ปริกษาวิทยานิพนธ์หลัก: ผศ.ดร.นันทรี ชัยชนะวงศาโรจน์, อ. ที่ปริกษาวิทยานิพนธ์ร่วม:รศ.นพ.ดร.รัฐกร วิไลชนม์, 253 หน้า.

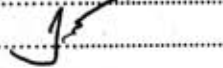
Helicobacter pylori เป็นเชื้อแบคทีเรียที่เป็นสาเหตุหลักของการก่อโรคแผลในกระเพาะอาหารและมะเร็งกระเพาะอาหาร เชื้อ *H. pylori* สามารถอยู่ในสภาวะที่เรียกว่าไบโอฟิล์ม ซึ่งมีส่วนช่วยในการดำรงชีวิตในสภาพแวดล้อม ที่เป็นอันตรายต่อตัวเชื้อ ฤทธิ์ของเคอร์คิวมินคือการยับยั้งการเจริญและการเกาะติดเซลล์ของเชื้อ *H. pylori* ได้มีการศึกษาอย่างกว้างขวาง การวิจัยนี้มีวัตถุประสงค์เพื่อที่จะศึกษาฤทธิ์ของเคอร์คิวมินต่อไบโอฟิล์มของเชื้อ *H. pylori* และกลไกหรือฮิสทีดามีน รวมไปถึงฮิสทีดามีนที่ควบคุมการสร้างไบโอฟิล์ม บทบาทของฮิสทีดามีนได้แก่ *flaA*, *flgR*, และ *flgQ* ได้ถูกทำการศึกษาผ่านการทำให้เกิดการกลายพันธุ์ โดยวิธี inverse PCR mutagenesis ฤทธิ์ของเคอร์คิวมิน ในการยับยั้งการสร้างไบโอฟิล์มของเชื้อ *H. pylori* สายพันธุ์ปกติ, สายพันธุ์ที่ฮิสทีดามีนกลายพันธุ์, และสายพันธุ์ ATCC43504 ได้ถูกศึกษาทั้งในเชิงคุณภาพโดยวิธี pellicle assay และเชิงปริมาณโดยการย้อมสีคริสตัลไวโอเลต โครงสร้างสามมิติของไบโอฟิล์มได้ทำการศึกษา ด้วยกล้องอิเล็กตรอนแบบส่องกราด (SEM) และยังได้ศึกษาฤทธิ์ของเคอร์คิวมินต่อการยับยั้งการเกาะติดเซลล์ เชื้อ HEp-2 ของเชื้อ *H. pylori* ในครั้งนี้ด้วย พบว่าเชื้อสายพันธุ์ทั้งหมด 6 สายพันธุ์ ได้แก่ PA315 และ NA2 (ฮิสทีดามีน *flaA* กลายพันธุ์), PR611 และ NR2 (ฮิสทีดามีน *flgR* กลายพันธุ์), และ PQ และ NQ (ฮิสทีดามีน *flgQ* กลายพันธุ์) เชื้อที่มีฮิสทีดามีน *flgR* กลายพันธุ์พบว่ามีการสร้างไบโอฟิล์มที่ลดลงอย่างมีนัยยะสำคัญทางสถิติ เมื่อเปรียบเทียบกับสายพันธุ์ปกติ (ATCC26695 และ N6) และสายพันธุ์ที่ฮิสทีดามีนอื่น ๆ กลายพันธุ์ นอกจากนี้ยังพบว่าความสามารถในการเกาะติดเซลล์เชื้อ HEp-2 ของเชื้อที่มีฮิสทีดามีน *flgR* และ *flgQ* กลายพันธุ์ลดลงอย่างมีนัยยะสำคัญทางสถิติ เคอร์คิวมินที่ระดับได้ความเข้มข้นน้อยที่สุดที่ยับยั้งเชื้อ (sub-MICs) สามารถยับยั้งการสร้างไบโอฟิล์มของเชื้อ *H. pylori* ได้โดยแปรผันตามกับระดับความเข้มข้นของสารเคอร์คิวมิน อย่างไรก็ตาม เชื้อ *H. pylori* สามารถกลับมาสร้างไบโอฟิล์มได้ใหม่เมื่อเพิ่มระยะเวลาเพาะบ่มเชื้อ โครงสร้างของไบโอฟิล์มเมื่อศึกษาด้วยกล้องอิเล็กตรอนแบบส่องกราด พบเซลล์ของเชื้อถูกปกคลุมด้วยสาร extracellular polymeric และเรียงตัวเชื่อมต่อกันเป็นชั้น นอกจากนี้ยังพบลักษณะของการสร้างสาร extracellular polymeric ที่น้อยลง เซลล์มีการเปลี่ยนแปลงรูปร่างเป็นลักษณะกลมและเซลล์ถูกทำลายเนื่องมาจากฤทธิ์ของเคอร์คิวมิน และยังพบว่าเคอร์คิวมินยับยั้งการเกาะติดเซลล์เชื้อ HEp-2 ของเชื้อ *H. pylori* อย่างมีนัยยะสำคัญทางสถิติ การศึกษาเปรียบเทียบโปรตีโอมิกส์เพื่อดูการแสดงออกของโปรตีนระหว่างที่เป็นไบโอฟิล์มกับเชื้อที่เป็นเซลล์เดี่ยว ทั้งในสภาวะที่มีและไม่มีเคอร์คิวมิน พบว่าโปรตีนที่แสดงออกมาเฉพาะในส่วน of เชื้อที่เป็นไบโอฟิล์ม ได้แก่ โปรตีนในกลุ่มของการเคลื่อนที่, โปรตีน chaperone, โปรตีน stress response, โปรตีนที่ทำหน้าที่ขนส่งอิเล็กตรอน, โปรตีนที่ทำหน้าที่ในกระบวนการเผาผลาญในโครเจนและการโบไฮเดรต, และโปรตีน metabolic intermediate biosynthesis ขณะที่ในสภาวะที่มีเคอร์คิวมินความเข้มข้น 1/4 ของความเข้มข้นที่น้อยที่สุดที่ยับยั้งเชื้อจะพบการแสดงออกของโปรตีน chaperone ในเชื้อ *H. pylori* ทั้งที่เป็นไบโอฟิล์มกับเชื้อที่เป็นเซลล์เดี่ยว ข้อมูลที่ได้นี้เป็นการรายงานครั้งแรกของฮิสทีดามีนที่เกี่ยวข้องกับ กลไกการสร้างไบโอฟิล์มของเชื้อ *H. pylori* ได้แก่ ฮิสทีดามีน *flgR*, *flgE*, *flgD*, *flgI*, *flaA*, *tig*, *hsp 60*, *grpE*, *cfp*, *kata*, *trxB*, *tsaA*, *porB*, *flaA*, *ureA*, *ureB*, *acnB*, *gltA*, และ *fadA* ประโยชน์ของเคอร์คิวมินในการยับยั้งการสร้างไบโอฟิล์มและการเกาะติดเซลล์เชื้อของเชื้อ *H. pylori* นำมาซึ่งการคิดค้นเพื่อพัฒนาเป็นยาหรือสารที่ใช้ในการรักษาโรคติดเชื้อ *H. pylori* ที่มีสาเหตุที่เกี่ยวข้องกับไบโอฟิล์ม

สาขาวิชา.....ชีวเวชศาสตร์.....

ลายมือชื่อ.....  Punsin p.m

ปีการศึกษา.....2552.....

ลายมือชื่อ.....ที่ปริกษาวิทยานิพนธ์หลัก.....  นันทรี ชัยชนะวงศาโรจน์

ลายมือชื่อ.....ที่ปริกษาวิทยานิพนธ์ร่วม.....  รศ.ดร.รัฐกร วิไลชนม์

4789717920: MAJOR BIOMEDICAL SCIENCES

KEYWORDS: *Helicobacter pylori* / biofilm / flagella / curcumin / proteomics /SEM
PANAN PATTIYATHANEE: INHIBITORY ACTIVITY OF CURCUMIN
AGAINST *HELICOBACTER PYLORI* BIOFILMS : THE ROLE OF
FLAGELLAR GENES AND COMPARATIVE PROTEOMICS
ANALYSIS. THESIS ADVISOR: ASST. PROF. NUNTAREE
CHAICHANAWONGSAROJ, Ph.D. THESIS CO-ADVISOR: ASSOC.
PROF. RATHA-KORN VILAICHONE, MD. Ph.D., 253 pp.

Helicobacter pylori is a leading etiologic agent causing peptic ulcer and gastric cancer. The bacterium is shown to have alternate life style as a biofilm, which facilitates bacterial survival in the hazardous environments. The antimicrobial as well as anti-adhesive activities of curcumin (diferuloylmethane) against *H. pylori* have been widely described. Objectives of this study were to investigate inhibitory effect of curcumin on *H. pylori* biofilm and mechanisms or genes, including flagellar genes that regulate the biofilm formation. The roles of flagellar genes, including *flaA*, *flgR*, and *fliQ* genes, in *H. pylori* were investigated by the construction of isogenic mutants using inverse PCR mutagenesis. The effect of curcumin was investigated on *H. pylori* wild type, flagellar mutants and ATCC43504 against biofilm formation both qualitatively by pellicle assay and quantitatively by crystal violet staining. Three-dimensional structure of biofilm was imaged by scanning electron microscopy (SEM). The effect of curcumin on *H. pylori* adherence to HEP-2 cells was also investigated. Six flagellar mutants were obtained, including PA315 and NA2 (*flaA* mutants), PR611 and NR2 (*flgR* mutants), and PQ and NQ (*fliQ* mutants). The *flgR* mutants formed a significant reduction of biofilm level compared to their wild types (ATCC26695 and N6) and other mutants. Additionally, an ability to adhere to the HEP-2 cells of both *flgR* and *fliQ* mutants was significantly decreased. Sub-minimum inhibitory concentrations (sub-MICs) of curcumin inhibited *H. pylori* biofilm in dose dependent manner. However, *H. pylori* could restore ability to form biofilm during extended time of incubation. SEM revealed a dense mature biofilm characterized by a presence of cells encased in extracellular polymeric matrix and connected together forming multicellular layers. The less amorphous matrix, slow of morphological conversion to coccoid form with cell damage was demonstrated after curcumin treatment. Curcumin significantly decreased the ability of *H. pylori* to adhere to the HEP-2 cells. A proteomics analysis was performed in order to investigate the difference in protein profile expression between biofilm and planktonic counterparts with an absence and presence of sub-MICs of curcumin. Proteins involving in biofilm formation in *H. pylori* belonged to chemotaxis and motility, chaperone, stress response, electron transport, nitrogen and carbohydrate metabolism, and metabolic intermediate biosynthesis. With a presence of 1/4 MIC curcumin, a chaperone group protein was up-regulated both in biofilm and planktonic counter parts. This is the first report showing genes, including *flgL*, *flgE*, *flgD*, *fliD*, *flaA*, *tufA*, *tig*, *hsp60*, *grpE*, *efp*, *katA*, *trxB*, *tsaA*, *porB*, *fldA*, *ureA*, *ureB*, *acnB*, *gltA*, and *fadA*, which being possibly involved in mechanism of *H. pylori* biofilm formation. The advantages of curcumin to inhibit biofilm formation and adherence by *H. pylori*, making it as an alternative complimentary medicine for curing of *H. pylori*-biofilm related infections.

Field of study...Biomedical Sciences.. Student's signature.....
Academic year..2009..... Advisor's signature.....
Co-advisor's signature.....

ACKNOWLEDGEMENTS

Completing this thesis was a long and difficult task. Many people supported and encouraged me in many different ways during the process, and it is now my pleasure to thank those who helped this thesis come to be.

I would like to express my sincere gratitude to my advisor as well as my mentor, Asst. Prof. Nuntaree Chaichanawongsaroj for her invaluable guidance and consolation throughout my thesis. My deep gratitude is extended to Assoc. Prof. Ratha-korn Vilaichone, my co-advisor, for his suggestion and bacterial strains providing. I would like to thank all members of the committee, Asst. Prof. Tewin Tencomnao, Dr. Siriporn Chuchawankul, Dr. Rachaneeporn Tiyawisutsri, and the invited external examiner Asst. Prof. Pitak Santanirand for giving helpful comments and suggestions.

My appreciation also goes to Prof. Dr. Pornthep Tiensiwakul for giving me the HEp-2 cells. I also would like to thank the Department of Transfusion Medicine, Faculty of Allied Health Sciences and the Halal Science Center, Chulalongkorn University for providing laboratory facilities.

A special note of thank goes to Ph.D. classmate of Biomedical Sciences and people in the Pathogen Molecular Biology Unit, London School of Hygiene and Tropical Medicine for assistance and experience sharing.

I would like to acknowledge the Commission of Higher Education, Ministry of Education for a Ph.D. scholarship.

This study was supported by the Asahi Glass Foundation and “90 years Chulalongkorn University Grant” from the Ratchadaphiseksomphot Endowment Fund.

Finally, I could not finish this thesis without the moral support and encouragement of my family and my loved ones. Thank you very much from the deepest of my heart.

CONTENTS

| | Page |
|--|------|
| ABSTRACT (THAI)..... | iv |
| ABSTARCT (ENGLISH) | v |
| ACKNOWLEDGEMENTS..... | vi |
| CONTENTS..... | vii |
| LIST OF TABLES..... | xv |
| LIST OF FIGURES..... | xvii |
| LIST OF ABBREVIATIONS | xxi |
| CHAPTER | |
| I INTRODUCTION..... | 1 |
| II LITERATURE REVIEW..... | 5 |
| 1. The Discovery of <i>Helicobacter pylori</i> | 5 |
| 2. General Aspects of <i>H. pylori</i> | 6 |
| 2.1 Taxonomy | 6 |
| 2.2 Metabolism and physiology..... | 9 |
| 2.3 Genome..... | 11 |
| 2.4 Microbiology and laboratory culture..... | 12 |
| 2.5 Epidemiology..... | 13 |
| 2.6 Transmission..... | 14 |
| 2.7 Pathogenesis and clinical relevance..... | 15 |
| 2.8 Virulence..... | 16 |
| 2.9 Treatment | 19 |
| 3. <i>H. pylori</i> Biofilms..... | 21 |
| 3.1 Biofilms: City of microbes..... | 21 |

| Chapter | Page |
|--|------|
| | viii |
| | Page |
| 3.1.1 Stages in biofilm formation..... | 22 |
| 3.1.2 Architecture of Biofilm..... | 23 |
| 3.1.3 Biofilm pathogenicity and disease..... | 24 |
| 3.2 Biofilms: Alternative life style of <i>H. pylori</i> contributing to host infection | 27 |
| 3.3 Potential regulators relating to biofilm formation of..... <i>H. pylori</i> | 30 |
| 3.3.1 Gene responsible in <i>H. pylori</i> biofilm..... formation | 30 |
| 3.3.2 Bacterial adhesin and biofilm formation..... | 31 |
| 3.3.3 <i>H. pylori</i> flagellum: A component mediating... in biofilm formation | 33 |
| 3.4 Antimicrobial resistance in <i>H. pylori</i> resulted by..... biofilm formation | 40 |
| 3.5 Strategies for control of biofilms: A novel approach..... treating infections | 42 |
| 4. Potential Action of Herbal Medicines in Treatment of <i>H. pylori</i> .. Infection | 44 |
| 4.1 Pharmaceutical properties of curcumin..... | 45 |
| 4.1.1 General aspects of curcumin..... | 45 |
| 4.1.2 Chemotherapeutic effects of curcumin..... against <i>H. pylori</i> | 47 |
| 4.2 Potential anti-biofilm property of curcumin..... | 48 |

| Chapter | Page |
|--|------|
| 5. Proteomics Study in <i>H. pylori</i> | 49 |
| 5.1 Proteomics analysis: an alternative approach to study... biofilms | 49 |
| 5.1.1 Proteomics overview..... | 50 |
| 5.1.2 Two-dimentional gel electrophoresis..... | 50 |
| 5.1.3 Mass spectrometry..... | 51 |
| 5.2 Proteomic analysis of bacterial biofilm..... | 54 |
| 5.3 A proteomic analysis of protein expression in <i>H. pylori</i> .. | 55 |
| III RESEACH QUESTIONS AND OBJECTIVES..... | 57 |
| 1. Research questions..... | 57 |
| 2. Objectives..... | 59 |
| 3. Hypotheses..... | 59 |
| 4. Conceptual framework..... | 60 |
| VI MATERIALS AND METHODS..... | 61 |
| 1. Chemicals, reagents, scientific instruments and bacterial strains.. | 62 |
| 2. Preparation of Bacterial Strains and Curcumin Stock Solution.... | 64 |
| 2.1 Preparation of bacterial strains..... | 64 |
| 2.2 Preparation of curcumin suspension..... | 65 |
| 3. Construction of <i>H. pylori flaA, flgR, and fliQ</i> Mutants..... | 66 |
| 3.1 Chromosomal DNA extraction..... | 66 |
| 3.2 Primer designation for PCR and inverse PCR | 67 |
| amplification | |
| 3.3 Flagellar gene PCR amplifications..... | 73 |
| 3.4 Agarose gel elctrophoresis..... | 73 |

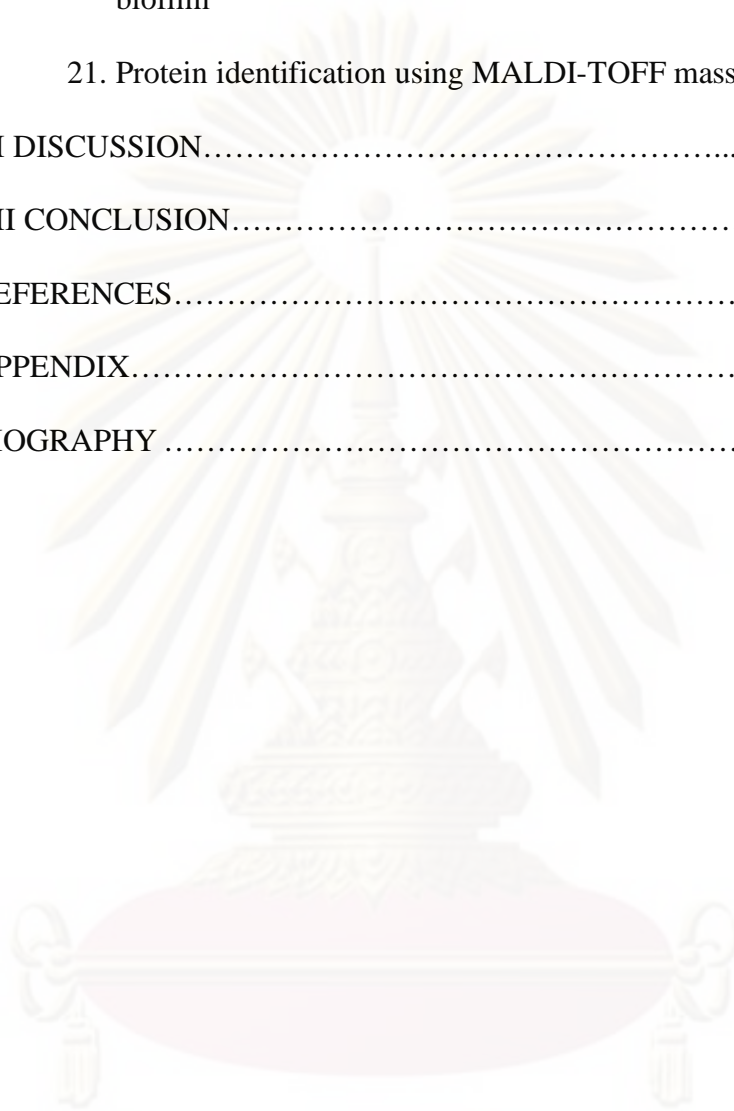
| Chapter | Page |
|--|------|
| | x |
| 3.5 PCR purification..... | 74 |
| 3.6 Cloning of <i>flaA</i> , <i>flgR</i> , and <i>fliQ</i> genes into pGEM® | 74 |
| T-Easy vector for <i>H. pylori</i> mutagenesis | |
| 3.7 Colony PCR..... | 75 |
| 3.8 Plasmid DNA isolation..... | 76 |
| 3.9 Restriction enzyme analysis..... | 77 |
| 3.10 DNA sequencing..... | 77 |
| 3.11 Inverse PCR mutagenesis (IPCRM) | 78 |
| 3.12 Kanamycin resistance cassette (kan ^R) insertion into... | 80 |
| IPCRM products | |
| 3.13 Bacterial transformations..... | 81 |
| 3.13.1 Natural transformation of <i>H. pylori</i> | 81 |
| 3.13.2 Electroporation..... | 81 |
| 4. Assessment for Minimum Inhibitory Concentration (MIC)..... | 82 |
| of Curcumin against <i>H. pylori</i> | |
| 5. Investigation of Biofilm Formation by Pellicle Assay..... | 84 |
| 6. Optimization of Biofilm Formation in <i>H. pylori</i> | 85 |
| 6.1 Optimization of curcumin concentration against..... | 85 |
| <i>H. pylori</i> biofilm | |
| 6.2 Optimization of incubation period against <i>H. pylori</i> | 86 |
| biofilms in the presence and absence of curcumin | |
| 7. Quantification of Biofilm Formation..... | 86 |
| 7.1 Quantification of biofilm formation using glass coverslip | 86 |

| Chapter | Page |
|--|------|
| 7.2 Quantification of biofilm formation using pellicle assay | 87 |
| 8. Investigation of anti-adhesive property of curcumin against..... | 88 |
| <i>H. pylori</i> | |
| 8.1 Preparation of human laryngeal epithelial cells..... | 88 |
| 8.1.1 Culture of human laryngeal epithelial cells..... | 88 |
| 8.1.2 Counting cells..... | 89 |
| 8.2 Adhesion assay..... | 90 |
| 9. Analysis of 3-Dimensional Structure of <i>H. pylori</i> Biofilm Using | 92 |
| Scanning Electron Microscopic (SEM) | |
| 9.1 SEM sample preparation..... | 92 |
| 9.2 SEM analysis..... | 93 |
| 10. Proteomics Analysis of <i>H. pylori</i> Biofilm..... | 93 |
| 10.1 Protein sample preparation for proteomics analysis.... | 94 |
| 10.1.1 Sample collection | 94 |
| 10.1.2 Sonication of sample..... | 94 |
| 10.1.3 Lyophilization of sample..... | 95 |
| 10.1.4 Analysis of total protein concentration..... | 95 |
| 10.1.5 Protein purification..... | 95 |
| 10.2 The first dimensional gel electrophoresis: isoelectric... focusing (IEF) | 96 |
| 10.3 The second dimensional gel electrophoresis: sodium.. | 97 |

| | |
|---|-----|
| dodecyl sulfate-polyacrylamide gel electrophoresis (SDS-PAGE) | |
| 10.3.1 IPG strip equilibration..... | 97 |
| 10.3.2 SDS-PAGE preparation..... | 98 |
| 10.3.3 SDS-PAGE condition..... | 98 |
| 10.4 Gel staining..... | 98 |
| 10.5 Gel image analysis..... | 99 |
| 10.6 Spot picking..... | 99 |
| 10.7 Mass spectrometry analysis..... | 100 |
| 10.8 Protein data analysis..... | 100 |
| 11. Statistical Analysis..... | 100 |
| V RESULTS..... | 102 |
| 1. Primer designation..... | 102 |
| 2. The <i>flaA</i> , <i>flgR</i> , and <i>fliQ</i> genes amplification..... | 104 |
| 3. Cloning of PCR fragment into pGEM® T-Easy vector..... | 105 |
| 3.1 Colony PCR analysis of plasmid pGA, pGR, and pGQ.. | 110 |
| 3.2 Restriction analysis of plasmid pGA, pGR, and pGQ.... | 110 |
| 4. DNA sequence analysis of plasmid pGA, pGR, and pGQ..... | 115 |
| 5. Mutagenesis of plasmid pGA, pGR, and pGQ by inverse PCR... amplification | 115 |
| 6. Insertion of kan ^R cassette into mutated genes for <i>H. pylori</i> mutagenesis | 124 |
| 7. Transformation of mutated <i>flaA</i> , <i>flgR</i> , and <i>fliQ</i> genes into..... <i>H. pylori</i> ATCC26695 and N6 | 126 |

| | |
|---|-----|
| 8. Antimicrobial activity of curcumin against <i>H. pylori</i> | 130 |
| wild types and flagellar mutants | |
| 9. Comparison of biofilm formation among <i>H. pylori</i> wild types... 131 | |
| and flagellar mutants | |
| 10. Effect of curcumin against biofilm formation among <i>H. pylori</i> .. | 132 |
| wild types and flagellar mutants | |
| 11. Quantification of biofilm formation performed by modified..... | 136 |
| assay in polystyrene plates | |
| 12. Adhesion of <i>H. pylori</i> wild types and their isogenic mutants.... | 140 |
| against the HEP-2 cells | |
| 13. Screening for biofilm formation..... | 143 |
| 14. The antimicrobial activity of curcumin against <i>H. pylori</i> strains | 147 |
| 15. Inhibitory activity of curcumin on <i>H. pylori</i> biofilm..... | 149 |
| 15.1 Effect of curcumin concentration against <i>H. pylori</i> | 149 |
| biofilm formation | |
| 15.2 Effects of curcumin at various incubation times on..... | 151 |
| <i>H. pylori</i> biofilm formation | |
| 16. Quantification of biofilm formation by modified..... | 153 |
| crystal violet assay | |
| 17. Scanning electron microscopy of <i>H. pylori</i> biofilm..... | 156 |
| 18. Anti-adhesive property of curcumin against <i>H. pylori</i> | 159 |
| 19. 2-D gel electrophoresis..... | 161 |
| 19.1 Total protein quantification..... | 161 |
| 19.2 Proteomic mapping..... | 162 |

| Chapter | Page |
|--|------|
| 20. Image analysis and comparison of proteomic map of <i>H. pylori</i> biofilm | 169 |
| 21. Protein identification using MALDI-TOFF mass spectrometry | 172 |
| VI DISCUSSION..... | 188 |
| VII CONCLUSION..... | 204 |
| REFERENCES..... | 206 |
| APPENDIX..... | 242 |
| BIOGRAPHY | 253 |



ศูนย์วิทยทรัพยากร
 จุฬาลงกรณ์มหาวิทยาลัย

LIST OF TABLES

| Table | Page |
|--|------|
| 1. Characteristics of cultivated <i>H. pylori</i> species..... | 8 |
| 2. Virulence factors identified in <i>H. pylori</i> | 19 |
| 3. Partial list of common human infection involving biofilm..... | 26 |
| 4. <i>H. pylori</i> adhesins and host cell receptors..... | 32 |
| 5. Flagellar genes identified in the two published genome sequences..... | 39 |
| 6. Curcumin and other derivatives from <i>C. longa</i> L..... | 46 |
| 7. The oligonucleotide sequences of PCR and IPRCM primers for amplification.. | 103 |
| of <i>flaA</i> , <i>flgR</i> , and <i>fliQ</i> genes and the relative product sizes | |
| 8. <i>H. pylori</i> wild type strains and their isogenic mutants constructed by..... | 127 |
| inverse PCR mutagenesis | |
| 9. Average MICs and sub-MICs of curcumin of individual <i>H. pylori</i> wild..... | 130 |
| type strains, ATCC26695 and N6, and their isogenic mutants, PA315, | |
| PR611, PQ, NA2, NR2, NQ | |
| 10. Pellicle and attached biofilm levels observed among <i>H. pylori</i> wild types..... | 134 |
| and their isogenic mutants, in an absence and presence of curcumin | |
| 11. A development of biofilm levels of fourteen strains of <i>H. pylori</i> | 146 |
| 12. Average MICs of twelve strains of <i>H. pylori</i> | 148 |
| 13. Inhibitory effects of curcumin at subinhibitory concentrations on <i>H. pylori</i> ... | 150 |
| ATCC43504 biofilm formation | |
| 14. Effects of curcumin at various incubation times on <i>H. pylori</i> ATCC43504..... | 152 |
| biofilm formation | |

| Table | Page |
|---|------|
| 15. Total protein concentrations of individual samples quantified..... by Bradford assay. | 162 |
| 16. Identification of the entire proteins expressed and up-regulated in both <i>H. pylori</i> biofilm and planktonic cells without curcumin treatment, with 1/4 and 1/2 MIC of curcumin treatment | 175 |
| 17. Comparison of proteomic map patterns of <i>H. pylori</i> ATCC43504 biofilm..... and planktonic without curcumin treatment, with 1/4 and 1/2 MIC of curcumin treatment | 180 |
| 18. Identified proteins that were present and up-regulated in biofilm and..... planktonic sample without curcumin treatment | 182 |
| 19. Identified proteins that were present and up-regulated in biofilm and..... planktonic sample with 1/4 MIC of curcumin treatment | 183 |
| 20. Identified proteins that were present and up-regulated in biofilm sample without and with 1/4 MIC, and planktonic sample with 1/2 MIC of curcumin treatment | 184 |
| 21. Identified proteins that were present and up-regulated in planktonic sample... without, with 1/4 MIC, and 1/2 MIC of curcumin treatment | 186 |
| 22. The correlation between the final concentration at standard protein..... (BSA) and its corresponding absorbance value at 595 nm | 251 |

LIST OF FIGURES

| Figure | Page |
|--|------|
| 1. The chemical reaction of urea hydrolysis..... | 10 |
| 2. Potential environmental and cultural factors in biofilm development..... | 22 |
| 3. SEM micrograph of a 4-day-old biofilm of <i>H. pylori</i> grown as..... stationary batch culture | 29 |
| 4. Electron micrograph displaying flagellated <i>H. pylori</i> (A) and distal end of..... a sheath with shaft, narrowing, and terminal club (B) | 35 |
| 5. Flagellar proteins and their putative locations and interactions..... | 37 |
| 6. The sequence of <i>flaA</i> gene from <i>H. pylori</i> ATCC26695..... | 68 |
| 7. The sequence of <i>flgR</i> gene from <i>H. pylori</i> ATCC26695..... | 70 |
| 8. The sequence of <i>fliQ</i> gene from <i>H. pylori</i> ATCC26695..... | 72 |
| 9. Schematic representation of IPCRM..... | 79 |
| 10. Hemacytometer-counting chamber..... | 90 |
| 11. Agarose gel electrophoresis of PCR amplified product of <i>flaA</i> , <i>flgR</i> ,..... and <i>fliQ</i> genes | 104 |
| 12. The physical map and multiple cloning regions of pGEM® T-Easy vector..... | 106 |
| 13. The schematic picture of pGA..... | 107 |
| 14. The schematic picture of pGR..... | 108 |
| 15. The schematic picture of pGQ..... | 109 |
| 16. Agarose gel electrophoresis of colony PCR product of plasmid pGA..... amplified by T7 and SP6 primers | 112 |
| 17. Agarose gel electrophoresis of colony PCR product of plasmid pGR..... amplified by T7 and SP6 primers | 112 |

| Figure | Page |
|---|------|
| 18. Agarose gel electrophoresis of colony PCR product of plasmid pGQ..... amplified by T7 and SP6 primers | 113 |
| 19. Agarose gel electrophoresis of plasmid pGA and pGR cut with <i>Not</i> I..... enzyme | 114 |
| 20. Agarose gel electrophoresis of plasmid pGQ cut with <i>Eco</i> R I..... enzyme | 114 |
| 21. Agarose gel electrophoresis of IPCRM amplified product of plasmid pGA,... pGR, and pGQ | 118 |
| 22. Agarose gel electrophoresis of <i>Bgl</i> II restricted colony PCR product..... of the self-ligated plasmid I-pGA | 119 |
| 23. Agarose gel electrophoresis of <i>Bgl</i> II restricted colony PCR product..... of the self-ligated plasmid I-pGR | 119 |
| 24. Agarose gel electrophoresis of <i>Bgl</i> II restricted colony PCR product..... of the self-ligated plasmid I-pGR | 120 |
| 25. Agarose gel electrophoresis of self-ligated plasmid I-pGA and I-pGR..... cut with <i>Not</i> I and <i>Bgl</i> II enzyme | 123 |
| 26. Agarose gel electrophoresis of self-ligated plasmid I-pGQ cut with <i>Eco</i> R I and <i>Bgl</i> II enzyme | 123 |
| 27. Agarose gel electrophoresis of colony PCR product of the I-pGA/ <i>kan</i> ^R and I-pGR/ <i>kan</i> ^R | 125 |
| 28. Agarose gel electrophoresis of colony PCR product of the I-pGA/ <i>kan</i> ^R and I-pGR/ <i>kan</i> ^R | 125 |

| Figure | Page |
|---|------|
| 29(A). PCR amplification of <i>flaA</i> gene from <i>H. pylori</i> wild type and..... mutated strains | 128 |
| 29(B). PCR amplification of <i>flgR</i> gene from <i>H. pylori</i> wild type and..... mutated strains | 128 |
| 29(C). PCR amplification of <i>flaA</i> and <i>fliQ</i> genes from <i>H. pylori</i> wild type..... and mutated strains | 129 |
| 29(D). PCR amplification of <i>flgR</i> gene from <i>H. pylori</i> wild type and..... mutated strains | 129 |
| 30. Biofilm characteristics represented by pellicle and attached..... biofilm formation following 7-d incubation | 135 |
| 31. Biofilm level quantification of <i>H. pylori</i> wild types and flagellar mutants..... performed by modified assay in polystyrene plates | 138 |
| 32. Biofilm level quantification of curcumin-treated <i>H. pylori</i> wild types and..... flagellar mutants compared to the untreated | 139 |
| 33. Percentile of adhesion of <i>H. pylori</i> wild types and flagellar mutants..... | 142 |
| 34. Photograph of pellicle assay showing 7-day biofilm formed by <i>H. pylori</i> ATCC43504 | 145 |
| 35. Biofilm level quantification of <i>H. pylori</i> ATCC43504 performed by..... modified crystal violet assay | 154 |
| 36. Biofilm formation of <i>H. pylori</i> ATCC43504 in a presence of various..... curcumin concentrations | 155 |

| Figure | Page |
|--|------|
| 37. SEM photomicrograph of biofilm development of <i>H. pylori</i> ATCC43504..... at a magnification of X 15,000 | 158 |
| 38. Percentile of adhesion of <i>H. pylori</i> ATCC43504 in a presence and absence..... of 1/2 MIC of curcumin | 160 |
| 39. Proteomic map of <i>H. pylori</i> ATCC43504 biofilm in an absence of curcumin.. | 164 |
| 40. Proteomic map of <i>H. pylori</i> ATCC43504 planktonic in an absence..... of curcumin | 165 |
| 41. Proteomic map of <i>H. pylori</i> ATCC43504 biofilm in a presence..... of curcumin at 1/4 MIC | 166 |
| 42. Proteomic map of <i>H. pylori</i> ATCC43504 planktonic in a presence..... of curcumin at 1/4 MIC | 167 |
| 43. Proteomic map of <i>H. pylori</i> ATCC43504 planktonic in a presence..... of curcumin at 1/2 MIC | 168 |
| 44. A schematic picture of comparative proteome analysis of individual sample...169 | 169 |
| 45. The correlation between final concentration ($\mu\text{g ml}^{-1}$) of standard BSA and... their absorbance value at 595 nm | 251 |

ศูนย์วิทยทรัพยากร

จุฬาลงกรณ์มหาวิทยาลัย

ABBREVIATIONS

| | |
|------|---|
| % | Percent |
| 2-D | Two-dimensional |
| 3-D | Three-dimensional |
| 3-d | Three-day |
| ATCC | American Type Culture Collection |
| ATP | Adenosine triphosphate |
| BCD | Beta-cyclodextrin |
| BHI | Brain heart infusion |
| bp | Base pair |
| CAC | Citric acid cycle |
| CFU | Colony forming unit |
| CLSI | Clinical and Laboratory Standards Institute |
| CV | Crystal violet |
| DDW | Deionized distilled water |
| DMEM | Dulbecco's modified of eagle medium |
| DMSO | Dimethyl sulfoxide |
| DPBS | Dulbecco's phosphate buffer saline |
| DW | Distilled water |
| ESI | Electrospray ionization |
| FBS | Fetal bovine serum |
| g | Gram |

| | |
|------------------|---|
| h | Hour |
| IEF | Isoelectric focusing |
| IPCRM | Inverse PCR mutagenesis |
| IPTG | Isopropyl-beta-D-thiogalactopyranoside |
| kan ^R | Kanamycin resistance cassette |
| kb | Kilobase |
| LB | Luria-Bertani |
| MALDI | Matrix-assisted laser desorption/ionization |
| MBC | Minimum bactericidal concentration |
| MH | Mueller-Hinton agar |
| MIC | Minimum inhibitory concentration |
| min | Minute |
| µg | Microgram |
| µl | Microlitre |
| ml | Millilitre |
| ml ⁻¹ | per millilitre |
| OD | Optical density |
| OMPs | Outer-membrane proteins |
| PBS | Phosphate buffer saline |
| PCR | Polymerase chain reaction |
| PFGE | Pulsed-field gel electrophoresis |

| | |
|----------|--|
| pI | Isoelectric point |
| QS | Quorum sensing |
| RIP | Rinonucleic acid III-inhibiting peptide |
| rpm | Revolution per minute |
| SDS-PAGE | Sodium dodecyl sulfate-polyacrylamide gel electrophoresis |
| sec | Second |
| U | Unit |
| UV | Ultraviolet |
| VBNC | Viable but nonculturable |
| v/v | Volume by volume |
| w/v | Weight by volume |

ศูนย์วิทยทรัพยากร
จุฬาลงกรณ์มหาวิทยาลัย

CHAPTER I

INTRODUCTION

Infection with *Helicobacter pylori* occurs worldwide with approximately a half of the world population is infected with this bacterium. The prevalence in some developing countries and in Thailand is up to 90 and 70%, respectively. *H. pylori* infection has been implicated in the etiology of chronic gastritis and peptic ulcer. In addition, epidemiological studies have identified an association between *H. pylori* infection and the development of gastric cancer. Several virulence factors for gastric colonization, tissue damage, and survival have been identified in *H. pylori*, such as flagella, urease enzyme, and vacuolating cytotoxin. Recently, this pathogenic bacterium is shown to have alternate life style as a biofilm. The term biofilm has been defined as “matrix enclosed bacterial population adherent to each other and to surfaces or interfaces”. Biofilm formation is important, as it is associated with chronic nature of infection and resistance to antibiotic chemotherapy. The biofilm matrix can interfere the diffusion of antibiotics into the deeper layer of the film resulting in inefficient effect against the bacteria and leading to the eradication failure. Apart from that; general antibiotic resistant mechanisms do not seem to be responsible for the protection of bacteria in a biofilm. Biofilm forms in multiple steps. In response to quorum sensing signal, bacteria migrate and adhere to a surface, divide to form microcolonies, and expand laterally and vertically leading to a mature biofilm. Many regulators are involved in the *H. pylori* biofilm development. These include flagella that have been considered to play a role at the initial step of biofilm formation in bacteria. From one recent study, it has been suggested that the *luxS* and

cagE genes may associate with biofilm formation in *H. pylori*. However the precise underlying factors, which regulate *H. pylori* biofilm formation, remains unclear. Biofilm production by *H. pylori* is reported recently and thought to facilitate bacterial survival both in environment and during colonization *in vivo*. In several studies, *H. pylori* biofilms have been detected in water distribution systems and general water sources in several countries providing a route of infection. In human infection, a presence of dense mature biofilms attached to the cell surface of the gastric specimens has been documented. Additionally, many studies have hypothesized that *H. pylori* infections resulting in gastric ulcers may be a manifestation of biofilms.

It is well recognized that bacteria in biofilm are less susceptible to conventional antibiotic therapy resulting in a treatment failure. Therefore, a novel therapy schemes for stopping biofilm formation should be taken into account. Herbal medicines have been implicated for their bactericidal property for long centuries. Some studies have described the virtue of using medicinal plants as an alternative medicine, which could inhibit bacterial growth and decrease the incidence of antibiotic resistance. Several reports have prescribed about various plant materials in inhibitory action against *H. pylori*. Among various Thai folk medicinal plants possessing anti-*H. pylori* activity, turmeric is one of those well-known herbs. Curcumin, the major active compound found in tumeric, has been prescribed in extensive beneficial pharmacological effects, including antibacterial activity against methicillin-resistant *Staphylococcus aureus*, *Lactobacilli*, *Chlamydia pneumoniae*. Antibacterial activity of curcumin against *H. pylori* has also been recently documented. Although, effects of curcumin against *H. pylori* have been reported

previously, but the effect of this relative compound against *H. pylori* biofilms has never been documented before.

The precise mechanism controlling *H. pylori* biofilm formation is still being unclear and a study of regulation in biofilm formation of this organism is limited. A large-scale study of protein termed proteomic is considered as a new tool for analyzing the whole protein expression. Goal of proteomics is to quantify and identify proteins, which often give important clues about the differences in protein expression of a particular phenotype. Several tools are available for proteomics analysis including 2-dimensional (2-D) gel electrophoresis. This tool comprises isoelectric focusing in the 1st dimension and polyacrylamide gel electrophoresis in the 2nd dimension. The separated proteins from electrophoresis are further quantified and identify by mass spectrometry. Recently, some reports have described a study of protein in *H. pylori* using proteomic. The 2-D gel electrophoresis analysis has also revealed which proteins were up-regulated or down-regulated in the presence of chemotherapeutic treatment. The data obtained from proteomics analysis could clarify the role of different proteins relating to bacterial pathogenesis.

Thus, aim of this study was to investigate the regulation of *H. pylori* biofilm formation. The flagella mutants strain were constructed and tested for its ability to form biofilm *in vitro* compared with the wild type. *H. pylori* biofilm formation was evaluated both qualitatively and quantitatively. Whether curcumin enables to inhibit biofilm formation and adhesion of *H. pylori* were clarified. The 3-dimensional cytoarchitecture of biofilm was investigated by scanning electron microscope. Finally, proteomics study of *H. pylori* biofilm was performed by 2-D gel electrophoresis in order to analyze the pattern of protein expression involving in *H.*

pylori biofilm formation. The patterns of protein expression were also compared between curcumin-treated and –untreated *H. pylori* biofilms.



ศูนย์วิทยทรัพยากร
จุฬาลงกรณ์มหาวิทยาลัย

CHAPTER II

LITERATURE REVIEW

1. The Discovery of *Helicobacter pylori*

Gastric curved or spiral bacteria have first been observed in humans almost 100 years ago (1). These observations received little attention at that time. Attempts to isolate these unknown organisms did not succeed and examinations of gastric suction material failed to confirm the histological findings (2). The observed bacteria were often considered to be contaminating organisms from the mouth, bowel, or gastric contents. With the improvement of endoscopic techniques, it became possible to obtain biopsies of the antrum. Since the late 19th century, European pathologists have noticed the presence of curved bacterial cells in gastric biopsy specimens submitted to histological examination (3). Two Australian scientists, Robyn Warren and Barry Marshall, had observed patients with spiral organisms on their gastric mucosa since 1979 and documented the inflammation associated with the bacteria. They began an attempt to study this organism in patients with various upper gastrointestinal symptoms. However, they first published work reporting the plate culture of *Helicobacter pylori* in 1984 (4). In this study, *H. pylori* was isolated from biopsy specimens taken from intact areas of the antral mucosa of patients. The presence of bacterial colonies was accidentally observed on culture plates that forgotten to throw away before Easter holiday. They achieved the first time to culture the organisms using *Campylobacter* culture techniques with a prolonged incubation and isolated the bacterium that is now known as *H. pylori* (5).

However, the bacterium was first classified into *Campylobacter* species and called *Campylobacter pyloridis* (6), which was changed later to *Campylobacter pylori* (7). The sequence determination of 16S rRNA, has differentiated this organism from *Campylobacter* spp. and it was renamed *H. pylori* in 1989 (8).

Since then, the wide interest has resulted in a steady increase in research on *H. pylori*. This also has turned the bacteria into one of the hot-topics for scientists. Furthermore, *H. pylori* was also one of the first bacteria having the genome sequenced for two different strains 26695 (9) and J99 (10). Nowadays, the new *Helicobacter* species are being discovered (11,12). Most of them do not normally colonize the gastric mucosa, but instead colonize in the intestinal tract and/or the liver of host, and therefore classified as enterohepatic (13). Those inhabiting the stomach, such as *H. pylori*, are termed gastric *Helicobacter* species (14). So far, only *H. pylori* has been found to generally inhabit humans, even though *Helicobacter heilmannii* has been occasionally detected.

2. General Aspects of *H. pylori*

2.1 Taxonomy

H. pylori belongs to the phylum proteobacteria, which is the largest and most physiologically diverse of all bacteria. This certain phylum comprises normal flora of animals, broad-range of animal pathogens, and plants (15). Based on analysis of their 16S ribosomal RNA, *Helicobacter* is categorized into the *Campylobacteriaceae* family, which includes other genera such as *Campylobacter*, *Sulfurospirillum*, *Wolinella*, *Thiovulum*, and *Arcobacter* (16). This bacterial group survives in different environments,

from aquatic habitats (*Sulfurospirillum* spp.) to mucosal surfaces of the gastrointestinal and/or urogenital tract of bird and animals (*Campylobacter* spp. and *H. pylori*). They are all spiral-shaped, multiply by binary fission, and able to grow microaerobically or anaerobically.

The genus *Helicobacter* comprises 18 validated species, 2 *Candidatus* species, and 9 additional provisional species (17,18). The characteristic of individual *Helicobacter* species is as listed as in Table 1 (19). However, several new species have been discovered during the past years and mainly isolated from animals. *H. heilmannii* has been recognized regularly in the human gastric mucosa apart from *H. pylori* with 0.5-6% of infection rate (20).



ศูนย์วิทยทรัพยากร
จุฬาลงกรณ์มหาวิทยาลัย

| Taxon | Catalase production | Nitrate reduction | Alkaline phosphatase hydrolysis | Urease | Indoxyl acetate hydrolysis | Glutamyl transferase | Growth at 42°C | Growth with 1% glycine | Susceptibility to | | Peri-plasmic fibers | No. of flagella | Distribution of flagella | G + C content (mol%) |
|------------------------------------|---------------------|-------------------|---------------------------------|--------|----------------------------|----------------------|----------------|------------------------|------------------------|--------------------------|---------------------|-----------------|--------------------------|----------------------|
| | | | | | | | | | Nalidixic acid (30 µg) | Cephalothin (30 µg disc) | | | | |
| Gastric | | | | | | | | | | | | | | |
| <i>H. acinomyces</i> | + | - | + | + | - | + | - | - | R | S | - | 2-5 | Bipolar | 30 |
| <i>H. bizozeronii</i> | + | + | + | + | + | + | + | - | R | S | - | 10-20 | Bipolar | ND |
| <i>H. felis</i> | + | + | + | + | - | + | + | - | R | S | + | 14-20 | Bipolar | 42 |
| <i>H. mustelae</i> | + | + | + | + | + | + | + | - | S | R | - | 4-8 | Peritrichous | 36 |
| <i>H. nemestrinae</i> ^b | + | - | + | + | - | ND | + | - | R | S | - | 4-8 | Bipolar | 24 |
| <i>H. pylori</i> | + | - | + | + | - | + | - | - | R | S | - | 4-8 | Monopolar | 39 |
| <i>H. salomonis</i> | + | + | + | + | + | ND | - | ND | R | S | - | 10-23 | Bipolar | ND |
| " <i>H. suncus</i> " | + | + | + | + | - | - | ND | ND | R | R | - | 2 | Bipolar | ND |
| Enterohepatic | | | | | | | | | | | | | | |
| <i>H. bilis</i> | + | + | ND | + | - | ND | + | + | R | R | + | 3-14 | Bipolar | ND |
| " <i>H. canadensis</i> " | + | V | - | - | + | - | + | + | R | R | - | 1-2 | Bipolar | ND |
| <i>H. canis</i> | - | - | + | - | + | ND | + | ND | S | I | - | 2 | Bipolar | 48 |
| <i>H. cholecystus</i> | + | + | + | - | - | - | + | + | I | R | - | 1-3 | Monopolar | ND |
| <i>H. cinaedi</i> | + | + | - | - | - | - | - | + | S | I | - | 1-2 | Bipolar | 37-38 |
| <i>Helicobacter</i> sp. cotton-top | + | + | + | + | - | + | + | + | S | R | - | 2 | Bipolar | 31 |
| <i>H. fennelliae</i> | + | - | + | - | + | - | - | + | S | S | - | 2 | Bipolar | 35 |
| " <i>H. ganmani</i> " | V | + | - | - | - | ND | - | - | S | R | - | 2 | Bipolar | ND |
| <i>H. hepaticus</i> | + | + | ND | + | + | ND | - | + | R | R | - | 2 | Bipolar | ND |
| " <i>H. mesocricetorum</i> " | + | + | + | - | ND | - | + | - | S | R | - | 1 | Bipolar | ND |
| <i>H. muridarum</i> | + | - | + | + | + | + | - | - | R | R | + | 10-14 | Bipolar | 34 |
| <i>H. pametensis</i> | + | + | + | - | - | - | + | + | S | S | - | 2 | Bipolar | 38 |
| <i>H. pullorum</i> | + | + | - | - | - | ND | + | ND | R | S | - | 1 | Monopolar | 34-35 |
| <i>Helicobacter</i> sp. flexispira | + | - | - | + | ND | + | + | - | R | R | + | 10-20 | Bipolar | 34 |
| <i>H. rodentium</i> | + | + | - | - | - | - | + | + | R | R | - | 2 | Bipolar | ND |
| <i>H. trogonum</i> | + | + | - | + | ND | + | + | ND | R | R | + | 5-7 | Bipolar | ND |
| " <i>H. typhlonicus</i> " | + | + | - | - | - | - | - | + | ND | ND | - | 2 | Bipolar | ND |

^a +, positive reaction; -, negative reaction; S, susceptible; R, resistant; I, intermediate; ND, not determined; V, variable.

^b Unpublished data suggest that *H. nemestrinae* may be identical to *H. pylori* (see text).

Table 1: Characteristics of cultivated *H. pylori* species^a. The table was modified from *Helicobacter pylori*: physiology and genetic, page 41 (19)

2.2 Metabolism and physiology

H. pylori conserves energy in the form of adenosine triphosphate (ATP). The microorganism generates the necessary ATP molecules by creating a proton electrochemical gradient across the cytoplasmic membrane. The respiratory chain plays as the key generator of this gradient in *H. pylori*. The organic compounds such as D-glucose and formate, or inorganic such as H₂ (20) are substrates of oxidation process. The only known electron acceptors are O₂ and possibly fumarate (21, 22), explaining the obligate requirement for O₂ in this bacterium. Oppositely, several essential metabolic enzymes used in anaerobic metabolism are typically found in *H. pylori* (23). However, those enzymes are oxygen-labile (23). Taking into account together, these factors may partly account for the microaerophilic character of the bacteria, despite the fact that it possesses several oxidative stress response systems (24). Growth of the microorganism *in vitro* occurs at low concentrations of oxygen (<10%), which corresponds to oxygen concentrations found in the gastric mucosa (23). In term of the metabolic aspects of carbon flow in *H. pylori*, there is strong evidence supporting the presence of standard Embden-Meyerhof pathway (25). The citric acid cycle (CAC) also typically plays a key role both in catabolic and biosynthetic pathways and is present in most bacteria. Genomic analysis failed to identify homologs of several genes encoding enzymes necessary to the typical CAC. It has been suggested that the bacterium possesses a branched incomplete CAC (22, 26, 27).

To survive and replicate in the extreme acid environment of human stomachs, *H. pylori* developed certain features that are exceptional in the bacterial world. One of

such features is an enzyme called urease, which catalyzes the hydrolysis of urea into carbon dioxide and ammonia. Under acidic conditions, these ammonia molecules capture H^+ to form NH_4^+ resulting in a rise of the pH and conferring to the bacterial acid resistance (Figure 1) (28). Another strategy to avoid the acid environment of the human stomach is the spiral shape of *H. pylori* and the seven-sheathed flagella present in one of its poles. It allows the bacterium to be highly motile even in very viscous mucus and locates in the mucus layer overlaying the gastric mucosa (16). This mucus is relatively thick and viscous, and maintains a pH gradient from approximately pH 2 to pH 7.4 from the adjacent of the gastric lumen through the above of the epithelial cells (28). Adaptation of bacteria to the stomach niche has probably resulted in the absence of some bacterial amino acid synthesis pathways. As the bacteria are therefore dependent on many of the host's amino acids and these amino acids may also serve as main source of carbon. The adaptation of *H. pylori* to the human stomach has turned it into a very fastidious microorganism, requiring a complex medium and a few days to be grown *in vitro*.

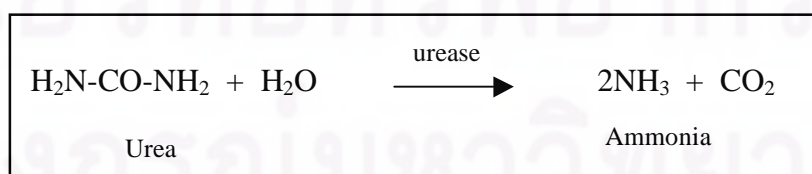


Figure 1: The chemical reaction of urea hydrolysis (28).

2.3 Genome

The genome of *H. pylori* contains approximate 1.7 megabase pairs (about one-third of *E. coli*), with a G+C content of 39% and approximate 1,500 predicted coding sequences (9). The two independent *H. pylori* genomes that have been completely sequenced have distinct origins. *H. pylori* 26695 was isolated from a gastritis patient and had been passaged repeatedly prior to sequence in 1980s by The Institute for Genomic Research, the United Kingdom. In contrast, *H. pylori* J99 was isolated from a duodenitis patient and had not been extensively passaged prior to sequence in 1994 by a collaborative effort between AstraZeneca PLC and Genome Therapeutics Corporation, the United State (29). Sequence comparisons between the genome of *H. pylori* strains 26695 and J99 demonstrate different chromosome organization in separated regions. However the genome size, genetic content, and gene order of these two sequenced strains are very similar (10). Both genomes contain two copies of the 16S and 23S-5S rRNA loci in the same two relative locations. Comparative analysis between the genomes of *H. pylori* 26695 and J99 have identified that between 6 to 7% of the genes are specific to each strain, with almost half of these genes being clustered in a single hypervariable region termed “plasticity zone” (30). The content of *H. pylori* plasticity zones may have an influence on the type or severity of diseases (31). There is, however, a remarkable diversity expressed by *H. pylori* strains. The physical maps generated by pulsed-field gel electrophoresis (PFGE) presented an extreme macrodiversity between independent *H. pylori* strains, even those isolated from similar geographical locations (32). It has been

suggested that common bacterial mechanisms such as endogenous point of mutation and intragenomic recombination are involved in such diversity in *H. pylori* (33, 34)

2.4 Microbiology and laboratory culture

H. pylori is a spiral-shaped, gram-negative, and non-sporeforming bacteria with cell size ranges from 0.2 to 1.2 μm wide and 1.5 to 10 μm long (19). *H. pylori* colonies are small (0.5 to 2 mm), translucent to yellowish or grayish. By observation with gram stain of a culture on solid medium, bacterial morphology appears as short spiral. In the stomach, it is present either as curved rods or as short spiral (35). Alternatively, the bacterial shape enables to change into coccoid form following an extended incubation period. The significance of each morphological type of *H. pylori* is uncertain. However, the spiral shape is commonly found *in vivo*, and it has been associated with an infectious form of the pathogen. Transformation to the coccoid form is commonly induced when organism exposing to sub-optimal conditions (36, 37). It has been suggested that the coccoid form is in fact a dormant growth phase playing a role in bacterial survival and transmission (38). Various deteriorated changes have been found in the coccoid cultures. These include fragmentation of DNA and RNA, protein degradation, loss of membrane potential, low level of mRNA produced, and reduction of ATP content (39, 40). The coccoid form of *H. pylori* has been categorized into three types including the dying coccoid form, the living with culturability form, and the viable but non-culturable form (41). *H. pylori* is motile with a rapid corkscrew-like motion due to flagellar activity. It possesses bundle of four to seven sheathed flagella with

monopolar distribution (19). Approximately half of the *H. pylori* strains carry a plasmid. However, no function has yet been identified and there is no difference in antibiotic resistant pattern between strains with or without plasmid (42).

H. pylori is microaerophilic and possesses respiratory capability. That means it requires only restricted oxygen concentration to grow. No growth is observed in aerobic conditions, but growth can occur under anaerobic conditions. The standard culture condition is 37 °C with 3 to 7% oxygen and 5 to 10% carbon dioxide (43). Culture is normally performed on rich media such as brain heart infusion agar, Columbia agar, or Brucella agar supplemented with 7 to 10% horse or sheep blood, or blood products such as lysed blood or serum. The colonies could be visible after 2 to 5 days of incubation. *H. pylori*-selective antibiotics like Skirrow's supplement (vancomycin, trimethoprim and polymyxin B) or Dent's supplement (vancomycin, trimethoprim, cefsulodin and amphotericin) are commonly added to the growth medium (44, 45). Its biochemical pattern is closely related to *Campylobacter*, *Acrobacter*, and *Wollinella* species. However, the key reactions for differentiation of *H. pylori* and other *Helicobacter* species are the production of urease, oxidase and catalase enzymes (19).

2.5 Epidemiology

H. pylori is a very common human gastrointestinal pathogen, which infection occurs worldwide with significant differences among countries (46). However, the majority of infections are asymptomatic (47). Overall, *H. pylori* prevalence varies widely by geographic area, age, race, sanitary, and socio-economic conditions. Inadequate

sanitation practices, low social class, and high-density living conditions seem to be related to a higher prevalence of *H. pylori* infection (48). In developing and underdeveloped countries such as in Africa and Asia, *H. pylori* can colonize as much as 90%, while in developed countries only 25 - 50% of the population is colonized (49). In Thailand, a seroprevalence of *H. pylori* is 55 - 70% (50). Whites race has a lower seroprevalence of *H. pylori* than either Blacks or Hispanics (48). Many have suggested that *H. pylori* is mostly acquired in childhood (51). However, no noteworthy gender differences exist in *H. pylori* prevalence (48).

2.6 Transmission

Even though the prevalence of *H. pylori* worldwide is over 50%, the bacterial isolation outside the human GI tract has been considered impossible. Humans are the principal reservoir. Whether *H. pylori* becomes widespread among human population still being questioned. Many epidemiological evidences have proposed several routes of transmission as person-to-person, by oral-oral, gastro-oral, or fecal-oral routes (52-54). The oral-oral route of infection is most likely responsible by saliva, dental plaque, and vomit. It has been suggested to occur by kissing (48). *H. pylori* DNA have been detected by PCR in the mouth of infected individuals (55). However, the bacterium has not been able to culture from oral cavity samples, which is recognized as gold standard for diagnosis. The gastro-oral route has been postulated to infect mainly in young children whom vomitus and gastro-oesophageal reflux are common (48). *H. pylori* has been cultured from all 80 vomitus samples collected from 16 seropositive subjects (53). *H.*

pylori DNA has also been detected in feces of infected subjects by some researchers, providing evidences for fecal-oral route of infection (48).

Apart from those previously mentioned modes of *H. pylori* transmission, waterborne, zoonotic or vectorborne, and iatrogenic transmission are other possible transmission pathways (48). It has been demonstrated that *H. pylori* can live several days to months in water resources (56). Support for waterborne transmission comes from studies conducted in Colombia, China, and Peru, which found that water sources may be related with *H. pylori* infection (57-59). Although the principal reservoir for *H. pylori* infection appears to be human, the organism has been occasionally shown to be related with animal reservoir such as domestic cat, sheep, or housefly (60-62). The higher prevalence of *H. pylori* infection was found among those who exposed to these relative animals rather than non-exposed ones. As for iatrogenic transmission, *H. pylori*-contaminated medical devices such as endoscopes or biopsy forceps have predisposed the patients who attending in the hospital (63).

2.7 Pathogenesis and clinical relevance

To date, *H. pylori* is firmly established as the etiologic agent of acute or chronic gastritis, and a predisposing factor in peptic ulcer disease and gastric cancer. Generally, the main causes for peptic ulcer were believed as stress and smoking. However, in February 1994, the National Institutes of Health Consensus Development Conference concluded that *H. pylori* represents the major cause of peptic ulcer disease and stated that all patients with peptic ulcer associated with *H. pylori* infection should

receive antimicrobial treatment (64). In June of the same year, the International Agency for Research on Cancer Working Group of the World Health Organization identified *H. pylori* as a group I, or definite, human carcinogen (65). Infection caused by *H. pylori* occurs worldwide as *H. pylori* is a very common human gastrointestinal pathogen (66). Persons infected with *H. pylori* may develop acute gastritis within 2 weeks with nausea and epigastric pain following infection. Most of infected individual establishes chronic gastritis of different types such as atrophic gastritis, gastric ulcer disease, gastric adenocarcinomas, and gastric mucosa-associated lymphoid tissue (MALT) lymphomas (43, 67). A well-known mucosal inflammation in chronic active gastritis is often evident in the antrum, predisposing to hyperacidity and duodenal ulcer disease. *H. pylori* has also been shown to induce apoptosis in gastric epithelial cell *in vitro* and *in vivo* (68). Various evidences implicate that apoptosis is the primary response of gastric epithelial cells to *H. pylori*, with epithelial hyperproliferation as a compensatory occurrence, resulting in a precursor of malignancy (69).

2.8 Virulence

H. pylori strains could be classified based on carriage of the cytotoxin-associated gene pathogenicity island (*cagPAI*) and expression of the vacuolating cytotoxin (VacA) (70). Type I strain (more virulent), which is the majority of *H. pylori*, possesses the *cagPAI* and secretes VacA. In contrast, type II strain (virulent) lacks the *cagPAI* and does not produce VacA. *cagPAI* is a 37-kb genomic fragment containing 29 genes with *cagA* appears to be a major virulent gene and molecular marker for *cagPAI*.

The *cagA* gene encodes a 120-kd protein, CagA, which is identified as the first protein of the PAI. The *H. pylori* PAI was originally named *cag* (cytotoxin associated gene) since it was thought to be associated with expression of the VacA. However, it was later shown that both factors are independent from each other. The ratio between *cag*⁺ and *cag*⁻ strains varies between different parts of the world. For example, approximately 40% of the strains are *cag*⁺ in the Netherlands, China, and Canada, while in Thailand and Peru are approximately 80% (71). The *cagPAI* also encodes a helicobacter-specific type IV secretion system involving in the secretion of CagA protein into host gastric epithelial cells (72). Translocated CagA is phosphorylated on tyrosine residues by the Src family kinases, and binds to SHP-2 domain. This complex results in cytoskeleton changes such as long cytoskeleton extension and pedestal formation known as the “hummingbird” phenotype (73). The strong direct correlation of the presence of *cagA* gene and disease has been reported (74). The interference of CagA to cell cycle has been conferred to involve to the increased risk of gastric cancer. *In vivo* study showed that *cagPAI*-positive strains induce gastric damage and implicate in extensive gastric ulceration and cancer, while *cagPAI*-negative strains resemble commensal bacteria (75, 76).

Almost of *H. pylori* strains contain a copy of the toxin gene, *vacA*, encoding for the vacuolating cytotoxin (VacA). The VacA is a 95 kD secreted exotoxin protein that causes epithelial cell vacuolation and has also been identified in more severe diseases (77). Sequence analysis of *vacA* gene has shown two variable regions; the signal region (‘S’-region) and the mid region (‘M’-region). The S region is divided in s1a, s1b, s1c, and s2, whereas the M region can be divided in m1 and m2 (78). Combinations of S and

M regions (such as s1a/m1, s1b/m1, s1a/m2, etc) resulted in an extensive recombination among *vacA* alleles (78). Numerous studies have shown that *H. pylori* strains that express vacuolating cytotoxin activity *in vitro* are more commonly associated with peptic ulcer disease than non-cytotoxin strains (78).

Although two important *H.pylori* factors contributing to the virulence and the colonization are *vacA* and *cagA*, other factors appear to promote bacterial pathogenesis. A unique array of features permits entry of *H. pylori* into the mucus. This starts from swimming and spatial orientation of *H. pylori* in the mucus, attachment to epithelial cells, evasion of immune response, and colonization. Several virulence factors for gastric colonization, tissue damage, and survival have been identified in *H. pylori* (Table 2) (16). However, the gastric mucosa is normally well protected against bacterial infections. Gastric acidity acts as the first-line defense against food-borne pathogens. Despite this, *H. pylori* is well adapted for this ecologic condition. *H. pylori* shows a remarkable acid-resistance response to the gastric environment by producing a neutral pH optimum urease (16, 79).

| Virulence factors | Effects |
|--------------------------------|--|
| Colonizing | |
| Flagella | Active movement through mucin |
| Urease | Neutralization of acid |
| Adhesins | Anchoring <i>H. pylori</i> to epithelium |
| Tissue damaging | |
| Proteolytic enzymes | Glucosulfatase degrades mucin |
| 120-k Da cytotoxin (Cag A) | Related to ulcer and severe gastritis |
| Vacuolating cytotoxin (Vac A) | Damage of the epithelium |
| Urease | Toxic effect on epithelial cells, disrupting cell tight junctions |
| Phospholipase A | Digest phospholipids in cell membranes |
| Alcohol dehydrogenase | Gastric mucosal injury |
| Survival | |
| Intercellular surveillance | Prevent killing in phagocytes |
| Superoxide dismutase | Prevent phagocytosis and killing |
| Catalase | Prevent phagocytosis and killing |
| Cocoid forms | Dormant form |
| Heat shock proteins | |
| Urease | Sheathing antigen |
| Other | |
| Lipopolysaccharide | Low biological activity |
| Lewis X/Y blood group homology | Autoimmunity |

Table 2: Virulence factors identified in *H. pylori* (16).

2.9 Treatment

Goal of *H. pylori* treatment is the complete elimination of organism (16).

Such goal has not been achieved with antibiotics alone. By principally, triple therapies by combination of two antibiotics with an antisecretory agent (e.g. H₂ antagonist or proton-pump inhibitor; PPI) have been extensively evaluated and approved as the most effective regimens. The combination of two or more antimicrobial agents increases

curing rates and reduces the risk of resistant problem. The chief antimicrobial agents used in several regimens are amoxicillin, clarithromycin, metronidazole, and tetracycline (80). Two regimens of first-line treatment that most often used are a PPI in conjunction with clarithromycin and amoxicillin, and a PPI in conjunction with clarithromycin and metronidazole (81). When first-line treatment fails, a second-line treatment of quadruple therapy is recommended. Some have proposed a quadruple therapy with proton pump, bismuth, metronidazole, and tetracycline as an effective second-line treatment (82). However, the particular *H. pylori* antibiotic susceptibility assessment is necessary in case of treatment failure (83).

Eradication failure rate for *H. pylori* has been markedly progressed accompanying with an increased rate of development of antibiotic resistant strains (84). The eradication failure rate remains as high as 5 to 20% along with frequent relapses of gastric ulcers, resulting the treatment of this bacterium is being troubled (83). This situation could be attributed to several reasons, including the cost, poor patient compliance, undesirable side effects, low penetration rate in the mucus, adverse effect on drug caused by gastric acidic pH, and particularly antibiotic resistance (84). Clarithromycin has emerged as the most important antibiotic combined therapy for eradication of *H. pylori* (85). To date, the frequency of clarithromycin resistance is approximately 12, 13, and up to 15% in North America, East Asia, and Europe, respectively (86). A review of literature on eradication therapy indicated that eradication rates of *H. pylori* infection have decreased to 53% if clarithromycin resistance was present and a clarithromycin-containing regimen was used (84). Metronidazole

resistance ranges between 20 to 30% in both men and women in developing countries (86), and ranges from about up to 40% in Canada (87) and 20% to more than 50% in the United State (88). Furthermore, stable high-level resistance to ampicillin, cephalothin, and penicillin has also been reported (89).

3. *H. pylori* Biofilms

3.1 Biofilms: City of microbes

The term “biofilm” has been used to describe the structure of complex bacteria ecosystems that allow bacteria to function together (90). “Biofilm” is stated from the macroscopic morphology that looks like a thin layer of slime (91). Costerton et al. defines biofilm as “ a microbially derived sessile community characterized by cells that are irreversibly attached to a substratum or interface or to each other”. Biofilms are embedded in a matrix of extracellular polymeric substances and exhibit an altered phenotype with respect to growth rate and gene transcription (92). Microbial biofilm phenotype is as common as planktonic microorganism phenotype (93). However, data came mostly from natural aquatic ecosystem showed that more than 99.9% of the bacteria grow in biofilms on a wide variety of surfaces (92). Transformation from planktonic to biofilm requires an up-regulation of specific genes that found only in the biofilm but not in planktonic organisms (92). Several key environmental and cultural characteristics affect the selection of biofilm inhabitants (Figure 2) (93). Of these characteristics, the four most important are organism attachment efficiency, nutritional resources, substrata, and environmental shear force (93).

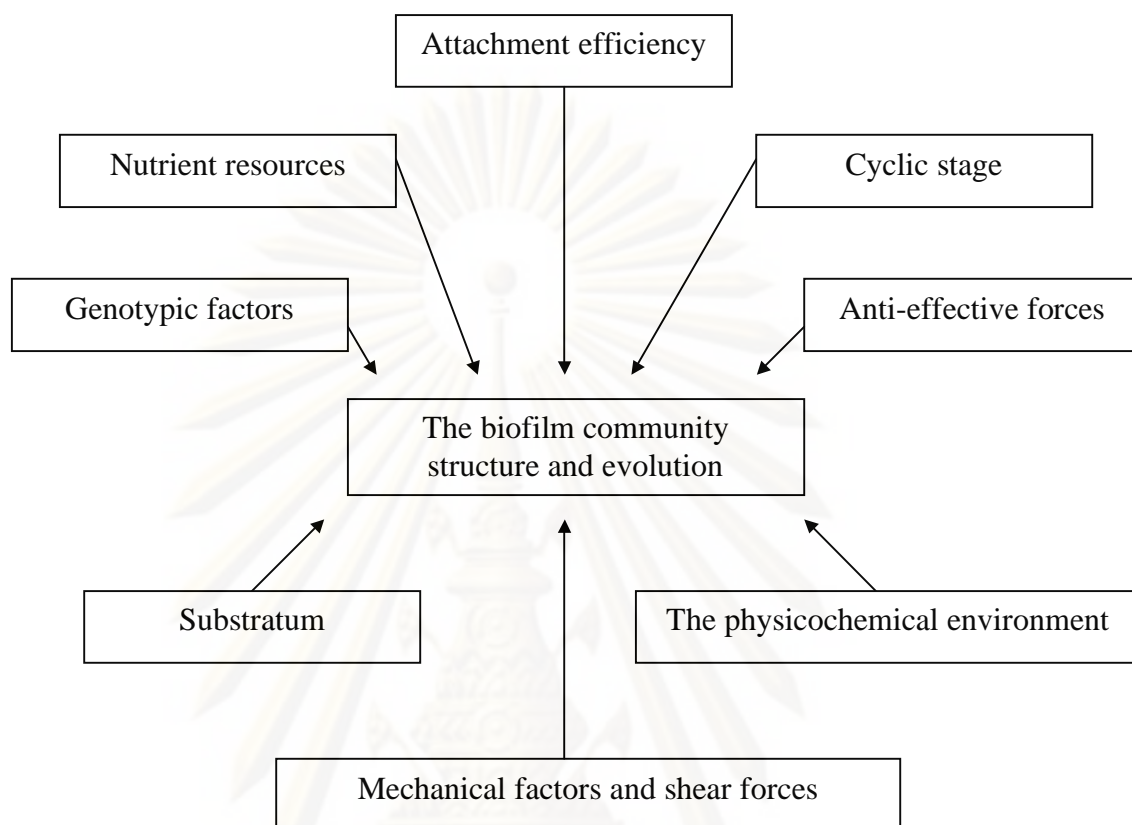


Figure 2: Potential environmental and cultural factors in biofilm development (93).

3.1.1 Stages in biofilm formation

By naturally, the formation of bacterial biofilm forms in multiple developmental stages (94). Five different stages of biofilm universal growth cycle have been proposed with common independent characteristics of the phenotype of the organism (93). Stage I, bacterial attachment phase can occur within only seconds in response to environmental signals. These signals include changes in nutrients and nutrient concentration, pH, temperature, oxygen concentration, osmolality, and iron. However, these signals vary by organism. Rough and hydrophobic (such as Teflon and

plastic) surfaces provide more susceptible surface area to form biofilm rather than smooth and hydrophilic (such as glass) ones. The initial stage I is irreversible and some cells still be able to detach from the substratum. This stage is mediated by a number of bacterial adhesion molecules. Bacterial cells exhibit a logarithmic growth rate during this stage. Stage II, where an irreversible binding occurs, begins minutes after stage I. Bacterial cell aggregation is formed and motility is decreased. During the end of this stage, exopolysaccharide is produced that is able to trap nutrients and planktonic bacteria. Stage III characterized by an observation of cell aggregate layers with thickness greater than 10 μm . When biofilm reaches the highest thickness, generally greater than 100 μm , this is referred to stage IV. During the last step, at stage V, cell dispersion is noted (93). Some of bacteria change to the planktonic phenotype and leave the biofilm. Although, progression from stage I to V takes several days, cycling of stage development is based on the organism pool and the growth characteristic of individual members (93).

3.1.2 Architecture of Biofilm

Three-dimensional architecture of clinical biofilm shares a similarity with the biofilm commonly found in animal, agricultural, industrial settings (93). The three-dimensional structure of mature biofilm often consists of three layers and stalks of mushroom-shaped microcolonies attached to the substratum surrounded by exopolysaccharide. Generally, up to 97% of the biofilm matrix is water. The rest compositions of the matrix include microbial cells (2 to 5%), exopolysaccharide (1 to 2%), proteins (<1 to 2%), and bacterial DNA or RNA (<1 to 2%) (93). Mature biofilm is

composed of three layers. The outermost layer of biofilm, where the most active organisms resembling their planktonic counterparts observed, is exposed to the highest nutrient and oxygen concentration. The second layer of biofilm, however, consists of metabolic down-regulated organisms. But these cells are still able to function as planktonic does, and have potential for multidrug resistance. The innermost layer of biofilm is anchored to surface of substratum and represents the earliest part of the biofilm. This layer is composed of very down-regulated organisms with the least metabolic activity. Most persister cells are located in this layer. Various forms of biofilms have been observed recently. For instant, bacterial aggregates, not attachment to a surface, are commonly termed flocs (95) and have been observed in *Campylobacter jejuni* (96). Other possible forms are pellicles, which are aggregate of bacterial cells that form at an air-liquid interface (97). Many of bacteria have been shown for the pellicle character, such as *C. jejuni* (96), *Salmonella enterica* (98), and *Pseudomonas aeruginosa* (97).

3.1.3 Biofilm pathogenicity and disease

The biofilm mode of growth is widespread (99). Monospecies biofilms are formed by many human pathogens such as *P. aeruginosa* (100), *Staphylococcus epidermidis* (101), *S. enterica* (102), *Vibrio cholerae* (103), *Burkholderia cepacia* (104). The mechanisms of biofilm pathogenicity have been considered to contribute to infectious diseases. Bacteria living as biofilm communities tend to attach to a solid surface. This initiates a colonization that is often an important first step in

infectious diseases. Thus biofilm may be an important mechanism of attachment to host tissue and indwelling medical devices. Biofilm can protect bacterial cells from natural host immune system, particularly the activity of phagocytic cells such as polymorphonuclear cells. The phagocytes are unable to penetrate through the biofilm and fail to eliminate organisms. In addition, biofilm may hide microbial antigens, preventing an immune response on blocking interaction with antibody. Biofilm can afford pH changes, nutrient deprivation and protect cells from hazardous substances including oxygen-reactive molecules and antimicrobial agents. However, mechanisms that mediate these protections are not completely known. Possibly, “sticky” exopolysaccharide provides a physical barrier to penetration by phagocytic cells and antibiotic molecules. Additional pathogenic mechanism responsible by biofilm is an ability to horizontally transfer genetic material, DNA, among microorganisms living in close proximity. This transfer may lead to the spread of antimicrobial resistance and result in more virulent strains of microorganisms. However, biofilm itself also has a potential to spread to other body sites. Biofilm disaggregation provides the potential of infection to the alternate body sites (93).

Many observations provide evidences of the significance of biofilm in the association with diseases. Biofilm colonization at medical devices often leads to many biofilm-associated infections. At least 30 bacteria and yeasts have been declared as causative agents for biofilm-associated infections. Table 3 presents several medical biofilm-associated conditions, which the biofilm plays a crucial role in promoting microorganism survival and distribution within the hosts.

| Infections or diseases | Common causative organisms |
|-------------------------------------|--|
| Native valve endocarditis (105) | Streptococci Staphylococci Gram-negative bacilli <i>Candida</i> and <i>Aspergillus</i> spp. |
| Otitis media (106) | <i>Streptococcus pneumoniae</i> <i>Haemophilus influenzae</i> <i>Moraxella catarrhalis</i> Group A streptococci <i>P. aeruginosa</i> <i>Staphylococcus aureus</i> |
| Chronic bacterial prostatitis (107) | <i>E. coli</i> <i>Klebsiella</i> Enterobacteria <i>Proteus</i> Coagulase-negative staphylococci |
| Cystic fibrosis (108) | <i>S. aureus</i> <i>H. influenzae</i> <i>P. aeruginosa</i> <i>Burkholderia cepacia</i> |
| Periodontitis (109) | <i>Fusobacterium nucleatum</i> <i>Peptostreptococcus micros</i> <i>Eubacterium brachy</i> <i>Lactobacillus</i> spp. |

Table 3: Partial list of common human infection involving biofilm.

3.2 Biofilms: Alternative life style of *H. pylori* contributing to host infection

A paradox is that, although *H. pylori* is extremely widespread, its microaerobic growth requirements mean that the organism does not multiply in the natural aerobic environment. However, *H. pylori* has been recently reported to have an alternate lifestyle as biofilm, which facilitate survival *in vivo*, in the hazardous environment, and during transmission (110). It has been shown previously that, in water, biofilm is a protective niche for several pathogens from stressful conditions. Several studies have identified *H. pylori* in water distribution systems (111, 112) and natural water sources (113) in several countries. These findings have been accompanied with the possibility that *H. pylori* may exist as a biofilm on surface exposed to water providing another route of infection (112). Several studies have described the roles of water sources and associated biofilms acting as environmental transmitters. *H. pylori* DNA was detected from drinking water storage pots in rural Gambia (114) and from cast iron water pipe sections in Scotland (110). These demonstrated the possibility of an increased rate of *H. pylori* colonization associated with contaminated water. In England, *H. pylori* DNA in domestic (houses) and school water distribution systems has been reported (112). The higher rate of *H. pylori* DNA was detected in biofilm setting samples rather than direct water and water net deposit samples. These confirmed hypothesis that biofilm might be able to act as bacterial reservoir in water resource (112). Water from natural sources such as river (113) and groundwater (115) have also been detected for *H. pylori* DNA suggesting *H. pylori* in biofilm could be found anywhere in the environment.

H. pylori infections resulting in gastric ulcers may be a manifestation of biofilm (116). A presence of dense mature biofilm attached to the cell surface of *H. pylori*-positive specimens has been documented (116). Cellini *et al.* (117) evaluated the expression of *glmM* and *luxS* genes from biopsies collected from dyspeptic patients, and found that 19 out of 21 samples gave positive of both. *luxS* is play a role in microbial quorum sensing which used as an indicator of *H. pylori* biofilm production. Coticchia *et al.* (118) demonstrated that 97.3% of the total surface area of human gastric mucosa, from the patients who tested urease positive for *H. pylori*, was covered by biofilms. While those testing negative had an average biofilm-covered area only 1.64%. In 2006, the existence of *H. pylori* biofilm on human gastric mucosa was first photographed (116). The dense mature biofilm was embedded in amorphous exopolysaccharide matrix. This biofilm was attached to the surface of *H. pylori*-positive specimens and absent in urease-negative controls (116). However, a prevalence of biofilm formation of *H. pylori* from clinical specimens is still limited and required more studies.

Biofilm formation of *H. pylori* is complicated by a number of factors. *H. pylori* does not adhere appreciably to plastic substratum and has been considered to form biofilms only at the air-liquid interface (119). *H. pylori* requires extended incubation (over 3 days of growth) in a microaerobic atmosphere for biofilm formation (119). *H. pylori* has been shown to produced a water-insoluble biofilm at the air-liquid interface of glass fermenter with a high carbon:nitrogen ratio (120). *H. pylori* enables to form a floating pellicle at the air-liquid interface in glass test tubes and glass coverlips (119). A scanning electron microscopy (SEM) of *H. pylori* biofilm reveals a cytoarchitecture of

bacterial cells under biofilm mode of growth (Figure 3). The bacteria (primarily coccoid) stacked several layers thick, and numerous holes could be observed.

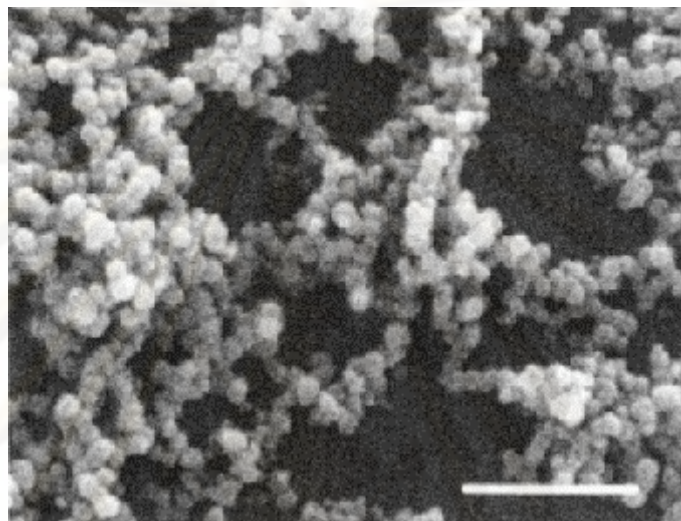


Figure 3: SEM micrograph of a 4-day-old biofilm of *H. pylori* grown as stationary batch culture (119). Bar, 1 μm .

During an extended incubation, *H. pylori* has a cellular conversion from bacilli to coccoid morphology which is viable but non-culturable (VBNC) forms (119). The VBNC bacteria could be integrated as the “persister” cells. This represent the non-growing population of cells in microbial biofilms which ensure the firmly adhesion to the surfaces (121). The precise composition and sequence structure of the polysaccharide produced by *H. pylori* biofilms have not been determined yet. However, carbohydrate analysis of crude extracted from *H. pylori* biofilms has been analyzed and shown the presence of fucose, glucose, galactose, and glycerol-manno-heptose, N-

acetylglucosamine and N-acetylmuramic acid (120). This sugar composition strongly indicates the presence of a polysaccharide as a component of *H. pylori* biofilm material. *H. pylori* biofilm also contains amino acid composition and lipid material, predominately tetradecanoic acid (C₁₄) and hexadecanoic acid (C₁₆) (120).

3.3 Potential regulators relating to biofilm formation of *H. pylori*

Many regulators, including signals and gene products are involved in the biofilm development under a dynamic process depending on different bacteria and different biotic and abiotic surfaces (122). The development of biofilm is mostly depended on quorum sensing which is the communication among bacterial cells via extracellular molecules or pheromones. (93). It is essential for biofilm formation by triggering expression of some genes and down-regulate of others. However, pheromones secreted by gram-negative and gram-positive are different. While, gram-negative bacteria utilizes low-molecular-weight homoserine molecules, such as N-acyl homoserine lactone. Gram-positive bacteria employs proteins or oligopeptides (93). However, factors important in favoring *H. pylori* to form biofilm both *in vitro* and *in vivo* are not well understood and more work is needed to fully elucidate.

3.3.1 Gene responsible in *H. pylori* biofilm formation

Biofilm formation has involved with number of global regulatory genes, which involved in virulence, cell-cell signaling, response to environmental signals (90). In 2004, Cole *et al.* (119) investigated the effect of specific mutation in several

genes on biofilm formation of *H. pylori*. Although, many genes including *ppk* (encodes for polyphosphokinase) and *clp* (encodes for protease) required for biofilm formation in other gram-negative bacteria, they did not affect *H. pylori* biofilms (123, 124). While, the *luxS* gene encodes for an autoinducer-2 (AI-2), a signaling molecule in quorum sensing system, and the *cagE* gene encodes for a type IV secretion are involved in *H. pylori* biofilm formation. A mutation in *luxS* increased monospecies biofilm formation by *H. pylori*. The *cagE* isogenic mutant was also found to adhere more strongly to glass surfaces rather than wild type. Both the *luxS* and the *cagE* gene mutants were found to form biofilms approximately twofold more efficiently than wild type (119). It has been suggested that the interplay between the *luxS* and *cagE* genes may involve in this matter. However, investigation of these interactions still requires more study.

3.3.2 Bacterial adhesin and biofilm formation

The first step in colonization begins with adhesion of bacteria to the human mucosal epithelium, triggering the pathogenesis (125). Although, epithelial mucosal surfaces possess several defense mechanisms to prevent adhesion. Colonizing bacteria have developed multiple adhesion mechanisms in order to overcome these obstacles. Numbers of specific mechanisms are used to improve a chance in successful attachment such as flagella, fimbriae, and pili. The bacterial adhesin has been shown to play a role in initial step of adhesion of many bacteria including *H. pylori* (16). Adhesins are bacterial proteins, glycoconjugates, or lipids that are involved in the initial stages of colonization by mediating the interaction between the bacteria and the host cell surfaces.

Many *H. pylori* adhesins are important virulence factors (Table 4). *H. pylori* adhesin-mediated colonization is clearly involved by several different elements and more than one adhesin may be crucial (16).

| <i>H. pylori</i> adhesins | Host cell receptors |
|--|--|
| AlpA, AlpB | Unknown |
| BabA | Lewis b |
| HopZ | Unknown |
| HpaA, Nap; 64 kDa, 62 kDa, 56 kDa, 20 kDa | N-acetylneuraminyllactose (sialic acid) |
| Hsp60, Hsp70 | Lactosylceramide sulfate, galactosylceramide sulfate (sulfatides) |
| LPS | 97-kDa mucin receptor |
| LPS core | Laminin |
| LPS O antigen (Lewis X); Nap | Lewis X |
| Nap | Gastric mucin |
| 19.6 kDa (ferritin) | Laminin |
| 25 kDa | Laminin |
| 61-kDa protein | H type 2 (O antigen), Lewis b, Lewis a |
| 63 kDa (Exoenzyme S-like adhesin) -catalase; Nap | Heparan sulfate and other sulfated polysaccharides; phosphatidylethanolamine, gangliosylceramide (GM3), gangliosylceramide (GM2), gangliosylceramide; gangliosylceramide |
| Unknown | Class II MHC |
| Unknown | beta-1 integrins |

Table 4: *H. pylori* adhesins and host cell receptors (16).

After adhesion, organism may undergo specific molecular changes to become pathogenic or establish biofilm (126). Without adhesion, the events leading to biofilm formation will generally not occur (127). Bacterial adhesin has been shown to be responsible in biofilm formation by *E. coli* (128). The decreased biofilm growth by Tn5 mutants of *E. coli* MS2027 was due to the disruption of genes encoding type 3 fimbriae (128). This adhesin was also suggested to contribute to biofilm formation by different gram-negative nosocomial pathogens including *Citrobacter koseri* and *Citrobacter freundii* (128). Up to date, several *H. pylori* adhesins have been demonstrated for their functions mediating in colonization (129). Several *H. pylori* putative outer-membrane proteins (OMPs), such as HopZ, HopO, and HopP (130), AlpA and AlpB (131), are responsible for colonization of the stomach and induction of host inflammatory reaction in animal models. When these relative genes were knockout, the mutants markedly impaired to colonize *in vivo*. However, whether *H. pylori* adhesin plays a significant role in the bacterial biofilm formation is still debated.

3.3.3 *H. pylori* flagellum: A component mediating in biofilm formation

Bacterial flagella is a crucial factor in the process of colonization and establishment of a successful infection (132). The participation of flagella is important in the growth of microcolony, especially in the early stages of biofilm formation (133). The flagella of a number of bacterial species play significant role in the rate of attachment to a surface and subsequent biofilm formation (134). In recently, studies have shown that *Aeromonas* flagella facilitate adherence to the epithelial cell lines as well as initial step of

biofilm formation on plastic surface (134). In *P. aeruginosa*, the mutation in flagellar genes renders the strains defective for biofilm formation in both static and flow cell systems (135). *C. jejuni* flagellum-deficient mutant showed reduced biofilm formation compared with the wild type strains. These findings have clearly shown that flagella are required for biofilm formation and maturation, in addition to colonization, attachment to a surface, and motility (136, 137). In *H. pylori*, flagella have been implicated as a critical factor for colonization and pathogenesis. However, whether flagella may play a role in biofilm formation in *H. pylori* have not been documented before.

The flagella of *H. pylori* have been extensively studied. This organelle acts as a key role in colonization of the human gastric mucosa. *H. pylori* cells normally possess a unipolar bundle of two to six sheathed flagella (Figure 4) that enable the bacteria to move in their ecological niche of the mucous layer of the gastric epithelium (138). Each *H. pylori* flagellum is about 3 μm long and exhibits a typical bulb-like structure at its distal end (139) (Figure 4). The sheath itself is an extension of the outer membrane and is thought to protect the acid-labile flagellar structure from the attack of the stomach acid (139).

ศูนย์วิทยทรัพยากร
จุฬาลงกรณ์มหาวิทยาลัย

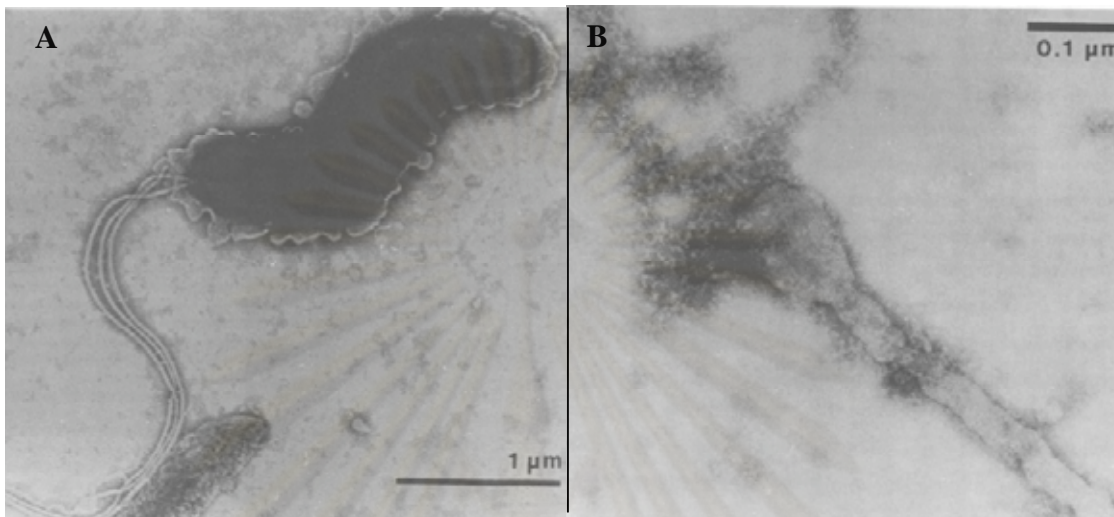


Figure 4: Electron micrograph displaying flagellated *H. pylori* (A) and distal end of a sheath with shaft, narrowing, and terminal club (B) (139).

H. pylori flagella comprises three structural elements like those of general enteric bacteria; a basal body, a flexible hook, and a flagellar filament (Figure 5) (140). The basal body is embedded in the cell wall and contains proteins that required for rotation and chemotaxis. The flexible hook locates, and serves as a joint between the basal body and the flagellar filament. The external helically shaped flagellar filament works as a screw when rotated at its base. A specific export apparatus forming at the cytoplasmic side of the MS ring secretes the external flagellar proteins that form the rod, hook, and filament. The proton gradient at the cytoplasmic membrane drives a proton flow that energizes flagellar motor rotation. The direction of rotation is determined by the interaction of FliM in the motor-switch complex with the chemotaxis regulator CheY, whose activity is regulated by the other components of the chemotaxis system. The

annotated genome sequences of *H. pylori* 26695 and J99 contain over 50 genes involving in flagellar expression, secretion, function and assembly (9,10) (Table 5). At least 20 of these proteins constitute the structural components of the *H.pylori* flagella. However, to date, only components of the filament and the hook have been characterized in some detail (Table 5). The filament is composed of two proteins, including the more abundant FlaA (141) and the second slightly larger protein; FlaB (142), localized close to the basis of the flagellum. The flagellin genes are under control of different promoter (σ^{28} for *flaA*; σ^{54} for *flaB*), however they are not genetically linked. Both flagellins have similar molecular mass (53 kDa) and share considerable amino acid homology (58% identity) (143). Expression of both flagellins appears to be necessary for fully motility (144) and for the establishment of persistent *H. pylori* infection in gnotobiotic piglet (136). The filament connected to the basal body by the flagella hook protein, which is a polymer of FlgE (145). The structural protein of the hook encoded by *flgE* gene. The *fliD* gene encodes a hook-associated protein (HAP2) localizing at the tip of the flagellar filament, promoting the incorporation of the flagellin monomers into the growing flagellar filament. The basal body-hook complex is encoded by NtrC orthologue, FlgR. The interaction of this complex is required for bacterial motility (146). The *flgR* gene also acts as a master transcriptional activator of σ^{54} -dependent genes, which transcribed by σ^{70} directs RNA polymerase (146). A model for flagellar gene expression in *H. pylori* has been proposed. The σ^{70} promoter directs transcription of genes encoding the early components required for flagellar assembly, including those for structural components of export apparatus, motor, basal body, and *flgR*. FlgR in turn activates transcription of σ^{54}

-dependent genes encoding the basal body-hook complex. It also represses *flaA* transcription as negative feedback for transcription of σ^{28} -regulated *flaA* flagellin gene promoter (146).

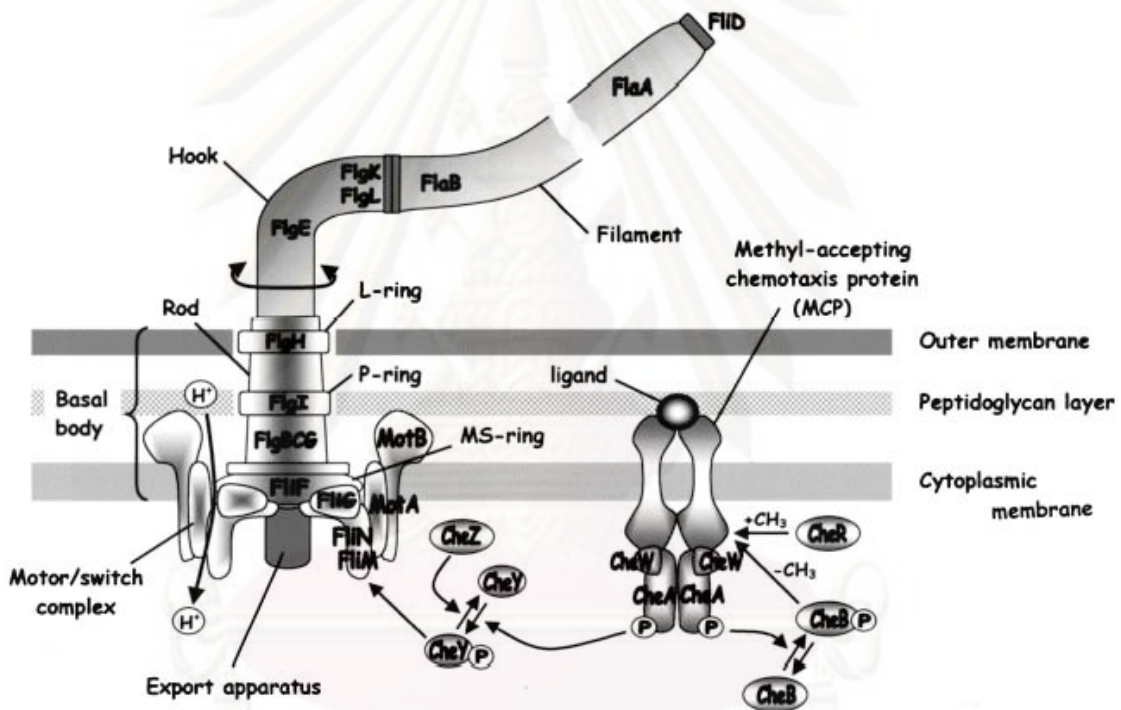


Figure 5: Flagellar proteins and their putative locations and interactions (140).

Symbols: H⁺, protons; P, phosphate; CH₃, methyl group.

In *H. pylori* the export apparatus is assembled from the proteins encoded by the *fliH*, *fliI*, *fliQ*, *fliL*, *fliP*, *fliR*, *flhA* (*flbA*), and *flhB* genes (Table 5). To date, only the *fliI*, *fliQ*, *flhA*, and *flhB* genes have been analyzed in some detail. Knockout mutants of *fliI* and *flhA* (*flbA*), members of the LcrD/FlbF family, were shown to be non-motile and aflagellate (147-149). In the functional analysis of gene involved in flagellar expression of *H. pylori* has shown that mutation in *fliQ*, *fliI*, and *flhB* genes results in non-motile and aflagellate strains. This demonstrated an essential role in flagellar biosynthesis (150). While *fliQ* mutant has reduced ability to adhere to AGS cells and *flhB* mutant showed a level of adherence similar to the wild type strain (150).

| Genes/Proteins | Functions | Genes/Proteins | Functions |
|--------------------|---|----------------------|--|
| <u>Structural</u> | | <u>Biosynthetic</u> | |
| <u>Basal body</u> | | HP1575/JH1483 | Flagellar biosynthetic protein (<i>flhB</i>) |
| HP1031/JH393 | Flagellar motor switch protein (<i>fliM</i>) | HP1419/JH1314 | Flagellar biosynthetic protein (<i>fliO</i>) |
| HP584/JH531 | Flagellar switch protein (<i>fliN</i>) | HP809/JH745 | Flagellar biosynthetic protein (<i>fliL</i>) |
| HP352/JH326 | Flagellar motor switch protein (<i>fliG</i>) | HP770/JH707 | Flagellar biosynthetic protein (<i>flhB</i>) |
| HP815/JH751 | Flagellar motor rotation protein (<i>motA</i>) | HP685/JH625 | Flagellar biosynthetic protein (<i>fliP</i>) |
| HP816/JH752 | Flagellar motor rotation protein (<i>motB</i>) | HP173/JH159 | Flagellar biosynthetic protein (<i>fliR</i>) |
| HP351/JH325 | Flagellar basal-body M-ring protein (<i>fliF</i>) | HP1041/JH383 | Flagellar biosynthetic protein (<i>flhA/flhA</i>) |
| HP325/JH308 | Flagellar basal-body L-ring protein (<i>flgH</i>) | HP684/JH625 | Flagellar biosynthetic protein (<i>fliP</i>) |
| HP246/JH231 | Flagellar basal-body P-ring protein (<i>flgI</i>) | HP353/JH327 | Flagellar export protein (<i>fliH</i>) |
| HP1558/JH1466 | Flagellar basal-body rod protein (proximal rod protein) (<i>flgC</i>) | HP1035/JH389 | Flagellar biosynthetic protein (<i>flhF</i>) |
| HP1559/JH1467 | Flagellar basal-body rod protein (<i>flgB</i>) | HP1420/JH1315 | Flagellar export protein ATP synthase (<i>fliI</i>) |
| HP1585/JH1492 | Flagellar basal-body rod protein (<i>flgG</i>) | <u>Regulatory</u> | |
| HP1557/JH1465 | Flagellar basal-body protein (<i>fliE</i>) | <u>Chemotaxis</u> | |
| HP1092/JH333 | Flagellar basal-body rod protein (<i>flgG</i>) | HP19/JH17 | Chemotaxis protein (<i>cheV</i>) |
| HP1030/JH394 | FliY protein (<i>fliY</i>) | HP99/JH91 | Methyl-accepting chemotaxis protein (<i>tlpA</i>) |
| <u>Hook</u> | | HP103/JH95 | Methyl-accepting chemotaxis protein (<i>tlpB</i>) |
| HP753/JH690 | Flagellar protein (<i>fliS</i>) | HP82/JH75 | Methyl-accepting chemotaxis transducer (<i>tlpC</i>) |
| HP870/JH804 | Flagellar hook protein (<i>flgE</i>) | HP599/JH546 | Methyl-accepting chemotaxis protein |
| HP908/JH844 | Flagellar hook protein homolog (<i>flgE</i>) | HP1067/JH358 | Chemotaxis protein (<i>cheV</i>) |
| HP907/JH843 | Hook assembly protein (<i>flgD</i>) | HP392/JH989 | Histidine kinase/chemotaxis protein (<i>cheAY</i>) |
| HP1119/JH1047 | Flagellar hook-associated protein 1 (HAP1/ <i>flgK</i>) | HP393/JH988 | Chemotaxis protein (<i>cheV</i>) |
| HP752/JH689 | Flagellar hook-associated protein 2 (HAP2/<i>fliD</i>) | HP616/JH559 | Chemotaxis protein (<i>cheV</i>) |
| HP295/JH280 | Flagellar hook-associated protein 3 (HAP3/ <i>flgL</i>) | HP391/JH990 | Purine-binding chemotaxis protein (<i>cheW</i>) |
| <u>Filament</u> | | HP1274/JH1195 | Paralyzed flagella protein (<i>pflA</i>) |
| HP115/JH107 | Flagellin B (<i>flaB</i>) | <u>Transcription</u> | |
| HP601/JH548 | Flagellin A (<i>flaA</i>) | HP244/JH229 | Histidine kinase |
| HP797/JH733 | Flagellar sheath adhesin <i>hpaA</i> | HP703/JH643 | Response regulator (<i>flgR</i>) |
| HP492/JH444 | Paralog of <i>hpaA</i> | HP714/JH652 | Alternative sigma factor sigma 54 |
| HP410/JH971 | Paralog of <i>hpaA</i> | HP1032/JH392 | Alternative sigma factor sigma 28 (<i>fliA</i>) |
| HP751/JH688 | Polar flagellin (<i>flaG</i>) | | |
| HP327/JH310 | Polar flagellin (<i>flaG</i>) | | |

^aCharacterized genes and proteins are in bold letters. Numbers labeled “HP” refer to the sequence published by Tomb *et al.* (9), those labeled “JH” to the one published by Alm *et al.* (10).

Table 5: Flagellar genes identified in the two published genome sequences^a.

3.4 Antimicrobial resistance in *H. pylori* resulted by biofilm formation

Biofilms are a major problem on a variety of medical devices and damaged tissues that can become the cause of persistent infections. By the fact that biofilm is often less susceptible to antibiotics (151) and host defense mechanisms (119) leading to a treatment failure and/or a chronic nature of infection. *In vivo*, antibiotics might suppress symptoms of infection by killing free-floating bacteria shed from the attached population, but fail to eradicate those bacterial cells embedded in the biofilm (152). When antimicrobial therapy stopped, the biofilm can act as a reservoir for the recurrence of infection. The biofilm usually persists the infection until the colonized surface is removed from the body (152).

It is well recognized that bacteria in biofilms are less susceptible to conventional antibiotic therapy (151). Biofilm-associated infections are 10 to 1,000 times more resistant to antimicrobial agents (153). The general antibiotic resistant mechanisms, such as efflux pumps, modifying enzymes, and target mutation, do not seem to be responsible for the protection of bacteria in a biofilm. Even sensitive bacteria that do not have a known genetic basis for resistance can have reduced susceptibility when entering into biofilm mode of growth (151). One interesting study has shown that *Klebsiella pneumoniae* grown as aqueous suspension had a minimum inhibitory concentration (MIC) of 2 $\mu\text{g ml}^{-1}$ ampicillin. While, high MIC of 5,000 $\mu\text{g ml}^{-1}$ was determined for biofilm state (154). However, when bacteria are dispersed from a biofilm, they rapidly become susceptible to antibiotics (155). This suggests that resistance of bacteria in biofilm is not acquired by mutations or mobile genetic elements. Several hypotheses have been described. First, it has been suggested that the biofilm matrix can either prevent or delay the diffusion of

antibiotics into the deeper layer of bacterial cells embedded in community (151). In case of aminoglycoside antibiotic, for example, positively charged agents bind to negatively charged polymers in the biofilm substance (156). Absorption of antibiotic agent into biofilm matrix may result in a retarded and/or slow penetration of aminoglycoside molecules (157). Second, a limitation of nutrient concentration is a well-known characteristic of biofilm feature as well as oxygen depletion in the deep layers of the biofilm. These factors probably promote some bacteria transiting from exponential to slow or no growth, which is generally less susceptible to growth-dependent antimicrobial agents (151). The third hypothesis depends on an altered chemical microenvironment within biofilm setting. Local accumulation of acidic waste products might lead to pH differences, probably greater than 1, between the bulk fluid and the biofilm interior. These changes could directly antagonize the action of an antibiotic (151). The fourth hypothesis is based on the induction of a biofilm phenotype in bacterial cells (153). A subpopulation of microorganism in biofilm forms a unique, and highly protected phenotype state, similarly to spore formation. In addition, the bacteria found within a biofilm are phenotypically different from their planktonic counterparts and have altered surfaces rendering them less susceptible to antibiotics (158).

Failure to eradicate *H. pylori* infection is associated with a significant increase in the prevalence of *H. pylori* resistant strains and development of multiple antimicrobial resistances (84). The rise of metronidazole and clarithromycin resistance in *H. pylori* is responsible by a significant role of biofilm formation (159). *In vivo*, the biofilm-related resistance in *H. pylori* was suggested to be due to the cluster of slow-growing biofilms embedded in an extracellular matrix during human

gastric mucosa colonization (121). Moreover, a production of water-insoluble biofilms in *H. pylori* enhanced resistance to antibiotics *in vivo* (120). While entering biofilm mode of growth, transformation of *H. pylori* cells into VBNC state is able to overcome stressful conditions, such as sub-inhibitory drug concentrations (121).

3.5 Strategies for control of biofilms: A novel approach to treating infections

Taken together with the fact that biofilm mode of growth in *H. pylori* facilitates the higher rate of antibiotic resistance (116). Many works are now focusing on elucidation of antibiotic resistant mechanisms in biofilm and development of new therapeutic strategies. In the meantime, some have reviewed an alternative strategy for treatment of *H. pylori* infection, instead of using antibiotics. Potential strategies for controlling biofilm include inhibition of microbial quorum sensing (160), degradation of extracellular matrix (161) and bioelectric effect (162). Rinonucleic acid III-inhibiting peptide (RIP) can inhibit eliminate biofilm formation in *S. aureus* and *S. epidermidis* by disrupting quorum-sensing mechanisms (160). The RIP seems to be synergistic with conventional antimicrobial agents as well. Lysostaphin, a constituent of human secretions, has been demonstrated to disrupt the extracellular matrix of *S. aureus* biofilm on plastic and glass surface (161). The low electric current (bioelectric effect) with an antimicrobial agent has also been shown to enhance the killing of biofilm-associated bacteria compared with the antimicrobial agent alone (162). However, a variety of further approaches are being defined to overcome biofilm-associated antimicrobial resistance.

Due to biofilm formation depends on the virtue of the ability of bacteria to adhere (163), one another possible strategy is an inhibition of microbial adherence.

Adhesion is a necessary first step in microbial colonization and pathogenesis (164). Organism may develop specific molecular change since adhesion has taken place, and may establish biofilm eventually (125). Establishment of novel alternative strategies to stop bacterial adhesion in order to overcome biofilm has been documented recently (164). For example, the development of carbohydrate-based anti-adhesive (165). This bases on the synthesis of short oligosaccharides to blocking bacterial carbohydrate ligands that mediate attachment (165). Generally, bacterial adhesion is mediated by carbohydrate-protein interactions between surface adhesions of microorganisms and the host cells. This can be interrupted by an antagonistic polyvalent carbohydrates compound. *H. pylori* possesses multiple binding mechanisms and many of those may mediate biofilm formation. Several *H. pylori* binding ligands may be use as the targets for anti-adhesion. The blockage of these mechanisms might inhibit or decrease the ability of bacteria to form biofilm (164).

Recently, natural products such as herbal compounds have been demonstrated for ability to inhibit microbial biofilm formation. Allicin, a sulfur-containing compound derived from fresh garlic, has been shown to diminish *S. epidermidis* and *Candida albicans* biofilms (166, 167). Xanthorrhizol, isolated from java turmeric (*Curcuma xanthorrhiza* Roxb.), has displayed a potent activity in preventing *Streptococcus mutants* biofilm (168). The significant reduction of adherent bacterial cells was observed on polystyrene microtiter plates coated with 5 $\mu\text{g ml}^{-1}$ of xanthorrhizol extract (168). No report of the effect of natural herbal compounds on *H. pylori* biofilm formation has been documented. In the other hand, most studies were concentrated on anti-*Helicobacter pylori* activity. Also, anti-adhesive property of some natural compounds against *H. pylori* has been investigated.

For example, the glycosylated compounds from okra (*Abelmoschus esculentus* Moench.) could prevent binding of *H. pylori* to human gastric mucosa (169). A high molecular weight polysaccharide component of black current seeds have also shown to inhibit adhesion to gastric epithelial cells (170). The polysaccharide extract-pretreated *H. pylori* had an impaired ability for the epithelial binding. The polymer identified as galactan has been considered to be responsible for this (170). One has demonstrated that acidic carbohydrate play important role in the anti-adhesion against *H. pylori* (171). Bacterial attachment to the human gastric adenocarcinoma epithelial cell was inhibited by *Panax ginseng* and *Artemisia capillaries* polysaccharide, which contained high amount of uronic acid (171). Some culinary plants, for example turmeric, borage, and parsley exhibited both bactericidal and anti-adhesive properties against *H. pylori* providing alternate therapy for *H. pylori* infection (172).

4. Potential Action of Herbal Medicines in Treatment of *H. pylori* Infection

In many countries, herbal medicines have been use for traditional treatment of many diseases for long centuries. The inhibitory action against *H. pylori* have been reviewed in various plant materials. For instance, about five and twenty-six of 50 Taiwanese folk medicinal plants have been demonstrated to possess higher and intermediate anti-*Helicobacter pylori* activities, respectively (173). While the Greek herbal medicine including *Anthemis melanolepis*, *Cerastium candididimum*, *Chamomilla recutita*, *Conyza albida*, *Dittrichia viscosa*, *Origano vulgare*, and *Stachys alopecuros* have been proved to be active against *H. pylori* with MICs ranging from 0.625 to 5 mg ml⁻¹ (174). In Thailand, six medicinal plants including *Myristica fragrans*, *Barringtonia acutangula*, *Kaempferia galanga*, *Cassia grandis*,

Cleome viscosa and *Syzygium aromaticum*, have exhibited active MICs range of 12.5-50 $\mu\text{g ml}^{-1}$ (175) against *H. pylori*. In Cameroon, ten-methanol plant extracts demonstrated antimicrobial activity against 15 *H. pylori* isolates, determined by disk diffusion method (176). Of those plants, *Ageratum conyzoides*, *Scleria striatinux* and *Lycopodium cernua* showed very potent anti-bacterial activity with the lowest MIC and minimum bactericidal concentration (MBC) of 0.032 mg mL^{-1} and 0.098 mg mL^{-1} , respectively (176). Additionally, *Alchornea triplinervia*, a medicinal plant commonly used for treatment of gastrointestinal ulcers in Brazil, has been observed for anti-*H. pylori* effect (177). The methanolic extracted of *A. triplinervia*, particularly the ethyl acetate fraction, has revealed anti-bacterial activity against *H. pylori* as well as anti-secretory and gastroprotective properties (177).

4.1 Pharmaceutical properties of curcumin

4.1.1 General aspects of curcumin

There are various Thai folk medicinal plants that have been used in traditional medicine for gastric ailment such as galangal (*K. galanga*) (178), common ginger (*Zingiber officinale*), sweet basil (*Ocimum basilicum*) (179). Turmeric is one of those well-known herbs. In India, current traditional medicine claims the use of turmeric powder against biliary disorders, anorexia, diabetic wound, hepatic disorder, rheumatism, and sinusitis (180). Turmeric (*Curcuma longa* Linn.) is naturally found in tropical and subtropical geographic countries, including Thailand. It belongs to *Zingiberaceae* family and is generally used in number of foods as an Asian condiment and also used as an essential ingredient in traditional medicine (181). Among various compound exhibited in turmeric, curcumin

(diferuloylmethane), the polyphenol yellow and non-toxic pigment, is considered as a predominant compound. The best characterized chemopreventive agent derived from the rhizomes. Curcumin has an extensive range of beneficial pharmacological effects, including anti-inflammatory, antioxidant, anti-viral, anti-bacterial, anti-angiogenic, anti-tumorigenic, and anti-ulcerogenic effects (182, 183). Curcumin melts at 176-177 °C and is soluble in ethanol, alkalis, ketone, acetic acid, and chloroform, but not in water (181). The chemical structure consists of unsaturated aliphatic with the aryl group that can be either substituted or not (Table 6) (184).

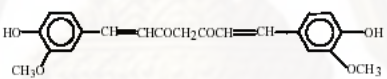
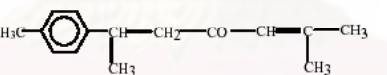

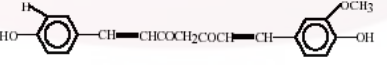


| Compounds | Chemical structure | Activity |
|-----------------------|--|--|
| Curcumin |  | anti-bacteria <i>Leishmania amazonensis</i> anti-HIV antioxidant anti-inflammatory anti-tumor |
| Ar-turmerone |  | snakebite |
| Methylcurcumin |  | <i>L. amazonensis</i> |
| Demethoxy curcumin |  | antioxidant |
| Bisdemethoxy curcumin |  | antioxidant |
| Sodium curcuminat |  | anti-inflammatory |

Table 6: Curcumin and other derivatives from *C. longa* L. (184).

For pharmacological purposes, seven to nine month-old turmeric rhizome is recommended for harvest and preparation (185). The amount of curcumin in turmeric extract should be at least 3 and 5% (w/w) as recommended by the WHO (186) and the Medicinal Plant Research Institute, Department of Medical Sciences, Ministry of Public Health, Thailand, respectively (185). There is data showing the administration of turmeric powder in patients with rheumatoid arthritis. A real improvement of disease was accomplished by treatment with 120 mg per day of turmeric orally (187). The WHO has recommended dose of turmeric powder for treatment of dyspeptic conditions in about 1.5-4 g per day orally (186).

The pharmacokinetic study of curcumin in rats demonstrated that this compound in dose of 1 to 5 g kg⁻¹ apparently did not cause any adverse effect. Curcumin was excreted mainly in the faeces (about 75%), the traces appeared in the urine. It seems that curcumin is rapidly metabolized in circulation (188). Metabolism of curcumin start from rapidly reduction into hexahydrocurcumin and then to hexahydrocurcuminol in human and rat livers (189). While the predominant metabolites of curcumin in rat plasma are curcumin glucuronide and curcumin sulfate. The hexahydrocurcumin and hexahydrocurcuminol occur in hepatocyte suspensions in only small amounts (189). However, little is known about the entire metabolic pathway of curcumin and its derivatives, and it is necessary to study more about it.

4.1.2 Chemotherapeutic effects of curcumin against *H. pylori*

Pharmaceutical benefit of curcumin against bacteria has been widely described (190). However, this relative property against *H. pylori* has been meagerly reported. O' Mahony *et al.* have shown that turmeric exhibited significant

bactericidal and anti-adhesive effects against *H. pylori* (172). Curcumin could inhibit the growth of 19 strains of *H. pylori in vivo* with MICs range of 6.25-50 $\mu\text{g ml}^{-1}$ (191). Consistently with a recent work of Han *et al.*, curcumin displayed moderate inhibitory activity against *H. pylori* with MIC value of 16 $\mu\text{g ml}^{-1}$ (192). Curcumin also had a combination effect with methanol extract of ginger root in inhibiting growth of *H. pylori*, with a ratio 1 to 1 (193). Curcumin could block the activation of NF- κ B which involving in some pro-inflammatory secretor such as cytokine IL-8 (194). Therefore, novel therapy of phytomedicine should be taken into account for inhibiting *H. pylori* colonization and adhesion. Moreover, its anti-biofilm formation is also interesting as a new strategy for *H. pylori* eradication.

4.2 Potential anti-biofilm property of curcumin

There are several reports prescribing inhibitory activity of medicinal plants against microbial biofilm. However, the anti-biofilm property of curcumin, in particular, has been slightly reported. Animal pathogenicity models, including *Arabidopsis thaliana* and *Caenorhabditis elegans*, were employed for a study of effect of curcumin on the virulence of *P. aeruginosa*. It has been demonstrated that curcumin inhibited *P. aeruginosa* virulence factors, including biofilm formation and acyl homoserine lactone production. In addition, a transcriptome analysis of curcumin-treated *P. aeruginosa* showed down-regulation of 31 quorum sensing genes (195). This data showed the involvement of curcumin in quorum sensing interruption in *P. aeruginosa* that reduces bacterial pathogenicity. Although, effects of curcumin against *H. pylori* have been reported previously, the effect against *H. pylori* biofilms has never been documented before.

5. Proteomics Study in *H. pylori*

5.1 Proteomics analysis: an alternative approach to study biofilms

Over 80% of human infections involve with biofilm, as claimed by the U.S. National Institutes of Health (196). It is now widely accepted that bacteria exist in two different modes of growth. The first being as single planktonic cells and the second as structured, multicellular communities know as bioiflm (196). *H. pylori* is one of those bacteria demonstrating biofilm mode of growth (116, 118, 119), which is thought to be important to facilitate bacteria to survive in the adverse conditions (110, 159). Nevertheless, the precise mechanism controlling *H. pylori* biofilm formation is still being unclear and a study of regulation in biofilm formation of this organism is limited. One strategy for improving these aspects is to analysis the whole related proteins. To date, a large-scale study of protein termed proteomic is considered as a tool for study of protein, particularly their structures and functions (197). Scientists are very interesting in proteomics because it gives a much better understanding of an organism than genomics (197). First, the level of transcription of a gene gives only a rough estimate of its level of expression into a protein. An mRNA produced in abundance may be degraded rapidly or translated inefficiently, resulting in a small amount of protein. Second, many proteins experience post-translational modifications that affect their activities; for example some proteins are not active until they become phosphorylated. Thus, methods such phosphoproteomics and glycoproteomics are used to study post-translational modifications. Third, many transcripts may give more than one protein through alternative splicing or post-translational modifications. Finally, many proteins form complexes with other

proteins or RNA molecules, and may only function in the presence of these other molecules (197).

5.1.1 Proteomics overview

The term “proteomics” was gained to make an analogy with genomics, the study of genes. Goal of proteomics is to quantify and identify proteins, which often give important clues about the differences in expression of discovered proteins resulted in a particular phenotype (197). Additionally, proteomics study is able to retrieve to the corresponding genes (197). Several tools are available for proteomics analysis including 2-dimensional (2-D) gel electrophoresis, which is able to analyze mixtures of proteins for over 1,800 types in one performance (198). The 2-D gel electrophoresis comprises isoelectric focusing in the 1st dimension, where proteins are separated based on isoelectric point, and polyacrylamide gel electrophoresis in the 2nd dimension, where proteins are separated based on size/mass (199). It is unlikely that two molecules will be similar in two distinct properties, so proteins are well separated by this principle. Proteins are resolved on a gel as spots after staining with silver, fluorescent dyes or Coomassie blue (200). The complete separated proteins could be then applied to mass spectrometry for identification by comparing with the database (199).

5.1.2 Two-dimensional gel electrophoresis

The 2-D gel electrophoresis begins with 1-D electrophoresis followed by a second dimension in a direction 90 degrees from the first run (199). For the 1st dimension, proteins were separated by isoelectric point called isoelectric

focusing (IEF). The proteins will move along a pH gradient gel, where an electric potential is applied across the gel, making one end more positive than the other. At all pH other than their isoelectric point, proteins will be charged. If they are positively charged, they will be pulled towards the negative end, or *vice versa*. The protein will accumulate at their isoelectric point, the point that the overall charge on the protein is zero (a neutral charge) (199).

In the second dimension, the protein complexes are denatured and separated by sodium dodecyl sulphate-polyacrylamide gel electrophoresis (SDS-PAGE) (199). SDS is an anionic detergent that denatures proteins by wrapping around the polypeptide backbone, and SDS binds to proteins fairly specifically in mass ratio of 1.4:1. The denatured polypeptides become negative charge of straight molecules in proportion to its length (charge densities per unit length). It is also necessary to reduce disulphide bridges, with 2-mercaptoethanol or dithiothreitol. Therefore, SDS-PAGE, protein migration is determined by the molecular weight (199).

The separated spots identified on a 2D-gel electrophoresis are usually attributable to one protein (199). The protein spots are enzymatically digested into smaller peptides using proteases such as trypsin or pepsin after electrophoretic separation. The collections of peptide products are then introduced to the mass analyzer.

5.1.3 Mass spectrometry

Mass spectrometry is an analytical technique that identifies the chemical composition of a compound or sample based on the mass-to-charge ratio of

charged particles (200). A sample undergoes chemical fragmentation, thereby forming charged particles (ions). The ratio of charge to mass of the particles is calculated by passing them through electric and magnetic fields in a mass spectrometer. The design of a mass spectrometer has three essential modules: an ion source, which transforms the molecules in a sample into ionized fragments; a mass analyzer, which sorts the ions by their masses by applying electric and magnetic fields; and a detector, which measures the value of some indicator quantity and thus provides data for calculating the abundances of each ion fragment present (200).

Mass spectrometry is an important emerging method for protein characterization. The two primary methods for ionization of whole proteins are electrospray ionization (ESI) and matrix-assisted laser desorption/ionization (MALDI) (201). Two approaches are used for characterizing proteins. First, intact proteins are ionized by either of the two techniques described above, and then introduced to a mass analyzer. Second, proteins are enzymatically digested into smaller peptides using a protease such as trypsin. Subsequently these peptides are introduced into the mass spectrometer and identified by peptide mass fingerprinting or tandem mass spectrometry (202). Whole protein mass analysis is primarily conducted using either time-of-flight (TOF) MS, or Fourier transform ion cyclotron resonance (FT-ICR). However, the most widely used instrument for peptide mass analysis is the MALDI time-of-flight (MALDI-TOF) because it allows a high sample throughput which several proteins can be analyzed in a single experiment (201).

Two mass spectrometry methods are used to identify proteins. Peptide mass fingerprinting is an analytical technique for protein identification that was developed in 1993. The unknown protein of interest is first cleaved into smaller

peptides. The absolute masses can be measured with a mass spectrometer such as MALDI-TOF or ESI-TOF. The mass spectrometrical analysis produces a list of molecular weights, which is called peak list. And these masses are then *in silico* compared to a huge database of predicted masses, such as Genbank containing known protein sequences information (203). The results are statistically analyzed to find the best match (204). If a protein sequence in the reference list gives rise to a significant number of predicted masses that match the experimental values, this protein was possibly present in the original sample. Tandem mass spectrometry, or also known as MS/MS, is becoming popular experimental method for identifying proteins. It involves multiple stages of mass analysis separation. A tandem mass spectrometer can be thought as two mass spectrometers in series connected by a collision cell that can break a molecule into pieces. A sample is sorted and weighed in the first mass spectrometer, then broken into pieces in the collision cell. A piece or pieces sorted and weighed in the second mass spectrometer subsequently. The advantages of peptide mass fingerprinting are that it is not time consuming, and it provides efficient data of mass of the peptides. A disadvantage is the protein sequence has to be present in the database of interest. Additionally most peptide mass fingerprinting algorithms consider that the peptides come from a single protein. An isolated protein is required for the identification based on peptide mass finger printing. The presence of a mixture can significantly complicate the analysis and compromise the results. Mixtures containing a number of 2-3 proteins typically require the additional use of MS/MS based protein identification to achieve sufficient specificity of identification.

5.2 Proteomic analysis of bacterial biofilm

Proteomic comparisons of biofilm-grown and planktonic cells of bacteria have been demonstrated in order to identify different protein expression between the two stages of growth. These provide source of data and help scientists to gain more knowledge about mechanism mediating bacterial biofilm formation. Some proteomics analyzes of bacterial biofilm are reviewed. Comparison of the two-dimensional proteome maps from *C. jejuni* planktonic and biofilm-grown cells demonstrated differences in protein expression level. The total of 30 proteins with 2-fold or more increased in biofilm-grown cells have been identified by nano-liquid chromatography-tandem mass spectrometry. The findings revealed that the largest group of proteins enhanced expression in biofilms. Most were related to the motility complex including the flagellin structural proteins, hook and basal body proteins, filament cap protein, and chemotaxis protein. Other groups of enhanced proteins involved in the oxidative and stress responses (205).

Soni *et al.* have examined the level of protein expression in *E. coli* O157:H7, between wild type and isogenic *luxS* mutant, and between wild type and *luxS* mutant supplemented with AI-2 molecule, using proteomic approach (206). In this study, 11 proteins were differently expressed between wild type and isogenic *luxS* mutant, whereas 18 proteins were differently expressed between wild type and *luxS* mutant supplemented with AI-2 molecule. Among those proteins, the FliC protein involving in flagellar synthesis and motility was up-regulated in the wild type but was not in the *luxS* mutant supplemented with AI-2 molecule. Thus, other signaling molecule rather than AI-2 may be responsible on flagellar synthesis in this organism (206).

With a virtue of proteomics analysis, particularly 2-D gel electrophoresis analysis, a panel of interested proteins can be analyzed and identified efficiently. From the above studies demonstrate the potential of proteomics technology, which can be employed for studying the underlying mechanism responsible for biofilm formation in many other organisms.

5.3 A proteomic analysis of protein expression in *H. pylori*

Recently, some reports have described a study of proteins in *H. pylori* in several objectives using proteomic. Proteome components of 71 clinical isolates of *H. pylori* have been analyzed quantitatively to determine protein expression associated with gastric diseases. The expression levels of CagA, UreB, GroEL, EF-Tu, TagD, and FldA showed significant differences among the gastric disease patterns (207). This provides data for disease-associated proteins and clustering clinical strains of *H. pylori* based on the expressed pathogenic proteins. A proteomics analysis demonstrated the distinct patterns of protein expression between chronic gastritis and duodenal ulcers. , It was suggested that *H. pylori* was able to express proteins differently while colonizing in different parts of human body (208). This leads to a better understanding of pathogenic mechanism of this organism, *in vivo*, Even though bismuth-based therapy is commonly recommended for eradicating *H. pylori*, the precise molecular mechanisms underlying bismuth against *H. pylori* still need to be clarified. Ge *et al.* have identified bismuth-binding protein in *H. pylori*, before and after treatment with bismuth citrate, using 2-D gel electrophoresis followed by peptide mass fingerprinting. From their studies, four proteins, including HspA, HspB, TsaA, and NapA, and bismuth-induced oxidative stress proteins were

found to be significantly up-regulated. The presence of bismuth also down-regulated the cellular protease activities (209). This data suggested that the activation of oxidative stress and homeostasis proteins, with inhibition of proteases might be the important factors underlying the molecular mechanism of bismuth's actions against *H. pylori* (209). Govorun *et al.* have found that four *H. pylori* isolates collected from two different regions in Russia demonstrated different proteome map. Some proteins varied in expression level among strains. For instance, the *cag26* pathogenicity factor was absent in two strains. In contrast, one of *H. pylori* strains lacked of hypothetical protein but it has *frxA* reductase. In this study, those four isolates could subdivided into two groups depending on the lack of *cag26* pathogenicity factor and the different expression level of transcription regulator (210). Even though subdivision of the four isolates into two groups does not correspond to their geographic distribution, the potential of proteome technology should be useful for clarifying the role of different proteins related to bacterial pathogenesis.

CHAPTER III

RESEARCH QUESTIONS AND OBJECTIVES

1. Research Questions

Infection of *H. pylori* occurs worldwide with approximately 50% of world's population. Carriage of *H. pylori* in the human stomach is associated with increased risk for gastroduodenal diseases, including gastric cancer. *H. pylori* is able to form biofilms both in environmental conditions and in human resulting in a persistent survival of bacteria. Many have hypothesized that *H. pylori* infections resulting in chronic gastric ulcers may be a manifestation of biofilms. However, to date data describing a prevalence of biofilm formation of *H. pylori* is still limited. Moreover, factors involving the mechanism of biofilm formation of *H. pylori* are not fully elucidated. Some adhesins including flegalla have been thought to mediate bacterial adhesion, colonization, and biofilm formation. However, more work is still required for understanding the process and regulation of *H. pylori* biofilms. Additionally, bacteria in biofilm state seemed to be less susceptible to antibiotic compared with those in planktonic state. These lead to a growing problem of antibiotic resistance in *H. pylori*.

Several considerable interests have focused on alternative medicines such as biologically active compounds. The pharmaceutical activity of curcumin, an active compound predominantly found in turmeric, against *H. pylori* has been previously documented. Although curcumin exhibited antimicrobial and anti-adhesive activity against *H. pylori*, the effect of curcumin on *H. pylori* biofilms remains unknown. In this study, flagellar mutant strains of *H. pylori* were constructed and investigated for

the effect against biofilm formation. The amount of biofilm production between *H. pylori* wild types and flagellar mutants were compared qualitatively by pellicle assays, and quantitatively by crystal violet staining. The ability of *H. pylori* to adhere to the HEP-2 cells was also studied. In addition, anti-biofilm and anti-adhesive activities of curcumin against *H. pylori* biofilm and adherence were investigated. Scanning electron microscopic examination was performed in order to study a 3-dimensional structure of *H. pylori* biofilm. Furthermore, protein profile expressions of *H. pylori* biofilm with a presence and absence of curcumin were analyzed in order to elucidate all biofilm related proteins of *H. pylori*. The protein data was thought to be useful for understanding the precise mechanism of biofilms and the effect of curcumin against biofilms.

The following questions were answered;

1. Did flagella possess a role in regulation of biofilm formation of *H. pylori*?
2. Did curcumin possess inhibitory effect against *H. pylori* biofilm formation?
3. Did curcumin possess inhibitory effect against *H. pylori* adherence to the epithelial cells?
4. What were mechanisms regulating biofilm formation of *H. pylori*?
5. What were mechanisms of curcumin in inhibiting *H. pylori* biofilm formation?

2. Objectives

1. To determine a role of *H. pylori* flagella in regulation of biofilm formation *in vitro*.
2. To determine inhibitory effect of curcumin against *H. pylori* biofilm formation *in vitro*.
3. To determine inhibitory effect of curcumin against *H. pylori* adherence *in vitro*.
4. To determine protein profile expression between biofilm and planktonic state of *H. pylori in vitro* in a presence and absence of curcumin.

3. Hypotheses

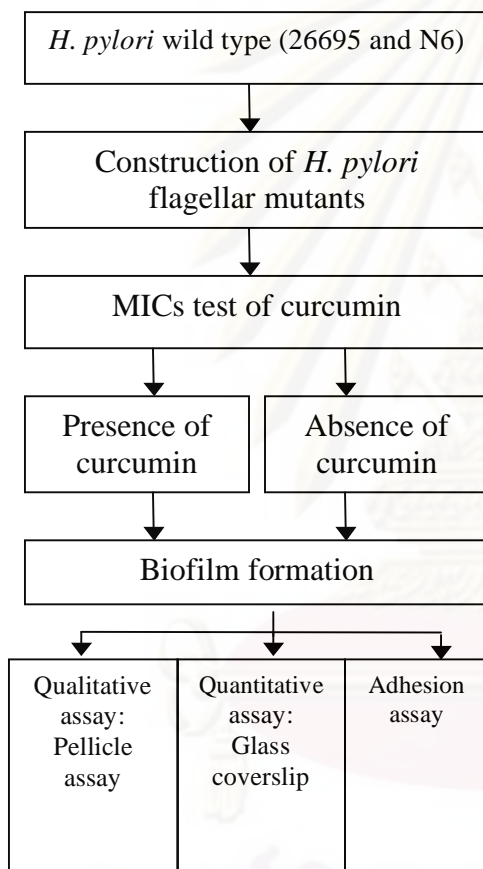
1. *H. pylori* flagella had an important role in regulation of biofilm formation.
2. Curcumin could be able to inhibit *H. pylori* biofilm formation.
3. Curcumin could be able to inhibit *H. pylori* adherence to the epithelial cells.
4. Protein profiles might express differently between curcumin-treated and – untreated *H. pylori* biofilm and planktonic state.

ศูนย์วิทยทรัพยากร
จุฬาลงกรณ์มหาวิทยาลัย

4. Conceptual Framework

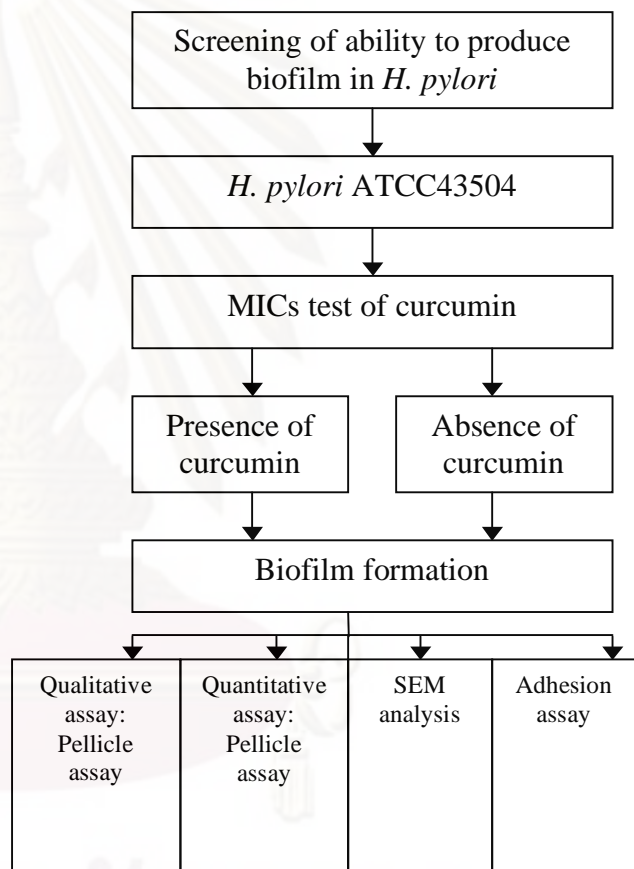
Phase I:

Roles of flagella in biofilm formation of *H. pylori*



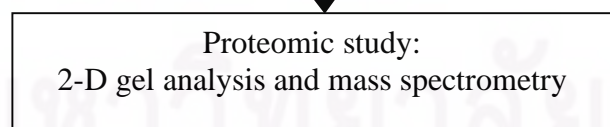
Phase II:

Effect of curcumin against *H. pylori* Biofilm formation and adhesion of *H. pylori* against HEp-2 cells



Phase III:

Proteomic analysis of *H. pylori* biofilm formation



CHAPTER IV

MATERIALS AND METHODS

Phase I: Roles of Flagella in Biofilm Formation of *H. pylori*

Flagella have been considered to have a possible role during initial step of biofilm formation (134). Thus, this study aimed to investigate their roles in the production of biofilm and adherence function against HEp-2 cells in *H. pylori*. Three putative flagellar genes of *H. pylori* were investigated. Those genes included *flaA* with likely a main flagellar composition, *flgR* with likely a regulatory gene and *fliQ* with likely an exported apparatus. Isogenic mutants of these genes was constructed and examined for their abilities to form biofilm and adhere to HEp-2 cells. Additionally, effect of curcumin against flagellar-mutant *H. pylori* biofilm formation and adherence to HEp-2 cells were also investigated. This phase of work was established at London School of Hygiene and Tropical Medicine, UK.

Phase II: Effect of Curcumin Against *H. pylori* Biofilm Formation and Adhesion of *H. pylori* Against HEp-2 Cells

A persistent infection and resistance to antimicrobial agents by bacteria living as biofilms are well documented (152). Stopping bacterial biofilm formation may be one of a key in resolving the infection and leads to a successful therapy. Several of *H. pylori* strains were screened to compare for the ability to form biofilm. The inhibitory effect of curcumin against *H. pylori* biofilm formation was investigated extensively with the chosen strain. Due to biofilm formation depends on the ability of bacterial adherence (95), so the effect of curcumin against bacterial adhesion was also

determined. A 3-dimensional cytoarchitecture of biofilm for curcumin-treated and -untreated *H. pylori* was observed by scanning electron microscope.

Phase III: Proteomics Analysis of *H. pylori* Biofilm Formation

As a precise mechanism regulating biofilm formation of *H. pylori* is still required for more elucidation. Moreover, the mechanism of curcumin, which affects *H. pylori* biofilm formation, is still not known. Thus an expression of protein profile of *H. pylori* biofilm in a presence and absence of curcumin was performed by 2-D gel electrophoresis analysis in order to achieve information about these. The proteins were subsequently sequenced by mass spectrometry to identify species.

1. Chemicals, reagents, scientific instruments and bacterial strains

All of chemicals and reagents used in this study were analytical grade or the pure grade available. Chemicals and reagents including curcumin, DMSO, β -cyclodextrin, isopropyl-beta-D-thiogalactopyranoside, (IPTG), 5-bromo-4-chloro-3-indolyl-beta-D-galacto-pyranoside (X-Gal) were purchased from Sigma. Agarose was purchased from Gibco.

Bacterial culture media including Blood agar base no. 2, Bacto agar, Brain heart infusion broth, Mueller-Hinton broth and agar were purchased from Oxoid. Supplemental media including lysed horse blood, and Dent's selective supplement were purchased from Oxoid. Sheep blood was purchased from Faculty of Veterinary Medicine, Chulalongkorn University, Thailand. Antibiotics including ampicillin, kanamycin, were purchased from Sigma.

Taq DNA polymerase was purchased from BioLabs. AccuPrime™ *Taq* DNA Polymerase High Fidelity was purchased from Invitrogen. pGEM® T-Easy vector was purchased from Promega. Loading dye was purchased from New England Biolabs. 10K-bp DNA molecular ladder was purchased from Fermentas Life Sciences. Restriction enzymes including *Bgl* II, *Not* I, *Eco*R I, and *Dpn* I were purchased from Promega. Commercial kit including QIAquick PCR Purification Kit, QIAprep Spin Miniprep Kit were purchased from QIAGEN. PUREGENE™ DNA Purification Kit was purchased from Gentra System. PRISM™ sequencing kit was purchased from Applied Biosystems.

Reagents used in cell culture experiments including Dulbecco's phosphate buffer saline, Dulbecco's modified Eagle's medium, and trypan blue were purchased from Gibco. Fetal bovine serum and Antibiotic-Antimycotic were purchased from PAA Laboratories.

T75 tissue culture flask, 6- and 12-well polystyrene plates were purchased from Corning. Electroporation cuvette was purchased from Bio-Rad. Glass bead was purchased from Jencons PLS. Glass coverslip was purchased from VWR International. Anaero Pack-MicroAero purchased from Mitsubishi Gas Chemical. Anaerobic jar was purchased from Oxoid. Membrane filter 0.22 and 0.45 µm was purchased from Millipore.

Bio-Rad Protein Assay, ammonium persulfate, TEMED were purchased from Bio-Rad. Immobiline™ DryStrip, IPG buffer, Immobiline™ Drystrip Cover Fluid, urea, CHAPS, dithiothreitol, iodoacetamide were purchased from Amersham Biosciences.

H. pylori standard strains including ATCC43504, ATCC43526, ATCC51932 were purchased from the American Type Culture and Collection, Rockville, MD, USA. *H. pylori* strain DMST20165 and DMST20885 were purchase from the Department of Medical Sciences, Thailand. XL2-blue MRF' *Escherichia coli* ultra-competent cells was purchased from Stratagene.

2. Preparation of Bacterial Strains and Curcumin Stock Solution

2.1 Preparation of bacterial strains

H. pylori strains used in the **phase I** included ATCC26695 and N6 strains (available in the Pathogen Molecular Biology Unit, London School of Hygiene and Tropical Medicine, the UK). Bacteria were grown on *Helicobacter* selective agar consisting of blood agar base number 2 supplemented with 7% (v/v) lysed horse blood and Dent's selective supplement. Bacterial plates were incubated at 37 °C in variable atmosphere incubator (Don Whitley Scientific) under microaerobic condition (N₂, 85%; O₂, 5%; CO₂, 10%). In the **phase II** and **III**, *H. pylori* ATCC43504 was used and grown on brain heart infusion (BHI) agar supplemented with 7% (v/v) sheep blood. Bacterial plates were incubated at 37 °C under microaerobic condition (O₂, 6-12%; CO₂, 5-8%) using Anaero Pack-MicroAero in anaerobic jar. Bacteria were routinely subcultured every three days. However, for minimum inhibitory concentration (MIC) test, additional 11 strains of *H. pylori* were also incorporated. These included *H. pylori* ATCC43526, ATCC51932, DMST20165 and DMST20885, and clinical strains C7, C42, 742, 749, 849, 867, and 928. These clinical strains were isolated from specimens with endoscopic diagnosis as following; gastritis (strains C42, 742, 749, and 867), peptic ulcer (strains C7 and 849), and duodenitis (strain

928). For a screening of ability of *H. pylori* to form biofilm in pellicle assay, 14 strains of *H. pylori* were tested. These included *H. pylori* ATCC43526, ATCC51932, and DMST20165 and DMST20885, and clinical strains 1203, 1260, 1261, 1264, 1265, 1268, 1275, LP25 and UT142. These clinical strains were isolated from specimens with endoscopic diagnosis as following; gastritis (strains 1260, 1261, 1268, LP25, and UT142), peptic ulcer (strains 1203 and 1275), and duodenitis (strains 1264 and 1265). All the clinical strains used in this project were kindly provided by Associate Professor Dr. Ratha-korn Vilaichone, Faculty of Medicine, Thammasat University, Thailand.

As for *H. pylori* mutant construction processes, XL2-blue MRF' *Escherichia coli* was used as competent cells. Bacteria were grown on Luria-Bertani (LB) agar at 37 °C. The antibiotic used for mutant selection purposes were ampicillin (100 µg ml⁻¹) and kanamycin (50 µg ml⁻¹ for *E coli* and 20 µg ml⁻¹ for *H. pylori*), whereas medium plate for routine subculture of *H. pylori* isogenic mutants is Dent's plate supplemented with 20 µg ml⁻¹ kanamycin.

2.2 Preparation of curcumin suspension

Curcumin was prepared as a stock solution by dissolving in DMSO and the final concentration was set as 50 mg ml⁻¹. The stock solution was sterilized through a 0.22 µm filter and transferred into aliquot tubes. The stock solution was stored at -20 °C until used.

3. Construction of *H. pylori* *flaA*, *flgR*, and *fliQ* Mutants

3.1 Chromosomal DNA extraction

One plateful of 3-d *H. pylori* ATCC26695 colony was harvested and suspended in 5 ml of Dulbecco's phosphate buffer saline (DPBS). Bacterial suspension was centrifuged at 1,000 rpm for 3 min, and bacterial pellet was collected. *H. pylori* chromosomal DNA was extracted from the pellet by PUREGENE™ DNA Purification Kit, following a manufacturer's instruction. Briefly, 3 ml of cell lysis solution was added into the pellet and incubated at 80 °C for 5 min to lyse cells. Fifteen µl of Rnase A solution was added into the cell lysate and mixed by inverting. Sample was incubated at 37 °C for 60 min. Then 1 ml of protein precipitation solution was added to the cell lysate and mix vigorously. The sample was incubated on ice for 5 min and then centrifuged at 2,000 rpm for 10 min in order to precipitate protein. Supernatant containing DNA was transferred into a clean centrifuge tube containing 3 ml of 100% isopropanol. The sample was mixed and centrifuged at 2,000 rpm for 3 min. The supernatant was then poured off and a visible DNA pellet was left in the tube. The sample was added with 70% ethanol and centrifuged at 2,000 rpm for 1 min to wash the DNA. After the ethanol was removed, 500 µl of DNA hydration solution was added into the sample and incubated 65 °C for 60 min. Tube was gently tapped to disperse the DNA. The DNA concentration and purity were measured by Nanodrop™ 1000 spectrophotometer (Thermo Scientific). The *H. pylori* ATCC26695 chromosomal DNA was stored at -20 °C until used.

3.2 Primer designation for PCR and inverse PCR amplification

Gene specific primers were designed from published sequences of *flaA*, *flgR*, and *fliQ* genes (Figure: 6, 7, and 8, respectively) by the Primer3 program (<http://fokker.wi.mit.edu/primer3/input-030.htm>). The details of each primers were summarized in Table 7 (in the Chapter IV). In this meanwhile, primers for inverse PCR mutagenesis (IPCRM) were manually generated by consideration of the published sequences of individual gene. The IPCRM primers were considerate from gene sequence locating around the middle of fragment. Both forward and reverse primers of each gene were designated to orient in the reverse direction of the usual direction and to start away from each other as following; 24 bp for *flaA*, 15 bp for *flgR*, and 4 bp for *fliQ*. A *Bgl* II restriction sequence (AGATCT) and two additional guanine (G) bases were added at the 5' end of each IPCRM primer. All of the oligonucleotide primers were synthesized by Sigma, UK.

DEFINITION *Helicobacter pylori* flaA gene
 ACCESSION HP0601 REGION: 637282..638814
 VERSION HP0601.1 GI:15644634
 SOURCE *Helicobacter pylori* 26695
 ORGANISM *Helicobacter pylori* 26695
 Bacteria; *Proteobacteria*; *Epsilonproteobacteria*; *Campylobacteriales*;
Helicobacteraceae; *Helicobacter*.

REFERENCE 1 (bases 1 to 1533)
 AUTHORS Tomb,J.-F., White,O., Kerlavage,A.R., Clayton,R.A., Sutton,G.G.
 Fleischmann,R.D., Ketchum,K.A., Klenk,H.P., Gill,S., Dougherty,B.A., Nelson,K., Quackenbush,J.,
 Zhou,L., Kirkness,E.F., Peterson,S., Loftus,B., Richardson,D., Dodson,R.,
 Khalak,H.G., Glodek,A., McKenney,K., Fitzgerald,L.M., Lee,N., Adams,M.D.,
 Hickey,E.K., Berg,D.E., Gocayne,J.D., Utterback,T.R., Peterson,J.D.,
 Kelley,J.M., Karp,P.D., Smith,H.O., Fraser,C.M. and Venter,J.C.

TITLE The complete genome sequence of the gastric pathogen *Helicobacter pylori*
 JOURNAL Nature 388 (6642), 539-547 (1997)
 PUBMED 9252185

CDS 1..1533
 /locus_tag="HP0601"
 /note="FlaA; structural flagella protein; in *Helicobacter* flagella are composed of
 flagellin A and flagellin B; the amounts of each seem to be controlled by
 environmental conditions"

 /translation="MAFQVNTNINAMNAHVQSALTQNALKTSLERLSSGLRINKA
 ADDASGMTVADSLRSQASSLGQAIANTNDGMGIIQVADKAMDEQLKILD
 TVKVKATQAAQDGQTTERKAIQSDIVRLIQGLDNIGNTTTTYNGQALLSG
 QFTNKEFQVGAYSNQSIKASIGSTTSKIGQVRIATGALITASGDISLTFKQ
 VDGVNDVTLESVKVSSSAGTGIGVLAEVINKNSNRRTGVKAYASVIT TSDV
 AVQSGSLSNLTNLNGIHLGNIADIKKNSDGRLLVAAINAVTSETGVEAYTD
 QKGRLLNLRSIDGRGIEIKTDSVSNGPSALTMVNGGQDLTKGSTNYGRSL
 TRLDKXSINVVSASDSQHLGFTAIGFGESQVAETTVNLRDVTGNFNANVK
 SASGANYNVAVIASGNQSLGSGVTTLRGAMVVIDIAESAMKMLDKVRSDL
 GSVQNQMISTVNNISITQVNVKAAESQIRDVDFAEESANFNKNNILAQSGS
 YAMSQANTVQQNILRLLT"

ORIGIN
 1 atggcttttc aggtcaatac aaatatcaat gcgatgaatg cgcgatgtgca atccgcactc
 61 actcaaaacg cgcttaaaac ttcattggag cgattgagtt caggtttaag gattaataaa
 121 gcggtgatg acgcatcagg catgacgggtg gcggtattctt tgcgttcaca agcgagcagt
 181 ttgggtcaag cgattgccaac cacgaatgac ggcattgggga ttatccaggt tgccgataag
 241 ^{flaAF} → gctatggatg agcagttaaa aatcttagac accgtaagg ttaaagcgac tcaagcggt
 301 caagatgggc aaactacaga atctcgtaaa gcgattcaat ctgacatcgt tcgtttgatt
 361 caaggttag acaatatcgg taatacgact acttataacg ggcaagcgtt attgtctggt
 421 caattacca acaaagaatt ccaagtaggg gcttattcta accaaagcat taaagcttct

LOCUS AE000511 1146 bp DNA linear BCT 22-SEP-2008
 DEFINITION *Helicobacter pylori* 26695, complete genome.
 ACCESSION HP0703 REGION: 755465..756610
 VERSION HP0703.1 GI:15644634
 SOURCE *Helicobacter pylori* 26695
 ORGANISM *Helicobacter pylori* 26695
 Bacteria; Proteobacteria; Epsilonproteobacteria; Campylobacterales;
 Helicobacteraceae; Helicobacter.

REFERENCE 1 (bases 1 to 1146)
 AUTHORS Tomb,J.-F., White,O., Kerlavage,A.R., Clayton,R.A., Sutton,G.G.,
 Fleischmann,R.D., Ketchum,K.A., Klenk,H.P., Gill,S.,
 Dougherty,B.A., Nelson,K., Quackenbush,J., Zhou,L., Kirkness,E.F.,
 Peterson,S., Loftus,B., Richardson,D., Dodson,R., Khalak,H.G.,
 Glodek,A., McKenney,K., Fitzgerald,L.M., Lee,N., Adams,M.D.,
 Hickey,E.K., Berg,D.E., Gocayne,J.D., Utterback,T.R.,
 Peterson,J.D., Kelley,J.M., Karp,P.D., Smith,H.O., Fraser,C.M. and
 Venter,J.C.

TITLE The complete genome sequence of the gastric pathogen *Helicobacter pylori*
 JOURNAL Nature 388 (6642), 539-547 (1997)
 PUBMED 9252185

CDS 1..1146
 /locus_tag="HP0703"
 /note="similar to PID:777754 percent identity: 44.20; identified by sequence
 similarity; putative"

 /translation="MKIAIVEDDINMRKSLELFFELQDDLEIVSFKNPKDALAKLDE
 SFDLVITDINMPHMDGLEFLRLLLEGKYESIVITGNATLNKAIDSIRLGVKDF
 FQ KPFKPELLLESYRTRKKVLEFQKKHPLEKPLKPKPKHSFLAASKALEES
 KRQALKVASTDANVMLLGESGVGKEVFAHFIHQHSQRSKHPFIANMSAI
 PEHLLESELFGYQKGAFTDATAKEITRLGDNKSVKIDVRFISATNANMKE
 KIAAKEFREDLFFRLQIVPITIAPLRERVEEILPIAEIKLKEVCDAYHLGPKSF
 SKNAAKCLLEYSWHGNVRELLGVVERAAILSEETIEQEKDLFLER"

ORIGIN
 1 atgaaaatcg ccattgtaga agatgatatt aacatgcgta aaagcctgga gcttttttt
flgRF →
 61 gagcttcaag acgatttaga gattgtgagt ttaaaaacc ctaaagacgc tttagcgaaa
 121 cttgatgaaa gctttgattt agtcatcagc gatattaaca tgcccatat ggacggcttg
 181 gaatttttac gccttttaga aggcaaatc gaatccattg tgattaccgg taatgcgacc
 241 ttgaataaag ccattgattc cattcgttta ggcgtgaaag acttttcca aaagccttt
 301 aaaccagaat tgcttttaga atccatctat cgcacaaaa aagttttaga attcaaaaa
 361 aaacacctt tagaaaaacc ttaaaaaaaa ccacacaaac acagctttt agccgcttca
 421 aaagcttag aagagagcaa acggcaggcc ttaaaagtgc caagcacgga cgctaatgct
 481 atgctattag gcgaaagcgg ggtgggtaag gaagttttg ctcatttcat ccaccagcat

LOCUS NC_000915 267 bp DNA linear BCT 22-SEP-2008
 DEFINITION *Helicobacter pylori* 26695, complete genome.
 ACCESSION HP1419 REGION: 1489408..1489674
 VERSION HP1419.1 GI:15644634
 SOURCE *Helicobacter pylori* 26695
 ORGANISM *Helicobacter pylori* 26695
 Bacteria; Proteobacteria; Epsilonproteobacteria; Campylobacteriales;
 Helicobacteraceae; Helicobacter.

REFERENCE 1 (bases 1 to 267)
 AUTHORS Tomb,J.-F., White,O., Kerlavage,A.R., Clayton,R.A., Sutton,G.G.,
 Fleischmann,R.D., Ketchum,K.A., Klenk,H.P., Gill,S.,
 Dougherty,B.A., Nelson,K., Quackenbush,J., Zhou,L., Kirkness,E.F.,
 Peterson,S., Loftus,B., Richardson,D., Dodson,R., Khalak,H.G.,
 Glodek,A., McKenney,K., Fitzgerald,L.M., Lee,N., Adams,M.D.,
 Hickey,E.K., Berg,D.E., Gocayne,J.D., Utterback,T.R.,
 Peterson,J.D., Kelley,J.M., Karp,P.D., Smith,H.O., Fraser,C.M. and
 Venter,J.C.

TITLE The complete genome sequence of the gastric pathogen *Helicobacter pylori*
 JOURNAL Nature 388 (6642), 539-547 (1997)
 PUBMED 9252185

CDS complement(1..267)
 /gene="fliQ"
 /locus_tag="HP1419"
 /note="with proteins FliP and FliR forms the core of the central channel in the
 flagella export apparatus"
 /translation="MESQLMKLAIETYKITLMISLPVLLAGLVVGLLVVSIFQATTQIN
 EMTLSFVVPKILAVIGVLILTMPWMTNMLLDYTKTLIKLIPKIIG"

ORIGIN
 1 atggaatcac aactcatgaa actcgccatt ^{fliQF} gagacttata aatcacttta gatgattct
 61 ttaccggtat tactagcggg attagtggtg gggctgtag tcagtatttt tcaagcgacc
 ← fliQR fliQIF →
 121 acccaaatca atgaaatgac ttgtctttt gtcgctaaga ttttagccgt gattgggggtg
 181 ctgattttaa ccatgccgtg gatgacgaac atgcttttag attacaccaa aaccttaatc
 ← fliQR
 241 aagctcattc ccaaaatcat cggctag

Figure 8: The sequence of *fliQ* gene from *H. pylori* ATCC26695 (from genbank accession number HP1419, <http://www.ncbi.nlm.nih.gov/entrez/>)

Forward primer (*fliQF*) = 5' TCATGAAACTCGCCATTGAG3'

Reverse primer (*fliQR*) = 5' CCGATGATTTTGGGAATGAG3'

Inverse PCR forward primer (*fliQIF*) = 5' GGAGATCTTTTGTCTTTTGTGCC3'

Inverse PCR forward primer (*fliQIF*) = 5' GGAGATCTTTTCATTGATTGGG3'

3.3 Flagellar gene PCR amplifications

In order to gain *H. pylori* flagellar mutant strains, three putative *H. pylori* flagellar genes were individually knocked out. These genes included *flaA*, *flgR*, and *fliQ* genes. *H. pylori* ATCC26695 chromosomal DNA was served as template for PCR amplification of individual gene. To amplify individual specific gene, 400 ng of the DNA template was subjected to PCR amplification in 100 μ l reaction mixtures containing 50 pmol of each gene specific primer (as described in Figure 6-8), 200 μ M of each deoxynucleotide triphosphate (dATP, dCTP, dGTP, and dTTP), 1x PCR buffer, 25 μ M MgCl₂ and 1 U of *Taq* DNA polymerase. DNA amplification was carried out with following conditions; 35 cycles of amplification (94 °C, 15 sec, 50 °C, 1 min, 72 °C, 1 min) and a final extension at 72 °C for 7 min. For negative control, sterile deionized distilled water (DDW) was used instead of DNA. Twenty μ l of PCR products was analyzed on 1.5% agarose gel. A 10K-bp DNA ladder was used as standard marker.

3.4 Agarose gel electrophoresis

Agarose gel electrophoresis was performed using a submerged horizontal electrophoresis apparatus (Wide Mini-Sub Cell GT Cell; Bio-Rad). Agarose gel concentrations ranged from 0.7-1.5%, were prepared and electrophorated in 1x TBE buffer (0.045M Tris-borate, 0.001 M EDTA). One μ g ml⁻¹ of ethidium bromide was added into agarose gel. To load the sample, 5 μ l of DNA was mixed with 1 μ l of 6x loading dye. The electrophoresis was performed at 120 volt for 40-50 min. The gel was visualized and photographed under UV light by gel documentation system

(Syngene). A 10K-bp DNA ladder was used as standard marker to estimate the molecular size of the DNA fragments.

3.5 PCR purification

The remaining 80 μ l of each PCR product was clean up by QIAquick PCR Purification Kit, following a manufacturer's instruction. Briefly, 400 μ l of buffer PBI was added into 80 μ l of PCR product. The mixture was transferred into the QIAquick column and centrifuged at 10,000 x g for 1 min. The flow-through was discarded. The 750 μ l of buffer PE was added into the QIAquick column and centrifuged at 10,000 x g for 1 min. The flow-through was discarded and the column was placed into a clean 1.5 ml microcentrifuge tube. To elute DNA, 50 μ l of buffer EB (10mM Tris-Cl, pH 8.5) was dispensed to the center of the QIAquick membrane and centrifuged at 10,000 x g for 1 min. The eluted DNA of PCR products were collected and rechecked on 1.5% agarose gel, with 10K-bp DNA ladder served as size marker. The PCR products concentration and purity were examined by Nanodrop™ 1000 spectrophotometer. The PCR products were stored at -20 °C until used.

3.6 Cloning of *flaA*, *flgR*, and *fliQ* genes into pGEM® T-Easy vector for *H. pylori* mutagenesis

Ten μ g of the individual amplified PCR product was separately inserted into pGEM® T-Easy vector with following ligation reaction; 50 ng of pGEM® T-Easy vector, 10X rapid ligation buffer, 3U of T4 DNA ligase, and DDW to final volume of 10 μ l. The ligation reactions were incubated overnight at 4 °C. Ligation

reaction of the inserted plasmid was introduced into XL2-blue MRF' *E. coli* ultra-competent cells by heat-shock transformation technique. Three μl of each ligation reaction was added into a sterile 1.5 ml microcentrifuge tube. The XL2-blue MRF' *E. coli* ultra-competent cells were removed from $-80\text{ }^{\circ}\text{C}$ and placed in an ice bath until just thawed. Thirty μl of *E. coli* ultra-competent cells was carefully transferred into tubes containing the ligation reaction. The tubes were gently mixed and placed on ice for 20 min. The cells were then incubated for 45-50 sec in a water bath at $42\text{ }^{\circ}\text{C}$, and then immediately placed on ice for 2 min. The cells were added with 950 μl of SOC broth (Sigma), and incubated at $37\text{ }^{\circ}\text{C}$ for 1.5 h with shaking (~ 150 rpm).

The transformants were selected on LB agar containing $100\text{ }\mu\text{g ml}^{-1}$ ampicillin, $32\text{ }\mu\text{g ml}^{-1}$ isopropyl-beta-D-thiogalactopyranoside (IPTG; Sigma), and $40\text{ }\mu\text{g ml}^{-1}$ 5-bromo-4-chloro-3-indolyl-beta-D-galacto-pyranoside (X-Gal; Sigma). These transformants were incubated at $37\text{ }^{\circ}\text{C}$ for 16 h. Positive colonies were distinguished by blue/white colony screening assay. The positive white colonies were picked up and restreaked onto fresh LB plate containing $100\text{ }\mu\text{g ml}^{-1}$ ampicillin and incubated overnight at $37\text{ }^{\circ}\text{C}$. The positive clones were confirmed by colony PCR amplification and restriction enzyme analysis.

3.7 Colony PCR

In order to check the inserted of positive clones, one loopful of bacteria was picked up and suspended in 100 μl of DDW. After vortex, samples were boiled in heat-block at $95\text{ }^{\circ}\text{C}$ for 10 min and centrifuged at 13,000 rpm for 5 min. Supernatants were collected as a boilate sample. The boilates were amplified with T7

and SP6 promoter primers in 25 µl reaction mixtures containing 1 µl of boilate, 50 pmol of each primer, 200 µM of each deoxynucleotide triphosphate, 1x PCR buffer, 25 µM MgCl₂ and 1 U of *Taq* DNA polymerase. Colony PCR amplification was carried out with following conditions; 35 cycles of amplification (94 °C, 15 sec, 50 °C, 1 min, 72 °C, 1 min) and a final extension at 72 °C for 7 min. Analysis of PCR products was performed on 0.7% agarose gel using 10K-bp DNA ladder as size marker. The expected sizes of colony PCR product for *flaA*, *flgR*, and *fliQ* clones were 983, 1197, and 391 bp, respectively.

3.8 Plasmid DNA isolation

Positive clones were grown overnight in 10 ml of LB broth containing ampicillin at 37 °C in shaking incubator at 200 rpm. The cultures were centrifuged at 4,000 rpm for 10 min and pellets were collected. The pellets were performed miniprep isolation for plasmid DNA using QIAprep Spin Miniprep Kit, following a manufacturer's instruction. Briefly, the pellets were resuspended in 250 µl of buffer P1 and transferred into microcentrifuge tubes. The samples were added with 250 µl of buffer P2, and subsequently with 350 µl of buffer N3 and immediately inverted 4-6 times. The samples were centrifuged at 13,000 rpm for 10 min and the supernatants were transferred into QIAprep spin columns by pipetting. The columns were centrifuged for further 1 min and the flow-through was discarded. The columns were then washed by adding 750 µl of buffer PE and centrifuged for 1 min. The flow-through was discarded and the columns were centrifuged for additional 1 min to remove residual wash buffer. The columns were placed in a clean 1.5 ml

microcentrifuge tube. To elute plasmid DNA, 50 µl of buffer EB (10mM Tris-Cl, pH 8.5) was dispensed to the center of the QIAprep spin column and centrifuged at 13,000 rpm for 1 min. The miniprep products concentration and purity were checked by Nanodrop™ 1000 spectrophotometer, and stored at -20 °C until used. The inserted fragment was further confirmed by restriction enzyme analysis and sequencing.

3.9 Restriction enzyme analysis

The correct inserted sizes were checked with restriction enzyme analysis using *Not* I for *flaA* and *flgR* and *EcoR* I for *fliQ*, genes. One µg of individual plasmids was incubated with each particular restriction enzyme and buffer at 37 °C in water bath for 1 h. The restricted digestion products were analyzed on 0.7% agarose gel using 10K-bp DNA ladder as size marker. The expected sizes of digested inserted fragment of *flaA*, *flgR*, and *fliQ* were 842, 1056, and 250 bp, respectively.

3.10 DNA sequencing

The positive clones were confirmed further by sequencing with a PRISM™ sequencing kit and T7 and SP6 primers. The plasmid of positive clones was subjected to sequence at the Pathogen Molecular Biology Unit, London School of Hygiene and Tropical Medicine, the UK. The sequences were then compared with nucleotide sequence databases on the TIGR website (<http://www.tigr.org>).

3.11 Inverse PCR mutagenesis (IPCRM)

The plasmids containing individual *flaA*, *flgR*, and *fliQ* genes were carried out for a mutagenesis. A linker fragment, defined deletion plus unique *Bgl*III restriction site, was introduced into the *flaA*, *flgR*, and *fliQ* clones by IPCRM using primers described in Figure 6-8. The IPCRM was carried out in 100 μ l reaction and prepared with following conditions; 1U of AccuPrime™ *Taq* DNA Polymerase High Fidelity, 10x AccuPrime™ PCR buffer I, 10 ng of plasmid DNA, 50 pmol of each gene specific inverse PCR primer. The amplification was carried out with following conditions; 94 °C for 15 sec and 30 cycles of amplification (94 °C, 15 sec, 52 °C, 15 sec, 68 °C, 5 min). Fifteen μ l of IPCRM products was analyzed on 0.7% agarose gel. A 10K-bp DNA ladder was used as size marker. The remaining 85 μ l of each IPCRM product was processed to clean by QIAquick PCR Purification Kit. The IPCRM products concentration and purity were examined by Nanodrop™ 1000 spectrophotometer.

The remaining IPCRM products were digested with 20U of both *Bgl* II and *Dpn* I in total volume of 100 μ l at 37 °C in water bath for 3 h. The restricted digestion products were analyzed on 0.7% agarose gel using 10K-bp DNA ladder as size marker. The digested products then purified using QIAquick PCR Purification Kit. The digested IPCRM products concentration and purity were rechecked by Nanodrop™ 1000 spectrophotometer. The digested IPCRM products were processed to self-ligation with following reactions; 80 ng of digested IPCRM product, 10X rapid ligation buffer, 9U of T4 DNA ligase, and DDW to final volume of 50 μ l. The ligation reactions were incubated overnight at 4 °C. The schematic picture

representing IPCRM is shown in Figure 9. After that, 3 μl of each ligation reaction was transformed into 30 μl of XL2-blue MRF' *E. coli* ultra-competent cells. The transformants were selected on LB agar containing IPTG, and X-Gal as described previously. The positive colonies were restreaked onto fresh LB plate containing 100 $\mu\text{g ml}^{-1}$ ampicillin and incubated overnight at 37 °C. The colony PCR was set up in a total volume of 50 μl using reactions as described previously for cloning verification. Then, 5 unit of *Bgl* II was added directly into 25 μl of PCR product and incubated at 37 °C for 60 min. The uncut PCR product and *Bgl* II digested product were analyzed on 0.7% agarose gel for *flaA* and *flgR* clones, and 1.5% agarose gel for *fliQ* clone using 10K-bp DNA ladder as size marker. Positive were identified by successful digestion of the colony PCR product by *Bgl* II. The expected sizes of digested positive clones for *flaA*, *flgR*, and *fliQ* were 480, 591, and 194 bp, respectively. Plasmid DNA was isolated from overnight LB broth culture of the positive colony PCR by QIAprep Spin Miniprep Kit and checked by restriction enzyme analysis as previously described for cloning verification.



Figure 9: Schematic representation of IPCRM. Solid boxes represent cloned DNA. U represents the *Bgl* II and *Dpn* I unique restriction site.

3.12 Kanamycin resistance cassette (kan^R) insertion into IPCRM products

Two µg of plasmid DNA containing cloned mutated individual gene was digested with 20U of *Bgl* II in a total volume of 100 µl at 37 °C for 3 h. The digested plasmid DNA was then purified using QIAquick PCR Purification Kit, and product concentration and purity were checked by Nanodrop™ 1000 spectrophotometer. The ligation reactions were set up as following; 80 ng of digested plasmid DNA/*Bgl* II, 1.44 kb of kan^R/*Bam*H I fragment (available in the Pathogen Molecular Biology Unit, London School of Hygiene and Tropical Medicine, the UK), 10X rapid ligation buffer, 9U of T4 DNA ligase. The ligation reactions were incubated overnight at 4 °C. After that, 3 µl of each ligation reaction was transformed into 30 µl of XL2-blue MRF' *E. coli* ultra-competent cells. The transformants were selected on LB agar containing IPTG, and X-Gal as described previously. The positive colonies were restreaked onto fresh LB plate containing 100 µg ml⁻¹ ampicillin and incubated for overnight at 37 °C and the boilates were prepared from the restreaks. Colony PCR was set up in a total volume of 25 µl using reactions as described previously for cloning verification. Plasmid DNA containing cloned mutated individual gene plus kan^R was isolated from overnight LB broth culture of the positive colony PCR using miniprep protocol and checked by restriction enzyme analysis as previously described for cloning verification.

3.13 Bacterial transformations

The constructed plasmid DNA of *flaA*, *fliQ*, and *flgR* genes was introduced into *H. pylori* 26695 and N6 wild-type strains by natural transformation and electroporation, respectively.

3.13.1 Natural transformation of *H. pylori*

For natural transformation, a heavy loop of 3-d *H. pylori* ATCC26695 cells ($\sim 10^8$ to 10^9 cells) was spread on 4 °C Dent's plates within diameter of 8 to 10 mm. Incubation was continued at 37 °C under microaerobic condition for 5 h. Two μg of constructed plasmid DNA was spotted directly onto the bacterial lawn. The bacteria were reincubated at 37 °C under microaerobic condition for further 24 h. The bacteria were then scraped and resuspended in 0.5 ml of BHI broth. One-hundred μl aliquot of bacterial suspension was spread onto Dent's plates supplemented with 20 $\mu\text{g ml}^{-1}$ kanamycin and incubated at 37 °C under microaerobic condition for 3 to 5 days. Kanamycin-resistant colony was restreaked to prepare bacterial stock.

3.13.2 Electroporation

For electroporation, a 3-d *H. pylori* N6 strain was collected from medium plate and resuspended in 10 ml of cold EBF buffer (15% (v/v) and 10% (w/v) sucrose) in centrifuge tube. Bacterial pellet was collected by centrifugation at 4,000 rpm for 10 min. The pellet was resuspended in 1 ml of cold EBF buffer and transferred to 1.5 ml tube. The pellet was washed twice by centrifugation at 13,000 rpm for 2 min and resuspended in 250 μl cold EBF. Five μl of ice-cold plasmid

containing 5 μg of constructed plasmid DNA was added to 50 μl of *H. pylori* host cells suspension. The suspension was mixed by pipetting and incubated on ice for 10 min. Electroporation mixture was transferred to a cold electroporation cuvette. The cuvette was placed in the safety chamber slide. Electroporation was performed at 25 μFD and 2500 V, and the pulse controller to 200 Ω by using Gene Pulser Xcell microbial system (Bio-Rad). The cuvette was then removed from the chamber immediately. One-hundred μl of room temperature SOC broth was added immediately to recover the cells. The cells were spotted onto Dent's plates supplemented with 20 $\mu\text{g ml}^{-1}$ kanamycin and incubated at 37 $^{\circ}\text{C}$ under microaerobic condition for 3 days. The bacterial cells were harvested and resuspended in 0.5 ml of BHI broth. One-hundred μl aliquot of bacterial suspension was spread onto Dent's plates supplemented with 20 $\mu\text{g ml}^{-1}$ kanamycin and incubated at 37 $^{\circ}\text{C}$ under microaerobic condition for 3 to 5 days. Kanamycin-resistant colony was restreaked to prepare bacterial stock.

The successful recombination between particular plasmid DNA and bacterial host DNA was confirmed by PCR using gene specific primers as described in Figure 6-8. The PCR amplifications were performed with the conditions as described previously.

4. Assessment for Minimum Inhibitory Concentration (MIC) of Curcumin against *H. pylori*

The MIC of curcumin was determined using agar dilution technique as described by the Clinical and Laboratory Standards Institute (CLSI). Curcumin stock

solution, prepared as described above, was diluted with Mueller-Hinton (MH) broth. In the **phase I**, final concentrations of curcumin were set up as 1.25 to 50 $\mu\text{g ml}^{-1}$. A 3-d bacterial colony, including ATCC26695, N6, and their *flaA*, *flgR*, and *fliQ* mutants, were harvested and resuspended in MH broth. The bacterial final concentrations were adjusted equivalently to 5×10^7 CFU ml^{-1} (OD_{600} of 0.1). Subsequently, the inoculum of 3 μl per spot was replicated onto MH agar containing curcumin, supplemented with 5% lysed horse blood, followed by incubating at 37 °C for 3 days, microaerophilically. The MIC was reported as the lowest concentration of compound that inhibited the complete growth of the bacterium tested. Curcumin-free plate and plates containing ampicillin ranged from 0.15 to 9.6 $\mu\text{g ml}^{-1}$ were co-assayed as a control. Experiments were performed in duplicate on three separated occasions.

In the **phase II**, final concentrations of curcumin were set up as 0.125 to 128 $\mu\text{g ml}^{-1}$. A 3-d bacterial colony of *H. pylori* strains, including ATCC43504, ATCC43526, ATCC51932, DMST20165, DMST20885, C7, C42, 742, 749, 849, 867, and 928 were harvested and resuspended in MH broth. The bacterial final concentrations were adjusted equivalently to 5×10^7 CFU ml^{-1} (OD_{600} of 0.1). The inoculum of 3 μl per spot was replicated onto curcumin-containing MH agar, supplemented with 5% sheep blood, followed by incubating at 37 °C for 3 days, microaerophilically. Curcumin-free plate, plates containing ampicillin ranged from 0.15 to 9.6 $\mu\text{g ml}^{-1}$, and plate containing 0.24% (v/v) DMSO were co-assayed as a control. Experiments were performed in duplicate on three separated occasions.

5. Investigation of Biofilm Formation by Pellicle Assay

Biofilm formation of *H. pylori* was investigated by pellicle assay. To establish this, 3-d *H. pylori* cells were suspended in 10 ml of brain heart infusion (BHI) broth supplemented with 2% (w/v) β -cyclodextrin (BCD) in sterile glass test tubes. A bacterial final concentration in broth was adjusted to an OD₆₀₀ of 0.2 ($\sim 10^8$ CFU ml⁻¹). The test tubes were left to stand in stationary phase at 37 °C for 7 days under microaerobic conditions in variable atmosphere incubator or anaerobic jar with Anaero Pack-MicroAero. Freely floating bacterial cells that formed at an air-liquid interface were determined as pellicle, whereas attached bacterial cells formed over interior surface of glass test tube at an air-liquid interface were determined as attached biofilm. These two characteristics were represented for biofilm formation in this study. A development of pellicle and/or attached biofilm was examined daily. The productions of biofilm were scored as (-, absent); not any form of biofilm seen, (+, just visible); thin pellicle film or a fine attached biofilm, (++, intermediate); accumulated pellicle covering just the center of liquid surface or a thin attached biofilm, (+++, extensive); a mature pellicle covering whole liquid surface or a dense attached biofilm.

Effect of curcumin against pellicle and attached biofilm formation was co-investigated. The culture broths of pellicle assay of individual strain were added with curcumin stock solution diluted in BHI broth, supplement with 2% (w/v) BCD. Curcumin final concentrations were adjusted equivalently to sub-MIC value of each *H. pylori* strain. A development of pellicle and/or attached biofilm in these curcumin-treated broths were examined daily along with those-untreated ones. All experiments were performed in duplicate on three separated occasions.

6. Optimization of Biofilm Formation in *H. pylori*

Prior to establish *H. pylori* biofilm contributing to subsequent proteomic analysis, curcumin concentration required in co-culture and precise time of incubation were optimized in the **phase II**. These optimizations were performed in order to evaluate the most suitable condition for being used in proteomic analysis, where the effect of curcumin against *H. pylori* biofilm formation was expected to be clearly observable. The optimum of curcumin concentration and time of incubation were investigated by biofilm qualification technique using pellicle assay.

6.1 Optimization of curcumin concentration against *H. pylori* biofilm

Pellicle assay was set in test tubes containing 10 ml of BHI supplemented with 2% BCD. Suspension of *H. pylori* cells in BHI broth was added and a bacterial final concentration was adjusted at an OD₆₀₀ of 0.2 (~10⁸ CFU ml⁻¹). The culture broths were co-cultivated with curcumin at different concentrations as following; 1/2, 1/4, 1/8, 1/16, and 1/32 MIC, and 0 µg ml⁻¹. The test tubes were left to stand in stationary phase at 37 °C for 7 days under microaerobic conditions in anaerobic jar with Anaero Pack-MicroAero. A development of pellicle and/or attached biofilm was examined daily through 7 days and scored as in the same manner as previous pellicle assay. Experiments were performed in duplicate on three separated occasions. The curcumin concentrations that presented inhibitory effect against *H. pylori* biofilm were then taken into account for further optimization process.

6.2 Optimization of incubation period against *H. pylori* biofilms in the presence and absence of curcumin

Pellicle assay was set with a presence of curcumin at concentrations displaying significant effect against *H. pylori* biofilm from the previous experiments. A development of pellicle and/or attached biofilm was examined daily through 21 days under microaerobic conditions in anaerobic jar with Anaero Pack-MicroAero and scored as previously. Experiments were performed in duplicate on three separated occasions.

7. Quantification of Biofilm Formation

7.1 Quantification of biofilm formation using glass coverslip

In the **phase I**, quantification of biofilm level produced by *H. pylori* ATCC26695, N6, and their *flaA*, *flgR*, and *fliQ* mutants was performed with a modified assay in polystyrene plate. The wells of 12-well polystyrene plates (Corning) were filled with 8 pieces of sterile glass bead (approximate 5-mm). Then, a sterile glass coverslip (approximate 13-mm diameter) was positioned on the top of glass beads in each well providing area for *H. pylori* to adhere at the air-liquid interface. The wells were seeded with *H. pylori* suspended in BHI broth supplemented with BCD to an OD₆₀₀ of 2 (10⁹ CFU ml⁻¹). However, the well supplemented with only 2% (w/v) BCD was served as blank control. In order to investigate effect of curcumin, the wells containing individual strain were added with curcumin stock solution diluted in BHI broth, supplemented with 2% (w/v) BCD. Curcumin final concentrations were adjusted equivalently to sub-MIC value of each *H. pylori* strain. The plates were incubated under microaerobic conditions at 37 °C

for 5 days under microaerobic condition in variable atmosphere incubator. Unseeded wells, either with a presence and absence of sub-MIC of curcumin, were set up as controls. Following incubation, medium was removed. The wells were washed twice with PBS and dried at 60 °C for 30 min. Two ml of 0.1% (w/v) crystal violet was added into each well and incubated for 5 min at room temperature. The unbound crystal violet was then discarded. The wells were dried again at 60 °C for 15 min and washed with 3 ml of PBS for further three times. The coverslips deposited in each well were transferred to new plates. The bound crystal violet was destained with 3 ml of ethanol/acetone (80:20, v/v) for 1 min. The solution was then transferred to disposable cuvette and absorbance at 570 nm was measured using spectrophotometer (WPA) to determine level of biofilm formation. Experiments were performed in duplicate on three separated occasions. Biofilm level was expressed by mean of tested OD subtracted with mean of blank OD.

7.2 Quantification of biofilm formation using pellicle assay

In the **phase II**, quantification of biofilm level produced by *H. pylori* ATCC43504 was performed with a modified assay in glass test tube. The glass test tubes were established as pellicle assay with a presence of curcumin at varied concentrations as following; 1/2, 1/4, 1/8, 1/16, and 1/32 MIC, and 0 µg ml⁻¹. However, BHI broths supplemented with 2% (w/v) BCD and 0.016% (v/v) DMSO were incorporated as controls. The unseeded culture conditions with a presence of varied sub-MICs of curcumin and absence of curcumin were served as blank controls. The 3-d *H. pylori* cells were suspended in BHI broth and added into individual test tubes. A bacterial final concentration in broth was adjusted to an OD₆₀₀ of 0.2 (~10⁸

CFU ml⁻¹). The test tubes were left to stand in stationary phase at 37 °C for 7 days under microaerobic conditions in anaerobic jar using Anaero Pack-MicroAero. At the end of 7 days of incubation, a whole liquid compartment of every tube was removed. The glass test tubes were then rinsed twice with 11 ml of PBS and dried at 60 °C for 30 min. The test tubes were filled up with 11 ml of 0.1% (w/v) crystal violet and incubated for 5 min at room temperature. The unbound crystal violet was then discarded. The test tubes were dried again at 60 °C for 15 min and washed with 11 ml of PBS three times. The bound crystal violet was destained with 11 ml of ethanol/acetone (80:20, v/v) for 1 min. The solution was then transferred to disposable cuvette and absorbance at 570 nm was measured using spectrophotometer (Hitachi) to determine level of biofilm formation. Experiments were performed in duplicate on three separated occasions. Biofilm level was expressed by mean of tested OD subtracted with mean of blank OD.

8. Investigation of anti-adhesive property of curcumin against *H. pylori*

8.1 Preparation of human laryngeal epithelial cells

8.1.1 Culture of human laryngeal epithelial cells

Human laryngeal epithelial cells (HEp-2), kindly provided by Dr.Pornthep Tiensiwakul, Faculty of Allied Health Sciences, Chulalongkorn University, Thailand, was used to study adherence of *H. pylori* in this study. The cells were grown in T75 tissue culture flask containing working medium; Dulbecco's modified of Eagle's medium (DMEM) supplemented with 10% (v/v) fetal bovine serum (FBS) and 1% (v/v) Antibiotic-Antimycotic. The cells were routinely split into fresh medium once confluence reached to 90% of cellular density. In order to split

the cells, the medium was discarded and the cells were washed twice with 5 ml of DPBS. The cells were disaggregated by adding 1 to 3 ml of 0.1% (v/v) trypsin and were left for 1 min. The activity of trypsin was stopped by adding 10 ml of fresh working medium. Cell suspension was thoroughly mixed by pipetted up and down several times. One ml of cell suspension was transferred into new T75 tissue culture flask containing 14 ml of fresh working medium, giving a split ratio of 1:10. The T75 flask was then incubated in CO₂ incubator at 37 °C under an atmosphere of 5% CO₂ and 95% humidity. The cellular confluence was observed by microscope.

8.1.2 Counting cells

In order to prepare an appropriate cell number for subculturing and adhesion assay, HEp-2 cells were counted using hemocytometer-counting chamber (Figure 10). After trypsinization and suspension in fresh working medium, an aliquot 100 µl of cell suspension was mixed with 100 µl of trypan blue and left for 3 to 5 min. The cells were applied into the counting chamber covered with coverslip using Pasteur pipette. The cells depositing in the central grid and the four outer grids were counted under microscope with 100 times magnification. Theoretically, viable cells are not stained with trypan blue, whereas dead cells are permeable and will take up the stain. Number of cells was calculated from following formula.

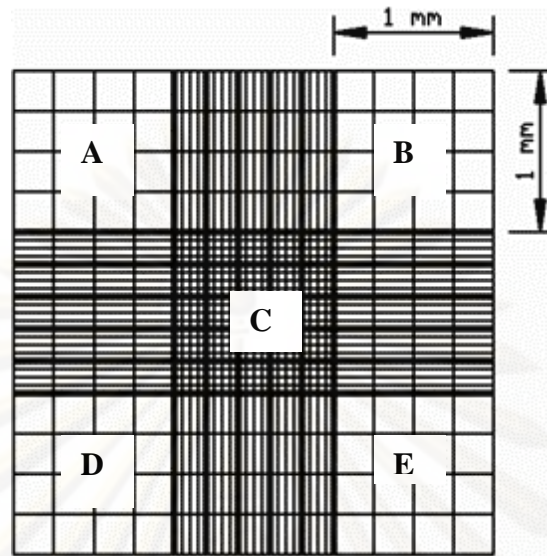


Figure 10: Hemacytometer-counting chamber. Areas marked A, B, C, D and E were used to count the cells.

$$\text{Number of viable cells in ml (cells ml}^{-1}\text{)} = \frac{\text{number of unstained cells} \times 10^4 \times \text{df}^*}{5}$$

*df ; dilution factor should be taken into account if any dilution was performed

8.2 Adhesion assay

The cells were split into 6-well polystyrene plates containing 3 ml of DMEM supplemented with 10% FBS. Cellular density was set at 3×10^6 cells per well. The cells were left to adhere for 24 h at 37 °C under an atmosphere of 5% CO₂ and 95% humidity, and then washed twice with 1 ml of DPBS. Subsequently, the

cells were grown in 1 ml of DMEM and co-cultivated with *H. pylori* at density of 3×10^8 CFU ml⁻¹ (OD₄₅₀ of 1) per well. Curcumin was added into co-culture and the final concentrations were adjusted equivalently to 1/2 MIC of each *H. pylori* strain. Curcumin-free co-culture was served as control. However in the **phase II**, following controls were further established; co-culture of *H. pylori* and 1/2 MIC of curcumin, co-culture of the cells with *H. pylori* and 0.016% (v/v) DMSO, co-culture of the cells with 1/2 MIC of curcumin.

Adhesion of *H. pylori* to HEP-2 cells was allowed to proceed for 2 h in CO₂ incubator. At the end of incubation period, medium was removed and the cells were washed approximately three times with DPBS in order to remove unattached bacteria. The cells were lysed with sterile distilled water (DW) for 15 min on shaking platform at 150 rpm, at room temperature. Cell lysate solutions were serially diluted from 10⁻¹ to 10⁻⁶ with DMEM. In the **phase I**, the lysate solutions were plated out onto Dent and Dent containing kanamycin plates supplemented with 7% lysed horse blood for wild type and flagellar mutant strains, respectively. While in the **phase II**, the lysate solutions were plated out onto BHI agar supplemented with 7% sheep blood. The plates in both **phase I** and **II** were incubated for 5 to 7 days at 37 °C under microaerobic condition. Plates with >25 and <250 colonies were enumerated. Experiments were performed in duplicate on three separated occasions. Visible colonies counted from the plates were expressed by mean. Number of the adherent bacterial, the percentile of bacterial adhesion, and the percentile of control were calculated from following formula.

$$\text{Adherent bacteria} = \frac{\text{mean of colony count}}{\text{x pipetting volume x dilution factor}}$$

$$\text{Percentile (\% of adhesion)} = \frac{\text{adherent bacteria x 100}}{\text{bacterial inoculum size}}$$

$$\text{Percentile (\% of control)} = \frac{\% \text{ adhesion (test) x 100}}{\% \text{ adhesion (control)}}$$

9. Analysis of 3-Dimensional Structure of *H. pylori* Biofilm Using Scanning Electron Microscopic (SEM)

9.1 SEM sample preparation

SEM analysis of *H. pylori* pellicle was performed to analyze bacterial 3-D structure of biofilms. In order to observe the 3-D structure among different ages of bacterial biofilm and determine the effect of curcumin resulting in this structural change, bacteria were grown as described in pellicle assay with an absence or presence of curcumin for 4, 5, 6, and 7 days. If no apparent pellicle was observed, planktonic cells were examined instead. However, bacteria grown in the test tubes containing only BHI broth without 2% (w/v) BCD at day 7 and colonies grown on BHI agar supplemented with 7% sheep blood for 3 days were served as controls. At the end of designed incubation period, sample both in pellicle and planktonic phases were separately collected. The pellicle compartment was firstly collected by gently pouring into a clean tube and left the planktonic behind in the culture tube. The

planktonic compartment was then transferred into another clean tube. The tubes were centrifuged at 3,000 rpm for 5 min and the supernatants were discarded. The pellets of both pellicle and planktonic were washed twice with 1 ml PBS. The samples were proceeded immediately for SEM analysis.

9.2 SEM analysis

SEM was performed by the Scientific and Technological Research Equipment Center, Chulalongkorn University, Thailand. The washed pellicles and planktonic cells were then fixed in 2.5% (v/v) glutaraldehyde in 0.1 M PBS (pH 7.2) for 1 h. Samples were washed twice by PBS followed by DW. The liquid was then removed. All samples were then successive dehydrated through a graded series of ethanol as following steps; 10 min per step; 30%, 50%, 70%, 90%, 3 x 100%; (v/v), respectively. The samples were dried at a critical point and positioned onto stub. The dehydrated samples were coated with gold-palladium. Finally, the samples were examined and the 3-D images were computerized documented with SEM (JEOL).

10. Proteomics Analysis of *H. pylori* Biofilm

In order to gain information regarding to biofilm formation mechanisms in *H. pylori*, 2-dimensional (2-D) gel electrophoresis was performed for protein analysis profile. Furthermore, mechanism of curcumin against *H. pylori* biofilm formation was also elucidated. The certain differential protein expression of *H. pylori* either in biofilm (pellicle) or planktonic states was compared both with a presence and absence of curcumin.

10.1 Protein sample preparation for proteomics analysis

10.1.1 Sample collection

H. pylori was grown as pellicle assay as previously described, in an absence and presence of curcumin at 1/4 and 1/2 MIC. All the cultures were established as maximized volume as enough for triplicate performances. Five samples of *H. pylori* biofilm and planktonic were prepared for 2-D gel electrophoresis including pellicle and planktonic cells without curcumin, pellicle and planktonic cells derived from 1/4 MIC of curcumin treated tube, and planktonic cells derived from 1/2 MIC of curcumin treated tube. Both pellicle and planktonic from every culture conditions were separately collected after 6 days of incubation, at 37 °C under microaerobic condition using Anaero Pack-MicroAero in anaerobic jar. The pellicle compartment of each culture condition was collected by gently pouring into a clean collection tube and left the planktonic behind in the culture tube. The planktonic compartment was then transferred into another clean collection tube. The tubes were centrifuged at 3,000 rpm for 5 min and the supernatants were discarded. The pellets of both pellicle and planktonic were washed twice with 5 ml PBS and subsequently resuspended in 35 ml of PBS.

10.1.2 Sonication of sample

The 35 ml suspension of both pellicle and planktonic samples of were then lysed by sonication (Vibra Cell™; Sonics & Materials Inc) as following conditions; 30 times of 10-s pulses on ice, amplitude of 40 μm. Following sonication, unlysed cells and cell debris were removed by centrifugation at 12,000 rpm for 15

min. The supernatants were collected and stored at $-80\text{ }^{\circ}\text{C}$ until ready for lyophilized.

10.1.3 Lyophilization of sample

The frozen samples were lyophilized using Modulyod Freeze Dryer (Thermo Electron Corporation) and operated under vacuum condition at $-45\text{ }^{\circ}\text{C}$ for 3 days until samples completely dried. The samples were then resuspended in 1 to 2 ml of PBS to prepared protein stock solutions and measured for protein concentrations.

10.1.4 Analysis of total protein concentration

Protein concentration was measured using Bradford assay (Bio-Rad Protein Assay). Each protein sample stock solution was diluted at 1:10 or 1:100. Eight-hundred μl of diluted sample was pipetted into a clean tube and mixed with 200 μl of dye reagent concentrate, and vortex vigorously. The tube was incubated at room temperature for 5 min. The sample was then transferred to disposable cuvette and absorbance at 595 nm was measured using spectrophotometer. The protein concentration was calculated and expressed as $\mu\text{g ml}^{-1}$ comparing with a standard curve of bovine serum albumin (see appendix).

10.1.5 Protein purification

Additional salt, lipid, and contaminant removals were performed in all samples by 2D Cleanup Kit (Amersham Biosciences), following a

manufacturer's instruction. Briefly, 1 mg of bacterial protein was transferred into a centrifuge tube. For each volume of sample, 3 volumes of precipitant reagent were added into the tube and mixed vigorously. The protein sample was incubated on ice for 15 min. For each original volume of sample, 3 volumes of co-precipitant reagent were added into the tube and mixed vigorously. The tube was centrifuged at 8,000 x *g* for 10 min and the supernatant was removed as much as possible. The co-precipitant, 3 times the size of the protein pellet, was added into the tube. The tube was centrifuged at 8,000 x *g* for 5 min and the supernatant was removed. The enough DDW was pipetted on top of pellet and the sample was mixed several times by vortex. One ml of pre-chilled wash buffer was added following by 5 μ l wash additive. The sample was mixed by vortex until fully dispersed. The sample was incubated at -20°C for 30 min with vortex once every 10 min. The tube was centrifuged again at 8,000 x *g* for 10 min and the supernatant was removed. The pellet was air-dried for 2 to 5 min. The pellet was solubilized in 250 μ l immobilized pH gradient (IPG) rehydration buffer. The sample was centrifuged at 8,000 x *g* for 10 min to remove any insoluble material. The supernatant of cleaned protein was transferred to clean microcentrifuge tube and stored at -80°C until used.

10.2 The first dimensional gel electrophoresis: isoelectric focusing (IEF)

Prior to IEF, the samples suspended in IPG rehydration buffer as mentioned above were allowed to thaw and incubate at room temperature for 30 min. Two-hundred and fifty μ l of individual samples containing 1 mg of total protein was load into strip holder. A 13-cm Immobiline™ DryStrip, pH 3-10 NL was positioned

into each strip holder with the gel side down. An Immobiline™ Drystrip Cover Fluid was applied thoroughly the entire IPG strip. Rehydration process was performed on Ettan™ IPGphor II™ unit platform (Amersham Biosciences) for 12 h. Following the rehydration, the first-dimension IEF was carried out. Running conditions were programmed as following, current limited 50 μ A/IPG strip, voltage step and hold mode; 1, step 500 voltage (500 volt-hours), 2, step 1,000 voltage (1000 volt-hours), 3, step 8,000 voltage (14,500 volt-hours), to a total volt-hour of 16,000 volt-hours.

10.3 The second dimensional gel electrophoresis: sodium dodecyl sulfate-polyacrylamide gel electrophoresis (SDS-PAGE)

10.3.1 IPG strip equilibration

After IEF, IPG strip was removed from the strip holder and IPG strip equilibration was performed immediately prior to the second-dimension run. The IPG strips were placed in individual tubes with support film toward tube wall. For the first equilibration, 5 ml of DTT-containing SDS equilibration buffer was added to each tube. The tubes were equilibrated at room temperature on shaking platform at 110 rpm for 20 min. The second equilibration was performed with 5 ml of iodoacetamide (IAA)-containing SDS equilibration buffer (without DTT). The tubes were then equilibrated again at room temperature on shaking platform at 110 rpm for 20 min. After equilibration, the IPG strips were immediately subjected to the SDS-PAGE.

10.3.2 SDS-PAGE preparation

The second dimension gel electrophoresis was then performed. A 12% polyacrylamide gel was prepared by mixing 10 ml of 4x resolving gel buffer, 16 ml of 30% T, 2.6% C monomer stock solution, 400 μ l of 10% SDS, 400 μ l of freshly prepared 10% ammonium persulfate, 16 μ l of TEMED, and adjusted the volume to 40 ml with DDW. The gel was set up in a casting stand and was allowed to completely polymerize for 45 min approximately. The gel was then rinsed several times with SDS electrophoresis buffer (25 mM Tris-HCL, pH 8.3, 192 mM glycine, 0.1% SDS) to eliminate unpolymerized acrylamide.

10.3.3 SDS-PAGE condition

The equilibrated IPG strip was placed between the precast plates with the plastic backing against one of the glass plates. Agarose sealing solution was laid over the placed IPG strip. Once the sealing solution was set, the precast gel cassette was inserted into SDS-PAGE unit (PROTEAN II xi cell; Bio-Rad). SDS electrophoresis buffer was filled into the unit both in the upper and lower chambers. The gel was electrophorated at constant current 50 mA per gel for 3 to 4 h until a tracking dye reached bottom of the gel.

10.4 Gel staining

After the second dimension gel electrophoresis, the gels were fixed with fixative solution containing 10% (v/v) CH_3COOH and 40% (v/v) methanol for at least 1 h with gentle agitation (60 rpm). The fixative solution was removed and replaced with DDW. The gels were washed for 10 min three times with agitation. The gels

were then stained with colloidal coomassie brilliant blue G-250 overnight. Subsequently, the gels were destained with warm DDW (45-55 °C) until clear background obtained.

10.5 Gel image analysis

The stained 2-D gels were placed on scanner and gel images were acquired using LabScan software on Imagescanner (Amersham Biosciences). ImageMaster 2D Elite 3.01 analysis software was used for spot-intensity calibration, spot and spot boundary detection, background abstraction, filtering out nonprotein spot, and matching. The biological variation analysis mode was used to match all images for comparative cross-gel statistical analysis of the two groups. To avoid experimental variations, triplicate gels were analyzed for each sample. The gel spot pattern of each gel was summarized obtaining one standard gel for each sample. These standard gels were then matched to yield information about differences in abundance up- or down-regulation of spots. A student's *t* test was used for this comparative analysis. Spots existing in only either pellicle or planktonic of each condition, and spots displaying *P* values of less than 0.05 were selected for identification by mass spectrometry.

10.6 Spot picking

Considered spots of interest as described above were then picked up for identification. Such protein spots were excised using pipette tip and dispensed into clean microcentrifuge tubes containing 200 µl of DDW. The protein spots were stored at 4 °C until proceeded for mass spectrometry analysis.

10.7 Mass spectrometry analysis

The protein spots were delivered to the Bio-technology Service Unit (BSU), National Science and Technology Development Agency, Pathumthani, Thailand, where mass spectrometry analysis was performed. Protein samples were digested with 20 mM trypsin/ambic. Mass spectrometry analyzes were performed with MALDI-TOF mass spectrometry model reflex V (Bruker Daltonik GmbH).

10.8 Protein data analysis

Proteins were identified by the BSU. Protein identifications were obtained using MASCOT (MatrixScience) and by searching for matching peptide mass fingerprints in a protein database from the NCBI. The search criteria used were fixed modification of carboxamidomethylation of cysteine, variable modification of methionine oxidation, and considered the accuracy of the experimental to theoretical pI and molecular weight. Protein scores were significant when P value was less than 0.05 (P value was the probability that the observed match is a random event).

11. Statistical Analysis

Experiment of MIC, investigation of biofilm formation by pellicle assay, optimization of biofilm formation, quantification of biofilm formation, adhesion assay, in *H. pylori*, and proteomics analysis of *H. pylori* biofilm were carried out independently in triplicate. Results obtained from MIC, investigation of biofilm formation by pellicle assay, optimization of biofilm formation in *H. pylori* were expressed as means from three independent experiments. Results obtained from the

quantification of biofilm formation, the adhesion assay, and the proteomics analysis were expressed as means \pm SD from three independent experiments.

For statistical analysis, in the **phase I**, One-way analysis of variance (One-way ANOVA) was used to determine the differences among wild types and mutants in quantification of biofilm formation and adhesion assay. Student's *t*-test was used to determine the differences between the means of curcumin-untreated and -treated samples in quantification of biofilm formation. Probability values $P \leq 0.05$ were considered significantly. A multiple comparison between sample pairs considered significantly was determined by Tukey test. In the **phase II**, One-way ANOVA was used to determine the differences among sample groups in quantification of biofilm formation, student's *t*-test was used to determine the differences between the means of curcumin-untreated and -treated samples and the adhesion assay. Probability values $P \leq 0.05$ were considered significantly. A multiple comparison between sample pairs considered significantly was determined by Tukey test. In the **phase III**, student's *t*-test was used to determine the differences between protein profile expressions of the two sample groups. Probability values $P \leq 0.05$ were considered significantly. All statistical analyses were performed using SPSS Statistic Base 17.0 (SPSS Co., Ltd., Thailand, Server IP Address; dc1.win.chula.ac.th)

CHAPTER V

RESULTS

Phase I: Roles of Flagella in Biofilm Formation of *H. pylori*

1. Primer designation

All primers used for specific gene amplification and IPCRM were designed from published sequences of flagellar gene; *flaA*, *flgR*, and *fliQ* genes as previously mentioned in the Chapter IV. Primers for *flaA* (*flaAF*; forward primer, *flaAR*; reverse primer) were designed from nucleotide sequence at position 232-1073. Primers for *flgR* (*flgRF*; forward primer, *flgRR*; reverse primer) were designed from nucleotide sequence at position 32-1087. Primers for *fliQ* (*fliQF*; forward primer, *fliQR*; reverse primer) were designed from nucleotide sequence at position 14-263.

Primers for IPCRM amplification were designed from the published sequences of individual gene to hybridize in reverse orientation and possess a unique restriction site at their 5' ends. The pairs of forward and reverse primers for *flaA*, *flgR*, and *fliQ* were designed to start at 24, 15, and 4-bp away from each other, respectively, in order to introduce a defined deletion in the amplified products. The IPCRM primers for *flaA* (*flaAIF*; forward primer, *flaAIR*; reverse primer) were designed from nucleotide sequence at position 657-696. IPCRM primers for *flgR* (*flgRIF*; forward primer, *flgRIR*; reverse primer) were designed from nucleotide sequence at position 546-590. IPCRM primers for *fliQ* (*fliQIF*; forward primer, *fliQIR*; reverse primer) were designed from nucleotide sequence at position 122-155. Additionally, each IPCRM primer was added with *bgl* II restriction endonuclease site

(AGATCT) and two additional guanine (G) bases at the 5' end. Table 7 shows all primers used in study.

| Primer name | Gene | PCR method | Primer sequence (5'-3')* | Position | T _m (°C) | Product size (bp) |
|----------------|-------------|------------|--------------------------|----------|---------------------|-------------------|
| <i>flaA</i> F | <i>flaA</i> | PCR | GCGGATAAGGCTATGGATGA | 232-1073 | 51.8 | 842 |
| <i>flaA</i> R | | PCR | GAGTCAGAAGCCGAAACGAC | | | |
| <i>flgR</i> F | <i>flgR</i> | PCR | ACATGCGTAAAAGCCTGGAG | 32-1087 | 51.8 | 1056 |
| <i>flgR</i> R | | PCR | CTCTTTCCACGACGCCTAAA | | | |
| <i>fliQ</i> F | <i>fliQ</i> | PCR | TCATGAAACTCGCCATTGAG | 14-263 | 49.7 | 250 |
| <i>fliQ</i> R | | PCR | CCGATGATTTTGGGAATGAG | | | |
| <i>flaA</i> IF | <i>flaA</i> | IPRCM† | GGAGATCTACAGGCGTTAAAGCC | 657-696 | 57.1 | 818 |
| <i>flaA</i> IR | | IPRCM | GGAGATCTTTCTGCTAACACGCC | | | |
| <i>flgR</i> IF | <i>flgR</i> | IPRCM | GGAGATCTCATGTCCGCAATCCC | 546-590 | 58.8 | 1041 |
| <i>flgR</i> IR | | IPRCM | GGAGATCTGGGTGCTTGGATCGC | | | |
| <i>fliQ</i> IF | <i>fliQ</i> | IPRCM | GGAGATCTTTTGTCTTTTGTGCC | 122-155 | 53.5 | 246 |
| <i>fliQ</i> IR | | IPRCM | GGAGATCTTTTCATTGATTTGGG | | | |

* Underlined nucleotides represent *bg*III restriction endonuclease sites.

† Inverse PCR mutagenesis

Table 7: The oligonucleotide sequences of PCR and IPRCM primers for amplification of *flaA*, *flgR*, and *fliQ* genes and the relative product sizes.

2. The *flaA*, *flgR*, and *fliQ* genes amplification

PCR amplification was performed as previously described in the Chapter IV. *H. pylori* ATCC26695 chromosomal DNA was served as template. The *flaA* fragment, size 842 bp, was obtained using primer *flaAF* and *flaAR*. The *flgR* fragment, size 1056 bp, was obtained using primer *flgRF* and *flgRR*. The *fliQ* fragment, size 250 bp, was obtained using primer *fliQF* and *fliQR*. These PCR products were analyzed by 1.5% agarose gel electrophoresis comparing with standard molecular weight marker (Figure 11; lane 1, 2, and 3, respectively).

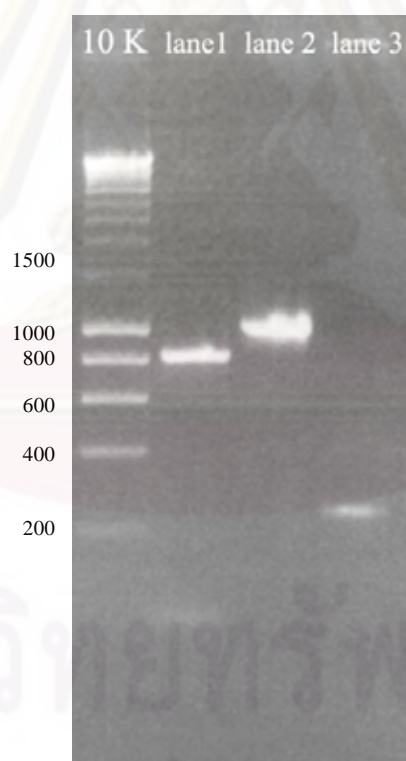


Figure 11: Agarose gel electrophoresis of PCR amplified product of *flaA*, *flgR*, and *fliQ* genes. Lane 1; *flaA* gene amplified from ATCC26695. Lane 2; *flaA* gene amplified from ATCC26695. Lane 3; *flgR* gene amplified from ATCC26695. 10K was standard marker.

3. Cloning of PCR fragment into pGEM® T-Easy vector

The PCR products of all three genes were separately cloned in to pGEM® T-Easy vector. This commercially available vector is 3051 bp and is a linear DNA fragment containing thymine (T) overhang at the 3' end. The PCR products possessing the adenine (A) overhang, which matched with T overhang, were then able to clone into the vector easily. Figure 12 illustrates a physical map of pGEM® T-Easy vector. The PCR fragments of individual genes, as above described, were individually ligated to the pGEM® T-Easy vector as previously described in the Chapter IV. The ligated products were transformed into XL2-blue MRF' *E. coli* ultra-competent cells. Clones carrying the inserted fragment were named as following; pGA (designed for clone with 842 bp of *flaA* gene), pGR (designed for clone with 1056 bp of *flgR* gene), and pGQ (designed for clone with 250 bp of *fliQ* gene). The schematic pictures of all inserted plasmids were illustrated in Figure 13 to 15. The transformants were then selected on LB agar containing 100 $\mu\text{g ml}^{-1}$, 32 $\mu\text{g ml}^{-1}$, and 40 $\mu\text{g ml}^{-1}$ of ampicillin, IPTG, and X-Gal, respectively. The white colonies that considered as positive colony containing the inserted fragment were randomly picked up and restreaked onto fresh LB agar containing 100 $\mu\text{g ml}^{-1}$ of ampicillin. The overnight positive clones were preceded to verify by colony PCR and restriction analysis.

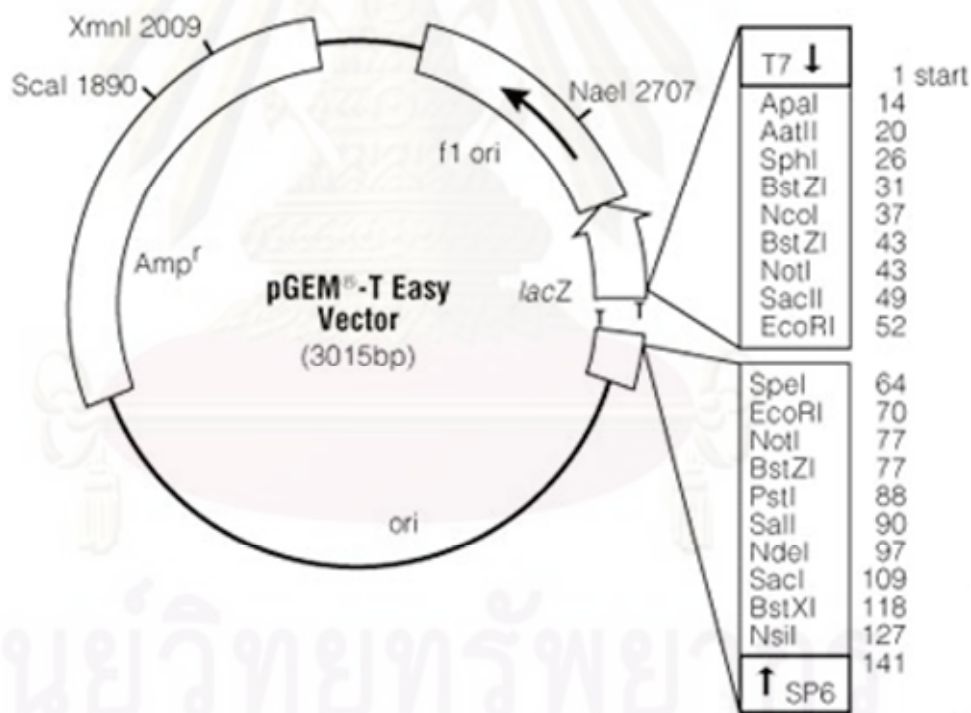


Figure 12: The physical map and multiple cloning regions of pGEM® T-Easy vector.

(Figures derived from <http://www.promega.com>)

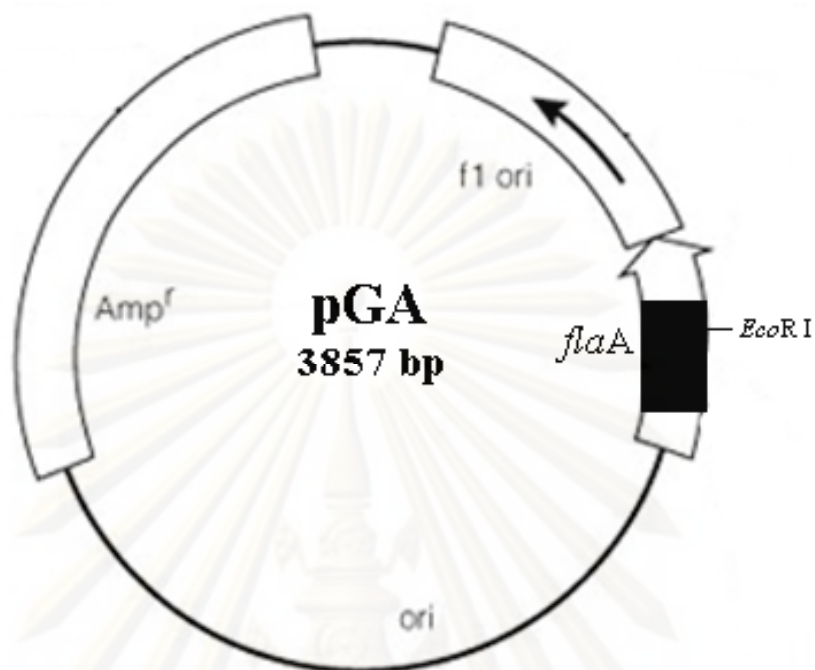


Figure 13: The schematic picture of pGA. PCR product of *flaA* gene was inserted into pGEM® T-Easy vector to obtain plasmid pGA.

ศูนย์วิทยทรัพยากร
จุฬาลงกรณ์มหาวิทยาลัย

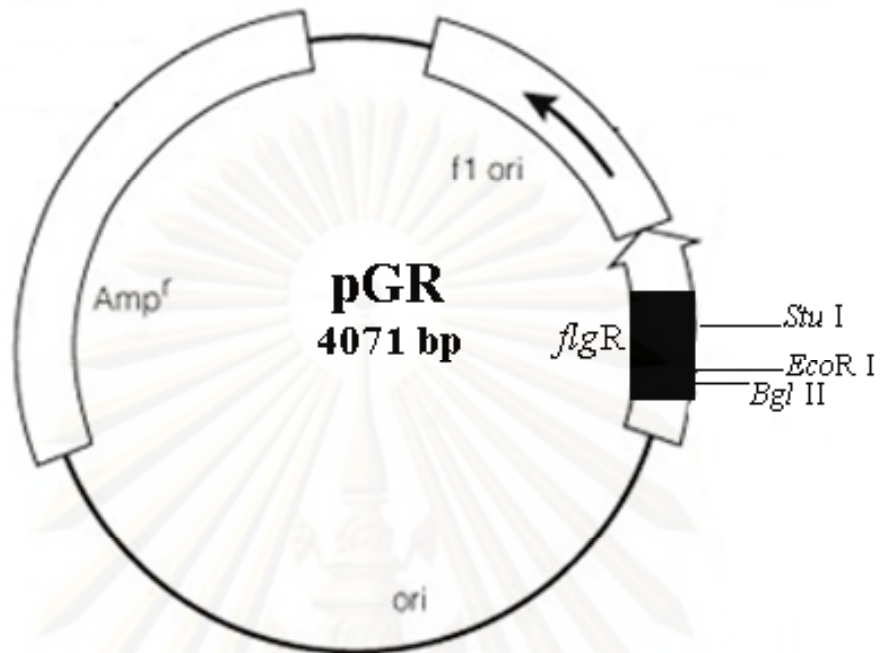


Figure 14: The schematic picture of pGR. PCR product of *flgR* gene was inserted into pGEM® T-Easy vector to obtain plasmid pGR.

ศูนย์วิทยทรัพยากร
จุฬาลงกรณ์มหาวิทยาลัย

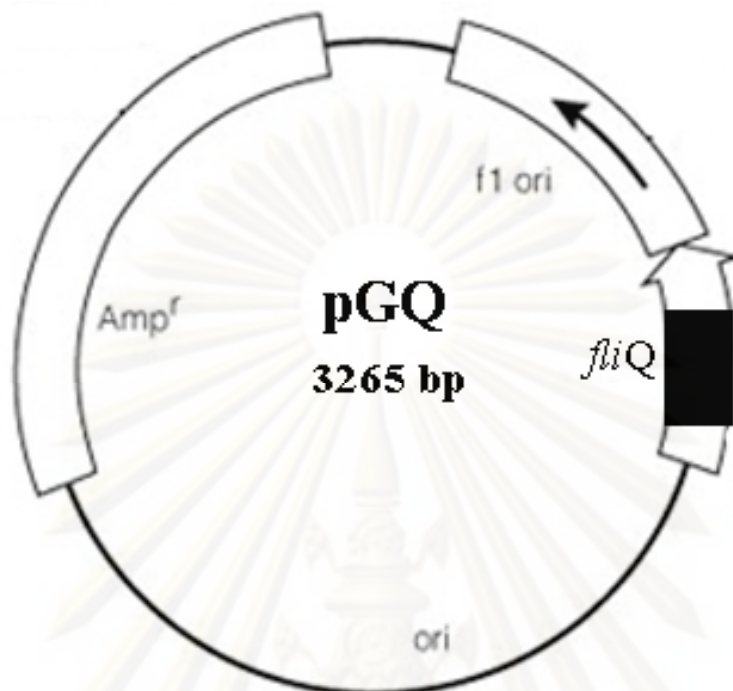


Figure 15: The schematic picture of pGQ. PCR product of *fliQ* gene was inserted into pGEM® T-Easy vector to obtain plasmid pGQ.

ศูนย์วิทยทรัพยากร
จุฬาลงกรณ์มหาวิทยาลัย

3.1 Colony PCR analysis of plasmid pGA, pGR, and pGQ

One loopful of bacteria from positive clone of individual genes was boiled in DDW. The boilates were amplified with T7 and SP6 promoter primers, as previously described in the Chapter IV, in order to confirm a presence of inserted fragment. Each amplified product was analyzed by 0.7% agarose gel electrophoresis comparing with standard molecular weight marker.

The colony PCR product of plasmid pGA (Figure 16) showed single DNA band of 983 bp fragment, composed of 842 and 141 bp of *flaA* gene and T7-SP6 fragment, respectively. The colony PCR product of plasmid pGR (Figure 17) showed single DNA band of 1197 bp fragment, composed of 1056 and 141 bp of *flgR* gene and T7-SP6 fragment, respectively. The colony PCR product of plasmid pGQ (Figure 18) showed single DNA band of 391 bp fragment, composed of 250 and 141 bp of *fliQ* gene and T7-SP6 fragment, respectively.

3.2 Restriction analysis of plasmid pGA, pGR, and pGQ

The positive clones were subjected to restriction enzyme analysis, as previously described in the Chapter IV, in order to reconfirm the fragment insertion. The plasmid pGA and pGR were digested with *Not* I, while plasmid pGQ was digested with *EcoR* I. To analyze the restriction pattern of each gene, the digested plasmids were electrophorated through 0.7% agarose gel electrophoresis comparing with standard molecular weight marker.

The *Not* I restricted pGA (Figure 19) showed two DNA bands, 842 and 3015 bp fragments. The 842 bp band was corresponded to the size of inserted *flaA* gene. The *Not* I restricted pGR (Figure 19) showed two DNA bands, a 1056 and 3015

bp fragments. The 1056 bp band was corresponded to the size of inserted *flgR* gene. The *EcoR* I restricted pGQ (Figure 20) showed two DNA bands, a 250 and 3015 bp fragments. The 250 bp band was corresponded to the size of inserted *fliQ* gene. The additional 3015 bp presented in all three constructs were the size of pGEM® T-Easy vector. Thus, from these restriction enzyme analysis patterns, pGA, pGR, and pGQ plasmids showed to carry the interested PCR amplified gene fragments. DNA sequencing was performed to confirm the nucleotide sequence of all the genes in these plasmids.



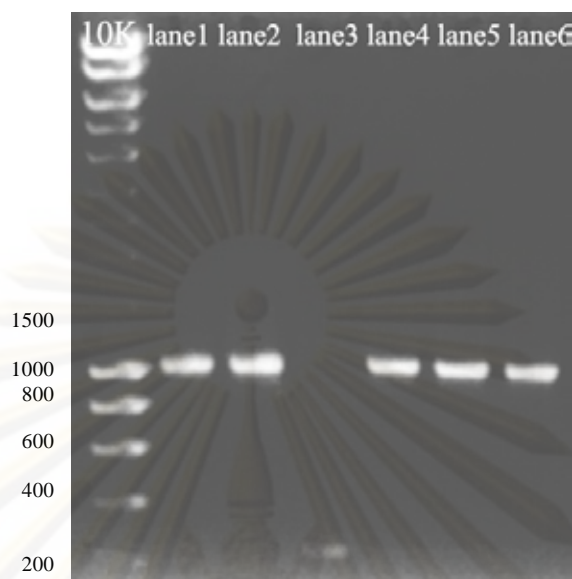


Figure 16: Agarose gel electrophoresis of colony PCR product of plasmid pGA amplified by T7 and SP6 primers. Lane 1, 2, 4, 5, and 6; positive bands of *flaA* gene. Lane 3; no positive band shown. 10K was standard marker.

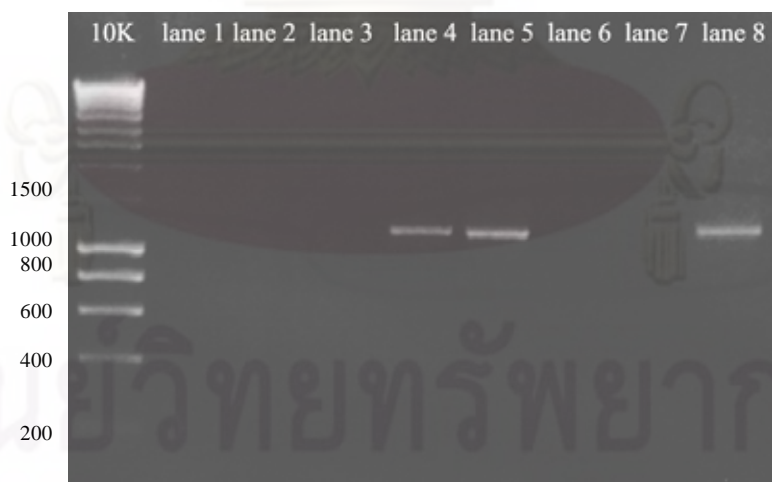


Figure 17: Agarose gel electrophoresis of colony PCR product of plasmid pGR amplified by T7 and SP6 primers. Lane 4, 5, and 8; positive bands of *flgR* gene. Lane 1, 2, 3, 6, and 7; no positive band shown. 10K was standard marker.



Figure 18: Agarose gel electrophoresis of colony PCR product of plasmid pGQ amplified by T7 and SP6 primers. Lane 1, 2, 5, 6, and 7; positive bands of *fliQ* gene. Lane 3 and 4; no positive band shown. 10K was standard marker.

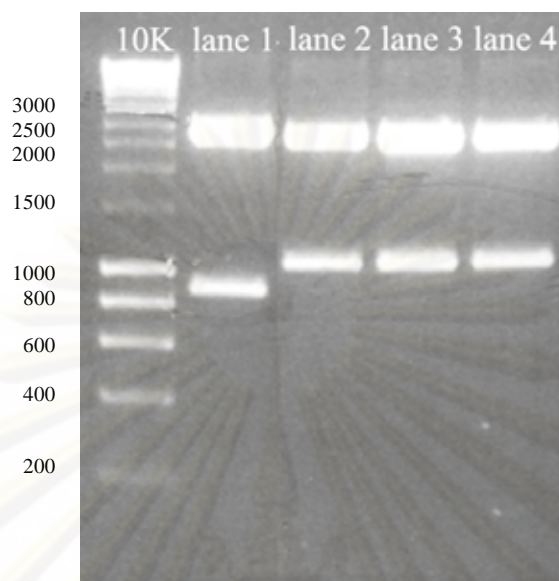


Figure 19: Agarose gel electrophoresis of plasmid pGA and pGR cut with *Not I* enzyme. Lane 1; plasmid pGA digested with *Not I*. Lane 2-4; plasmid pGR digested with *Not I*. 10K was standard marker.

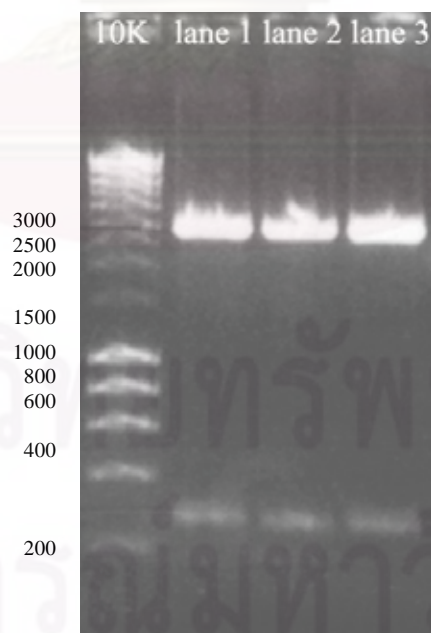


Figure 20: Agarose gel electrophoresis of plasmid pGQ cut with *EcoR I* enzyme. Lane 1-3; plasmid pGQ cut with *EcoR I*. 10K was standard marker.

4. DNA sequence analysis of plasmid pGA, pGR, and pGQ

DNA sequence analysis of individual plasmids carrying PCR amplified gene fragments were performed using T7 and SP6 primers as previously described in the Chapter IV. Data of nucleotide sequences were obtained and compared with the published nucleotide sequences (Figure 6 to 8). The nucleotide sequences of *flaA* gene in plasmid pGA showed an *EcoR* I site and genomic sequence compatible with *H. pylori* ATCC26695 *flaA* published sequence. The nucleotide sequences of *flgR* gene in plasmid pGR showed *EcoR* I and *Bgl* II sites and a genomic sequence compatible with *H. pylori* ATCC26695 *flgR* published sequence. The nucleotide sequences of *fliQ* gene in plasmid pGQ showed a genomic sequence compatible with *H. pylori* ATCC26695 *fliQ* published sequence. The sequence analysis data obtained here confirmed all the cloned plasmids carried the correct nucleotide sequences of individual interested genes.

5. Mutagenesis of plasmid pGA, pGR, and pGQ by inverse PCR amplification

To perform mutagenesis, plasmids carrying PCR amplified gene fragments were proceeded to amplify in an inverse direction using primer as previously described in Table 7. According to the primer designation and process of IPCRM, the products presumably had a defined deletion plus unique introduced *Bgl* II restriction site locating in the middle of individual genes. These resulted by the IPCRM forward and reverse primers that designated to amplify the gene of interest at the middle of fragment with starting point 24-, 15-, 4-bp away from each other for *flaA*, *flgR*, and *fliQ*, respectively, leading to nucleotide deletion. The *Bgl* II restriction sites were also introduced at both of these starting points. Thus these resulted in a successful

mutagenesis accompanied with the specific site promptly to link with a restricted kanamycin cassette in next step. Each IPCRM product was analyzed by 0.7% agarose gel electrophoresis comparing with standard molecular weight marker. The IPCRM product of plasmid pGA (designated as I-pGA; Figure 21) showed single DNA band of 3833 bp fragment, composed of 818 and 3015 bp of mutated *flaA* gene and pGEM® T-Easy vector, respectively. The IPCRM products of plasmid pGR (designated as I-pGR; Figure 21) showed single DNA band of 4056 bp fragment, composed of 1041 and 3015 bp of mutated *flgR* gene and pGEM® T-Easy vector, respectively. The IPCRM products of plasmid pGQ (designated as I-pGQ; Figure 21) showed single DNA band of 3261 bp fragment, composed of 246 and 3015 bp of mutated *fliQ* gene and pGEM® T-Easy vector, respectively.

The IPCRM products were then digested by *Bgl* II and *Dpn* I. The *Dpn* I was used in order to digest methylated and hemimethylated DNA in the original plasmids. Any plasmid generated by PCR, however, is non-methylated and resistant to digestion of *Dpn* I. Thus this offers a removal of original plasmid resulting in a reduction of background. After a complete digestion, the IPCRM products of all plasmids were then purified as previously described in the Chapter IV and a self-ligation of all digested IPCRM products was setup.

The *Bgl* II/*Dpn* I-digested self-ligated IPCRM products were transformed into *E. coli* ultra-competent cells and the transformants were selected on LB agar as previously described. The positive colonies were randomly picked up and restreaked onto fresh LB agar containing 100 µg ml⁻¹ of ampicillin. The overnight positive clones were performed a colony PCR as previously described in the Chapter IV. The colony PCR products from this step were then incubated with *Bgl* II in order to

confirm the introduction of *Bgl* II restriction site into the IPCRM amplified gene plasmids. Positives were identified by successful digestion compared to the uncut plasmids. To analyze the restricted digestion, both the *Bgl* II digested and undigested colony PCR products of I-pGA and I-pGR were electrophorated through 0.7% agarose gel electrophoresis, while the I-pGQ were electrophorated through 1.5% agarose gel electrophoresis comparing with standard molecular weight marker.

The *Bgl* II restricted of the self-ligated I-pGA (Figure 22) showed single DNA band, a 480 bp fragments. The 480 bp band was corresponded to the size of *Bgl* II restricted-mutated *flaA* gene with 24-bp deletion plus T7-SP6 fragment. The undigested of I-pGA showed single band of a 959 bp fragment. The *Bgl* II restricted of the self-ligated I-pGR (Figure 23) showed two DNA bands, 591 and 1182 bp fragments. The 591 bp band was corresponded to the size of *Bgl* II restricted-mutated *flgR* gene with 15-bp deletion plus T7-SP6 fragment. Another 1182 bp band was presumably an incomplete digested product. The undigested of I-pGR also showed single band of a 1182 bp fragment. The *Bgl* II restricted of the self-ligated I-pGQ (Figure 24) showed two DNA bands, 194 and 387 bp fragments. The 194 bp band was corresponded to the size of *Bgl* II restricted mutated *fliQ* gene with 4-bp deletion plus T7-SP6 fragment. Another 387 bp band was presumably an incomplete digested product. The undigested of I-pGQ also showed single band of a 387 bp fragment.

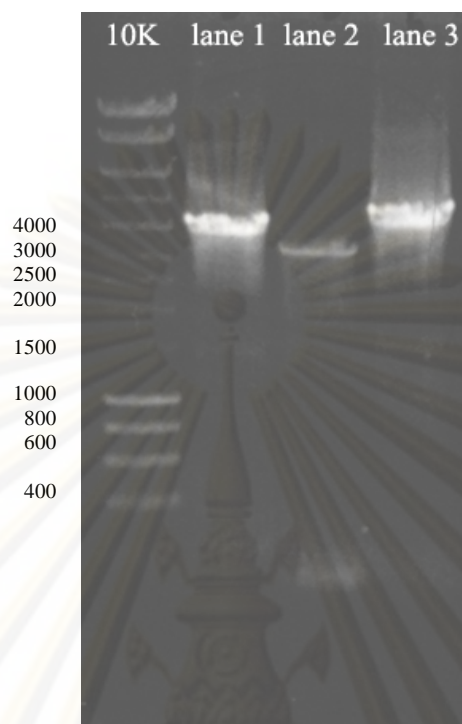


Figure 21: Agarose gel electrophoresis of IPCRM amplified product of plasmid pGA, pGR, and pGQ. Lane 1; I-pGA amplified from ATCC26695. Lane 2; I-pGQ amplified from ATCC26695. Lane 3; I-pGR amplified from ATCC26695. 10K was standard marker.

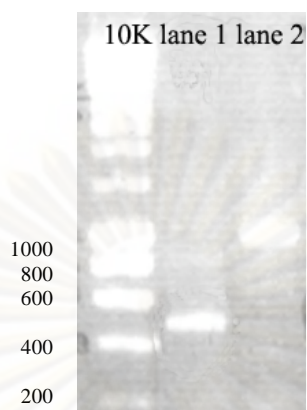


Figure 22: Agarose gel electrophoresis of *Bgl* II restricted colony PCR product of the self-ligated plasmid I-pGA. Lane 1; *Bgl* II digested mutated *flaA* gene. Lane 2; undigested mutated *flaA* gene. 10K was standard marker.

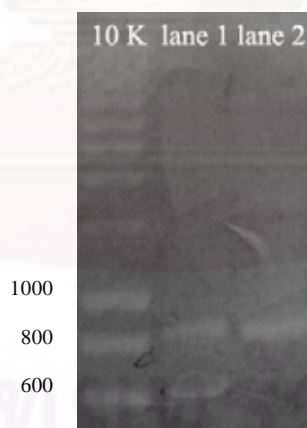


Figure 23: Agarose gel electrophoresis of *Bgl* II restricted colony PCR product of the self-ligated plasmid I-pGR. Lane 1; *Bgl* II digested mutated *flgR* gene. Lane 2; undigested mutated *flgR* gene. 10K was standard marker.



Figure 24: Agarose gel electrophoresis of *Bgl* II restricted colony PCR product of the self-ligated plasmid I-pGR. Lane 1; *Bgl* II digested mutated *fliQ* gene Lane 2; undigested mutated *fliQ* gene. 10K was standard marker.

ศูนย์วิทยทรัพยากร
จุฬาลงกรณ์มหาวิทยาลัย

The constructs of self-ligated IPCRM were also subjected to restriction analysis, as previously described in the Chapter IV, in order to reconfirm. Plasmid containing self-ligated IPCRM product was then extracted from overnight culture broth of individual clones, as previously described in the Chapter IV. The plasmid I-pGA and I-pGR were digested with *Not* I, while plasmid I-pGQ was digested with *EcoR* I. The *Bgl* II was co-digested in all plasmids. To analyze the restriction pattern, the digested plasmids of I-pGA and I-pGR were electrophorated through 0.7% agarose gel electrophoresis, while the I-pGQ were electrophorated through 1.5% agarose gel electrophoresis comparing with standard molecular weight marker.

The *Not* I/*Bgl* II restricted I-pGA (Figure 25) showed three DNA bands, 409, 818 and 3015 bp fragments. The 409 bp band was corresponded to the size of I-pGA that was digested by both *Not* I/*Bgl* II. The 818 bp band corresponded to the size of I-pGA that was probably digested by only *Not* I but not by *Bgl* II. The additional 3015 bp was the size of pGEM® T-Easy vector. The *Not* I/*Bgl* II restricted I-pGR (Figure 25) showed three DNA bands, 521, 1041 and 3015 bp fragments. The 521 bp band was corresponded to the size of I-pGR that was digested by both *Not* I/*Bgl* II. The 1041 bp band corresponded to the size of I-pGR that was probably digested by only *Not* I but not by *Bgl* II. The additional 3015 bp was the size of pGEM® T-Easy vector. The *EcoR* I/*Bgl* II restricted I-pGQ (Figure 26) showed three DNA bands, 123, 246 and 3015 bp fragments. The 123 bp band was corresponded to the size of I-pGQ that was digested by both *EcoR* I/*Bgl* II. The 246 bp band corresponded to the size of I-pGQ that was probably digested by only *EcoR* I but not by *Bgl* II. The

additional 3015 bp was the size of pGEM® T-Easy vector. All the checked positive plasmids were ready for kan^R cassette insertion in the next step.



ศูนย์วิทยทรัพยากร
จุฬาลงกรณ์มหาวิทยาลัย

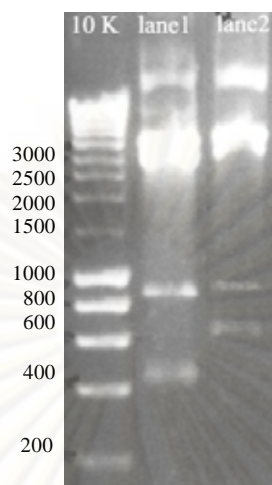


Figure 25: Agarose gel electrophoresis of self-ligated plasmid I-pGA and I-pGR cut with *Not* I and *Bgl* II enzyme. Lane 1; mutated *flaA* gene cut with *Not* I/*Bgl* II. Lane 2; mutated *flgR* gene cut with *Not* I/*Bgl* II. 10K was standard marker.

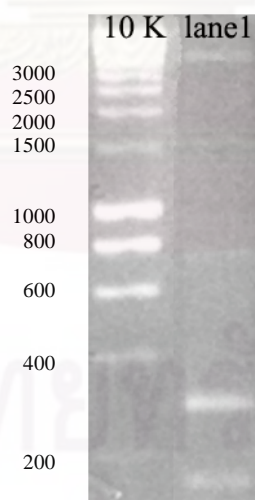


Figure 26: Agarose gel electrophoresis of self-ligated plasmid I-pGQ cut with *EcoR* I and *Bgl* II enzyme. Lane 1; mutated *fliQ* gene cut with *EcoR* I/*Bgl* II. 10K was standard marker.

6. Insertion of kan^R cassette into mutated genes for *H. pylori* mutagenesis

The plasmids containing mutated individual genes were digested with *Bgl* II and purified. The digested plasmids were then ligated together with *Bam*H I-cut kan^R cassette. The ligated products were transformed into *E. coli* ultra-competent cells and the transformants were selected on LB agar, as previously described. The positive colonies were randomly picked up and restreaked onto fresh LB agar containing 100 µg ml⁻¹ of ampicillin. The overnight positive clones were performed a colony PCR and restriction enzyme analysis. The kan^R cassette-ligated I-pGA, I-pGR, and I-pGQ plasmids were designated as I-pGA/kan^R, I-pGR/kan^R, and I-pGQ/kan^R, respectively.

Colony PCR products were analyzed by 0.7% agarose gel electrophoresis comparing with standard molecular weight marker. The colony PCR product of I-pGA/kan^R (Figure 26) showed single DNA band of 2399 bp fragment, composed of 818, 1440, and 141 bp of mutated *flaA* gene, kan^R cassette, and T7-SP6 fragments, respectively. The colony PCR product of I-pGR/kan^R (Figure 27) showed single DNA band of 2622 bp fragment, composed of 1041, 1440, and 141 bp of mutated *flgR* gene, kan^R cassette, and T7-SP6 fragments, respectively. The colony PCR product of I-pGQ/kan^R (Figure 28) showed single DNA band of 1827 bp fragment, composed of 246, 1440, and 141 bp of mutated *fliQ* gene, kan^R cassette, and T7-SP6 fragments, respectively.

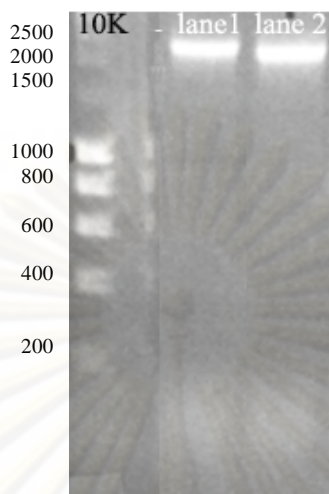


Figure 27: Agarose gel electrophoresis of colony PCR product of the I-pGA/kan^R and I-pGR/kan^R. Lane 1; mutated *flaA* plus inserted kan^R cassette. Lane 2; mutated *flgR* plus inserted kan^R cassette. 10K was standard marker.

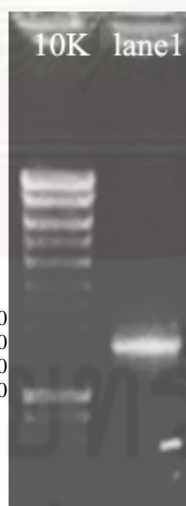


Figure 28: Agarose gel electrophoresis of colony PCR product of the I-pGQ/kan^R. Lane 1; mutated *fliQ* plus inserted kan^R cassette. 10K was standard marker.

The positive clones from the colony PCR analysis were subjected to restriction analysis, as previously described in the Chapter IV, in order to reconfirm the introduction of kan^R cassette into the mutated genes. Plasmid containing mutated gene plus kan^R cassette was then extracted as previously described in the Chapter IV. The I-pGA/kan^R and I-pGR/kan^R were digested with *Not* I, while I-pGQ/kan^R was digested with *EcoR* I. To analyze the restriction pattern, the digested plasmids were electrophorated through 0.7% agarose gel electrophoresis comparing with standard molecular weight marker. The *Not* I restricted I-pGA/kan^R showed two DNA bands corresponding to the size of mutated *flaA* gene plus kan^R cassette. The *Not* I restricted I-pGR/kan^R showed two DNA bands corresponding to the size of mutated *flgR* gene plus kan^R cassette. The *EcoR* I restricted I-pGQ/kan^R showed two DNA bands corresponding to the size of mutated *fliQ* gene plus kan^R cassette. All the checked positive plasmids were ready for transforming into *H. pylori* wild type cells in the next step.

7. Transformation of mutated *flaA*, *flgR*, and *fliQ* genes into *H. pylori* ATCC26695 and N6

After a complete construction performed by IPCRM, the I-pGA/kan^R, I-pGR/kan^R, and I-pGQ/kan^R plasmids were separately introduced into *H. pylori* wild type both ATCC26695 and N6 strains by natural transformation and electroporation, respectively. The Transformants were selected on Dent's plate supplemented with 20 µg ml⁻¹ kanamycin. Six flagellar mutant strains were obtained as summarized in Table 8. The PA315 and NA2 were *flaA* mutants, PR611 and NR2 were *flgR*

mutants, and PQ and NQ were *fliQ* mutants of ATCC26695 and N6, respectively. Successful recombination was checked by PCR using gene specific primer pairs as described in Table 7 in this Chapter. The amplified PCR product of PA315 (Figure 29A; lane 2) and NA2 (Figure 29C; lane 6) showed similar single DNA band of 2258 bp fragment, composed of 818 and 1440 bp of mutated *flaA* gene and kan^R cassette, respectively. The amplified PCR product of PR611 (Figure 29B; lane 4) and NR2 (Figure 29D; lane 6) showed similar single DNA band of 2481 bp fragments, composed of 1041 and 1440 bp of mutated *flgR* gene and kan^R cassette, respectively. The amplified PCR product of PQ (Figure 29C; lane 3) and NQ (Figure 29C; lane 12) showed similar single DNA band of 1686 bp fragments, composed of 246 and 1440 bp of mutated *fliQ* gene and kan^R cassette, respectively.

| Strains | Relevant characteristics |
|-----------|--|
| ATCC26695 | Virulent wild type strain |
| PA315 | Kan ^R † <i>H. pylori</i> 26695 <i>flaA</i> mutant |
| PR611 | Kan ^R <i>H. pylori</i> 26695 <i>flgR</i> mutant |
| PQ | Kan ^R <i>H. pylori</i> 26695 <i>fliQ</i> mutant |
| N6 | Virulent wild type (mouse-adapted) strain |
| NA2 | Kan ^R <i>H. pylori</i> N6 <i>flaA</i> mutant |
| NR2 | Kan ^R <i>H. pylori</i> N6 <i>flgR</i> mutant |
| NQ | Kan ^R <i>H. pylori</i> N6 <i>fliQ</i> mutant |

†Kanamycin resistant

Table 8: *H. pylori* wild type strains and their isogenic mutants constructed by inverse PCR mutagenesis.

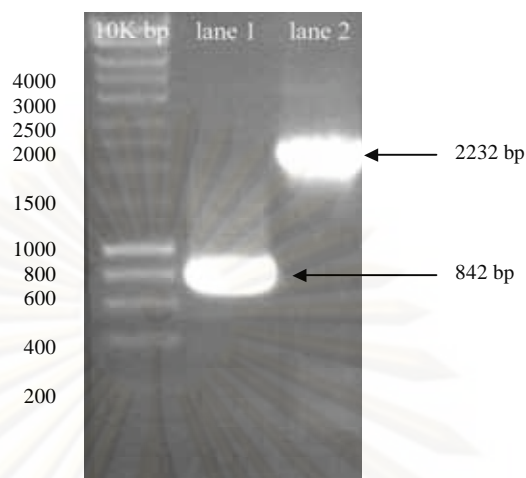


Figure 29(A): PCR amplification of *flaA* gene from *H. pylori* wild type and mutated strains. The 10K bp was served as a molecular weight marker. Lane 1; *flaA* gene amplified from ATCC26695 wild type strain (842 bp). Lane 2; *flaA* gene amplified from *flaA* mutant strain PA315 (2232 bp).

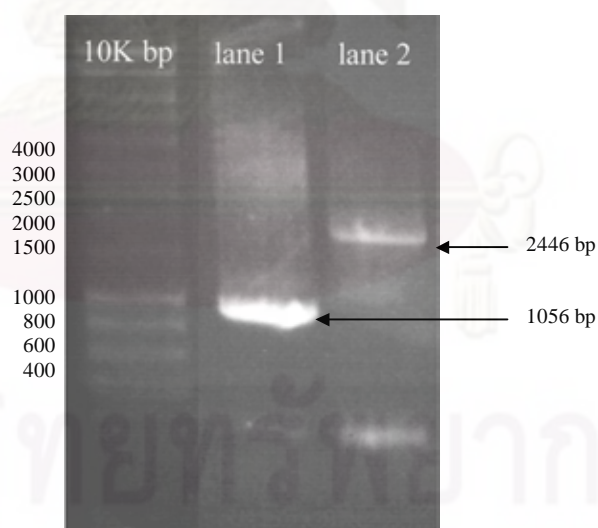


Figure 29(B): PCR amplification of *flgR* gene from *H. pylori* wild type and mutated strains. The 10K bp was served as a molecular weight marker. Lane 1; *flgR* gene amplified from ATCC26695 wild type strain (1056 bp). Lane 2; *flgR* gene amplified from *flgR* mutant strain PR611 (2446 bp).

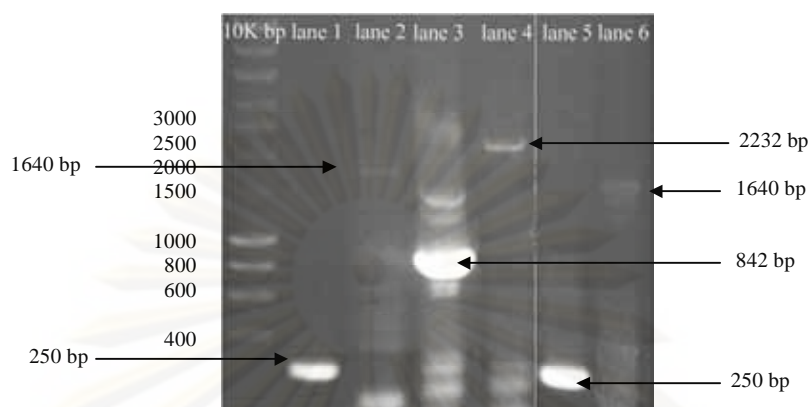


Figure 29(C): PCR amplification of *flaA* and *fliQ* genes from *H. pylori* wild type and mutated strains. The 10K bp was served as a molecular weight marker. Lane 1; *fliQ* gene amplified from ATCC26695 wild type strain (250 bp). Lane 2; *fliQ* gene amplified from *fliQ* mutant strain PQ (1640 bp). Lane 3; *flaA* gene amplified from N6 wild type strain (842 bp). Lane 4; *flaA* gene amplified from *flaA* mutant strain NA2 (2232 bp). Lane 5; *fliQ* gene amplified from N6 wild type strain (250 bp). Lane 6; *fliQ* gene amplified from *fliQ* mutant strain NQ (1640 bp).

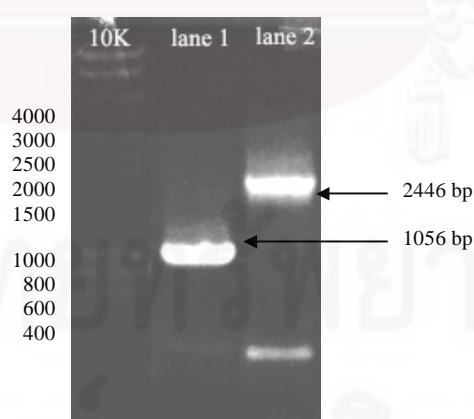


Figure 29(D): PCR amplification of *flgR* gene from *H. pylori* wild type and mutated strains. The 10K bp was served as a molecular weight marker. Lane 1; *flgR* gene amplified from N6 wild type strain (1056 bp). Lane 2; *flgR* gene amplified from *flgR* mutant strain NR2 (2446 bp).

8. Antimicrobial activity of curcumin against *H. pylori* wild types and flagellar mutants

The antimicrobial activity of curcumin against both *H. pylori* wild types and flagellar mutants were examined *in vitro* by agar dilution method. The compound significantly inhibited growth of *H. pylori* with MICs of 20 $\mu\text{g ml}^{-1}$ for ATCC26695, N6, and NQ; 30 $\mu\text{g ml}^{-1}$ for PA315, PQ, NA2, and NR2; and 40 $\mu\text{g ml}^{-1}$ for PR611. All the strains were sensitive to ampicillin with MICs $\leq 0.15 \mu\text{g ml}^{-1}$. Table 9 shows MICs of ampicillin and curcumin of individual strains. Sub-MICs of curcumin were considered as 1-fold concentration under MICs, and were applied in the subsequent experiments beyond this.

| Strains | Average MICs of ampicillin ($\mu\text{g ml}^{-1}$) | Average MICs of curcumin ($\mu\text{g ml}^{-1}$) | Average sub-MICs of curcumin ($\mu\text{g ml}^{-1}$) |
|-----------|--|--|--|
| ATCC26695 | ≤ 0.15 | 20 | 10 |
| PA315 | ≤ 0.15 | 30 | 20 |
| PR611 | ≤ 0.15 | 40 | 30 |
| PQ | ≤ 0.15 | 30 | 20 |
| N6 | ≤ 0.15 | 20 | 10 |
| NA2 | ≤ 0.15 | 30 | 20 |
| NR2 | ≤ 0.15 | 30 | 20 |
| NQ | ≤ 0.15 | 20 | 10 |

Table 9: Average MICs and sub-MICs of curcumin of individual *H. pylori* wild type strains, ATCC26695 and N6, and their isogenic mutants, PA315, PR611, PQ, NA2, NR2, NQ. Experiments were performed in duplicate on three separated occasions. Results are expressed in mean.

9. Comparison of biofilm formation among *H. pylori* wild types and flagellar mutants

We established *H. pylori* biofilm using pellicle assay as described in the Chapter IV. Two types of biofilm were observed which were pellicle and attached biofilm. The biofilm levels of both wild type and mutated strains were graded as following; (-, absent); not any form of biofilm seen, (+, just visible); thin pellicle film or a fine attached biofilm, (++, intermediate); accumulated pellicle covering just the center of liquid surface or a thin attached biofilm, (+++, extensive); a mature pellicle covering whole liquid surface or a dense attached biofilm. The results of biofilm scoring are summarized in Table 10. The result shown that every strain that produced pellicle was also capable to form attached biofilm. Notably, the attached biofilms of both *H. pylori* ATCC26695 and N6 were initially observed on day 3 after incubation following with the pellicle formation, which was detected on day 4 and 3, respectively. Both of *H. pylori* ATCC26695 and N6 wild type strains extensively formed pellicle and attached to the surface of glass test tube, at the air-liquid interface since day 6 and 5 of incubation, respectively. Figure 30 (test tubes in the left panel) shows pellicle and attached biofilm established by *H. pylori* both wild types and mutants observed on day 7 of incubation. Figure 30A and E show biofilm characteristics of ATCC26695 and N6, respectively. The pellicle floating at air-liquid interface clearly detached from the attached biofilm (Figure 30E). However, the floating pellicle tended to drop easily to bottom of test tube when disturbed, whilst the attached biofilm stuck firmly to glass test tube even after removal of all medium (data not shown).

We also assessed the effect of *flaA*, *flgR*, and *fliQ* on *H. pylori* biofilm formation. The isogenic *H. pylori* mutants of these relative genes were therefore tested for their ability to form biofilm using pellicle assay as performed with their wild types. All the mutants demonstrated a delayed biofilm formation. The earliest biofilm formation was initially observed on day 4 of incubation in PQ, NA2, and NQ (Table 10). The NR2 started to form biofilm on day 5 of incubation, whereas PA315 and PR611 firstly produced biofilm on day 6 of incubation. Comparison of biofilm level between wild types and flagellar mutants on day 7 of incubation, it was found that no mature biofilm in either pellicle or attached biofilm were detected in all *H. pylori* flagellar mutants. The level of pellicle and attached biofilm was reduced in PA315, PQ, NA2 and NQ mutants (Table 10). Only small floating pellicle and thin line of attached biofilm were detected in almost flagellar mutants. In the meantime, the PR611 and NR2 mutants showed markedly decreased of pellicle rather than other strains, which only a pellicle assembled as thin floating layer and a just visible attached biofilm were observed. Figure 30B, C, and D (test tubes in the left panel) show biofilm produced by PA315, PR611, and PQ (the *flaA*, *fliQ*, and *flgR* mutants of ATCC26695), respectively. Figure 30F, G, and H (test tubes in the left panel) show biofilm produced by NA2, NR2, and NQ (the *flaA*, *fliQ*, and *flgR* mutants of N6), respectively.

10. Effect of curcumin against biofilm formation among *H. pylori* wild types and flagellar mutants

We investigated inhibitory action of curcumin against *H. pylori* wild type and mutant strains using pellicle assay as described in the Chapter IV. All the strains

were co-cultured with a presence of curcumin at sub-MICs as shown in Table 9. Curcumin showed inhibitory effect on biofilm produced by both *H. pylori* wild types and mutants. As summarized in Table 10, all curcumin treated strains obviously inhibited the biofilm formation, both pellicle and attached biofilm characteristics. Four of eight strains, including PA315, PR611, PQ, and NR2, treated with sub-MICs were completely unable to produce attached biofilm even until day 7 of incubation. The other four, including ATCC26695, N6, NA315, and NQ, however, were still capable to produce attached biofilm but at low level when compared to the untreated. Almost the curcumin treated strains failed to produce pellicle even until day 7 of incubation, except for N6 and NQ that could produce at very low level. Figure 30A to H (test tubes in the right panel) show the curcumin treated strains, which impaired to produce pellicle and attached biofilm on glass test tubes.

| Curcumin concentration | ATCC26695 | | | | PA315 | | | | PR611 | | | | PQ | | | | N6 | | | | NA2 | | | | NR2 | | | | NQ | | | |
|------------------------|-----------------------|------------------|------------------------|------------------|-----------------------|------------------|------------------------|------------------|-----------------------|------------------|------------------------|------------------|-----------------------|------------------|------------------------|------------------|-----------------------|------------------|------------------------|------------------|-----------------------|------------------|------------------------|------------------|-----------------------|------------------|------------------------|------------------|-----------------------|------------------|------------------------|--|
| | 0 µg ml ⁻¹ | | 10 µg ml ⁻¹ | | 0 µg ml ⁻¹ | | 20 µg ml ⁻¹ | | 0 µg ml ⁻¹ | | 30 µg ml ⁻¹ | | 0 µg ml ⁻¹ | | 20 µg ml ⁻¹ | | 0 µg ml ⁻¹ | | 10 µg ml ⁻¹ | | 0 µg ml ⁻¹ | | 20 µg ml ⁻¹ | | 0 µg ml ⁻¹ | | 20 µg ml ⁻¹ | | 0 µg ml ⁻¹ | | 10 µg ml ⁻¹ | |
| Day | Pellicle | Attached biofilm | Pellicle | Attached biofilm | Pellicle | Attached biofilm | Pellicle | Attached biofilm | Pellicle | Attached biofilm | Pellicle | Attached biofilm | Pellicle | Attached biofilm | Pellicle | Attached biofilm | Pellicle | Attached biofilm | Pellicle | Attached biofilm | Pellicle | Attached biofilm | Pellicle | Attached biofilm | Pellicle | Attached biofilm | Pellicle | Attached biofilm | Pellicle | Attached biofilm | | |
| 1 | - | - | - | - | - | - | - | - | - | - | - | - | - | - | - | - | - | - | - | - | - | - | - | - | - | - | - | - | - | - | | |
| 2 | - | - | - | - | - | - | - | - | - | - | - | - | - | - | - | - | - | - | - | - | - | - | - | - | - | - | - | - | - | - | | |
| 3 | - | + | - | - | - | - | - | - | - | - | - | - | - | - | + | + | - | - | - | - | - | - | - | - | - | - | - | - | - | - | | |
| 4 | + | + | - | - | - | - | - | - | - | - | - | - | + | - | ++ | ++ | - | - | + | - | - | - | - | - | - | - | + | + | - | - | | |
| 5 | ++ | ++ | - | - | - | - | - | - | - | - | - | - | + | + | - | - | +++ | +++ | + | + | + | ++ | - | - | - | - | + | + | + | + | | |
| 6 | +++ | +++ | - | - | + | + | - | - | - | + | - | - | ++ | ++ | - | - | +++ | +++ | + | + | + | ++ | - | + | - | + | + | ++ | ++ | + | + | |
| 7 | +++ | +++ | - | + | ++ | ++ | - | - | + | + | - | - | ++ | ++ | - | - | +++ | +++ | + | + | + | ++ | - | + | + | + | ++ | ++ | + | + | | |

Table 10: Pellicle and attached biofilm levels observed among *H. pylori* wild types and their isogenic mutants, in an absence and presence of curcumin. A development of two biofilm characteristics (pellicle and attached biofilm) were daily observed and scored through 7 days. Level of individual biofilm type represent as (-, absent); not any form of biofilm seen, (+, just visible); thin pellicle film or a fine attached biofilm, (++, intermediate); accumulated pellicle covering just the center of liquid surface or a thin attached biofilm, (+++, extensive); a mature pellicle covering whole liquid surface or a dense attached biofilm. Experiments were performed in duplicate on three separated occasions. Representative scores were the major scores derived from three separated experiments. Biofilm grading was based on Josh *et al.* (96). Level of individual biofilm type represent as -, absent; +, small (just visible); ++, intermediate; +++, extensive. Revise table with everyday score

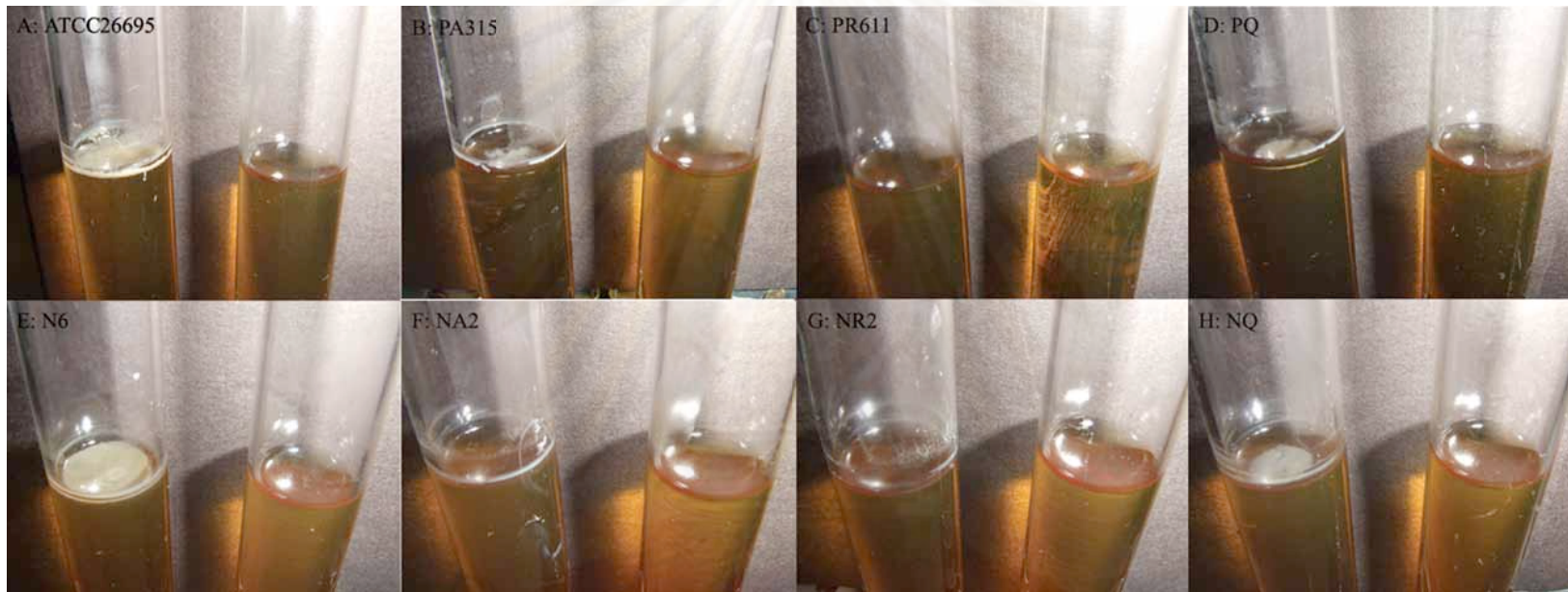


Figure 30: Biofilm characteristics represented by pellicle and attached biofilm formation following 7-d incubation. (A), (B), (C), and (D) show *H. pylori* ATCC26695, PA315, PR611, and PQ biofilms, respectively. (E), (F), (G), and (H) show N6, NA2, NR2, and NQ biofilms, respectively. The left panel test tubes are cultures without curcumin addition. The right panel test tubes are cultures with a presence of sub-MICs of curcumin of individual strains. Test tubes not to scale.

11. Quantification of biofilm formation performed by modified assay in polystyrene plates

We established a modified method to quantify biofilm formation of *H. pylori* in polystyrene plates containing glass coverslips, which allowed bacteria to adhere to the surface provided as described in the Chapter IV. The adherent bacterial community considered as biofilm was stained with crystal violet. The absorbance of biofilm-bound crystal violet was then measured by spectrophotometer at 570 nm. Figure 30 demonstrates absorbance of individual sample directly representing biofilm level produced by *H. pylori* wild types and their isogenic *flaA*, *flgR*, *fliQ* mutants in this study. *H. pylori* ATCC26695 formed biofilm level significantly higher than PR611 ($P= 0.021$). On a contrary, Strains PA315 and PQ produced no different biofilm level compared to the wild type ($P> 0.05$). The level of biofilm was expressed as mean of tested OD values subtracted by mean of blank OD. The biofilm level of ATCC26695, PA315, PR611, and PQ were 0.388, 0.215, 0.133, and 0.252 (Figure 31A). In addition, N6 wild type consistently produced higher biofilm level compared to its mutants. The N6 strain produced biofilm level significantly higher than both NR2 and NQ ($P= 0.003$ and 0.007 , respectively). However, no significance difference between N6 and NA2 biofilm levels ($P> 0.05$). Among mutant strains, NA2 significantly produced higher biofilm level than NR2 ($P= 0.037$), but not NQ ($P> 0.05$). The biofilm level of N6, NA2, NR2, and NQ were 0.341, 0.266, 0.138, and 0.163, respectively (Figure 31B).

The inhibitory activity of curcumin at sub-MICs (1/2 MICs) against *H. pylori* biofilm formation was examined quantitatively. Curcumin significantly inhibited the production of biofilm by *H. pylori* wild type ATCC26695 and mutant strain NA2. In

comparison to curcumin-untreated *H. pylori*, the treated-group decreasingly produced biofilm in these two strains. As shown in Figure 32, either curcumin-treated ATCC26695 (Figure 32A) or curcumin-treated flagellar mutants NA2 (Figure 32B) significantly produced biofilm level lower than their untreated-ones ($P= 0.015$ and 0.008 , respectively). The biofilm level of curcumin-treated ATCC26695 and NA2 were as low as 0.157 and 0.094 , respectively. However, other strains included PA315, PR611, PQ, N6, NR2, and NQ were not affected by curcumin ($P > 0.05$). The biofilm levels of these curcumin-treated strains were of 0.072 , 0.048 , 0.153 , 0.179 , 0.087 , and 0.079 , respectively (Figure 32A and B).

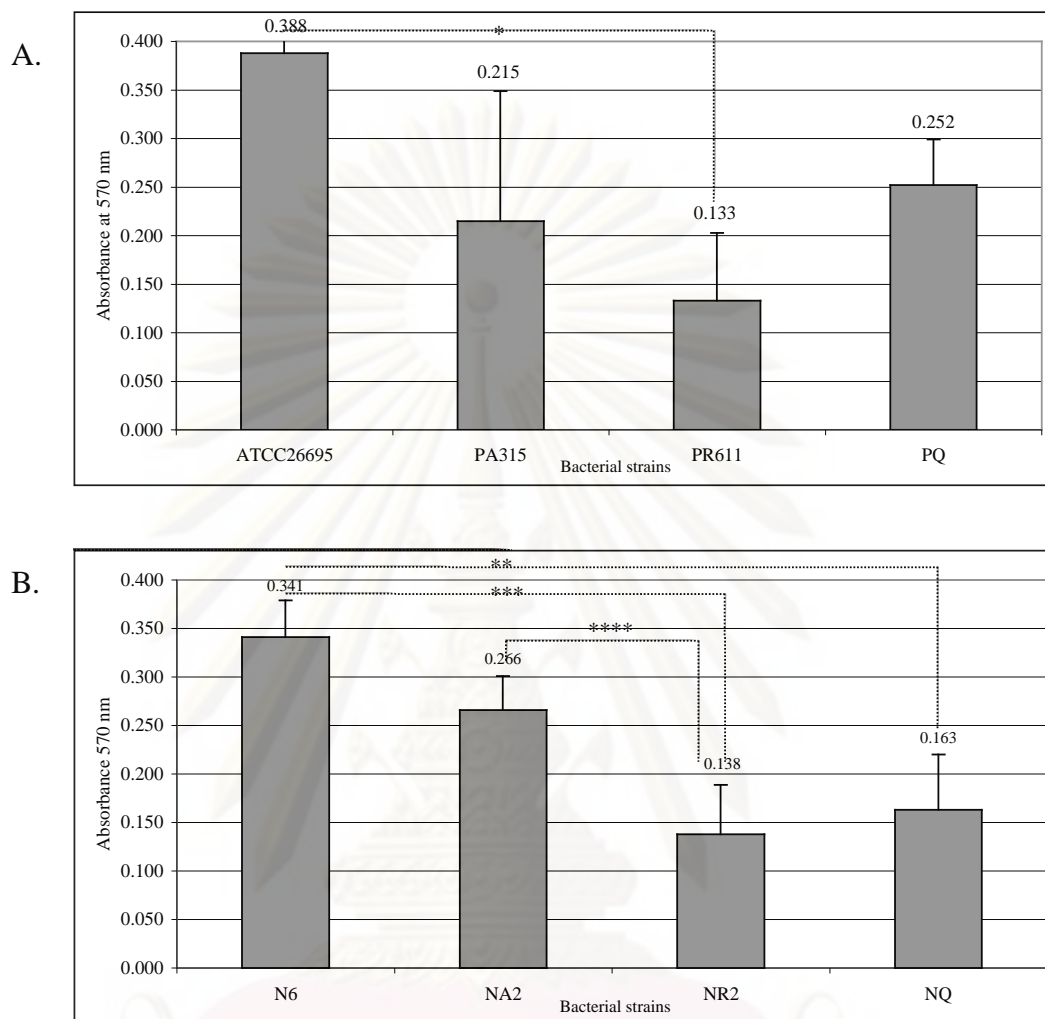


Figure 31: Biofilm level quantification of *H. pylori* wild types and flagellar mutants performed by modified assay in polystyrene plates. (A) Biofilm level quantification in ATCC26695, PA315, PR611, and PQ. (B) Biofilm level quantification in N6, NA2, NR2, and NQ. The level of biofilm was expressed as mean of tested OD values subtracted by mean of blank OD. Experiments were performed in duplicate on three separated occasions. Error bars represent \pm standard deviation from the mean. *, **, ***, and **** Statistical significant differences were accepted at the $P=0.021$, 0.007 , 0.003 , and 0.037 level, respectively.

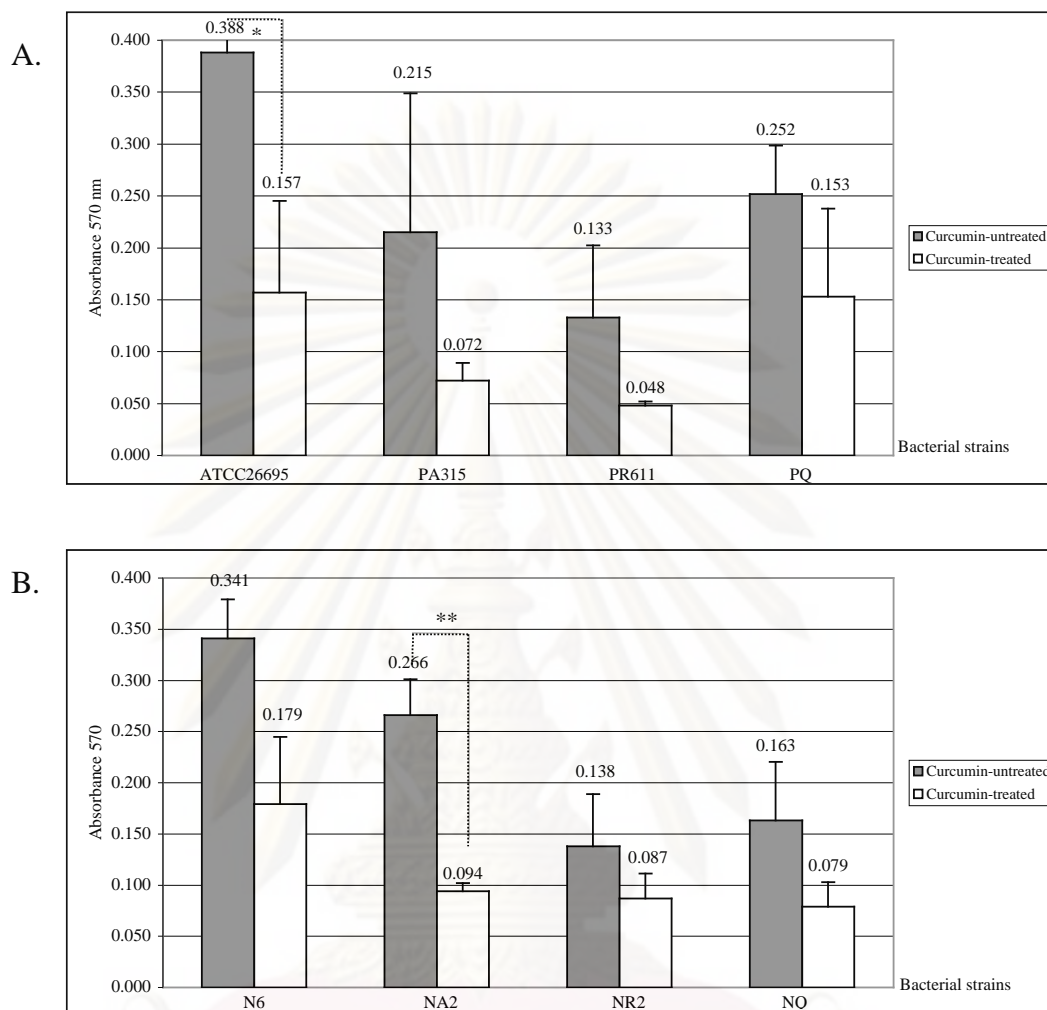


Figure 32: Biofilm level quantification of curcumin-treated *H. pylori* wild types and flagellar mutants compared to the untreated. The quantification was performed by modified assay in polystyrene plates. (A) Biofilm level quantification in ATCC26695, PA315, PR611, and PQ with an absence and presence curcumin. (B) Biofilm level quantification in N6, NA2, NR2, and NQ with an absence and presence curcumin. The level of biofilm was expressed as mean of tested OD values subtracted by mean of blank OD. Experiments were performed in duplicate on three separated occasions. Error bars represent \pm standard deviation from the mean. * and **Statistical significant differences were accepted at the $P= 0.015$ and 0.008 level, respectively.

12. Adhesion of *H. pylori* wild types and their isogenic mutants against the HEp-2 cells

In order to study the role of *flaA*, *flgR*, and *fliQ* genes in adherence to human epithelial cells, which thought to be the first step of biofilm formation *in vivo*. All the mutant strains were tested for the ability to adhere to human laryngeal epithelial HEp-2 cells compared with their wild types. The bacteria were co-cultured with the HEp-2 cells. The cells were lysed and the adherent bacteria were plated out. Number of growth colony was enumerated. The percent of adherence bacteria was expressed as a proportion of adherence bacteria versus control. The proportion of adherence bacteria was calculated as the rate of the number of adherence bacteria divided by the bacterial inoculum. PQ showed the most noticeably reduced level of adherence following by PR611 and PA315, respectively, compared to ATCC26695. In this study, the original bacterial inoculum volume was $3.00 \pm 0.00 \times 10^8$ CFU ml⁻¹. The numbers of colony count of *H. pylori* ATCC26695, PA315, PR611, and PQ were $9.43 \pm 5.87 \times 10^7$ CFU ml⁻¹, $2.37 \pm 2.57 \times 10^7$ CFU ml⁻¹, $1.63 \pm 2.15 \times 10^7$ CFU ml⁻¹, and $5.33 \pm 5.03 \times 10^6$ CFU ml⁻¹, respectively. In comparison to a percentile of adhesion of the ATCC26695 wild type as 100 %, it significantly reduced to 13.02% and 8.69% for the PR611 and PQ, respectively ($P= 0.010$ and 0.008 , respectively). The PA315 showed no significant difference of percentile of adhesion, which was 38.45% ($P > 0.05$) (Figure 33A). Consistent with the results seen in NR2 and NQ, a marked decrease of adherence in these mutants was observed. The NQ showed the most reduced adherent ability following by NR2 and NA2, respectively, compared to N6. The numbers of colony count of *H. pylori* N6, NA2, NR2, and NQ were

$8.27 \pm 2.85 \times 10^7$ CFU ml⁻¹, $4.30 \pm 5.02 \times 10^7$ CFU ml⁻¹, $8.67 \pm 8.02 \times 10^6$ CFU ml⁻¹, and $1.67 \pm 2.08 \times 10^6$ CFU ml⁻¹, respectively. Percentile of adherence significantly reduced to only 12.22% and 2.63% for the NR2 and NQ, respectively, compared to the N6 (100%) ($P = 0.006$ and 0.003 , respectively) (Figure 34B). The NA2 showed no significant difference of percentile of adhesion, which was 47.29% ($P > 0.05$) (Figure 33B).

Interestingly, curcumin at sub-MIC significantly affected the *H. pylori* adherence to the epithelial cell lines in all strains. As the result shown, all of strains treated with curcumin at 1/2 MIC completely failed to adhere to the HEp-2 cells (Figure 33A and B). Percentile of adherence was represented as 0% for all curcumin-treated strains.

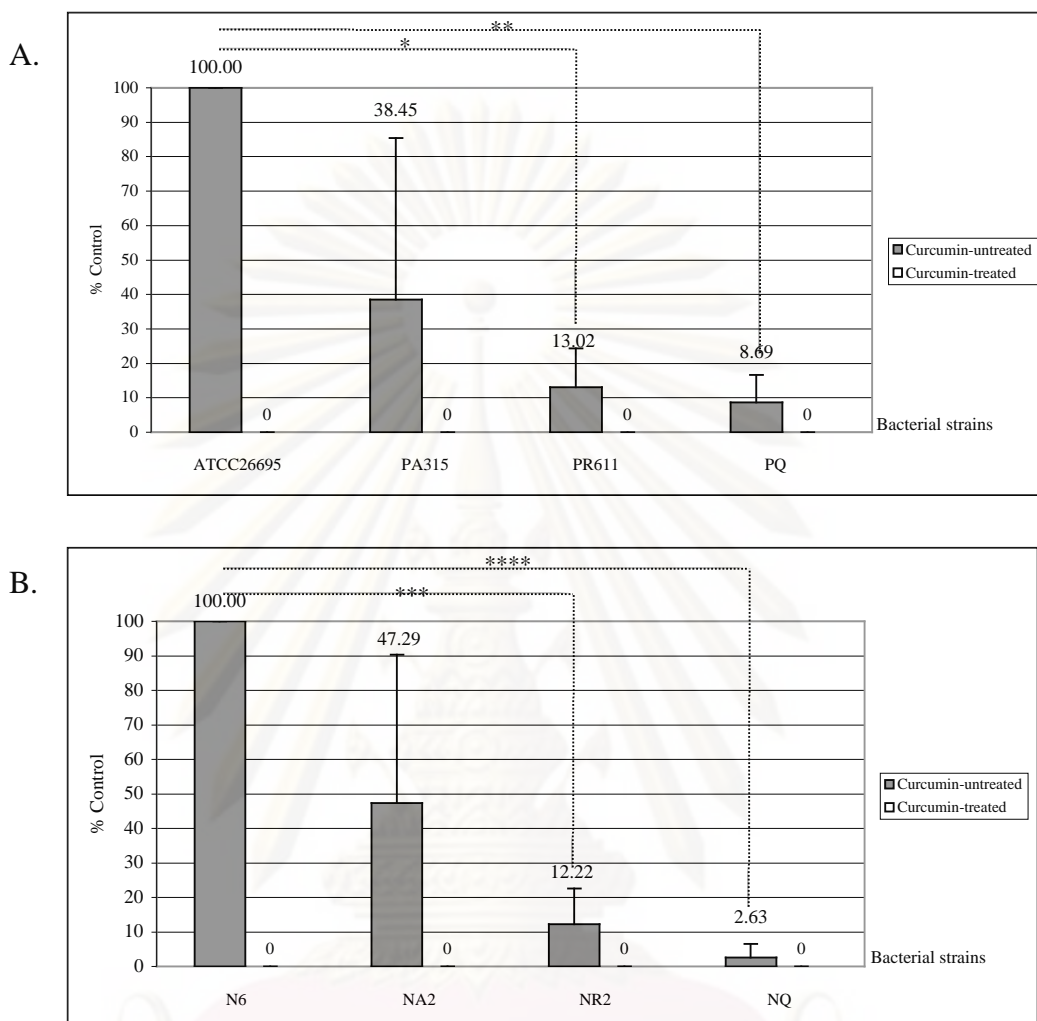


Figure 33: Percentile of adhesion of *H. pylori* wild types and flagellar mutants. (A) Percentile of adhesion of ATCC26695, PA315, PR611, and PQ with an absence and presence curcumin. (B) Percentile of adhesion of N6, NA2, NR2, and NQ with an absence and presence curcumin. Results expressed as the proportion of adherence bacteria versus control. Experiments were performed in duplicate on three separated occasions. Error bars represent \pm standard deviation from the mean. *, **, ***, and ****Statistical significant differences was accepted at the $P= 0.010, 0.008, 0.006,$ and 0.003 level, respectively.

Phase II: Effect of Curcumin Against *H. pylori* Biofilm Formation and Adhesion of *H. pylori* Against HEp-2 Cells

13. Screening for biofilm formation

In order to investigate the variability of *H. pylori* strains to produce biofilm and to find out for the most suitable *H. pylori* biofilm-producing strain for the subsequent analysis, 14 strains of *H. pylori* were preliminary screened for biofilm formation by pellicle assay as described in the Chapter IV. These strains included three reference strains (ATCC43504, ATCC43526, ATCC51932) and eleven isolates (DMST20165, DMST20885, and clinical strains 1203, 1260, 1261, 1264, 1265, 1268, 1275, LP25 and UT142). The development of biofilm formation was observed daily through 7 days of incubation. The biofilm levels were graded as score as previously described. Every strain exhibited ability to form biofilm in both two characteristics, including pellicle and attached biofilm, in the culture test tubes at the air-liquid interface (Figure 34). A development of these two characteristics of *H. pylori* biofilm is shown in Table 11. The biofilm of three strains, including ATCC43504, ATCC43526, and 1264, could be initially observed on day 3 of incubation. Almost strains, including DMST20885, 1203, 1260, 1261, 1265, 1268, 1275, and UT142, started to form biofilm on day 4 of incubation. However the other two strains, DMST20165 and LP25 initially formed biofilm after 5 days of incubation. Notably, ATCC51932 failed to form biofilm in the same period as others, which later started to form biofilm on day 7 of incubation. The biofilm levels, both in the form of pellicle and attached biofilm, produced by every strain increasingly developed from the first day that they were observed through day 7. At the end of incubation period, nine strains of *H. pylori*, including ATCC43504, ATCC43526, DMST20165,

DMST20885, 1261, 1264, 1265, 1268, and UT142, produced extensive levels of pellicle and attached biofilm as scored as ++++. Four strains, including 1203, 1260, 1275, and LP25, formed pellicle and attached biofilm in intermediate levels as scored as ++. Only one strain, ATCC51932, developed both two biofilm characteristics only low level as scored as +.

As the results shown, 3 strains, including ATCC43504, ATCC43526, and 1264, exhibited the most powerful potential in producing biofilm in similar levels. However, only the ATCC43504 strain was considered and chosen for subsequent study.



ศูนย์วิทยทรัพยากร
จุฬาลงกรณ์มหาวิทยาลัย

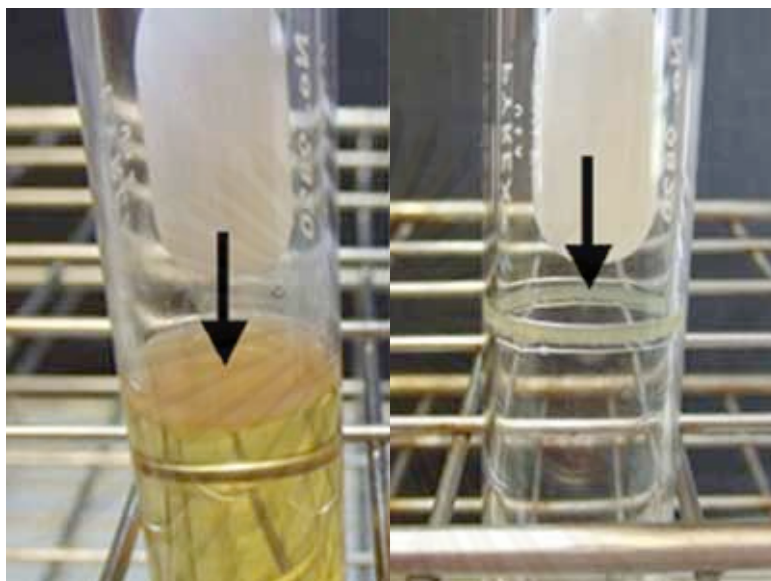


Figure 34. Photograph of pellicle assay showing 7-day biofilm formed by *H. pylori* ATCC43504. Left test tube, culture grown without curcumin demonstrating mature biofilm at air-liquid interface. Two biofilm characteristics were observed, including pellicle (left test tube) and attached biofilm (right test tube). Test tubes not to scale.

| Day | ATCC43504 | | ATCC43526 | | ATCC51932 | | DMST20165 | | DMST20885 | | 1203 | | 1260 | | 1261 | | 1264 | | 1265 | | 1268 | | 1275 | | LP25 | | UT142 | |
|-----|-----------|------------------|-----------|------------------|-----------|------------------|-----------|------------------|-----------|------------------|----------|------------------|----------|------------------|----------|------------------|----------|------------------|----------|------------------|----------|------------------|----------|------------------|----------|------------------|----------|------------------|
| | Pellicle | Attached biofilm | Pellicle | Attached biofilm | Pellicle | Attached biofilm | Pellicle | Attached biofilm | Pellicle | Attached biofilm | Pellicle | Attached biofilm | Pellicle | Attached biofilm | Pellicle | Attached biofilm | Pellicle | Attached biofilm | Pellicle | Attached biofilm | Pellicle | Attached biofilm | Pellicle | Attached biofilm | Pellicle | Attached biofilm | Pellicle | Attached biofilm |
| 1 | - | - | - | - | - | - | - | - | - | - | - | - | - | - | - | - | - | - | - | - | - | - | - | - | - | - | - | - |
| 2 | - | - | - | - | - | - | - | - | - | - | - | - | - | - | - | - | - | - | - | - | - | - | - | - | - | - | - | - |
| 3 | + | + | + | + | - | - | - | - | - | - | - | - | - | - | - | - | + | ++ | - | - | - | - | - | - | - | - | - | - |
| 4 | ++ | ++ | +++ | +++ | - | - | - | - | ++ | ++ | + | + | + | + | + | + | +++ | +++ | + | + | + | + | + | + | + | + | ++ | ++ |
| 5 | +++ | +++ | +++ | +++ | - | - | ++ | + | +++ | +++ | ++ | ++ | + | + | ++ | ++ | +++ | +++ | ++ | ++ | +++ | +++ | ++ | ++ | + | + | +++ | +++ |
| 6 | +++ | +++ | +++ | +++ | - | - | ++ | ++ | +++ | +++ | ++ | ++ | ++ | ++ | ++ | ++ | +++ | +++ | ++ | ++ | +++ | +++ | ++ | ++ | ++ | ++ | +++ | +++ |
| 7 | +++ | +++ | +++ | +++ | + | + | +++ | +++ | +++ | +++ | ++ | ++ | ++ | ++ | +++ | +++ | +++ | +++ | +++ | +++ | +++ | +++ | +++ | ++ | ++ | +++ | +++ | +++ |

Table 11: A development of biofilm levels of fourteen strains of *H. pylori*. A development of two biofilm characteristics (pellicle and attached biofilm) were daily observed and scored through 7 days. Level of individual biofilm type represent as (-, absent); not any form of biofilm seen, (+, just visible); thin pellicle film or a fine attached biofilm, (++, intermediate); accumulated pellicle covering just the center of liquid surface or a thin attached biofilm, (+++, extensive); a mature pellicle covering whole liquid surface or a dense attached biofilm. Experiments were performed in duplicate on three separated occasions. Representative scores were the major scores derived from three separated experiments. Biofilm grading was based on Josh *et al.* (96).

14. The antimicrobial activity of curcumin against *H. pylori* strains

We investigated the MIC of curcumin against 11 strains of *H. pylori* included ATCC43526, ATCC51932, DMST20165, DMST20885, and clinical strains C7, C42, 742, 749, 849, 867, and 928. Curcumin significantly inhibited the growth of strain 849, 867, and 928 at an MIC value of 8 $\mu\text{g ml}^{-1}$. Additionally, the compound inhibited growth of *H. pylori* with MICs of 9.33 $\mu\text{g ml}^{-1}$ for ATCC51932 and DMST20885; 14.67 $\mu\text{g ml}^{-1}$ for C7; 16 $\mu\text{g ml}^{-1}$ for ATCC43504, ATCC43526, and clinical strain 749; 22.67 $\mu\text{g ml}^{-1}$ for DMST20165; 24 $\mu\text{g ml}^{-1}$ for C42; 26.67 $\mu\text{g ml}^{-1}$ for 742. All the strains were sensitive to ampicillin with MICs $\leq 0.15 \mu\text{g ml}^{-1}$. DMSO at concentration of 0.24%, which was the highest concentration mixed in curcumin suspension, showed no effect against bacterial viability. Table 12 shows MICs of ampicillin and curcumin of individual strains.

| Strains | Average MICs of ampicillin ($\mu\text{g ml}^{-1}$) | Average MICs of curcumin ($\mu\text{g ml}^{-1}$) |
|-----------|---|---|
| ATCC43504 | ≤ 0.15 | 16 |
| ATCC43526 | ≤ 0.15 | 16 |
| ATCC51932 | ≤ 0.15 | 22.67 |
| DMST20165 | ≤ 0.15 | 22.67 |
| DMST20885 | ≤ 0.15 | 9.33 |
| C7 | ≤ 0.15 | 14.67 |
| C42 | ≤ 0.15 | 24 |
| 742 | ≤ 0.15 | 26.67 |
| 749 | ≤ 0.15 | 16 |
| 849 | ≤ 0.15 | 8 |
| 867 | ≤ 0.15 | 8 |
| 928 | ≤ 0.15 | 8 |

Table 12: Average MICs of twelve strains of *H. pylori*. The strains included ATCC43504, ATCC43526, ATCC51932, DMST20165, DMST20885, C7, C42, 742, 749, 849, 867, and 928. Experiments were performed in duplicate on three separated occasions. Results are expressed in mean.

15. Inhibitory activity of curcumin on *H. pylori* biofilm

15.1 Effect of curcumin concentration against *H. pylori* biofilm formation

In order to determine effect of curcumin concentration against *H. pylori* biofilm formation, curcumin was tested at various sub-MICs including 1/2, 1/4, 1/8, 1/16, and 1/32 MIC. *H. pylori* ATCC43504 was grown as pellicle assay, as previously described in the Chapter IV, in a presence of these relative curcumin concentrations. A development of biofilm was examined daily through 7 days. The biofilm levels were graded as score as previously described. The concentrations of curcumin at subinhibitory level; 1/2, 1/4, 1/8, 1/16, 1/32 MIC, and control, used for biofilm assay in this study were 8, 4, 2, 1, 0.5, and 0 $\mu\text{g ml}^{-1}$, respectively. Their inhibitory effects on biofilm formation of *H. pylori* ATCC43504 are shown in Table 13. In the control, both pellicle and attached biofilm were firstly detected since day 3 of incubation, following by an expansion of bacterial biofilm on the continuous days. The biofilm became fully mature and was clearly observed on day 5. This mature pellicle and attached biofilm were steadily maintained through day 7 of observation. The similar characteristic of biofilm production also appeared in curcumin treated at 1/8, 1/16 and 1/32 MIC. While, curcumin at 1/4 MIC markedly impaired biofilm formation, the complete inhibition of biofilm formation was demonstrated at 1/2 MIC. DMSO at concentration of 0.016%, which was the highest concentration, mixed in curcumin suspension, showed no effect against *H. pylori* biofilm production.

| Curcumin concentrations | 0 | | 1/32 MIC | | 1/16 MIC | | 1/8 MIC | | 1/4 MIC | | 1/2 MIC | | 0.016% DMSO | |
|-------------------------|----------|------------------|----------|------------------|----------|------------------|----------|------------------|----------|------------------|----------|------------------|-------------|------------------|
| | Pellicle | Attached biofilm | Pellicle | Attached biofilm | Pellicle | Attached biofilm | Pellicle | Attached biofilm | Pellicle | Attached biofilm | Pellicle | Attached biofilm | Pellicle | Attached biofilm |
| 1 | - | - | - | - | - | - | - | - | - | - | - | - | - | - |
| 2 | - | - | - | - | - | - | - | - | - | - | - | - | - | - |
| 3 | + | + | + | + | - | + | - | + | - | - | - | - | + | + |
| 4 | ++ | ++ | ++ | ++ | + | + | + | + | - | - | - | - | ++ | + |
| 5 | +++ | +++ | +++ | +++ | ++ | +++ | ++ | +++ | - | + | - | - | +++ | ++ |
| 6 | +++ | +++ | +++ | +++ | +++ | +++ | ++ | +++ | + | + | - | - | +++ | +++ |
| 7 | +++ | +++ | +++ | +++ | +++ | +++ | +++ | +++ | ++ | ++ | - | - | +++ | +++ |

Table 13: Inhibitory effects of curcumin at subinhibitory concentrations on *H. pylori*

ATCC43504 biofilm formation. A development of pellicle and/or attached biofilm was daily observed and until 7 days. Level of individual biofilm type represent as (-, absent); not any form of biofilm seen, (+, just visible); thin pellicle film or a fine attached biofilm, (++, intermediate); accumulated pellicle of liquid surface or a thin attached biofilm, (+++, extensive); a mature pellicle covering whole liquid surface or a dense attached biofilm. Experiments were performed in duplicate on three separated occasions. Representative scores were the major scores derived from three separated experiments. Biofilm grading was based on Josh *et al.* (96).

15.2 Effects of curcumin at various incubation times on *H. pylori* biofilm formation

In order to examine the effect of incubation time against biofilm formation of *H. pylori* ATCC 43504 both in curcumin treated and untreated condition, the biofilm production was observed daily through day 21. Curcumin concentrations at 1/4 and 1/2 MIC, which displayed significant effects against biofilm formation, were selected for prolonged treatment-time. The biofilm levels were graded as score as previously described. Interestingly, it was found that the ability of bacteria to form biofilm, which was initially suppressed by effect of curcumin, could be restored during prolong incubation (Table 14). The biofilm, initially produced in intermediate level, with a presence of curcumin at 1/4 MIC developed to be mature on day 9 for attached biofilm and day 10 for pellicle. Furthermore, the culture with a presence of curcumin at 1/2 MIC, which did not form biofilm in the first 7 days of incubation, restored ability to form biofilm during a prolonged incubation. The pellicle and attached biofilm were first observable on day 15 whilst biofilm became mature on day 17.

| Curcumin concentrations | 0 | | 1/4 MIC | | 1/2 MIC | |
|-------------------------|----------|------------------|----------|------------------|----------|------------------|
| | Pellicle | Attached biofilm | Pellicle | Attached biofilm | Pellicle | Attached biofilm |
| 1 | - | - | - | - | - | - |
| 2 | - | - | - | - | - | - |
| 3 | - | + | - | - | - | - |
| 4 | + | + | - | + | - | - |
| 5 | ++ | +++ | - | + | - | - |
| 6 | +++ | +++ | + | + | - | - |
| 7 | +++ | +++ | + | + | - | - |
| 8 | +++ | +++ | ++ | ++ | - | - |
| 9 | +++ | +++ | ++ | +++ | - | - |
| 10 | +++ | +++ | +++ | +++ | - | - |
| 11 | +++ | +++ | +++ | +++ | - | - |
| 12 | +++ | +++ | +++ | +++ | - | - |
| 13 | +++ | +++ | +++ | +++ | - | - |
| 14 | +++ | +++ | +++ | +++ | - | - |
| 15 | +++ | +++ | +++ | +++ | + | + |
| 16 | +++ | +++ | +++ | +++ | ++ | ++ |
| 17 | +++ | +++ | +++ | +++ | +++ | +++ |
| 18 | +++ | +++ | +++ | +++ | +++ | +++ |
| 19 | +++ | +++ | +++ | +++ | +++ | +++ |
| 20 | +++ | +++ | +++ | +++ | +++ | +++ |
| 21 | +++ | +++ | +++ | +++ | +++ | +++ |

Table 14: Effects of curcumin at various incubation times on *H. pylori* ATCC43504 biofilm formation. Biofilm developments were daily observed through 21 days in a presence of curcumin at 1/2 and 1/4 MIC. Level of individual biofilm type represent as (-, absent); not any form of biofilm seen, (+, just visible); thin pellicle film or a fine attached biofilm, (++, intermediate); accumulated pellicle of liquid surface or a thin attached biofilm, (+++), extensive); a mature pellicle covering whole liquid surface or a dense attached biofilm. Experiments were performed in duplicate on three separated occasions. Representative scores were the major scores derived from three separated experiments. Biofilm grading was based on Josh *et al.* (96).

16. Quantification of biofilm formation by modified crystal violet assay

Biofilm level of *H. pylori* ATCC43504 treated with various curcumin concentrations was quantitatively measured and compared with the untreated control using modified crystal violet assay as previously described in the Chapter IV. After complete 7-d incubation, a whole liquid compartment included pellicle was discarded. The left behind-attached biofilm was stained by crystal violet and the absorbance of biofilm bound-crystal violet was then measured by spectrophotometry at 570 nm. Although, quantification of biofilm formation was performed with only the attached biofilm compartment, this could still represent a trend of entire biofilm level in this study. The level of biofilm was expressed as mean of tested OD values subtracted by mean of blank OD. As shown in Figure 35, curcumin significantly decreased the biofilm formation in a dose dependent manner. Under the present of high curcumin concentrations, the less biofilm levels were measured. The biofilm treated with curcumin 1/2 and 1/4 MIC showed significant low level with the absorbance of 0.036 and 0.088, respectively ($P= 0.001$ and 0.000 , respectively). On a contrary, those treated with 1/8, 1/16, and 1/32 MIC exhibited higher biofilm level as almost similar as measured in the untreated one with no significant different biofilm level was detected ($P> 0.05$). The absorbance of 1/8, 1/16, 1/32 MIC and the control were 0.308, 0.307, 0.363, and 0.446, respectively. DMSO at concentration of 0.016% did not show any effect against *H. pylori* biofilm. The absorbance of DMSO control broth was 0.309, which did not differ from the curcumin-untreated broth ($P> 0.05$). Figure 36A shows biofilm formation of *H. pylori* ATCC43504 in both pellicle and attached biofilm forms with a presence of varied subinhibitory levels of curcumin,

while Figure 36B shows biofilm formation of the bacteria in control broth containing 0.016% DMSO, which was the highest concentration, mixed in curcumin suspension.

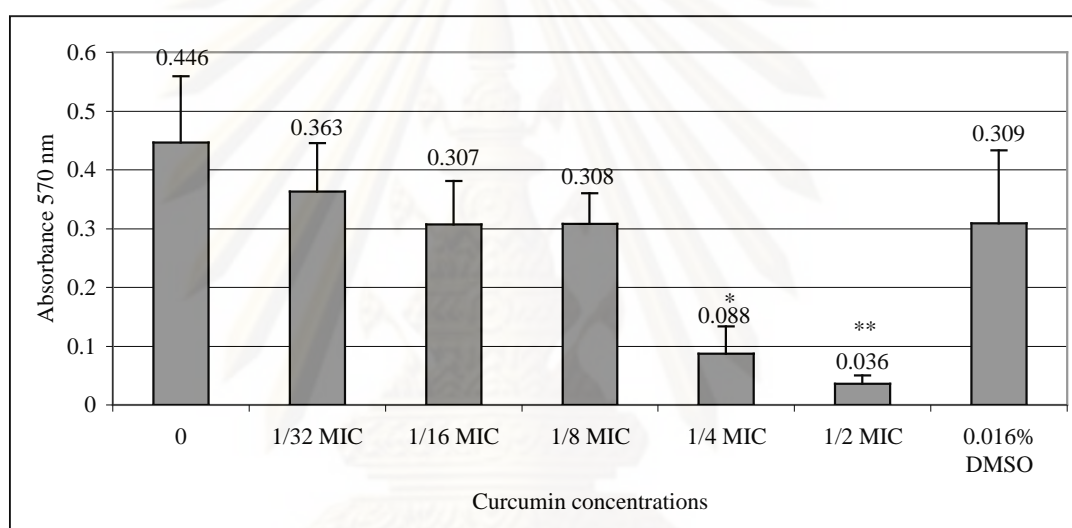


Figure 35: Biofilm level quantification of *H. pylori* ATCC43504 performed by modified crystal violet assay. The level of biofilm production was measured at absorbance 570 nm at 7 day. Experiments were performed in duplicate on three separated occasions. Error bars represent \pm standard deviation from the mean. * and **Statistical significant differences were accepted at the $P=$ 0.001 and 0.000, respectively

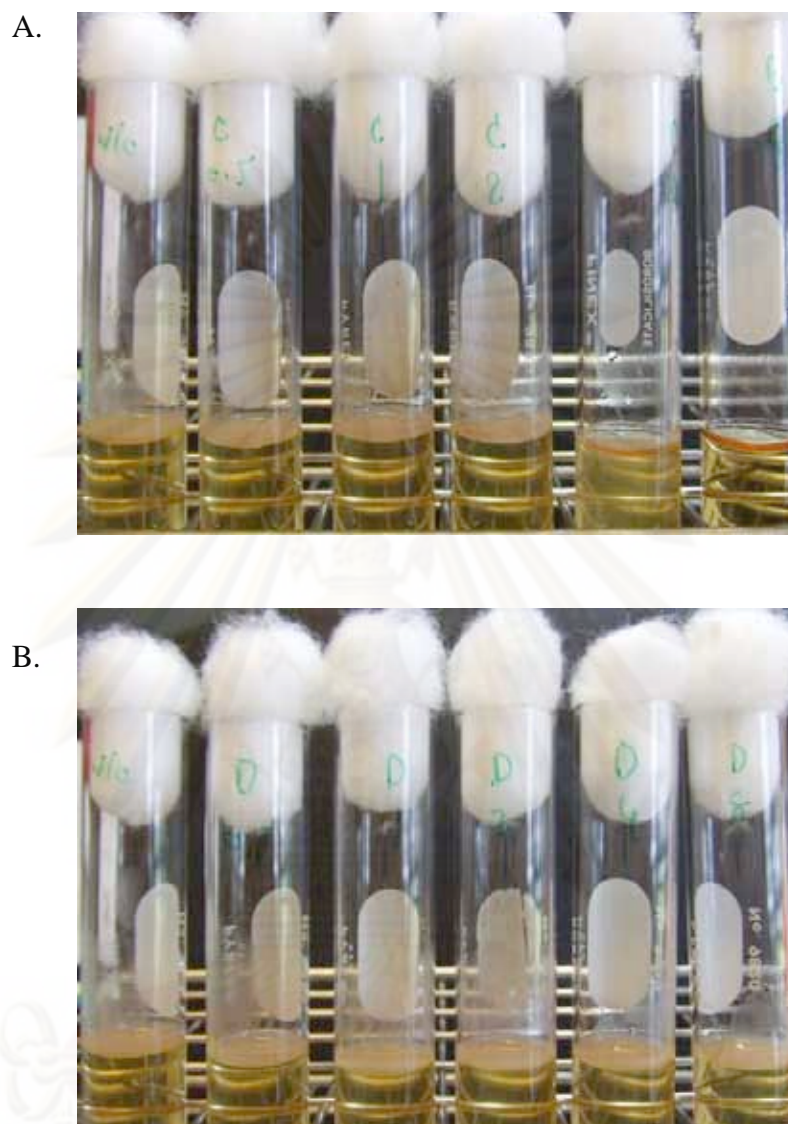


Figure 36: Biofilm formation of *H. pylori* ATCC43504 in a presence of various curcumin concentrations. Biofilm characteristics were represented by pellicle and attached biofilm. (A) Tubes, from left to right, show *H. pylori* ATCC43504 biofilms in an absence and presence of curcumin concentrations at subinhibitory levels; 0, 1/32, 1/16, 1/8, 1/4, and 1/2 MIC, respectively. (B) *H. pylori* ATCC43504 Biofilm in DMSO-free medium (the most far left tube) and *H. pylori* ATCC43504 in culture broth containing 0.016% DMSO (the most far right tube) Test tubes not to scale.

17. Scanning electron microscopy of *H. pylori* biofilm

We investigated a 3-D structure of *H. pylori* ATCC43504 biofilm and determined the effect of curcumin against its cytoarchitecture using SEM. Our SEM images were compared to the existing images from other works. Different ages of either *H. pylori* biofilm and/or planktonic grown as described in pellicle assay, in the Chapter IV, with an absence or presence of curcumin for 4, 5, 6, and 7 days were collected. The samples were 5 pellicles and 1 planktonic, comprising the 4-, 5-, 6-, and 7-d curcumin-untreated pellicles, the 7-d 1/4 MIC of curcumin-treated pellicle, and the 7-d 1/2 MIC of curcumin-treated planktonic which no biofilm observed. In our study, the SEM images of untreated *H. pylori* ATCC43504 taken from pellicle on day 4, 5, 6, and 7 (Figure 37A to D) reveal uniform biofilm architecture with dense accumulation of bacteria within an amorphous extracellular matrix. The cells embedded in the matrix connecting to each other by long fibrils and formed multicellular layers. Examination of adherent layers indicated the abundant of cross-linked fibrils that were associated with mature biofilms. The cells encased in the 7- and 6-d old pellicles without curcumin showed to produce more extensive amorphous extracellular substance and formation of the matrix of cross-linked fibrils, compared to those younger pellicles. Moreover, the bacterial morphology changed from bacillary to coccoid form in the older culture. The photographic evidences show the coccoid was predominant on day 7 following by day 6, 5, and 4, respectively.

In comparison to the biofilm architecture of curcumin-untreated, a fiber-like structure was found to adhere to rod shape bacteria, instead of coccoid form, in the biofilm derived from day 7 of 1/4 MIC treated *H. pylori* (Figure 37E). The SEM image show the cells predominately appeared in rod shape but, however, shorter than

those grown on routine solid medium (Figure 37G). In addition, the amorphous substance appeared to be lesser than the untreated sample (Figure 37A) taken from the same incubation period.

Interesting, there was no conspicuous evidence of biofilm formation observed from 7-d planktonic bacteria of 1/2 MIC treated *H. pylori* (Figure 37F). Neither amorphous extracellular substance nor complex bacterial layers were observed. The photographic evidence shows the bacterial cell dispersed thoroughly over a filter membrane. The bacterial cells were found in coccoid-rod mixed population and tended to produce fiber-like structure. Surprisingly, the cell destruction, represented by a pore formation over cell wall surface (Figure 37F; arrowed) occurred. While, bacteria grown without 2% (w/v) BCD have a filamentous coccoid morphology and flagellar could be observed on the surface (Figure 37G). Instead, a long bacillary shape was seen from 3-day old colonies (Figure 37H).

Noteworthy, the entire pellicle samples firmly aggregated compared to the planktonic. The pellicle was only dispersed but not dissolved in broth medium even after heavily vortex, while the planktonic was vigorously dissolved (data not shown).

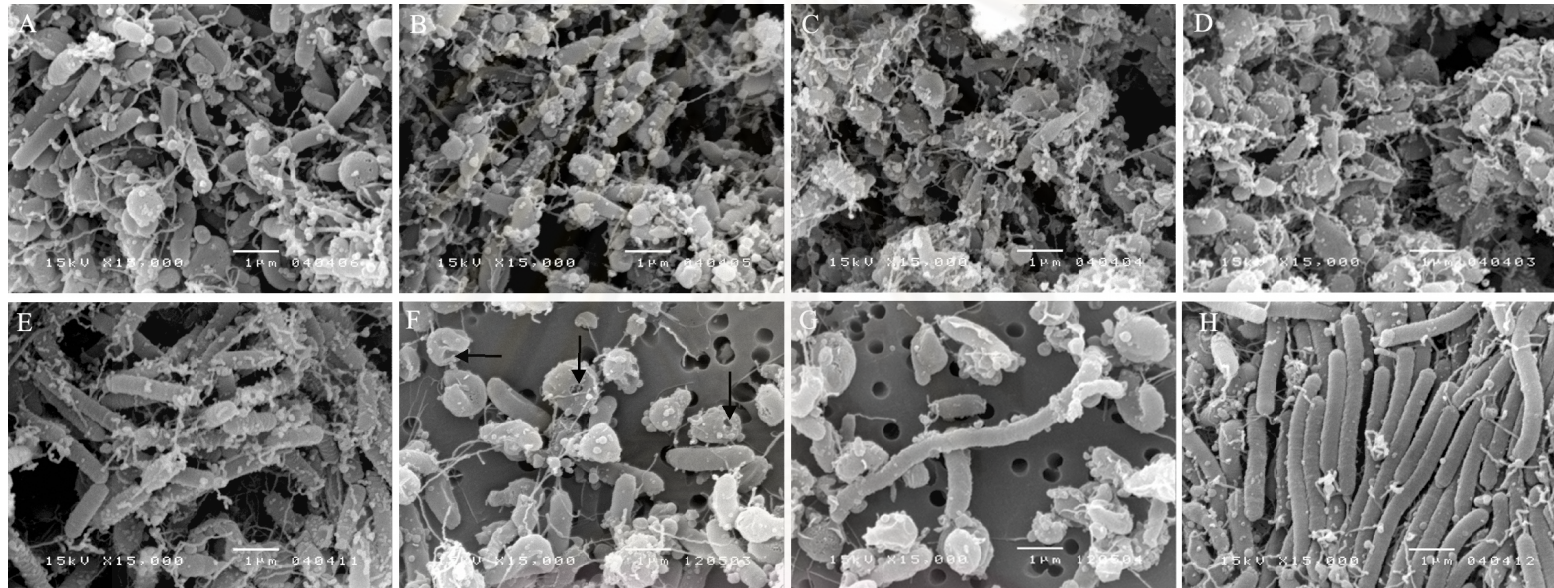


Figure 37: SEM photomicrograph of biofilm development of *H. pylori* ATCC43504 at a magnification of X 15,000. A-D; pellicle cells taken from bacterial culture without curcumin at day 4, 5, 6, and 7, respectively. E; pellicle cells taken from culture with 1/4 MIC of curcumin on day 7. F; planktonic cells taken from culture with 1/2 MIC of curcumin on day 7 show perforations on the cell surface (arrowed). G: bacterial cells taken from culture without 2% (w/v) BCD on day 7. H; Bacteria from 3-day direct colonies. Bars, 1µm.

18. Anti-adhesive property of curcumin against *H. pylori*

We analyzed an anti-adhesive property of curcumin against *H. pylori* ATCC43504 adhesion to the HEp-2 cells in this study in order to confirm our data earlier performed with *H. pylori* wild types and flagellar mutants. The anti-adhesive activity of curcumin at 1/2 MIC was assessed against *H. pylori* ATCC43504 on HEp-2 cells in this study. The cells were lysed after a complete co-cultivation, and the adherent bacteria were plated out. Number of growth colony was enumerated. The percent of adherence bacteria was expressed as a proportion of adherence bacteria in curcumin treated versus control in the untreated one. The proportion of adherence bacteria was calculated as the rate of the number of adherence bacteria divided by the bacterial inoculum. The curcumin-treated bacteria showed the prominent reduction of adherence ability to the HEp-2 cells compared to the untreated one. The original bacterial inoculum volume was $3.00 \pm 0.00 \times 10^8$ CFU ml⁻¹. However, the number of colony count of *H. pylori* co-cultured with the HEp-2 cells in an absence and presence of 1/2 MIC of curcumin were $3.67 \pm 4.03 \times 10^6$ CFU ml⁻¹ and $2.76 \pm 0.58 \times 10^5$ CFU ml⁻¹, respectively. In comparison to a percentile of adhesion of the curcumin-untreated *H. pylori* as 100 %, it significantly reduced to only 16.79 % for the curcumin-treated *H. pylori* ($P = 0.009$) (Figure 38). Curcumin at 1/2 MIC showed no effect on the viability of *H. pylori* and HEp-2 cells in this study. The number of colony count of *H. pylori* co-cultured with 1/2 MIC of curcumin was $2.20 \pm 0.53 \times 10^8$ CFU ml⁻¹, which did not significantly differ from the original bacterial inoculum ($P > 0.05$). The number of viable HEp-2 cells after treated with 1/2 MIC of curcumin was $2.73 \pm 0.16 \times 10^6$ cells per well, which did not significantly differ from the original cell number,

$3.00 \pm 0.00 \times 10^6$ cells per well ($P > 0.05$). DMSO at concentration of 0.016%, which was the concentration mixed in curcumin suspension, did not show any bactericidal effect against *H. pylori*. The number of colony count of *H. pylori* co-cultured with DMSO was $1.97 \pm 0.42 \times 10^8$ CFU ml⁻¹, which did not significantly differ from the original bacterial inoculum ($P > 0.05$).

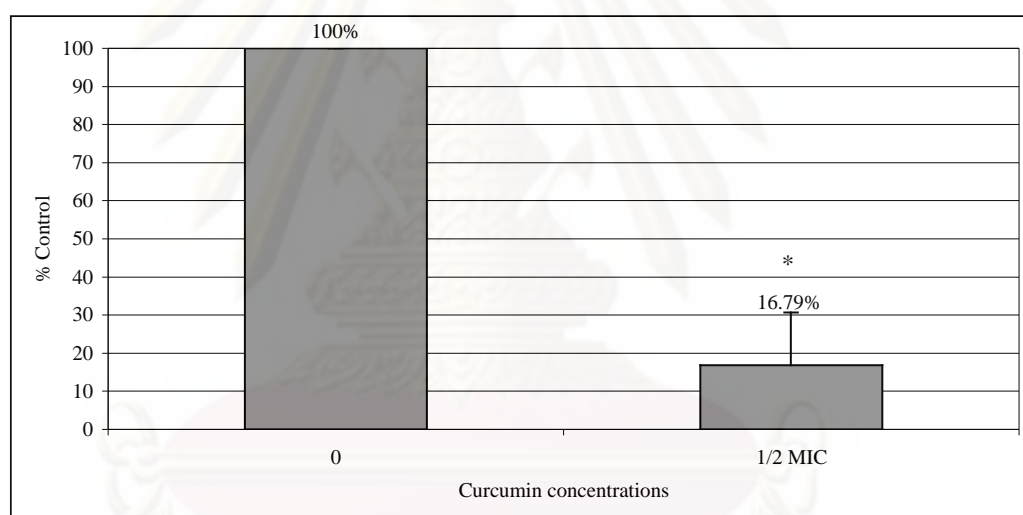


Figure 38: Percentile of adhesion of *H. pylori* ATCC43504 in a presence and absence of 1/2 MIC of curcumin. After co-cultured with HEP-2 cells for 2 h in an absence and presence of curcumin, bacteria were plated out. Results expressed as the proportion of adherence bacteria versus control. Experiments were performed in duplicate on three separated occasions. Error bars represent \pm standard deviation from the mean. *Statistical significant difference was accepted at the $P = 0.009$ level.

Phase III: Proteomics Analysis of *H. pylori* Biofilm Formation

H. pylori biofilm and planktonic were collected from culture condition established as pellicle assay as previously described in the Chapter IV. Total protein was extracted from the following samples including biofilm and planktonic cells of culture without curcumin, biofilm and planktonic cells of culture with 1/4 MIC of curcumin, and planktonic cells of 1/2 MIC of curcumin. All these samples were collected on day 6 of incubation (Table 14), as this was the earliest day that the differences of biofilm formation among sample groups were observed. Protein was extracted from individual sample by sonication as previously described in the Chapter IV. After sonication, an aliquot of bacteria were tested for viability by subculturing onto BHI agar and incubated at 37 °C for 3 to 5 days, microaerobically. None of bacterial colony was found. Individual protein sample was concentrated by lyophilization and the total protein was measured. The protein stock solutions were cleaned up and solubilized in IPG rehydration buffer. These protein samples were ready to process for proteomics analysis.

19. 2-D gel electrophoresis

19.1 Total protein quantification

Protein samples derived from 5 separate culture conditions were collected. These included biofilm and planktonic cultures without curcumin, biofilm and planktonic cultures with 1/4 MIC of curcumin, and planktonic culture with 1/2 MIC of curcumin. Total protein concentrations were measured using Bradford assay. The total protein concentrations of individual sample are summarized in Table 15.

| Sample type | Total protein concentration ($\mu\text{g ml}^{-1}$) |
|----------------------------------|---|
| Biofilm without curcumin | 3,712.68 |
| Planktonic without curcumin | 3,094.37 |
| Biofilm with 1/4 MIC curcumin | 3,139.44 |
| Planktonic with 1/4 MIC curcumin | 3,573.24 |
| Planktonic with 1/2 MIC curcumin | 3,241.69 |

Table 15: Total protein concentrations of individual samples quantified by Bradford assay.

19.2 Proteomic mapping

Two hundred and fifty μl IPG rehydration buffer containing 1 mg of protein of individual samples were separated on a 2-D gel electrophoresis covering the pH 3-10 non linear gradient ranges. After the first dimensional gel electrophoresis (IEF), the strips possessing proteins separated by their isoelectric points were transferred to the second dimensional gel electrophoresis (SDS-PAGE), where the proteins were then separated by their molecular weights. Gels were stained by colloidal coomassie brilliant blue G-250, which specifically bound to arginine, histidine, and tyrosine in proteins embedded in the gel. The gels were photographed by Imagescanner using LabScan software. Each culture condition was separately pooled. Each pooled sample was separately performed in triplicate in order to avoid any variation. The complete 2-D gel electrophoresis resulted in a proteomic map exhibiting a protein profile expression of individual sample. The proteomic maps of either pellicle and/or planktonic derived from culture without curcumin, with 1/4 MIC of curcumin, and with 1/2 MIC of curcumin are shown in Figure 39 to 43.

For biofilm and planktonic derived from culture without curcumin, a total of 74 and 69 spots were detected, respectively. Among these, 24 and 6 spots from biofilm and planktonic, respectively, were found to be differentially present. For biofilm and planktonic derived from culture conditions with 1/4 MIC of curcumin, a total of 81 and 53 spots were detected, respectively. Among these, 22 and 8 spots from biofilm and planktonic, respectively, were found to be differentially present. For planktonic derived from culture condition with 1/2 MIC of curcumin, a total of 48 spots were detected. Among these, 4 spots were found to be differentially present. Most of the spots from 5 proteomic maps were localized in the area of pH 5-8 and the protein mass ranged from 17 to 94 kDa. These proteomic maps were subsequently analyzed and compared with protein database NCBI.

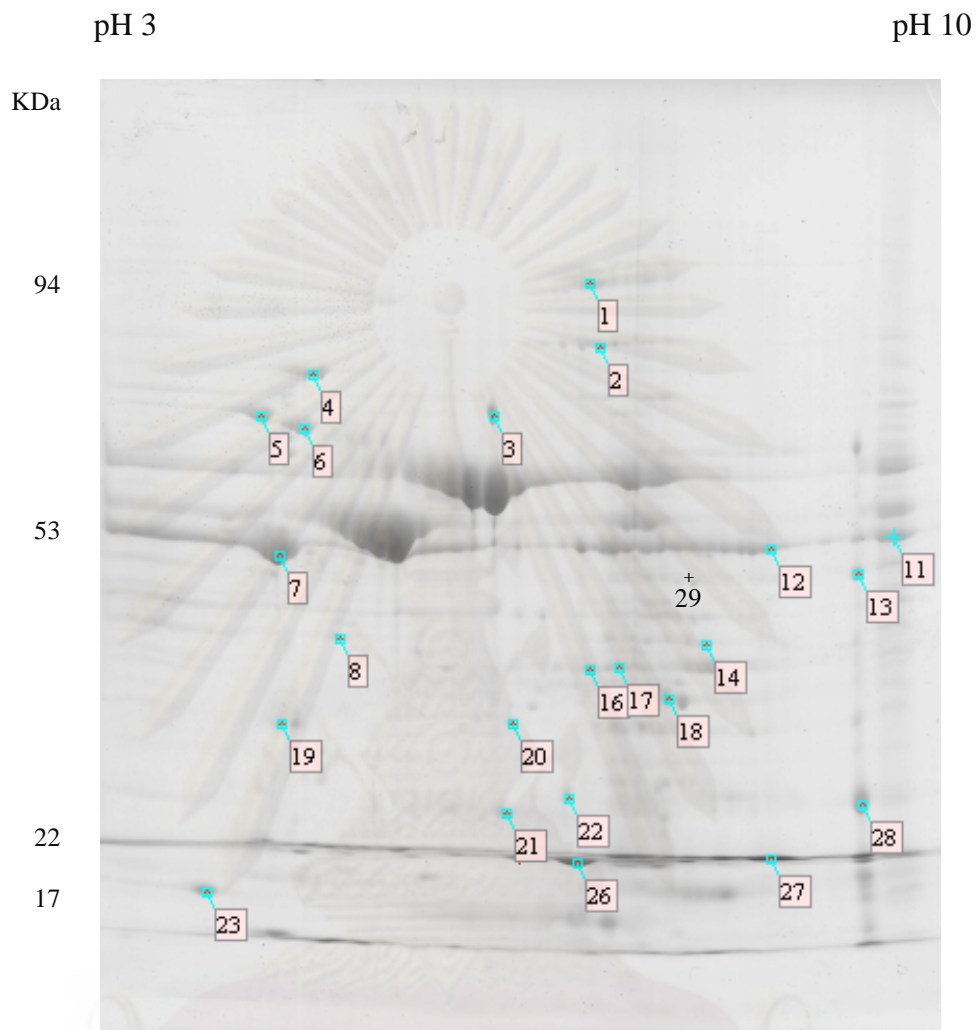


Figure 39: Proteomic map of *H. pylori* ATCC43504 biofilm in an absence of curcumin. Spots that were picked up to identify are marked with numbers.

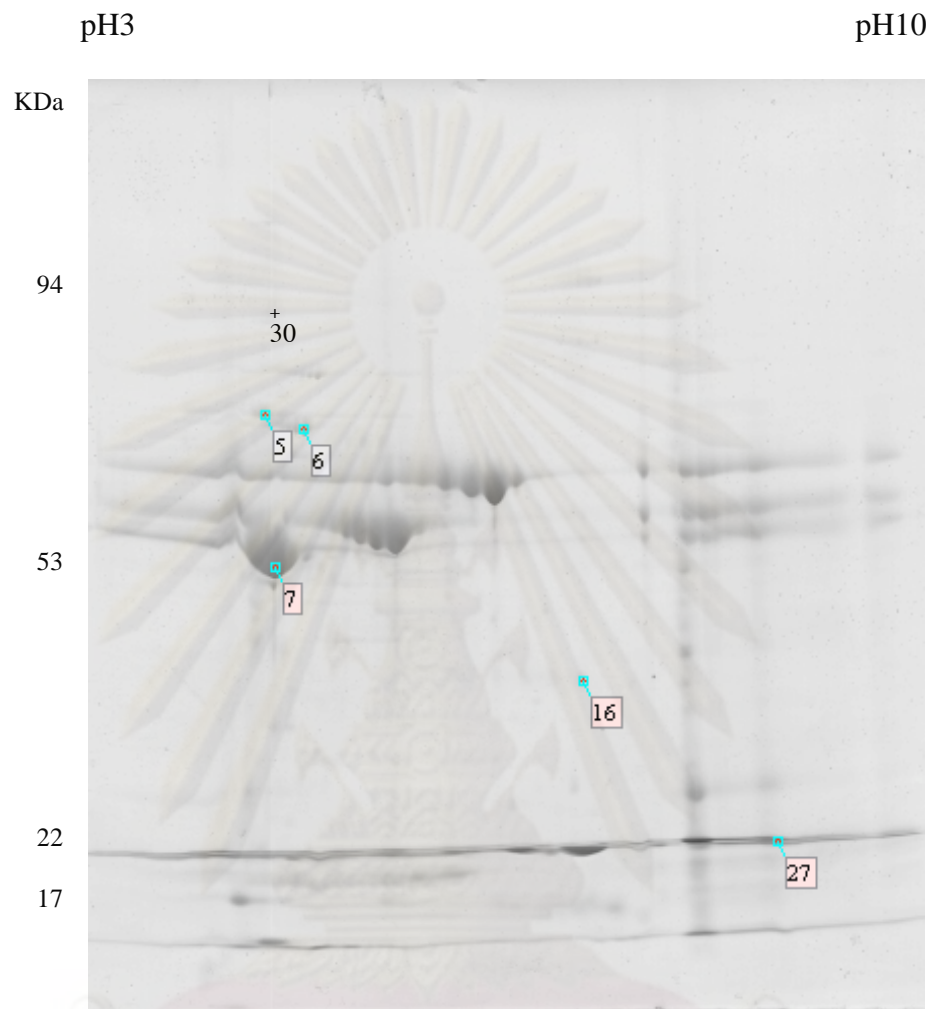


Figure 40: Proteomic map of *H. pylori* ATCC43504 planktonic in an absence of curcumin. Spots that were picked up to identify are marked with numbers.

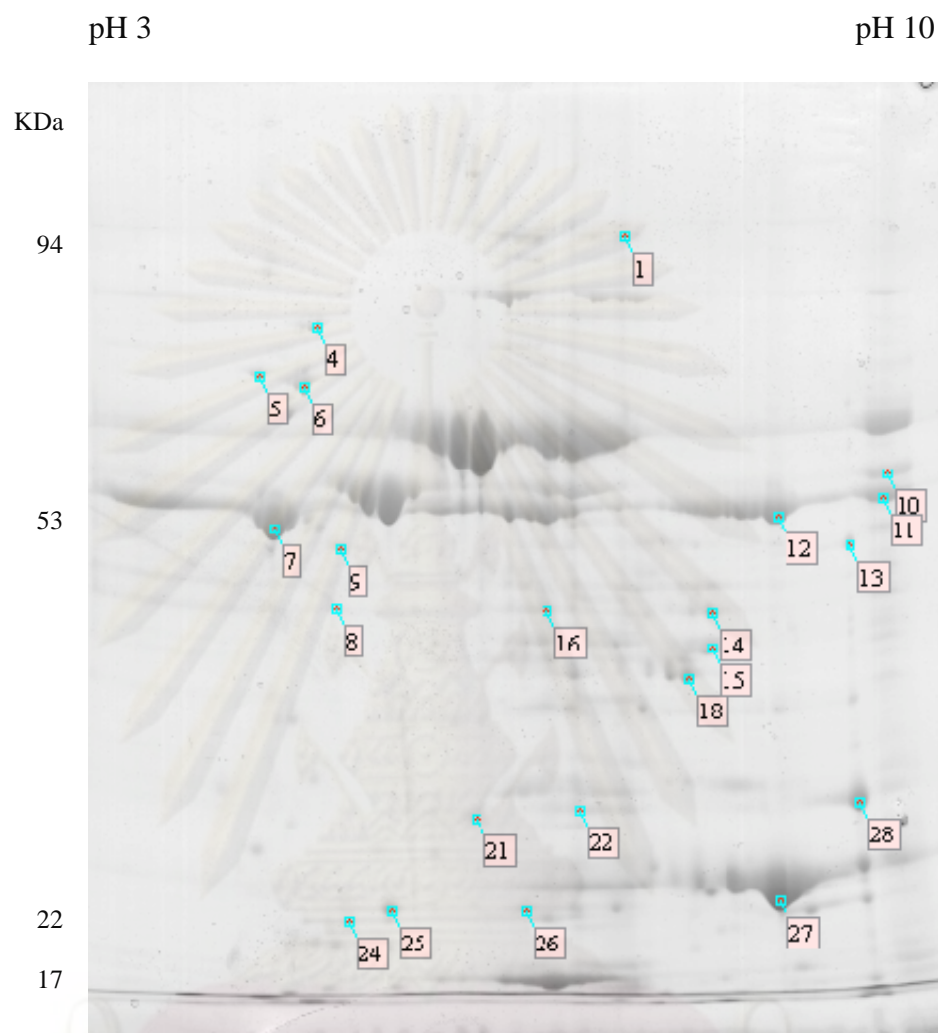


Figure 41: Proteomic map of *H. pylori* ATCC43504 biofilm in a presence of curcumin at 1/4 MIC. Spots that were picked up to identify are marked with numbers.

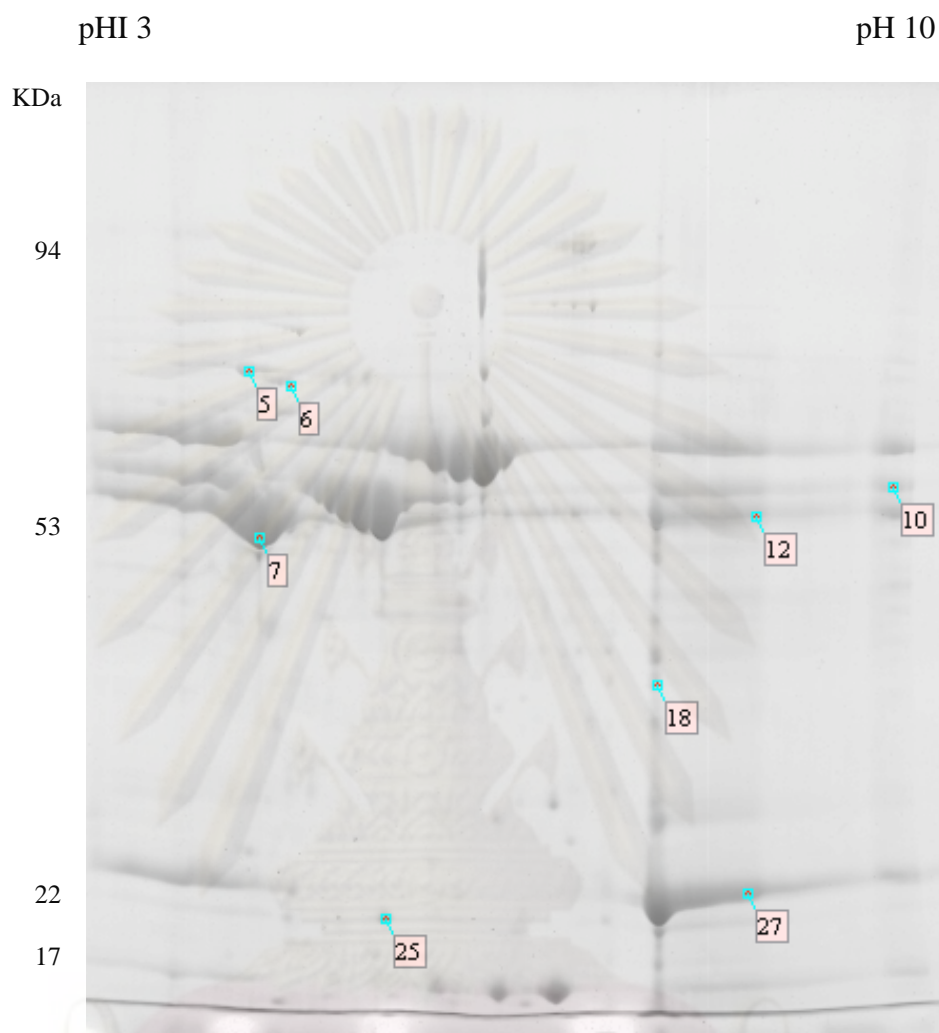


Figure 42: Proteomic map of *H. pylori* ATCC43504 planktonic in a presence of curcumin at 1/4 MIC. Spots that were picked up to identify are marked with numbers.

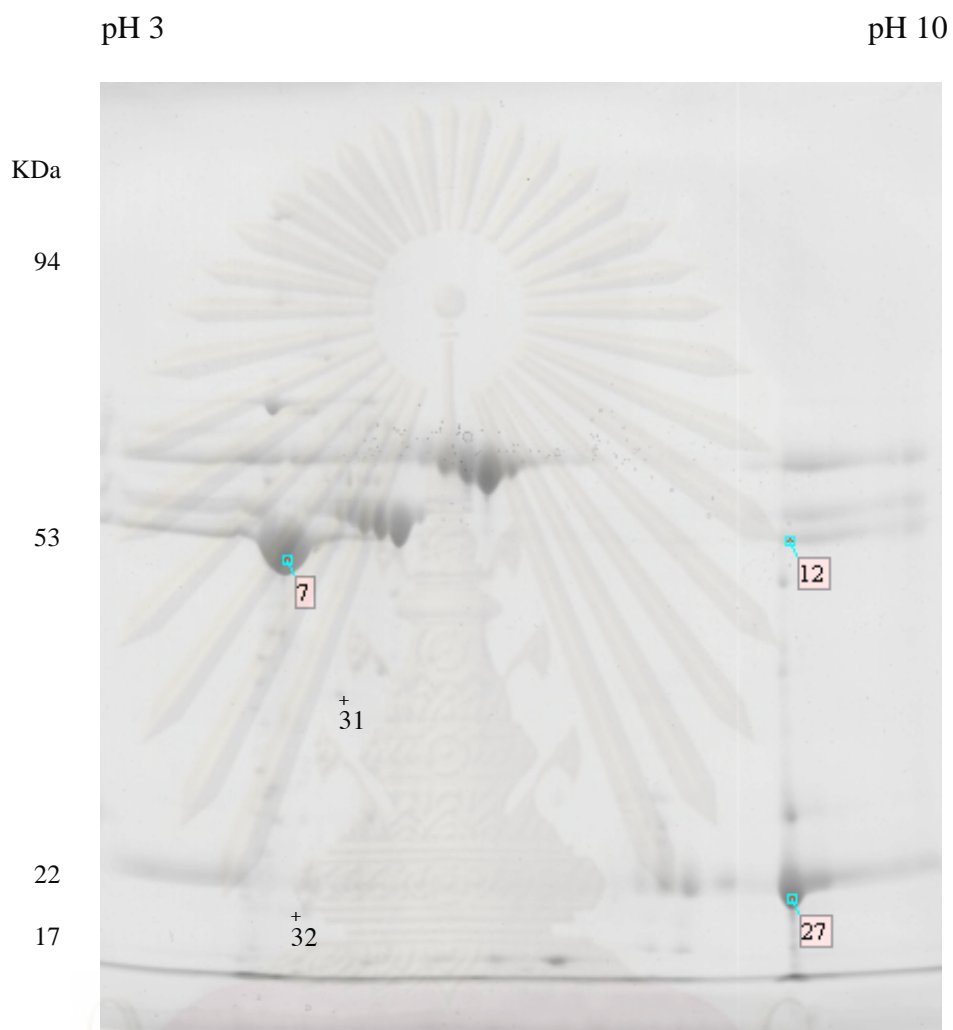


Figure 43: Proteomic map of *H. pylori* ATCC43504 planktonic in a presence of curcumin at 1/2 MIC. Spots that were picked up to identify are marked with numbers.

20. Image analysis and comparison of proteomic map of *H. pylori* biofilm

The proteomic maps of individual samples were then analyzed by ImageMaster 2D Elite 3.01 analysis software. A comparative proteome analysis was performed in order to gain information about either differentially present/absent spots or differences intensities of spots represented up- or down-regulation. A student's *t* test was used for this comparative analysis. Samples were compared as following schematic (Figure 44).

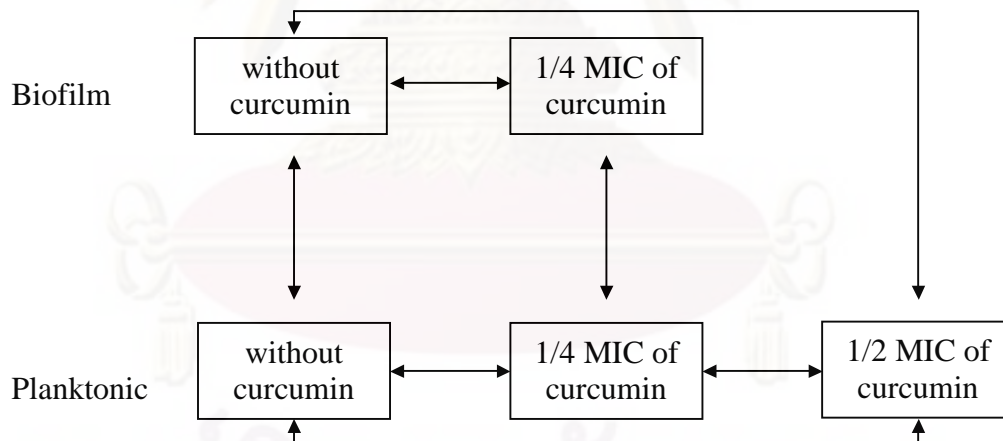


Figure 44: A schematic picture of comparative proteome analysis of individual sample. Arrows (\longleftrightarrow) indicate a pair of samples, which were compared to each other.

Several spots were found at the same position. However, differentially present spots observed only on one particular gel, but not on the others, as well as a significant up-regulated spots were also detected. These spots are marked with a square at the corresponding site in Figure 39 to 43.

The proteomic maps of biofilm without curcumin treatment and planktonic without curcumin treatment were matched (Figure 39 and 40). This matching analysis revealed 4 protein spots showed up-regulation ($P \leq 0.05$), and 19 and 1 spots were only present in the biofilm and planktonic sample, respectively, without curcumin treatment. Only one protein spot (no. 27) was present on both samples without a significant difference.

The proteomic maps of biofilm with 1/4 MIC of curcumin treatment and planktonic with 1/4 MIC of curcumin treatment were matched (Figure 41 and 42). This matching analysis revealed 7 protein spots showed up-regulation ($P \leq 0.05$) and 14 spots were only present in the biofilm sample with 1/4 MIC of curcumin treatment. Only one protein spot (no. 12) was present on both samples without a significant difference.

The proteomic maps of biofilm without curcumin treatment and biofilm with 1/4 MIC of curcumin treatment were matched (Figure 39 and 41). This matching analysis revealed 6 proteins spots showed up-regulation ($P \leq 0.05$) and 7 spots were only present in the biofilm sample without curcumin treatment. Additionally, there were 5 spots only present in the biofilm with 1/4 MIC of curcumin treatment. Eleven protein spots (no. 1, 5, 6, 7, 8, 11, 13, 14, 16, 18, and 21) were present on both samples without a significant difference.

The proteomic maps of biofilm without curcumin treatment and planktonic with 1/2 MIC of curcumin treatment were matched (Figure 39 and 43). This matching analysis revealed 3 proteins spots showed up-regulation ($P \leq 0.05$) and 21 spots were only present in the biofilm sample without curcumin treatment. Additional 2 protein spots were only present in the planktonic sample with 1/2 MIC of curcumin treatment.

The proteomic maps of biofilm with 1/4 MIC of curcumin treatment and planktonic with 1/2 MIC of curcumin treatment were matched (Figure 41 and 43). This matching analysis revealed 1 protein spot showed up-regulation ($P \leq 0.05$) and 19 spots were only present in the biofilm sample with 1/4 MIC of curcumin treatment. Additional 1 spot was only present in the planktonic sample with 1/2 MIC of curcumin treatment. Two protein spots (no. 12 and 27) were present on both samples without a significant difference.

The proteomic maps of planktonic without curcumin treatment and planktonic with 1/4 MIC of curcumin treatment were matched (Figure 40 and 42). This matching analysis revealed 1 protein spot showed up-regulation ($P \leq 0.05$) and 2 spot was only present in the planktonic sample without curcumin treatment. Additionally, there were 4 spots only present in the planktonic with 1/4 MIC of curcumin treatment. Three protein spots (no. 5, 7, and 27) were present on both samples without a significant difference.

The proteomic maps of planktonic without curcumin treatment and planktonic with 1/2 MIC of curcumin treatment were matched (Figure 40 and 43). This matching analysis revealed 2 protein spots showed up-regulation ($P \leq 0.05$) and 4

spots were only present in the planktonic sample without curcumin treatment. However, there were 3 spots (no. 12, 31, and 32) only present in planktonic with 1/2 MIC of curcumin treatment but not in planktonic without curcumin treatment.

The proteomic maps of planktonic with 1/4 MIC of curcumin treatment and planktonic with 1/2 MIC of curcumin treatment were matched (Figure 42 and 43). This matching analysis revealed 2 protein spots showed up-regulation ($P \leq 0.05$) and 5 spots were only present in the planktonic with 1/4 MIC of curcumin treatment. However, there were 2 spots (no.31 and 32) only present in planktonic with 1/2 MIC of curcumin treatment. Only one protein spot, no. 12, was present on both samples without a significant difference.

After matching analysis, all these revealed spots were picked up for protein identification in the next step.

21. Protein identification using MALDI-TOFF mass spectrometry

The picked up protein spots were delivered to the Bio-technology Service Unit (BSU) in order to perform mass spectrometry analysis. Peptide mass fingerprints were obtained by MALDI-TOF mass spectrometry. Protein identifications were also performed by searching for matching peptide mass fingerprints in the NCBI protein database. Total of 28 identified proteins, which belong to *H. pylori* proteins, are listed in Table 16. These proteins derived from spots marked with squared number as shown in Figure 39 to 43. These identified proteins were responsible in different cellular function as following described.

The predominant identified proteins consisted of those involved in chemotaxis and motility functions. These proteins included putative flagellar hook-associated

protein 3 (FlgL), flagellar hook protein (FlgE), flagellar capping protein (FliD), flagellin A (FlaA), and flagellar basal body rod modification protein (FlgD). Another predominant identified protein group was those involved in oxidative stress response. These proteins included catalase (KatA), thioredoxin reductase (TrxB), and alkyl hydroperoxide reductase (TsaA). Interestingly, group of proteins responsible in electron transport function were also identified, including pyruvate ferredoxin oxidoreductase beta subunit (PorB), bifunctional methionine sulfoxide reductase A/B protein (HPSH_01160), and flavodoxin (FldA). Three proteins involved in the protein synthetic function, which was elongation factor Tu (EF-Tu) and P (EF-P), trigger factor (Tig), 60kDa-heat shock protein (Hsp60), and co-chaperone and heat shock protein (GrpE). One protein having known function, acetyl coenzyme A acetyltransferase (FadA), was detected. Three another proteins, urease subunit alpha (UreA), urease subunit beta (UreB), and bifunctional urease subunit gamma/beta were involved in nitrogen metabolism, whereas additional two proteins included bifunctional aconitate hydratase 2/2-methylisocitrate dehydratase (AcnB) and citrate synthase (GltA) were involved in carbohydrate metabolism. However, three proteins (HPB128_25g37, HP1037, and HP0175) having no known function were also observed.

A positional shift of spot was observed among the proteomic maps. The positional shifts of spot number 16 and 17 corresponding to hypothetical protein HPB128_25g37 (Figure 39) and spot number 11 and 12 corresponding to catalase (Figure 41) were observed in gel of biofilm without curcumin treatment sample.

Four additional proteins identified as other bacterial proteins also differentially expressed here. These proteins marked with un-squared numbers.

Protein derived from spot number 29 (Figure 39) was identified as response regulator transcription regulator protein of *Ralstonia solanacearum*. Protein derived from spot number 30 (Figure 40) was identified as hypothetical protein of *Burkholderia mallei*. Protein derived from spot number 31 (Figure 43) was identified as gluconate 2-dehydrogenase (acceptor) protein of *Burkholderia ambifaria*. Protein derived from spot number 32 (Figure 43) was identified as UDP-galactopyranose mutase protein of *Caulobacter crescentus*.



ศูนย์วิทยทรัพยากร
จุฬาลงกรณ์มหาวิทยาลัย

| Spot | Protein | Gene | Homologs of the gene of strain 26695 or others* | Function | Mass (kDa) | pI |
|------|---|--------------|---|-------------------------------------|------------|------|
| 1 | Urease subunit alpha | <i>ureA</i> | JH0067 | Nitrogen metabolism/colonization | 61.82 | 5.64 |
| 2 | Bifunctional aconitate hydratase 2/2-methylisocitrate dehydratase | <i>acnB</i> | HP0779 | Carbohydrate Metabolism | 93.48 | 6.17 |
| 3 | Urease subunit beta | <i>ureB</i> | HPAG1_0073 | Nitrogen metabolism/colonization | 61.80 | 5.64 |
| 4 | Putative flagellar hook-associated protein 3 (HAP3) | <i>flgL</i> | HP1047 | Chemotaxis and motility | 92.16 | 5.29 |
| 5 | Flagellar hook protein | <i>flgE</i> | HP0870 | Chemotaxis and motility | 76.22 | 5.04 |
| 6 | Flagellar capping protein | <i>fliD</i> | HP0752 | Chemotaxis and motility | 72.82 | 5.23 |
| 7 | Flagellin A | <i>flaA</i> | HP0601 | Chemotaxis and motility | 53.28 | 6.04 |
| 8 | Elongation factor Tu | <i>tufA</i> | HP1205 | Peptide bond synthesis | 43.73 | 5.17 |
| 9 | Trigger factor | <i>tig</i> | HP0795 | Protein export | 52.01 | 5.33 |
| 10 | Heat shock protein 60 | <i>hsp60</i> | HP0010 | Protein folding and stabilization | 58.29 | 5.44 |
| 11 | Catalase | <i>katA</i> | HP0875 | Detoxification | 58.71 | 8.70 |
| 12 | Catalase | <i>katA</i> | HP0876 | Detoxification | 58.71 | 8.70 |
| 13 | Pyruvate ferredoxin oxidoreductase, beta subunit | <i>porB</i> | HP1111 | Electron transport | 35.39 | 8.31 |
| 14 | Citrate synthase | <i>gltA</i> | HP0026 | Carbohydrate Metabolism | 48.55 | 7.71 |
| 15 | Bifunctional methionine sulfoxide reductase A/B protein | | HPSH_01160 | Electron transport | 39.76 | 6.81 |
| 16 | Hypothetical protein HPB128_25g37 | | HPB128_25g37 | Unknown function | 42.98 | 5.77 |
| 17 | Hypothetical protein HPB128_25g38 | | HPB128_25g37 | Unknown function | 42.98 | 5.77 |
| 18 | Acetyl coenzyme A acetyltransferase | <i>fadA</i> | HP0690 | metabolic intermediate biosynthesis | 41.49 | 6.71 |
| 19 | Flagellar basal body rod modification protein | <i>flgD</i> | HP0907 | Chemotaxis and motility | 40.91 | 5.45 |
| 20 | Hypothetical protein HP1037 | | HP1037 | Unknown function | 40.94 | 5.82 |

*Numbers labeled “HP” refer to the sequence of *H. pylori* ATCC26695, “JH” to the sequence of *H. pylori* J99, “HPAG1” to the sequence of *H. pylori* HPAG1, “HPSH” to the sequence of *H. pylori* Shi470, “HPB128” to the sequence of *H. pylori* B128.

Table 16: Identification of the entire proteins expressed and up-regulated in both *H.*

pylori biofilm and planktonic cells without curcumin treatment, with 1/4 and 1/2 MIC of curcumin treatment.

| Spot | Protein | Gene | Homologs of the gene of strain 26695 or others* | Function | Mass (kDa) | pI |
|------|---|-------------|---|-----------------------------------|------------|------|
| 21 | Thioredoxin reductase | <i>trxB</i> | HP0285 | Electron transport | 34.03 | 5.93 |
| 22 | Hypothetical protein | | HPB128_25g37 | Unknown function | 42.98 | 5.77 |
| 23 | Flavodoxin | <i>fldA</i> | HP1161 | Electron transport | 17.48 | 4.45 |
| 24 | Co-chaperone and heat shock protein | <i>grpE</i> | HP0110 | Protein folding and stabilization | 22.20 | 5.30 |
| 25 | Elongation factor P (EF-P) | <i>efp</i> | HP0177 | Peptide bond synthesis | 20.83 | 5.43 |
| 26 | Alkyl hydroperoxide reductase Bifunctional urease subunit | <i>tsaA</i> | HP1563 | Detoxification | 22.34 | 5.88 |
| 27 | gamma/beta | | HP0073 | Nitrogen metabolism | 26.58 | 8.46 |
| 28 | Uncharacterized protein | | HP0175 | Unknown function | 34.01 | 9.29 |

*Numbers labeled "HP" refer to the sequence of *H. pylori* ATCC26695, "JH" to the sequence of *H. pylori* J99, "HPAG1" to the sequence of *H. pylori* HPAG1, "HPSH" to the sequence of *H. pylori* Shi470, "HPB128" to the sequence of *H. pylori* B128.

Table 16: Identification of the entire proteins expressed and up-regulated in both *H. pylori* biofilm and planktonic cells without curcumin treatment, with 1/4 and 1/2 MIC of curcumin treatment (Continued).

Among those identified *H. pylori* proteins, some were present only on one particular gel whereas some existing in more than one gel. Table 17 summarizes the protein spots expressing in individual 5 proteomic maps. Data obtained from protein identification combining with comparative proteome analysis demonstrated the known proteins present in particular samples. Furthermore, the significant up-regulated proteins in individual sample were also shown. Tables 18 to 21 summarize proteins that differently present among those comparative groups of samples either in the similar level of expression or up-regulated level.

For biofilm and planktonic samples without curcumin treatment, 23 and 5 proteins were successfully identified, respectively. The identified proteins are shown in Table 18. Four proteins were found to up-regulate in the biofilm. The main up-regulated proteins belonged to those involving in chemotaxis and motility function. Additional 18 proteins were only found in the biofilm sample but not planktonic. Only one protein, bifunctional urease subunit gamma/beta (spot no. 27), was express in both samples with no significant different level.

For biofilm and planktonic samples with 1/4 MIC of curcumin treatment, 22 and 8 proteins were successfully identified, respectively. The identified proteins are shown in Table 19. Seven proteins were found to up-regulated in the biofilm. The 3 out of 7 up-regulated proteins belonged to those involving in chemotaxis and motility function, whereas additional 4 up-regulated proteins were associated in oxidative stress response, electron transport, and nitrogen metabolism functions. Only one protein, catalase (spot no. 12), was express in both samples with no significant different level.

The identified proteins of biofilm sample without and with 1/4 MIC curcumin treatment, and planktonic sample with 1/2 MIC curcumin treatment are shown in Table 20. Eleven out of all 28 identified proteins was expressed with similar level in proteomic maps of biofilm sample both derived from culture without curcumin and with 1/4 MIC of curcumin treatment. Almost every protein associated with chemotaxis and motility function was identified in both biofilm samples, except for flagellar basal body rod modification protein. Other protein groups expressing in both biofilms belonged to the protein involved in protein synthesis, oxidative stress response, electron transport, nitrogen and carbon metabolisms. In comparison to biofilm with 1/4 MIC of curcumin, 6 proteins, including protein representing by spot no. 4, 12, 22, 26, 27, and 28, were up-regulated, whereas 6 proteins representing by spot no. 2, 3, 17, 19, 20, and 23 expressed in only biofilm sample without curcumin. On a contrary, additional 5 proteins expressed in only biofilm sample with 1/4 MIC of curcumin are representing by spot no. 9, 10, 15, 24, and 25. Although, 3 proteins included flagellin A (spot no. 7), catalase (spot no. 12), and bifunctional urease subunit gamma/beta (spot no. 27) were also found in all three compared sample types. But these 3 proteins were down-regulated in planktonic with 1/2 MIC of curcumin.

The identified proteins of planktonic sample without, with 1/4 and 1/2 MIC curcumin treatment are shown in Table 21. Three out of all 28 identified proteins was expressed with similar level in proteomic maps of planktonic sample both derived from culture without curcumin and with 1/4 MIC of curcumin treatment. These included flagellar hook protein (spot no. 5), flagellin A (spot no. 7), and bifunctional urease subunit gamma/beta proteins (spot no. 27). In comparison to planktonic with 1/4 MIC of curcumin, 1 protein (flagellar capping protein, spot no. 6) was up-

regulated, whereas another 1 protein (Hypothetical protein HPB128_25g37, spot no. 16) expressed in only planktonic sample without curcumin. On a contrary, additional 4 proteins expressed in only biofilm sample with 1/4 MIC of curcumin are representing by spot no. 10, 12, 18, and 25. Although, 2 proteins included flagellin A (spot no. 7) and bifunctional urease subunit gamma/beta (spot no. 27) were also found in all three compared sample types. But these 2 proteins were down-regulated in only planktonic sample without and with 1/2 MIC curcumin treatment. Interestingly, 1 protein (catalase, spot no. 12) was found in both planktonic samples treated with curcumin, but not in sample without curcumin.

| Spot | Protein | Protein sample types | | | | |
|------|---|--------------------------|-----------------------------|----------------------------|-------------------------------|-------------------------------|
| | | Biofilm without curcumin | Planktonic without curcumin | Biofilm + 1/4 MIC curcumin | Planktonic + 1/4 MIC curcumin | Planktonic + 1/2 MIC curcumin |
| 1 | Urease subunit alpha | + | - | + | - | - |
| 2 | Bifunctional aconitate hydratase 2/2-methylisocitrate dehydratase | + | - | - | - | - |
| 3 | Urease subunit beta | + | - | - | - | - |
| 4 | Putative flagellar hook-associated protein 3 (HAP3) | + | - | + | - | - |
| 5 | Flagellar hook protein | + | + | + | + | - |
| 6 | Flagellar capping protein | + | + | + | + | - |
| 7 | Flagellin A | + | + | + | + | + |
| 8 | Elongation factor Tu | + | - | + | - | - |
| 9 | Trigger factor | - | - | + | - | - |
| 10 | Heat shock protein 60 | - | - | + | + | - |
| 11 | Catalase | + | - | + | - | - |
| 12 | Catalase | + | - | + | + | + |
| 13 | Pyruvate ferredoxin oxidoreductase, beta subunit | + | - | + | - | - |
| 14 | Citrate synthase | + | - | + | - | - |
| 15 | Bifunctional methionine sulfoxide reductase A/B protein | - | - | + | - | - |
| 16 | Hypothetical protein HPB128_25g37 | + | + | + | - | - |
| 17 | Hypothetical protein HPB128_25g37 | + | - | - | - | - |
| 18 | Acetyl coenzyme A acetyltransferase | + | - | + | + | - |
| 19 | Flagellar basal body rod modification protein | + | - | - | - | - |
| 20 | Hypothetical protein HP1037 | + | - | - | - | - |

Note: Symbols "+" or "-" show the presence or absence of corresponding protein spot on the proteomic map, respectively.

Table 17: Comparison of proteomic map patterns of *H. pylori* ATCC43504 biofilm and planktonic without curcumin treatment, with 1/4 and 1/2 MIC of curcumin treatment.

| Spot | Protein | Protein sample types | | | | |
|------|--|----------------------|------------|----------------------------|-------------------------------|-------------------------------|
| | | Biofilm | Planktonic | Biofilm + 1/4 MIC curcumin | Planktonic + 1/4 MIC curcumin | Planktonic + 1/2 MIC curcumin |
| 21 | Thioredoxin reductase | + | - | + | - | - |
| 22 | Hypothetical protein | + | - | + | - | - |
| 23 | Flavodoxin | + | - | - | - | - |
| 24 | Co-chaperone and heat shock protein | - | - | + | - | - |
| 25 | Elongation factor P | - | - | + | + | - |
| 26 | Alkyl hydroperoxide reductase | + | - | + | - | - |
| 27 | Bifunctional urease subunit gamma/beta | + | + | + | + | + |
| 28 | Uncharaterized protein | + | - | + | - | - |

Note: Symbols "+" or "-" show the presence or absence of corresponding protein spot on the proteomic map, respectively.

Table 17: Comparison of proteomic map patterns of *H. pylori* ATCC43504 biofilm and planktonic without curcumin treatment, with 1/4 and 1/2 MIC of curcumin treatment (Continued).

ศูนย์วิทยทรัพยากร
จุฬาลงกรณ์มหาวิทยาลัย

| Spot | Protein | Protein sample types | |
|------|---|--------------------------|-----------------------------|
| | | Biofilm without curcumin | Planktonic without curcumin |
| 1 | Urease subunit alpha | + | - |
| 2 | Bifunctional aconitate hydratase 2/2-methylisocitrate dehydratase | + | - |
| 3 | Urease subunit beta | + | - |
| 4 | Putative flagellar hook-associated protein 3 (HAP3) | + | - |
| 5 | Flagellar hook protein | ↑ | ↓ |
| 6 | Flagellar capping protein | ↑ | ↓ |
| 7 | Flagellin A | ↑ | ↓ |
| 8 | Elongation factor Tu | + | - |
| 9 | Trigger factor | - | - |
| 10 | Heat shock protein 60 | - | - |
| 11 | Catalase | + | - |
| 12 | Catalase | + | - |
| 13 | Pyruvate ferredoxin oxidoreductase, beta subunit | + | - |
| 14 | Citrate synthase | + | - |
| 15 | Bifunctional methionine sulfoxide reductase A/B protein | - | - |
| 16 | Hypothetical protein HPB128_25g37 | ↑ | ↓ |
| 17 | Hypothetical protein HPB128_25g37 | + | - |
| 18 | Acetyl coenzyme A acetyltransferase | + | - |
| 19 | Flagellar basal body rod modification protein | + | - |
| 20 | Hypothetical protein HP1037 | + | - |
| 21 | Thioredoxin reductase | + | - |
| 22 | Hypothetical protein | + | - |
| 23 | Flavodoxin | + | - |
| 24 | Co-chaperone and heat shock protein | - | - |
| 25 | Elongation factor P | - | - |
| 26 | Alkyl hydroperoxide reductase | + | - |
| 27 | Bifunctional urease subunit gamma/beta | + | + |
| 28 | Uncharacterized protein | + | - |

Note: Symbols "+" or "-" show the presence or absence of corresponding protein spot on the proteomic map, respectively. Symbols "↑" or "↓" show up- or down-regulated protein expression, respectively.

Table 18: Identified proteins that were present and up-regulated in biofilm and planktonic sample without curcumin treatment.

| Spot | Protein | Protein sample types | |
|------|---|----------------------------------|-------------------------------------|
| | | Biofilm + 1/4 MIC curcumin | Planktonic + 1/4 MIC curcumin |
| 1 | Urease subunit alpha | + | - |
| 2 | Bifunctional aconitate hydratase 2/2-methylisocitrate dehydratase | - | - |
| 3 | Urease subunit beta | - | - |
| 4 | Putative flagellar hook-associated protein 3 (HAP3) | + | - |
| 5 | Flagellar hook protein | ↑ | ↓ |
| 6 | Flagellar capping protein | ↑ | ↓ |
| 7 | Flagellin A | ↑ | ↓ |
| 8 | Elongation factor Tu | + | - |
| 9 | Trigger factor | + | - |
| 10 | Heat shock protein 60 | ↑ | ↓ |
| 11 | Catalase | + | - |
| 12 | Catalase | + | + |
| 13 | Pyruvate ferredoxin oxidoreductase, beta subunit | + | - |
| 14 | Citrate synthase | + | - |
| 15 | Bifunctional methionine sulfoxide reductase A/B protein | + | - |
| 16 | Hypothetical protein HPB128_25g37 | + | - |
| 17 | Hypothetical protein HPB128_25g37 | - | - |
| 18 | Acetyl coenzyme A acetyltransferase | ↑ | ↓ |
| 19 | Flagellar basal body rod modification protein | - | - |
| 20 | Hypothetical protein HP1037 | - | - |
| 21 | Thioredoxin reductase | + | - |
| 22 | Hypothetical protein | + | - |
| 23 | Flavodoxin | - | - |
| 24 | Co-chaperone and heat shock protein | + | - |
| 25 | Elongation factor P | ↑ | ↓ |
| 26 | Alkyl hydroperoxide reductase | + | - |
| 27 | Bifunctional urease subunit gamma/beta | ↑ | ↓ |
| 28 | Uncharaterized protein | + | - |

Note: Symbols "+" or "-" show the presence or absence of corresponding protein spot on the proteomic map, respectively. Symbols "↑" or "↓" show up- or down-regulated protein expression, respectively.

Table 19: Identified proteins that were present and up-regulated in biofilm and planktonic sample with 1/4 MIC of curcumin treatment.

| Spot | Protein | Protein sample types | | |
|------|---|--------------------------|----------------------------|-------------------------------|
| | | Biofilm without curcumin | Biofilm + 1/4 MIC curcumin | Planktonic + 1/2 MIC curcumin |
| 1 | Urease subunit alpha | + | + | - |
| 2 | Bifunctional aconitate hydratase 2/2-methylisocitrate dehydratase | + | - | - |
| 3 | Urease subunit beta | + | - | - |
| 4 | Putative flagellar hook-associated protein 3 (HAP3) | ↑ | ↓ | - |
| 5 | Flagellar hook protein | + | + | - |
| 6 | Flagellar capping protein | + | + | - |
| 7 | Flagellin A | ↑ | ↑ | ↓ |
| 8 | Elongation factor Tu | + | + | - |
| 9 | Trigger factor | - | + | - |
| 10 | Heat shock protein 60 | - | + | - |
| 11 | Catalase | + | + | - |
| 12 | Catalase | ↑ | ↓ | ↓ |
| 13 | Pyruvate ferredoxin oxidoreductase, beta subunit | + | + | - |
| 14 | Citrate synthase | + | + | - |
| 15 | Bifunctional methionine sulfoxide reductase A/B protein | - | + | - |
| 16 | Hypothetical protein HPB128_25g37 | + | + | - |
| 17 | Hypothetical protein HPB128_25g37 | + | - | - |
| 18 | Acetyl coenzyme A acetyltransferase | + | + | - |
| 19 | Flagellar basal body rod modification protein | + | - | - |
| 20 | Hypothetical protein HP1037 | ↑ | - | - |

Note: Symbols "+" or "-" show the presence or absence of corresponding protein spot on the proteomic map, respectively. Symbols "↑" or "↓" show up- or down-regulated protein expression, respectively.

Table 20: Identified proteins that were present and up-regulated in biofilm sample without and with 1/4 MIC, and planktonic sample with 1/2 MIC of curcumin treatment.

| Spot | Protein | Protein sample types | | |
|------|--|--------------------------|----------------------------|-------------------------------|
| | | Biofilm without curcumin | Biofilm + 1/4 MIC curcumin | Planktonic + 1/2 MIC curcumin |
| 21 | Thioredoxin reductase | + | + | - |
| 22 | Hypothetical protein | ↑ | ↓ | - |
| 23 | Flavodoxin | + | - | - |
| 24 | Co-chaperone and heat shock protein | - | + | - |
| 25 | Elongation factor P | - | + | - |
| 26 | Alkyl hydroperoxide reductase | ↑ | ↓ | - |
| 27 | Bifunctional urease subunit gamma/beta | ↑ | ↓ | ↓ |
| 28 | Uncharaterized protein | ↑ | ↓ | - |

Note: Symbols "+" or "-" show the presence or absence of corresponding protein spot on the proteomic map, respectively. Symbols "↑" or "↓" show up- or down-regulated protein expression, respectively.

Table 20: Identified proteins that were present and up-regulated in biofilm sample without and with 1/4 MIC, and planktonic sample with 1/2 MIC of curcumin treatment (Continued).

| Spot | Protein | Protein sample types | | |
|------|---|-----------------------------|-------------------------------|-------------------------------|
| | | Planktonic without curcumin | Planktonic + 1/4 MIC curcumin | Planktonic + 1/2 MIC curcumin |
| 1 | Urease subunit alpha | - | - | - |
| 2 | Bifunctional aconitate hydratase 2/2-methylisocitrate dehydratase | - | - | - |
| 3 | Urease subunit beta | - | - | - |
| 4 | Putative flagellar hook-associated protein 3 (HAP3) | - | - | - |
| 5 | Flagellar hook protein | + | + | - |
| 6 | Flagellar capping protein | ↑ | ↓ | - |
| 7 | Flagellin A | ↑ | ↑ | ↓ |
| 8 | Elongation factor Tu | - | - | - |
| 9 | Trigger factor | - | - | - |
| 10 | Heat shock protein 60 | - | + | - |
| 11 | Catalase | - | - | - |
| 12 | Catalase | - | + | + |
| 13 | Pyruvate ferredoxin oxidoreductase, beta subunit | - | - | - |
| 14 | Citrate synthase | - | - | - |
| 15 | Bifunctional methionine sulfoxide reductase A/B protein | - | - | - |
| 16 | Hypothetical protein HPB128_25g37 | + | - | - |
| 17 | Hypothetical protein HPB128_25g37 | - | - | - |
| 18 | Acetyl coenzyme A acetyltransferase | - | + | - |
| 19 | Flagellar basal body rod modification protein | - | - | - |
| 20 | Hypothetical protein HP1037 | - | - | - |

Note: Symbols "+" or "-" show the presence or absence of corresponding protein spot on the proteomic map, respectively. Symbols "↑" or "↓" show up- or down-regulated protein expression, respectively.

Table 21: Identified proteins that were present and up-regulated in planktonic sample without, with 1/4 MIC, and 1/2 MIC of curcumin treatment.

| Spot | Protein | Protein sample types | | |
|------|--|-----------------------------|-------------------------------|-------------------------------|
| | | Planktonic without curcumin | Planktonic + 1/4 MIC curcumin | Planktonic + 1/2 MIC curcumin |
| 21 | Thioredoxin reductase | - | - | - |
| 22 | Hypothetical protein | - | - | - |
| 23 | Flavodoxin | - | - | - |
| 24 | Co-chaperone and heat shock protein | - | - | - |
| 25 | Elongation factor P | - | + | - |
| 26 | Alkyl hydroperoxide reductase | - | - | - |
| 27 | Bifunctional urease subunit gamma/beta | ↑ | ↑ | ↓ |
| 28 | Uncharacterized protein | - | - | - |

Note: Symbols "+" or "-" show the presence or absence of corresponding protein spot on the proteomic map, respectively. Symbols "↑" or "↓" show up- or down-regulated protein expression, respectively.

Table 21: Identified proteins that were present and up-regulated in planktonic sample without, with 1/4 MIC, and 1/2 MIC of curcumin treatment (Continued).

CHAPTER VI

DISCUSSION

In 1970s, the term “biofilm” has been used to describe the structure of complex bacteria ecosystems that allow bacteria to function in a coordinated fashion (90). Since then, it has been established that the majority of bacteria exist in naturally microbial ecosystems attached to surface and not as “free-floating” planktonic organisms. Hence, pure culture planktonic growth is not how bacteria normally exist in nature (90). Several clinically important bacteria enable to form biofilm (100-104). Over 60% of bacterial infections in human are responsible by biofilms (211), which are hardly to be eliminated either by host defense mechanisms and/or conventional antibiotic regimens (93). *H. pylori* is one of those bacteria that be able to establish the biofilm (110), which favoring the bacterium to survive in adverse conditions (120) as well as promoting the transmission of pathogen to human (146). Although, the main route of transmission of *H. pylori* has not been determined, several reports have described detection of *H. pylori* DNA in drinking and environmental water. These have suggested that *H. pylori* may be waterborne and its ability to form biofilm may be involved in the transmission (112,115).

Some have hypothesized regulatory genes controlling *H. pylori* biofilm formation (119,123,124), but further investigations still being required. Motility has been shown to be a key factor in the ability of *H. pylori* to colonize gastric mucosa (136). Interestingly, some of the current biofilm models indicate that the participation of flagella and pili is important in the growth of the microcolony, especially during the early stages of biofilm formation (92,212). Moreover flagella have been

considered to have a possible role as an adhesin during initial step of biofilm formation (134). We therefore studied the role of flagella genes in regulation of *H. pylori* biofilm formation. The three chosen genes included *flaA* with likely function in flagellar main composition (142), *flgR* with likely a regulatory gene (146), and *fliQ* with likely play a role in export apparatus (148).

The IPCRM technique was used in order to construct the mutant strains. The benefit of using IPCRM is that it has been proven to be a rapid and convenient method for mutating cloned DNA by simultaneously introducing a defined deletion and a unique restriction site (213). When used in conjunction with allelic replacement, this method has proven to be invaluable in the production of defined mutants from both gram-positive and gram-negative bacteria (214). In this study, mutated genes were transformed into *H. pylori* ATCC26695 and N6 host cells by natural transformation and electroporation, respectively. The efficiency of transformation rate of electroporation has been shown to be far higher than natural transformation (215). However, none of transformant *H. pylori* ATCC26695 clone was recovered from electroporation. This may cause by an electroporatic pulse that leading to cell damage or rupture (216). With this reason, the natural transformation was performed instead.

Here, we showed that *H. pylori* could form biofilm in liquid monoculture with two distinct characteristics. It can form a pellicle and attach to a glass surface at air-liquid interface indicating the most presumable its microaerobic, capnophilic character (119). Similar forms of biofilms have been observed previously in other bacteria such as *C. jejuni* (96) and *P. aeruginosa* (97). A monosaccharide analysis performed by gas-liquid chromatography/mass spectrometry revealed several sugars

served as major component in *H. pylori* biofilm materials (120). Whether these biofilm compositions are different among stages of growth may be further investigated with this relevant technique. Animal models have provided an invaluable resource to study *H. pylori* pathogenesis. Some animal models such as mouse and Mongolian gerbils have been shown to develop inflammation and cancer, respectively, when infected with *H. pylori* (217). Many cell lines such as HEp-2, AGS, and MKN45 cells have also been used in studies of *H. pylori* pathogenesis (218). Biofilm formation on human bronchial epithelial (HBE) cells by *Neisseria meningitidis* has demonstrated a role of nasopharyngeal colonization (219). This may be worth to establish and study *H. pylori* biofilm by these models in future. However, different levels of biofilm production were observed between wild type and flagellar mutant strains in this study. In comparison to the wild type *H. pylori* ATCC26695 and N6, all of the *flgR* mutants, PR611 and NR2, showed a significant reduction to form biofilm in both pellicle and attached biofilm characteristics, qualitatively and quantitatively. The *flaA* and *fliQ* mutants, however, demonstrated just slightly decreased biofilm levels.

FlgR is required for flagellar biosynthesis in the earlier stage (146). It is governed by housekeeping sigma factor σ^{70} directs RNA polymerase (146). The activated FlgR in turn activates subsequent genes and regulons (220). The FlgR has been required for the basal body-hook filament complex formation and a colonization of the upper gastrointestinal tract of chicken (221). Although, the involvement of *flgR* gene in bacterial biofilm formation still needs more elucidation. However its role in colonization may be associated.

Double mutation in both *flaA* and *flaB* caused loss of polar flagella and reduction of biofilm formation in *Aeromonas hydrophila* (222). Consistently, the insertional inactivation of *flaA* gene of *C. jejuni* has resulted in a stubby flagellation and delays a pellicle formation (205). FliQ is involved in an export apparatus (140). A *fliQ* mutation has yielded aflagellate and non-motile *H. pylori* (150). However, whether *fliQ* gene involved in biofilm formation has never been reported. From our data, we suggested that the requirement of FlgR for early flagellar biosynthesis (221) might be necessary for the initial stage of biofilm formation.

The ability to adhere to stratum could subsequently promote biofilm establishment (96). The impaired ability to adhere against the HEp-2 cells was observed among these *H. pylori* flagellar mutants, particularly *flgR* and *fliQ* mutants. While the *flgR* mutant had a strongly decreased ability to colonize in chicken (221), the *fliQ* mutant has been shown a reduced ability to adhere to AGS cells (150). The mechanism indicating FlgR regulates flagellar biosynthesis has been described (221). The FlgR also acts as a master transcriptional activator of σ^{54} -dependent genes (146). These σ^{54} -dependent genes cover all the proteins needed for assemble of the hook-basal body filament structure (223). The lack of FlgR, in our point of view, might result an improper or incapable early flagellar biosynthesis (221) that influenced bacterial adhesion as well as biofilm formation. The FliQ protein may be necessary for construction of the channel where the flagella-associated proteins would be transported in order to form the flagellum (148). The channel could not be constructed in an absence of FliQ, which might interrupt the precursor proteins required for the flagellum (148). However, *fliQ* genes did not appear much effect on the ability of *H. pylori* to form biofilm, suggesting that adhesion and biofilm formation presumably

separately controlled in *H. pylori*.

We also confirmed the ability of *H. pylori* to establish biofilm in other strains. Although, all the tested *H. pylori* strains here enabled to produce biofilm, but the dramatically different biofilm levels have been observed both in reference and clinical isolates. *H. pylori* ATCC51932, which is *cagA* negative strain, exhibited the lowest biofilm level among these. This effector protein, CagA, has been suggested to have a role in *H. pylori* colonization (224). Also, the *cagPAI* encodes a type IV secretion system (T4SS), has been noted to be associated in attachment and invasion of *H. pylori* into hepatocytes (225). Although postulated of the relevant of this virulent factor with biofilm formation has not been elucidated, its role in colonization and adhesion may be associated. In this study we aimed to use the reference strain as a representative for further ongoing studies. Although, *H. pylori* ATCC43504 and ATCC43526 exhibited high ability to form biofilm and they were both high reproducibility in this study. However, the ATCC43054 was the chosen one as, in generally, it is used for the quality control of the susceptibility tests (226) that more closely related to our point of study over curcumin.

The increased antimicrobial resistance of *H. pylori* in biofilm has been postulated (159). Production of biofilm by *H. pylori* may also be important for enabling its resistance to host defense factors (227). In general, antimicrobial agents show poor efficacy against biofilm-associated infection (158). In conjunction with a rapid development of bacterial resistance, these may result in a restrictive use of newer generations of antibiotics (228). Several potential strategies to overcome biofilm infections have been proposed. For example, the use of carbohydrate-based therapeutic as anti-adhesive (229), the use of phytomedicine to prevent biofilm

formation (230, 231), and the use of bacteriophage to hydrolyze biofilm extracellular polymers (232). Interestingly, the anti-biofilm activities have been demonstrated in a number of medicinal plants (233-236). In the traditional medicine, turmeric is one of the well-known herbs used for gastric ailment (181). Curcumin is major compound derived from the rhizomes of turmeric, which possesses a board pharmacological effect (237) and confers anti-*H. pylori* activity (191). Effect of curcumin on *H. pylori* biofilm formation was investigated. The sub-MICs of curcumin of individual *H. pylori* strains were used. The sub-MICs, but not exactly MIC levels, were chosen because these concentrations were considered as sufficient enough to effect on *H. pylori* biofilm but did not effect bacterial viability.

In the present study, anti-biofilm activity of curcumin against *H. pylori* flagellar wild types and their mutants, as well as ATCC43504 was clearly observed, both qualitatively and quantitatively. The ability to establish biofilm of *H. pylori* flagellar wild type ATCC26695 and flagellar mutant NA2 was decreased when curcumin treated. We suggested that among those flagellar mutants, curcumin played the most influence on *flaA* gene. Whether this natural compound play an effect against *H. pylori* adhesin has been reported (172). However, its direct activity against bacterial flagellar component, particularly *flaA* gene, has never been documented. Anyhow, the significant effect of anti-biofilm activity of curcumin was observed against *H. pylori* ATCC43504 with dose dependent manner. Although, curcumin effectively inhibited *H. pylori* biofilm formation, the ability could restore in the later period. However, in our point of view, curcumin could delay biofilm formation making most of bacterial cells being as planktonic, which is more sensitive to antimicrobial agents rather than in biofilm state (153). Curcumin has been shown to

down-regulated virulence factors, quorum sensing and biofilm initiation genes of *P. aeruginosa* (195). Use of natural products in combination with antimicrobial agents has improved inhibitory activity against bacterial biofilms (238). Curcumin, in conjunction with anti-tuberculosis agent, has been shown to improve the disease outcome in patients with active tuberculosis (239). The integration of turmeric with currently antibiotic treatment might be a new approach for effective therapy of biofilm-related infection. The virtue of anti-biofilm property of curcumin could not be crucial in only preventing biofilm formation but also in inhibition of pathogenesis caused by *H. pylori*. If biofilm formation is defeated, the host defense mechanism may be able to resolve infection easier (151). Also, antibiotics can act directly and more effectively to the pathogen (151). However, the precise mechanism of this agent against *H. pylori* biofilm requires further investigation.

Despite the fact that biofilm structure has been extensively studied, few standardized methods are available for quantification (240). Furthermore, the quantification of *H. pylori* biofilm seemed to be cumbersome because of its growth nature and biofilm characteristic (119). Few have demonstrated biofilm quantification techniques (98, 119) such as crystal violet staining of forming biofilm on the inner surface of glass flasks (98), quantification of biofilm formed on glass frit using 3-(4,5-dimethylthiazol-2-yl)-2,5-diphenyltetrazolium bromide (MTT) and direct colony count (119). Here we quantified biofilm level by crystal violet staining via two modified techniques. The first, modified from Cole *et al.* (119), was performed in polystyrene plate incorporated with glass coverslips. The *H. pylori* biofilm presumably attach to the provided glass coverslip, and subsequently stained by crystal violet. The second, modified from Anriany *et al.* (98), was performed with pellicle

assay. Once pellicle was removed and the attached biofilm adhering firmly at air-liquid interface was left behind (96), which was then stained by crystal violet. We noticed that there was a correlation between level of pellicle and attached biofilm while biofilm formation was progressing. Although, a quantification of biofilm formation was performed with only the attached biofilm compartment, this could still represent a trend of level of entire biofilm in this study. These two modified techniques required unequal period of incubations, which were 5 and 7 days for glass coverslip and pellicle assay, respectively. These periods seemed to be proper for *H. pylori* biofilm development as the mature biofilm was detected since day 5 of incubation in this study. Even these two techniques yielded the clear quantitative results, some limitations of each technique were noted. In our experiences, the glass coverslip assay required more devices to set up but less time of incubation. Although the pellicle assay required more period of incubation, however the pellicle could be able to collect for subsequent tests.

Stopping bacterial adhesion is thought to be one advantage strategy to overcome biofilm-associated infections (164). As well as looking at the anti-biofilm activity, the ability of curcumin to reduce adherence of *H. pylori*, including ATCC26695 and N6 both wild types and flagellar mutants, and ATCC43504, to the HEp-2 cells was also demonstrated here. Consistently, turmeric is one out of three plants showing to inhibit adhesion of *H. pylori* to the stomach sections previously (172). And this may results in preventing biofilm formation and/or leading to biofilm detachment on human gastric mucosa. Although, curcumin-treated *H. pylori* flagellar wild types (ATCC26695 and N6) and mutants, were still able to form biofilm at lower level on abiotic glass surface included coverslips and test tubes, all of them failed to

adhere to biotic surface; the HEp-2 cells. The concentration of curcumin might also be critical. Ability of adherence of *H. pylori* treated with curcumin at $8 \mu\text{g ml}^{-1}$ (for ATCC43504) was found to reduce, in comparison to those treated with $10 \mu\text{g ml}^{-1}$ or higher concentration (for ATCC26695, N6, and flagellar mutants), which the bacterial completely failed to adhere to the HEp-2 cells. We suggested that curcumin might abolish the bacterial adherence (241) as well as directly affected HEp-2 cells or cell receptors leading bacterial adherent failure. A blockage of *H. pylori* adhesin, BabA, by turmeric has been shown (172), which prescribed anti-adhesive effect of this plant material. Also the evidences that curcumin causing an alteration of protein pattern in cell lines (242) and cell receptor (243) have been reported.

The progression of biofilm formation by *H. pylori* mimics previous reports, beginning with individual bacteria adhering to the abiotic surface, expansion into colonies and formation of a 3-D structure (119). The architecture of *H. pylori* biofilms was observed by SEM revealed that the bacteria aggregated together surrounded by extracellular material and fibrillar network. This material is likely represents extracellular polymeric substance (EPS) (92). This observation associates with the mature biofilms previously explained (94). The bacterial cells encased in biopolymer matrix are represented as an ultrastructure of biofilm. The matrix mainly contains exopolysaccharide, proteins, and DNA (93). The polymeric matrix may be responsible for the biofilm volume and the protection of biofilm community (244). Moreover, most of the bacterial cell shape embedded in extracellular polymeric matrix changed from rod to coccoid. Marked differences were found in the older culture of biofilm, which demonstrated greater coccoid. This morphological conversion may lead bacteria to a dormant stage and a loss of culturability (121). The

bacterium tends to enter the VBNC state, which represents a non-growing population of cells in microbial biofilms in order to ensure firmly adhesion to the surfaces (245). Several human pathogens are able to convert to the VBNC form in order to response to sub-optimum conditions such as sub-inhibitory drug concentrations, nutrient depletion or adverse atmospheres (246). Those include *Campylobacter spp*, *E. coli*, *Francisella tularensis*, *Legionella pneumophila*, *Listeria monocytogenes*, *Mycobacterium tuberculosis*, *P. aeruginosa*, *Salmonella spp*, *Shigella spp*, *V. cholerae*, *V. parahaemolyticus*, *V. vulnificus*, and *H. pylori*. This VBNC state has been suggested to play a role in recurrent and drug resistant infections (246). The direct viable count-fluorescent in situ hybridization (DVC-FISH) was used to confirm the presence of VBNC *H. pylori* cells in water sample (247). This technique may be helpful to proof whether those coccoid bacteria cells encasing in EPS are VBNC. Noteworthy, in the curcumin-treated conditions, less amorphous substance with retardation of morphological change was investigated. Moreover, curcumin at 1/2 MIC absolutely inhibited the biofilm formation and perforation of cells was revealed in the planktonic cells from day 7. This could be associated with cell wall and cell membrane damage as similar as in *L. monocytogenes*, *S. typhimurium* and *E. coli* exposed to bacteriocin or hydostatic pressure (248). The evidence of cell injury has been observed with planktonic and sessile *Bacillus subtilis*, *Pseudomonas fluorescens*, *P. aeruginosa* after treatment with sanitizer against biofilms (249, 250). Proteomics has been used to study global protein expression and to identify proteins specific to *H. pylori* bismuth-binding proteins (209, 210), but has not been applied to *H. pylori* biofilms. The comparative proteomic study was performed in biofilm-grown and planktonic cells, with an absence and presence of curcumin, demonstrated

differences in protein expressions. Biofilm-grown *H. pylori* shared some similarity in up-regulated protein profile expression with other bacteria (205, 251-253). However, many of the proteins identified here in *H. pylori* currently have no known function. The largest group of proteins having up-regulated in *H. pylori* biofilms was related to the chemotaxis and motility. These included putative flagellar hook-associated protein 3 (HAP3) (FlgL), flagellar hook protein (FlgE), flagellar capping protein (FliD), flagellin A (FlaA), and flagellar basal body rod modification protein (FlgD). Although, it has been suggested that motility-associated genes are commonly repressed upon initiation of biofilm formation (254), the motility complex has recently been shown a role in biofilm formation (205). This finding is consistent with our proteomics analysis of *H. pylori* biofilm. Some have provided evidences suggesting these flagella are associated in bacterial biofilm formation (133, 134). FlgL and FlgE were up-regulated in *Shewanella livingstonensis* providing one of microbial adaptation mechanism against a defined stress condition (255). Additionally, a proteomic analysis in *C. jejuni* exhibited the up-regulation of FlaA in the sessile phase indicating its role in biofilm formation (205). FliD found to be up-regulated in biofilm not only in this study, but also in other work (205). The proteins FlgL, FlgE, FlaA, and FliD are required in flagellar biosynthesis and are present in the mature flagella (140). However, FlgD is required for hook assembly but has not been detected in the mature flagella (256). Furthermore this protein has never been reported in biofilm formation before. Thus this is the first time documented the presence of FlgD involved in biofilm formation. The explanation whether flagella being important in biofilm formation has been proposed (205). Flagellar filaments are perhaps as a component of extracellular matrix and important in aiding cell-to-cell

contact in the formation of 3-D matrix (205). Additional surface appendages such as fimbriae are also important in mature biofilm formation (257). Our data revealed a role for the motility complex in biofilm formation. This might be confirmed through the examination of those flagellum-deficient mutants, particularly in *flgR* gene, which significantly impaired the ability to form biofilm in this study. In our flagellar-gene inactivation analysis, the *flgR* gene was found to play the most influence on biofilm formation. However, whether *flgR* involves in biofilm formation has never been explained. Another striking finding in our work was that even *flgR* showed to influence in biofilm formation, the relative protein was not identified in this proteomic analysis. Several possibilities may be able to explain this. For example, proteins may form complexes with other proteins and only function in the presence of these other molecules, or post-translational modification of proteins may affect their activities (197). FlgR must be phosphorylated by FlgS to activate the transcription of subsequent genes (218). However, the phosphorylated FlgR, however, has been showed to be less stable (218). Neither unphosphorylation nor destabilization might be possibly responsible in the absence of the FlgR in this proteomics analysis.

A group of protein responsible as a chaperone in protein biosynthesis was found to be up-regulated in biofilm in this study. These included elongation factor Tu (EF-Tu) and P protein (EF-P), trigger factor protein (Tig), heat shock protein 60 (Hsp 60) and co-chaperone (GrpE). The elongation factor protein plays a role as translational machinery that required for expression of the genetic information encoded in cells (258). In *C. jejuni*, elongation factor G (EF-G) has been increasingly expressed in biofilm phase (205). These two proteins are proved to be important in cell viability (259) and facilitating organism to colonize (260). The Tig, one of

virulence genes, is a key protein in biofilm formation in *S. mutants* (253). A deficiency of Tig protein causes alterations in biofilm formation leading to acid and oxidative stress intolerance (253). The heat shock protein is a related protein expressing when cells are exposed to elevated temperatures or other stress (261). The Hsp 60 is involved in the synthesis of mycolic acid, which is responsible for the development of a wrinkled mature pellicle in *Mycobacterium smegmatis* (251). The chaperone proteins may be necessary for protein biosynthesis when grown under sub-optimal condition (255). Another group of proteins having up-regulated in the biofilm in this study are involved in the general stress response and detoxification. These included catalase (KatA), thioredoxin reductase (TrxB), alkyl hydroperoxide reductase (TsaA). Several microorganisms cope with the harmful oxidative stress molecules via an antioxidant system (262). By generally, KatA and TsaA are 2 out of three principal enzymes involving in resist to oxidative damage in *H. pylori* (23). KatA converts hydrogen peroxide to oxygen and water whereas TsaA catalyzes a reduction of alkyl hydroperoxide to the alcohol (263). *H. pylori* harbors TrxB, a chaperon which required as a reductant for many oxidative stress enzymes (262). The thioredoxin and TrxB have been shown to predominately exhibit in *C. albicans* biofilm and exert resistance to common antifungals (264). KatA contributes to the peroxide resistance of *P. aeruginosa* biofilm that propagate to a chronic infection (252). There are several modes of survivability of cells within biofilm (92) and the up-regulation of stress response proteins might be another survival capability (205).

Proteins responsible in electron transport function, including pyruvate ferredoxin oxidoreductase beta subunit (PorB), bifunctional methionine sulfoxide reductase A/B protein (HPSH_01160), and flavodoxin (FldA) were up-regulated in

biofilm. These proteins generally involve in coupled oxidation and reduction reactions in respiration (265-267). Among these proteins, only methionine sulfoxide reductase has been previously conferred for an increased level in biofilm compared to the planktonic counterparts (265). Acetyl coenzyme A acetyltransferase; FadA (or thiolase), which is function in metabolic intermediate biosynthesis (268), was also found to be up-regulated in the biofilm phase in this study. However, its presence in other biofilm-grown bacteria has never been reported. Enhanced expression of some energy generation or catabolic function proteins may indicate that the biofilm-grown cells remain in an active growth cell (205). Although, it is well known that cells entering in biofilm may convert to a slow growth phase (151), the cells in this stage still viable. Their metabolic functions have to balance which some proteins are down/up regulated.

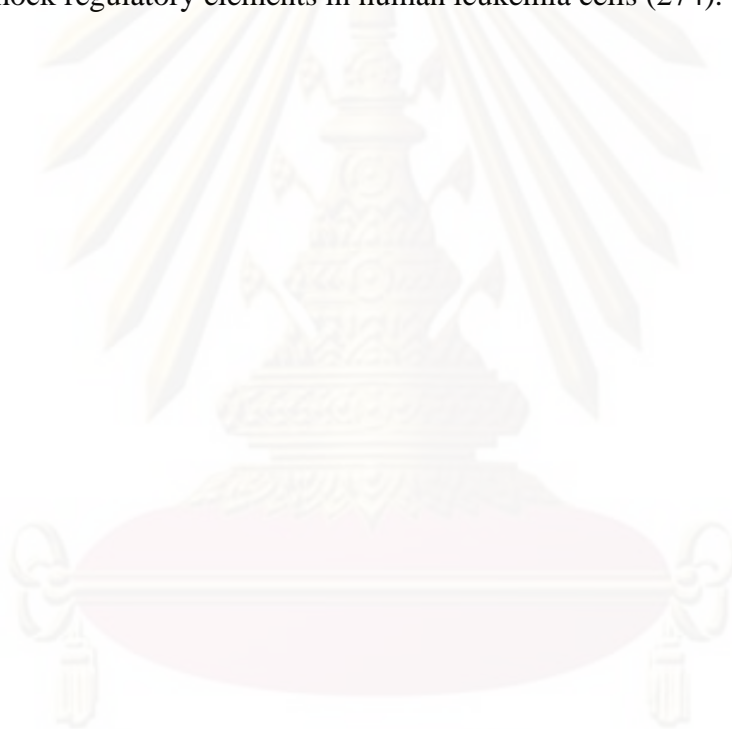
Proteins involving in nitrogen metabolism (urease subunit alpha; UreA and beta; UreB, and bifunctional urease subunit gamma/beta; HP0073) as well as carbohydrate metabolism (bifunctional aconitate hydratase 2/2 methylisocitrate dehydratase; AcnB and citrate synthase; GltA) were also detected in enhanced levels in *H. pylori* biofilm in this study. Urease involves in nitrogen metabolism (269) and also appears to be critical for *H. pylori* colonization (270). *Proteus mirabilis* urease negative strain failed to produce the rise in urinary pH, resulting in a failure to attach and become colonized by crystalline biofilm (271). However, whether or not this protein directly responsible in biofilm formation has never been purposed, its role in colonization may be involved. The citric acid cycle (CAC) is important central metabolic pathway in living cells (27). GltA and AcnB carry out the first and second steps in the oxidative branch of this cycle, respectively (27). In *P. aeruginosa*

biofilm, the increased transcription level of aconitate hydratase gene, *acnA*, has been shown (272).

Interestingly, urease and catalase are key enzymes used for a conventional *H. pylori* identification (19). In our point of view, these enzymes should be normally present in all *H. pylori* cells. Thus, the absence of these two proteins in planktonic sample was unusual. Uraese is one of essential factors for *H. pylori* adhesion (270), whereas catalase protects bacteria against damaging factors (16). The presence of these two proteins in biofilm, but not in planktonic counterpart, might be due to a role in adhesion associating biofilm formation (126) and a survival mode within biofilm (205). Weather these planktonics were still able to produce these enzymes could be performed by conventional urease and catalase tests (19).

All of the identified proteins here were found to be present in both cucumin-untreated biofilm and 1/4 MIC of curcumin-treated biofilm. These proteins were almost absent and/or down-regulated in their planktonic counterparts, suggesting that these proteins might be responsible in biofilm formation. With a presence of curcumin, biofilm and planktonic treated with 1/4 MIC showed almost similar pattern of protein profile expression as observed in cucumin-untreated biofilm and planktonic, respectively. Exceptionally, the chaperone proteins (EF-Tu, EF-P, Tig, Hsp 60 and GrpE) were expressed in response to a presence of 1/4 MIC but not 1/2 MIC of curcumin. Curcumin might induce the presence of these chaperone proteins that inhibited *H. pylori* biofilm. The presence of oregano essential oil component, carvacrol, caused *E. coli* O157:H7 to produce significant amounts of heat shock protein 60 and inhibited the synthesis of flagellin (273). Bacterial flagella have been shown to promote biofilm formation (133,134). Taken these into account, a

mechanism of curcumin that inhibit *H. pylori* might be responsible by the chaperone group protein. It was suggested that the chaperone proteins might facilitate proper folding of newly synthesized proteins during bacterial growth under sub-optimal condition (255). The absent of those relative proteins in 1/2 MIC of curcumin-treated planktonic might be due to effect of curcumin. Curcumin has been found to attenuate *P. aeruginosa* biofilm initiation genes (195). Moreover, it has been shown to activate the heat shock regulatory elements in human leukemia cells (274).



ศูนย์วิทยทรัพยากร
จุฬาลงกรณ์มหาวิทยาลัย

CHAPTER VII

CONCLUSION

H. pylori could form biofilm at the air-liquid interface with two distinctive characters included attached biofilm and pellicle. Role of three flagellar genes, *flaA*, *flgR*, and *fliQ*, on *H. pylori* biofilm formation was investigated. Six flagellar mutants were constructed from two wild types, including ATCC26695 and N6. Genes involved in flagellar synthesis, particularly *flgR*, presumably played an important role in biofilm formation of *H. pylori*. The mutagenesis of *flgR* showed the significant reduced ability to form biofilm in comparison to the wild types, while the biofilm level of *flaA* and *fliQ* mutants showed no significant reduction. Besides that, the *flgR* and *fliQ* were affected the ability of bacteria to adhere to the HEP-2 cells.

Curcumin could inhibit *H. pylori* biofilm formation in dose dependent manner. However, the ability to form biofilm could restore in extended incubation period. Cells encased in mature biofilm connected each other by the fiber-like structure, and were mostly present in coccoid shape covering with extracellular substance. Curcumin affected against cellular structure. The pore formation, represented as cell destruction, was observed over curcumin-treated cells. Curcumin demonstrated inhibitory effect against *H. pylori* biofilm and showed a greatly inhibitory action on adherence of *H. pylori* to the human epithelial cells. The virtue of anti-*H. pylori* property of curcumin could be crucial in inhibition of pathogenesis caused by this organism. Curcumin might be a potential supplemental material for the treatment of biofilm-involved *H. pylori* infection making a new approach for effective therapy.

Proteomics analysis demonstrated proteins possibly involved in biofilm formation of *H. pylori*. Such proteins included chemotaxis and motility proteins (FlgL, FlgE, FliD, FlaA, FlgD), chaperone proteins (TufA, Tig, Hsp60, GrpE, Efp), stress response proteins (KatA, TrxB, TsaA), electron transport proteins (PorB, HPSH_01160, FldA), nitrogen and carbohydrate metabolism proteins (UreA, UreB, HP0073, AcnB, GltA), and metabolic intermediate biosynthesis (FadA). Planktonic cells could express some proteins, but in decreased level, similar to those found in their biofilm counterpart. These proteins provided the first lines of evidence indicating mechanism involved in *H. pylori* biofilm formation. The proteins up-regulating in a presence of curcumin included Tig, Hsp60, HPSH_01160, GrpE, and Efp.

Further studies may be established to provide more understanding over *H. pylori* biofilm mechanisms. Curcumin inhibitory effect against *H. pylori* biofilm may be able to establish *in vivo* in animal models. Whether curcumin may possess synergistic effect with conventional antibiotics against biofilm may be investigated. However, other possible agents possessing anti-biofilm activity may be tested against *H. pylori* biofilm. In order to retrieve back to the corresponding genes and fulfill our proteomic data obtained here, a genetic inactivation of those genes encoding for proteins involved in *H. pylori* biofilm formation may be performed.

REFERENCES

- (1) Fung, W. P.; Papadimitriou, J. M.; and Matz, L. R. 1979. Endoscopic, histological and ultrastructural correlations in chronic gastritis. **Am. J. Gastroenterol.** 71:269-279.
- (2) Palmer, E. D. 1954. Investigation of the gastric spirochaetes of the human. **Gastroenterology.** 27:218-220.
- (3) Mashall, B. J. 2001. One hundred years of discovery and rediscovery of *Helicobacter pylori* and its association with peptic ulcer disease, In S. L. Hazell. (ed.), **Helicobacter pylori: physiology and genetic**, pp. 19-24. Washington DC: ASM Press.
- (4) Marshall, B. J., and Warren, J. R. 1984. Unidentified curved bacilli in the stomach of patients with gastritis and peptic ulceration. **Lancet.** 1:1311-1315.
- (5) Warren, J. R., and Marshall, B. J. 1983. Unidentified curved bacilli on gastric epithelium in active chronic gastritis. **Lancet.** 1:1273-1275.
- (6) Smith, A.; Price, A. B.; Dolby, J.: and Levi J. 1984. *Campylobacter pyloridis* in Peptic-Ulcer disease – Pathogen or Opportunist. **Gut.** 25:1136-1137.
- (7) Marshall, B. J., and Goodwin, C. S. 1987. Revised Nomenclature of *Campylobacter pyloridis*. **Int. J. Syst. Bacteriol.** 37:68.
- (8) Romaniuk, P. J., *et al.* 1987. *Campylobacter pylori*, the spiral bacterium associated with human gastritis, is not a true *Campylobacter* sp. **J. Bacteriol.** 169:2137-2141.

- (9) Tomb, J. F., *et al.* 1997. The complete genome sequence of the gastric pathogen *Helicobacter pylori*. **Nature**. 388:539-547.
- (10) Alm, R. A., *et al.* 1999. Genomic sequence comparison of two unrelated isolates of the human gastric pathogen *Helicobacter pylori*. **Nature**. 397:176-180.
- (11) Harper, C. G., *et al.* 2002. *Helicobacter cetorum* sp nov., a urease-positive *Helicobacter* species isolated from dolphins and whales. **J. Clin. Microbiol.** 40:4536-4543.
- (12) Harper, C. G., *et al.* 2003. Isolation and characterization of novel *Helicobacter* spp. from the gastric mucosa of harp seals *Phoca groenlandica*. **Dis Aquat. Organ.** 57:1-9.
- (13) Schauer, D. B. 2001. Enterohepatic *Helicobacter* species, In S. L. Hazell. (ed.), ***Helicobacter pylori: physiology and genetic***, pp. 533-548. Washington DC: ASM Press.
- (14) Danon, S. J., and Lee, A. 2001. Enterohepatic *Helicobacter* species, In S. L. Hazell. (ed.), ***Helicobacter pylori: physiology and genetic***, pp. 549-563. Washington DC: ASM Press.
- (15) Madigan, M.; Martinko, J.; and Parker, J. 2003. **Brock Biology of Microorganisms**. 10th ed. London: Prentice-Hall International.
- (16) Andersen, L. P., and Wadstrom, T. 2001. Basic Bacteriology and Culture, In Hazell, S. L. (ed.), ***Helicobacter pylori: physiology and genetic***, pp. 27-38. Washington DC: ASM Press.

- (17) Murray, R. G.; and Stackebrandt, E. 1995. Taxonomic note: implementation of the provisional status Candidatus for incompletely described prokaryotes. **Int. J. Syst. Bacteriol.** 45:186-187.
- (18) Page, R. D. M. 1996. TREEVIEW: an application to display phylogenetic trees on personal computers. **Comput. Applic. Biosci.** 12:357-358.
- (19) Solnick, J. V., and Vandamme, P. 2001. Taxonomy of the *Helicobacter* Genus, In S. L. Hazell.(ed.), ***Helicobacter pylori: physiology and genetic***, pp. 39-51. Washington DC: ASM Press.
- (20) Singhal, A. V., and Sepulveda, A. R. 2005. *Helicobacter heilmannii* gastritis: a case study with review of literature. **Am. J. Surg. Pathol.** 29:1537-1539.
- (21) Olson, J. W., and Maier, R. J. 2002. Molecular hydrogen as an energy source for *Helicobacter pylori*. **Science.** 298:1788-1790.
- (22) Lancaster, C. R., and Simon, J. 2002. Succinate:quinone oxidoreductases from epsilon-proteobacteria. **Biochem. Biophys. Acta.** 1553:84-101.
- (23) Marais, A.; Mendz, G. L.; Hazell, S. L.; and Megraud, F. 1999. Metabolism and genetics of *Helicobacter pylori*: the genome era. **Microbiol. Mol. Biol. Rev.** 63:642-674.
- (24) Kelly, D. B.; Hughes, N. J.; and Poole, R. K. 2001. Microaerobic physiology: aerobic respiration, anaerobic respiration and carbon dioxide metabolism, In S. L. Hazell.(ed.), ***Helicobacter pylori: physiology and genetic***, pp. 113-124. Washington DC: ASM Press.

- (25) Hildebrand, P.; Meyer-Wyss, B. M.; Mossi, S.; and Beglinger, C. 2000. Risk among gastroenterologists of acquiring *Helicobacter pylori* infection: case-control study. **Br. Med. J.** 321:149.
- (26) Hoffman, P. S.; Goodwin, A.; Johnsen, J.; Magee, K.; Veldhuyzen, S. J. O.; and vanZanten, S. J. O. V. 1996. Metabolic activities of metronidazole-sensitive and resistant strains of *Helicobacter pylori*: repression of puruvate oxidoreductase and expression of isocitrate lyase activity correlate with resistance. **J. Bacteriol.** 178:4822-4829.
- (27) Kelly, D. B., and Hughes, N. J. 2001. The citric acid cycle and fatty acid biosynthesis, In S. L. Hazell.(ed.), ***Helicobacter pylori: physiology and genetic***, pp. 135-146. Washington DC: ASM Press.
- (28) Mobley, L. T. 2001. Urease, In S. L. Hazell.(ed.), ***Helicobacter pylori: physiology and genetic***, pp. 179-191. Washington DC: ASM Press.
- (29) Baron, S., *et al.* 1996. **Medical Microbiology**. 4th ed. Galveston: The University of Texas Medical Branch at Galveston.
- (30) Alm, R. A., and Trust, T. J. 1999. Analysis of the genetic diversity of *Helicobacter pylori*: the tale of two genomes. **J. Mol. Med.** 77:834-846.
- (31) Alm, A. R., and Noonan, B. 2001. The genome, In S. L. Hazell.(ed.), ***Helicobacter pylori: physiology and genetic***, pp. 295-311. Washington DC: ASM Press.
- (32) Takami, S.; Hayashi, Y.; Tonokatsu, Y.; Shimoyama, T.; and Tamura, T. 1993. Chromosomal heterogeneity of *Helicobacter pylori* isolates by pulsed-field gel electrophoresis. **Zentralbl. Bakteriol.** 280:120-127.

- (33) Pride, D. T., and Blaser, M. J. 2002. Concerted evolution between duplicated genetic elements in *Helicobacter pylori*. **J. Mol. Biol.** 316:629-642.
- (34) Bjorkholm, B. M.; Sjolund, P. G.; Falk, P. G.; Berg, O. G.; Engstrand, L.; and Anderson, D. I. 2001. Mutation frequency and biological cost of antibiotic resistance in *Helicobacter pylori*. **Proceeding of the National Academy of Sciences of the United State of America.** 98:14607-14612.
- (35) Saito, N.; Konishi, K.; Kato, M.; Takeda, H.; Asaka, M.; and Ooi, H. K. 2008. Coccoid formation as a mechanism of species-preservation in *Helicobacter pylori*: an ultrastructural study. **Hokkaido. Igaku, Zasshi.** 83(5):291-295.
- (36) West, A. P.; Millar, M. R.; and Tompkins, D. S. 1990. Survival of *Helicobacter pylori* in water and saline. **J. Clin. Pathol.** 43:609.
- (37) Moshkowitz, M.; Gorea, A.; Arber, N.; Konikoff, F.; Berger, S.; and Gilat, T. 1994. Morphological transformation of *Helicobacter pylori* during prolonged incubation – association with decrease acid resistance. **J. Clin. Pathol.** 47:172-174.
- (38) Brenciaglia, M. I.; Fornara, A. M.; Scaltrito, M. M.; and Dubini, F. 2000. *Helicobacter pylori*: cultivability and antibiotic susceptibility of coccoid forms. **Int Antimicrob. Agent.** 13:237-241.
- (39) Enroth, H.; Wreiber, K.; Rigo, R.; Risberg, D.; Uribe, A.; and Engstrand, L. 1999. *In vitro* aging of *Helicobacter pylori*: changes in morphology, intracellular composition and surface properties. **Helicobacter.** 4:7-16.

- (40) Kusters, J.G.; Gerrits, M. M.; van Strijp, J. A.; and Vandenbroucke-Grauls, C. M. 1997. Coccoid forms of *Helicobacter pylori* are the morphologic manifestation of cell death. **Infect. Immun.** 65:3672-3679.
- (41) Saito, N., and *et al.* 2003. Plural transformation-processes from spiral to coccoid *Helicobacter pylori* and its viability. **J. Infect.** 46:49-55.
- (42) Goodwin, C. S., and Armstrong, J. A. 1990. Microbiological aspects of *Helicobacter pylori* (*Campylobacter pylori*). **Eur. J. Clin. Microbiol. Infect. Dis.** 9:1-13.
- (43) Versalovic, J., and Fox, JG. 2003. *Helicobacter*, In P. R. Murray (ed.), **Manual of Clinical Microbiology**, pp. 915-928. Washington DC: ASM Press.
- (44) Dent, J. C., and McNulty, C. A. 1988. Evaluation of a new selective medium for *Campylobacter pylori*. **Eur. J. Clin. Microbiol. Infect. Dis.** 7:555-558.
- (45) Goodwin, C. S.; Blincow, E. D.; Warren, J. R.; Waters, T. E.; Sanderson, C. R.; and on, L. 1985. Evaluation of cultural techniques for isolating *Campylobacter yloridis* from endoscopic biopsies of gastric mucosa. **J. Clin. Pathol.** 38:1127-1131.
- (46) Mitchell, H. M. 2001. Epidemiology of infection, In S. L. Hazell. (ed.), **Helicobacter pylori: physiology and genetic**, pp. 7-18. Washington DC: ASM Press.
- (47) Czinn, S. J. 2005. *Helicobacter pylori* infection: detection, investigation, and management. **J. Pediatr.** 146(3 Suppl):S21-26.

- (48) Brown, L. M. 2000. *Helicobacter pylori*: epidemiology and routes of transmission. **Epidemiol. Rev.** 22:283-297.
- (49) Parsonnet, J. 1995. The incidence of *Helicobacter pylori* infection. **Aliment. Pharmacol. Ther.** 9(2 Suppl):S45-51.
- (50) Perez-Perez, G. I.; Talor, D. N.; Bodhidatta, L.; and *et al.* 1990. Seroprevalence of *Helicobacter pylori* in Thailand. **J. Infect. Dis.** 161:1237-1241.
- (51) Mitchell, H. M., and *et al.* 1992. Epidemiology of *Helicobacter pylori* in Southern China-identification of early childhood as the critical period for acquisition. **J. Infect. Dis.** 166:149-153.
- (52) Madinier, I. M.; Fosse, T. M.; and Montiel, R. A. 1997. Oral carriage of *Helicobacter pylori*: a review. **J. Periodontol.** 68: 2-6.
- (53) Personnet, J.; Shmuelly, H.; and Haggerty, T. 1999. Fecal and oral shedding of *Helicobacter pylori* from healthy infected adults. **J. Am. Med. Assoc.** 23: 2240-2245.
- (54) Thomas, J. E.; Gibson, G.; Darboc, M.; Dale, A.; and Weaver, L. T. 1992. Isolation of *Helicobacter pylori* from human faeces. **Lancet.** 340: 1194-1195.
- (55) Khandaker, K.; Palmer, K. R.; Eastwood, M. A.; Scott, A. C.; Desai, M.; and Owen, R. J. 1993. DNA fingerprints of *Helicobacter pylori* from mouth and antrum of patients with chronic ulcer dyspepsia. **Lancet.** 342:751.
- (56) Hulten, K., and *et al.* 1996. *Helicobacter pylori* in the drinking water in Peru. **Gastroenterology.** 110(4):1031-1035.

- (57) Zhang, L., and *et al.* 1996. *Helicobacter pylori* antibodies in relation to precancerous gastric lesions in a high risk Chinese population. **Cancer. Epidemiol. Biomarkers. Prev.** 5:627-630.
- (58) Goodman, K. J., and *et al.* 1996. *Helicobacter pylori* infection in the Columbian Andes: a population-based study of transmission pathways. **Am. J. Epidemiol.** 144:290-299.
- (59) Klein, P. D.; Graham, D. Y; Gaillour, A.; Opekun, A. R.; and Smith, E. O. 1991. Water source as risk factor for *Helicobacter pylori* infection in Peruvian children. Gastrointestinal Physiology Working Group. **Lancet.** 337:1503-1506.
- (60) Dubois, A., and *et al.* 1996. Transient and persistent experimental infection of nonhuman primates with *Helicobacter pylori*: implications for human disease. **Infect. Immun.** 64:2885-2891.
- (61) Dore, M. P., and *et al.* 1999. High prevalence of *Helicobacter pylori* infection in shepherds. **Dig. Dis. Sci.** 44:1161-1164.
- (62) Grubel, P.; Hoffman, J. S.; Chong, F. K.; Burstein, N. A.; Mepani, C.; and Cave, D. R. 1997. Vector potential of houseflies (*Musca domestica*) for *Helicobacter pylori*. **J. Clin. Microbiol.** 35:1300-1303.
- (63) Rohr, M. R.; Castro, R.; Morais, M.; Brant, C. Q.; Castelo, F. A.; and Ferrari, J. A. P. Risk of *Helicobacter pylori* transmission by upper gastrointestinal endoscopy. **Am. J. Infect. Control.** 26:12-15.
- (64) Dore, M. P.; Leandro, G.; Realdi, G.; Sepulveda, A. R.; and Graham, D. Y. 2000. Effect of pretreatment antibiotic resistance to metronidazole and clarithromycin

- on outcome of *Helicobacter pylori* therapy: a meta-analytical approach. **Dig. Dis. Sci.** 45:68-76.
- (65) Park, S., and *et al.* 2005. Rescue of *Helicobacter pylori*-induced cytotoxicity by red ginseng. *Dig. Dis. Sci.* 59(7):1218-1227. Cited in International agency for research on cancer. **Schistosomes, Liver Fluke and Helicobacter pylori.** Lyon: IARC Scientific Publication no. 61, International Agency for Research on Cancer, 1994.
- (66) Dunn, B. E.; Cohen, H.; and Blaser, M. J. 1997. *Helicobacter pylori.* **Clin. Microbiol. Rev.** 10:720-741.
- (67) Uemura, N., and *et al.* 2001. *Helicobacter pylori* infection and the development of gastric cancer. **N. Engl. J. Med.** 345(11):784-789.
- (68) Chen, G.; Sordillo, E. M.; and Ramey, W. G. 1997. Apoptosis in gastric epithelial cells is induced by *Helicobacter pylori* and accompanied by increased expression of Bak. **Biochem. Biophys. Res. Commun.** 239:626-632.
- (69) Eguchi, H., and Moss, S. F. 2002. *Helicobacter pylori.* **J. Clin. Pathol.** 55:284-285.
- (70) Menaker, R. J.; Ceponis, P. J.; and Jones, N. L. 2004. *Helicobacter pylori* induces apoptosis of macrophages in association with alterations in the mitochondrial pathway. **Infect. Immune.** 72:2889-2898.
- (71) Perez-Perez, G. I., and *et al.* 1997. Country-specific constancy by age in *cagA*+ proportion of *Helicobacter pylori* infections. **Int. J. Cancer.** 72:453-456.

- (72) Backert, S., and *et al.* 2000. Translocation of the *Helicobacter pylori* CagA protein in gastric epithelial cells by type IV secretion apparatus. **Cell. Microbiol.** 2:155-164.
- (73) Segal, E. D.; Cha, J.; Lo, J.; Falkow, S.; and Tompkins, L. S. 1999. Altered states: involvement of phosphorylated CagA in the induction of host cellular growth changes by *Helicobacter pylori*. **Proc. Natl. Acad. Sci. USA.** 96. 14559-14564.
- (74) Blaser, M. J. 1998. *Helicobacter pylori* and gastric diseases. **Br. Med. J.** 316:1507-1510.
- (75) Moreira, K. R.; Darini, E.; Canavez, F. C.; de Carvalho, C. M.; Troquez, C. A.; and Camara-Lopes L. H. 2005. *Helicobacter pylori* and *cagA* gene detected by polymerase chain reaction in gastric biopsies: correlation with histological finding, proliferation and apoptosis. **Sao. Paulo. Med.** 123:113-118.
- (76) Censini, S., and *et al.* 1996. *cag*, a pathogenicity island of *Helicobacter pylori*, encodes type I specific and disease-associated virulence factors. **Proc. Natl. Acad. Sci. USA.** 93:14648-14653.
- (77) Atherton, J. C.; Peek, R. M. Jr.; Tham, K. T.; Cover, T. L.; and Blaser, M. J. 1997. Clinical and pathological importance of heterogeneity in *vacA*, the vacuolating cytotoxin gene of *Helicobacter pylori*. **Gastroenterology.** 112:92-99.
- (78) Atherton, J. C.; Cao, P.; Peek, R. M. Jr.; Tummuru, M. K. R.; Blaser, M. J.; and Cover, T. L. 1995. Mosaicism in vacuolating cytotoxin alleles of *Helicobacter pylori*. **J. Biol. Chem.** 270:17771-17777.

- (79) Suerbaum, S., and Michetti, P. 2002. *Helicobacter pylori* and infection. **N. Engl. J. Med.** 347:1175-1186.
- (80) Bartnik, W. 2008. Clinical aspects of *Helicobacter pylori* infection. **Pol. Arch. Med. Wewn.** 118(7-8):426-430.
- (81) Malfertheiner, P., and *et al.* 2002. Current concepts in the management of *Helicobacter pylori* infection-The Maastricht 2-200 Consensus Report. **Aliment. Pharmacol. Ther.** 16:167-180.
- (82) Kim, J. G. 2005. Treatment of *Helicobacter pylori* infection. **Korean. J. Gastroenterol.** 46:172-180.
- (83) Megraud, F. 2004. *H. pylori* antibiotic resistance: prevalence, importance, and advances in testing. **Gut.** 53(9):1374-1384.
- (84) Romano, M., and *et al.* 2008. Failure of first line eradication treatment significantly increase prevalence of anti-microbial resistant *Helicobacter pylori* clinical isolates. **J. Clin. Pathol.** 61(10):1112-1115.
- (85) Graham, D. Y. 1995. Clarithromycin for treatment of *Helicobacter pylori* infections. **Eur. J. Gastroenterol. Hepatol.** 7(Suppl):S55-S58.
- (86) Kwon, D. H., and *et al.* 2003. High-level β -lactam resistance associated with acquired multidrug resistance in *Helicobacter pylori*. **Antimicrob. Agents. Chemother.** 47:2169-2178.
- (87) Hunt, R., and Thomson, A. B. 1998. **Canadian Helicobacter pylori consensus conference.** **Canadian Association of Gastroenterology.** 12:31-41.

- (88) Meyer, J. M., and *et al.* 2002. Risk factor for *Helicobacter pylori* resistance in the United States: the surveillance of *H. pylori* antimicrobial resistance partnership HARP) study, 1993-1999. **Ann. Intern. Med.** 136(1):13024.
- (89) Dore, M. P., and Realdi, G. 2001. Stable amoxicillin resistance in *Helicobacter pylori*. **Helicobacter.** 6:79.
- (90) Davey, M. E., and O'Toole, G. A. 2000. Microbial biofilms: from ecology to molecular genetics. **Microbiol. Mol. Biol. Rev.** 64(4):847-867.
- (91) Sauer, K. 2003. The genomics and proteomics of biofilm formation. **Genome. Biol.** 4:219.
- (92) Donlan, R. M., and Costerton, J. W. 2002. Biofilms: survival mechanisms of clinically relevant microorganisms. **Clin. Microbiol. Rev.** 15:167-193.
- (93) Thomas, J. G., and Lehman, D. C. 2006. Biofilms: architects of disease, In C. Mahon; G. Manuselis; and D. Lehman (eds.), **Textbook of diagnostic microbiology**, pp. 884-895. Amsterdam: Elsevier.
- (94) Watnick, P., and Kolter, R. 2000. Biofilm, city of microbes. **J. Bacteriol.** 182:2675-2679.
- (95) Hall-Stoodley, L.; Costerton, J. W.; and Stoodley, P. 2004. Bacterial biofilms: from the natural environment to infectious diseases. **Nat. Rev. Microbiol.** 2:95-108.
- (96) Joshua, G. W. P.; Guthrie-Irons, C.; Karlyshev, A. V.; and Wren, B. W. 2006. Biofilm formation in *Campylobacter jejuni*. **Microbiology.** 152:387-396.
- (97) Friedman, L., and Kolter, R. 2004. Genes involved in matrix formation in *Pseudomonas aeruginosa* PA14 biofilms. **Mol. Microbiol.** 51:675-690.

- (98) Anriany, Y. A.; Weiner, R. M.; Johnson, J. A.; De Rezende, C. E.; and Joseph, S. W. 2001. *Salmonella enterica* serovar Typhimurium DT104 displays a rugose phenotype. **Appl. Environ. Microbiol.** 67:4048-4056.
- (99) Costerton, J. W.; Lewandowski, Z.; Caldwell, D. E.; Korber, D. R.; and Lappin-Scott, H. M. 1995. Microbial biofilms. **Annu. Rev. Microbiol.** 49:711-745.
- (100)Whitchurch, C. B.; Tolker-Nielsen, T.; Ragas, P. C.; and Mattick, J. S. 2002. Extracellular DNA required for bacterial biofilm formation. **Science.** 295:1487.
- (101) Mack, D., and *et al.* 2000. Identification of three essential regulatory gene loci governing expression of *Staphylococcus epidermidis* polysaccharide intercellular adhesin and biofilm formation. **Infect. Immun.** 68:3799-3807.
- (102) Solano, C., and *et al.* 2002. Genetic analysis of *Salmonella enteritidis* biofilm formation: critical role of cellulose. **Mol. Microbiol.** 43:793-808.
- (103) Nesper, J.; Lauriano, C. M.; Klose, K. E.; Kapfhammer, D.; Kraiss, A.; and Reidl, J. 2001. Characterization of *Vibrio cholerae* O1 El tor *galU* and *galE* mutant: influence on lipopolysaccharide structure, colonization, and biofilm formation. **Infect. Immun.** 69:435-445.
- (104) Huber, B., and *et al.* 2001. The *cep* quorum-sensing system of *Burkholderia cepacia* H111 controls biofilm formation and swarming motility. **Microbiology.** 147:2517-2528.
- (105)Tunkel, A. R., and Mandell, G. L. 1992. Infecting microorganisms, In Kaye, D. (ed.), **Infective endocarditis**, 2nd ed., pp. 85-97. New York: Raven Press.

- (106) Feigin, R. D.; Kline, M. W.; Hyatt, S. R.; and Ford, K. L. 1992. Otitis media, In Feigin, R. D. and Cherry, J. D. (ed.), **Textbook of pediatric infectious diseases**, 3rd ed., pp. 174-189. Philadelphia: W. B. Saunders.
- (107) Domingue, G. J., and Hellstrom, W. J. G. 1998. Prostatitis. **Clin. Microbiol. Rev.** 11:604-613.
- (108) Govan, J. R. W., and Deretic, V. 1996. Microbial pathogenesis in cystic fibrosis: mucoid *Pseudomonas aeruginosa* and *Burkholderia cepacia*. **Microbiol. Rev.** 60:539-574.
- (109) Moore, W. E. C., and *et al.* 1983. Bacteriology of moderate (chronic) periodontitis in mature adult humans. **Infect, Immun.** 42:510-515.
- (110) Park, S. R.; Mackay, W. G.; and Reid, D. C. 2001. *Helicobacter* sp. recovered from drinking water biofilm sampled from a water distribution system. **Water. Res.** 35:1624-1626.
- (111) Giao, M. S.; Azevedo, N. F.; Wilks, S. A.; Vieira, M. J.; and Keevil, C. W. 2008. Persistence of *Helicobacter pylori* in heterotrophic drinking water biofilms. **Appl. Environ. Microbiol.** 74(19):5898-5904.
- (112) Watson, C. L., and *et al.* 2004. Detection of *Helicobacter pylori* by PCR but not culture in water and biofilm samples from drinking water distribution systems in England. **J. Appl. Microbiol.** 97:690-698.
- (113) Enroth, H., and Engstrand, L. 1995. Immunomagnetic separation and PCR for detection of *Helicobacter pylori* in water and stool specimens. **J. Clin. Microbiol.** 33:2162-2165.

- (114) Bunn, J. E. G.; Mackay, W. G.; Thomas, J. E.; Reid, D. C.; and Weaver, L. T. 2002. Detection of *Helicobacter pylori* DNA in drinking water biofilms: implication for transmission in early life. **Lett. Appl. Microbiol.** 34:450-454.
- (115) Benson, J. A.; Fode-Vaughan, K. A.; and Collins, M. L. P. 2004. Detection of *Helicobacter pylori* in water by direct PCR. **Lett. Appl. Microbiol.** 39:221-225.
- (116) Carron, M. A.; Tran, V. R.; Sugawa, C.; and Coticchia, J. M. 2006. Identification of *Helicobacter pylori* biofilms in human gastric mucosa. **J. Gastrointest. Surg.** 10:712-717.
- (117) Cellini, L., and *et al.* 2005. Biofilm formation and modulation of *luxS* and *rpoD* expression by *Helicobacter pylori*. **Biofilms.** 2:1-9.
- (118) Coticchia, J. M.; Sugawa, C.; Tran, V. R.; Gurrola, J.; Kowalski, E.; and Carron, M. A. 2006. Presence and density of *Helicobacter pylori* biofilms in human gastric mucosa in patients with peptic ulcer disease. **J. Gastrointest. Surg.** 10:883-889.
- (119) Cole, S. P.; Harwood, J.; Lee, R.; She, R.; and Guiney, D. G. 2004. Characterization of monospecies biofilm formation by *Helicobacter pylori*. **J. Bacteriol.** 186:3124-3132.
- (120) Stark, R. M., and *et al.* 1999. Biofilm formation of *Helicobacter pylori*. **Lett. Appl. Microbiol.** 28: 121-126.
- (121) Cellini, L., and *et al.* 2007. Dynamic colonization of *Helicobacter pylori* in human gastric mucosa. **Scand. J. Gastroenterol.** 1:1-8.

- (122) Mizoguchi, H.; Fujioka, T.; Kishi, K.; Nishizono, A.; Kodama, R.; and Nasu, M. 1998. Diversity in protein synthesis and viability of *Helicobacter pylori* coccoid forms in response to various stimuli. **Infect. Immun.** 66:5555-5560.
- (123) Rashid, M. H., and *et al.* 2000. Polyphosphate kinase is essential for biofilm development, quorum sensing, and virulence of *Pseudomonas aeruginosa*. **Proc. Natl. Acad. Sci. USA.** 97:9636-9641.
- (124) O'Toole, G. A., and Kolter, R. 1998. Initiation of biofilm formation in *Pseudomonas fluorescens* WCS365 proceeds via multiple, convergent signaling pathways: a genetic analysis. **Mol. Microbiol.** 28:449-461.
- (125) Pizaro-Cerda, J., and Cossart, P. 2006. Bacterial adhesion and entry into host cells. **Cell.** 124(4):715-727.
- (126) Costerton, J. W.; Geesey, G. G.; and Cheng, K. J. 1978. How bacteria stick. **Sci. Am.** 238:86-95.
- (127) Vejborg, R. M., and Klemm, P. 2008. Blocking of bacterial biofilm formation by fish protein coating. **Appl. Environ. Microbiol.** 74:3551-3558.
- (128) Ong, C. Y., *et al.* 2008. Identification of type 3 fimbriae in uropathogenic *Escherichia coli* reveals a role in biofilm formation. **J. Bacteriol.** 190:1054-1063.
- (129) Evans, D. J. Jr., and Evans D. G. 2000. *Helicobacter pylori* adhesins: review and perspectives. **Helicobacter.** 5(4):183-195.

- (130) Yamaoka, Y., *et al.* 2002. *Helicobacter pylori* infection in mice: role of outer membrane proteins in colonization and inflammation. **Gastroenterology**. 123(6):1992-2004.
- (131) Jonge, R.; Durrani, Z.; Rijpkema, S. G.; Kuipers, E. J.; van Vliet, A. H. M.; and Kusters, J. G. 2004. Role of the *Helicobacter pylori* outer-membrane proteins AlpA and AlpB in colonization of the guinea pig stomach. **J. Med. Microbiol.** 53:375-379.
- (132) Ottemann, K. M., and Miller, J. F. 1997. Roles for motility in bacterial-host interactions. **Mol. Microbiol.** 24:1109–1117.
- (133) Guerry, P. 2007. *Campylobacter* flagella: not just for motility. **Trends. Microbiol.** 15(10):456-461.
- (134) Kirov, S. M.; Castrisios, M.; and Shaw, J. G. 2004. *Aeromonas* flagella (polar and lateral) are enterocyte adhesins that contribute to biofilm formation on surfaces. **Infect. Immun.** 72:1939-1945.
- (135) Toutain, C. M.; Caizza, N. C.; Zegans, M. E.; and O'Toole, G. A. 2007. Roles of flagella stators in biofilm formation by *Pseudomonas aeruginosa*. **Res. Microbiol.** 158:471-477.
- (136) Eaton, K. A.; Suerbaum, S.; Josenhans, C.; and Krakowka, S. 1996. Colonization of gnotobiotic piglets by *Helicobacter pylori* deficient in two flagellin genes. **Infect. Immun.** 64:2445-2448.

- (137) Reeser, R. J.; Medler, R. T.; Billinton, S. J.; Jost, B. H.; and Joens, L. A. 2007. Characterization of *Campylobacter jejuni* biofilms under defined growth conditions. **Appl. Environ. Microbiol.** 73:1908-1913.
- (138) Suerbaum, S. 1995. The complex flagella of gastric *Helicobacter* species. **Trends Microbiol.** 3:168–170.
- (139) Geis, G.; Laeyng, H.; Suerbaum, S.; Mai, U.; and Opferkuch, W. 1989. Ultrastructure and biochemical analysis of *Campylobacter pylori* flagella. **J. Clin. Microbiol.** 27:436-441.
- (140) Spohn, G., and Scarlato, V. 2001. Motility, Chemotaxis, and Flagella, In Hazell, S. L. (ed.), *Helicobacter pylori: physiology and genetic*, pp. 239-248. Washington DC: ASM Press.
- (141) Leying, H.; Suerbaum, S.; Geis, G.; and Haas, R. 1992. Cloning and genetic characterization of *Helicobacter pylori* flagellin gene. **Mol. Microbiol.** 6:2863-2874.
- (142) Kostrzynska, M.; Betts, J. D.; Austin, J. W.; and Trust, T. J. 1991. Identification, characterization, and spatial localization of two flagellin species in *Helicobacter pylori* flagella. **J. Bacteriol.** 173:973-946.
- (143) Suerbaum, S.; Josenhans, C.; and Labigne, A. 1993. Cloning and genetic characterization of the *Helicobacter pylori* and *Helicobacter mustelae* *flaB* flagellin genes and construction of *H. pylori* *flaA*- and *flaB*- negative mutants by electroporation-mediated alleic exchange. **J. Bacteriol.** 175:3278-3288.

- (144) Josenhans, C.; Labigne, A.; and Suerbaum, S. 1995. Comparative ultra structure and functional studies of *Helicobacter pylori* and *Helicobacter mustelae* flagellin mutants: both flagellin subunits, FlaA and FlaB, are necessary for full motility in *Helicobacter* species. **J. Bacteriol.** 177:3010-3020.
- (145) O'Toole, P. W.; Kostrzynska, M.; and Trust, T. J. 1994. Non-motile mutants of *Helicobacter pylori* and *Helicobacter mustelae* defective in flagellar hook production. **Mol. Microbiol.** 14:691-703.
- (146) Spohn, G., and Scarlato, V. 1999. Motility of *Helicobacter pylori* is coordinately regulated by the transcriptional activator FlgR, an NtrC homolog. **J. Bacteriol.** 181:593-599.
- (147) Jenks, P. J.; Foynes, S.; Ward, S. J.; Constantinidou, C.; Penn, C. W.; and Wren, B. W. 1997. A flagellar-specific ATPase (FliI) is necessary for flagellar export in *Helicobacter pylori*. **FEMS. Microbiol. Lett.** 152:205-211.
- (148) Porwollik, S.; Noonan, B.; and O'Toole, P. W. 1999. Molecular characterization of a flagellar export locus of *Helicobacter pylori*. **Infect. Immun.** 67:2060-2070.
- (149) Schmitz, A.; Josenhans, C.; and Suerbaum, S. 1997. Cloning and characterization of the *Helicobacter pylori flbA* gene, which codes for a membrane protein involved in coordinated expression of flagellar genes. **J. Bacteriol.** 179:987-997.
- (150) Foynes, S., and *et al.* 1999. Functional analysis of the roles of FliQ and FlhB in flagellar expression in *Helicobacter pylori*. **Microbiol. Lett.** 174:33-39.

- (151) Stewart, P. S., and Costerton, J. W. 2001. Antibiotic resistance of bacteria in biofilms. **Lancet**. 358:135-138.
- (152) Lewis, K. 2001. Riddle of biofilm resistance. **Antimicrob. Agents. Chemother.** 45:999-1007.
- (153) Thien-Fah, C. M., and O'Toole, G. A. 2001. Mechanisms of biofilm resistance to antimicrobial agents. **Trends. Microbiol.** 9:34-39.
- (154) Anderi, J. N.; Frankin, M. J.; and Stewart, P. S. 2000. Role of antibiotic penetration limitation in *Klebsiella pneumoniae* biofilm resistance to ampicillin and ciprofloxacin. **Antimicrob. Agents. Chemother.** 44(7):1818-1824.
- (155) Anwar, H.; van Biesen, T.; Dasgupta, M.; Lam, K.; and Costerton, J. W. 1989. Interaction of biofilm bacteria with antibiotics in a novel *in vitro* chemostat system. **Antimicrob. Agents. Chemother.** 33(10):1824-1826.
- (156) Shigeta, M.; Tanaka, G.; Komatsuzawa, H.; Sugai, M.; Suginaka, H.; and Usui, T. 1997. Permeation of antimicrobial agents through *Pseudomonas aeruginosa* biofilms: a simple method. **Chemotherapy.** 43(5):340-345.
- (157) Gordon, C. A.; Hodges, N. A.; and Marriott, C. 1988. Antibiotic interaction and diffusion through alginate and exopolysaccharide of cystic fibrosis-derived *Pseudomonas aeruginosa*. **J. Antimicrob. Chemother.** 22(5):667-674.
- (158) Patel, Robin. 2005. Biofilms and antimicrobial resistance. **Clin. Orthop. Relat. Res.** 437:41-47.
- (159) Graham, D. Y. 1998. Antibiotic resistance in *Helicobacter pylori*: implication for therapy. **Gastroenterology.** 115:1272-1277.

- (160) Balaban, N.; Stoodley, P.; Fux, C. A.; Wilson, S.; Costerton, J. W.; and Dell'Acqua, G. 2005. Prevention of staphylococcal biofilm-associated infections by te quorum sensing inhibitor RIP. **Clin. Orthop. Relat. Res.** 437:48-54.
- (161) Wu, J. A.; Kusuma, C.; Mond, J. J.; and Kokai-Kun, J. F. 2003. Lysosathpin disrupts *Staphylococcus aureus* and *Staphylococcus epidermidis* biofilms on artificial surfaces. **Antimicrob. Agents. Chemother.** 47(11):3407-3414.
- (162) Caubet, R., and *et al.* 2004. A radio frequency electric current enhances antibiotic efficacy against bacterial biofilms. **Antimicrob. Agents. Chemother.** 48(12):4662-4664.
- (163) Costerton, J. W.; Montanaro, L.; and Arciola, C. R. 2005. Biofilm in implant infections: its production and regulation. **Int. J. Artif. Organs.** 28:1062-1068.
- (164) Bavington, C., and Page, C. 2005. Stopping bacterial adhesion: a novel approach to treating infections. **Respiration.** 72:335-344.
- (165) Lloyd, D. H.; Viac, J.; Werling, D.; Reme, C. A.; and Gatto, H. 2007. Role of sugars in surface microbe-host interactions and immune reaction modulation. **Vet. Dermatol.** 18(4):197-204.
- (166) Shuford, J. A.; Steckelberg, J. M.; and Patel, R. 2005. Effects of fresh garlic extract on *Candida albicans* biofilm. **Antimicrob. Agents. Chemother.** 49:473.
- (167) Perez-Giraldo, C.; Cruz-Villalon, G.; Sanchez-Silos, R.; Martinez-Rubio, R.; Blanco, M. T.; and Gomez-Garcia, A. C. 2003. *In vitro* activity of allicin against *Staphylococcus epidermidis* and influence of subinhibitory concentration on biofilm formation. **J. Appl. Microbiol.** 95:709-711.

- (168) Rukayadi, Y., and Hwang, J. K. 2006. Effect of coating the wells of a polystyrene microtiter plate with xanthorrhizol on the biofilm formation of *Streptococcus mutans*. **J. Basic. Microbiol.** 46(5):410-415.
- (169) Lengsfeld, C.; Titgemeyer, F.; Faller, G.; and Hensel, A. 2004. Glycosylated compounds from okra inhibit adhesion of *Helicobacter pylori* to human gastric mucosa. **J. Agric. Food. Chem.** 52:1495-1503.
- (170) Lengsfeld, C.; Deters, A.; Faller, G.; and Hensel, A. 2004. High molecular weight polysaccharides from black current seeds inhibit adhesion of *Helicobacter pylori* to human gastric mucosa. **Planta. Med.** 70(7):620-626.
- (171) Lee, J. H.; Park, E. K.; Uhm, C. S.; Chung, M. S.; and Kim, K. H. 2004. Inhibition of *Helicobacter pylori* adhesion to human gastric adenocarcinoma epithelial cells by acidic polysaccharides from *Artemisia capillaris* and *Panax ginseng*. **Planta. Med.** 70(7): 615-619.
- (172) O'Mahony, R., and *et al.* 2005. Bactericidal and anti-adhesive properties of culinary and medicinal plants against *Helicobacter pylori*. **World. J. Gastroenterol.** 11:7499-7507.
- (173) Wang, Y. C., and Huang, T. L. 2005. Screening of anti-*Helicobacter pylori* herbs deriving from Taiwanese folk medicinal plants. **FEMS Immun. Med. Microbiol.** 43:295-300.
- (174) Stamatis, G.; Kyriazopoulos, P.; Golgou, S.; Basayiannis, A.; Skaltsas, S.; and Skaltsa, H. 2003. *In vitro* anti-*Helicobacter pylori* activity of Greek herbal medicines. **J. Ethnopharm.** 88:175-179.

- (175) Bhamarapavati, S.; Pendland, S. L.; and Mahady, G. B. 2003. Extracts of spice and food plants from Thai traditional medicine inhibit the growth of the human carcinogen *Helicobacter pylori*. **In Vivo**. 17:541-544.
- (176) Ndip, R. N., *et al.* 2007. *In vitro* anti-*Helicobacter pylori* activity of extracts of selected medicinal plants from North West Cameroon. **J. Ethnopharm.** 114(3):452-457.
- (177) Lima, Z. P., *et al.* 2008. Brazilian medicinal plant acts on prostaglandin level and *Helicobacter pylori*. **J. Med. Food**. 11(4):701-708.
- (178) Sirirugsa, P. 1998. Thai *Zingiberaceae*: species diversity and their uses. Pure. **Proceeding of the International Conference on Biodiversity and Bioresources Conservation and Utilization**. 70(11):2065-2145.
- (179) Manosroi, J.; Dhumtanom, P.; and Manosroi, A. 2006. Anti-proliferative activity of essential oil extracted from Thai medicinal plants on KB and P388 cell lines. **Cancer. Lett.** 235:114-120.
- (180) Ammon, H. P.; Anazodo, M. I.; Safavhi, H.; Dhawan, B. N.; and Srimal, R.C. 1992. Curcumin: a potent inhibitor of leukotriene B4 formation in rat peritoneal polymorphonuclear neutrophils (PMNL). **Planta. Med.** 58(2):226.
- (181) Araujo, C. A., and Leon, L. L. 2001. Biological activities of *Curcuma longa* L. **Mem. Inst. Oswaldo Cruz**. 96(5):723-728.
- (182) Jiao, Y., and *et al.* 2006. Iron chelation in the biological activity of curcumin. **Free. Radic. Biol. Med.** 40:1152-1160.

- (183) Duvoix, A., and *et al.* 2005. Chemopreventive and therapeutic effects of curcumin. **Cancer. Lett.** 223:181-190.
- (184) Roughley, P. J., and Whiting, D. A. 1973. Experiments in the biosynthesis of curcumin. **J. Chem. Soc.** 20:2379-2388.
- (185) . 2544. .
1. . . .
- (186) World Health Organization. 1999. WHO monographs on selected medicinal plants, Vol I. Malta. (Mimeographed).
- (187) Ammon, H. P., and Wahl, M. A. 1991. Pharmacology of *Curcuma longa*. **Planta. Med.** 57(1):1-7.
- (188) Whalstrom, B., and Blennow, G. 1978. A study on the fate of curcumin in the rat. **Acta. Pharmacol. Toxicol.** 43:86-92.
- (189) Ireson, C., and *et al.* 2001. Characterization of metabolites of the chemopreventive agent curcumin in human and rat hepatocytes and in the rat *in vivo*, and evaluation of their ability to inhibit phorbol ester-induced prostaglandin E₂ production. **Cancer. Res.** 61:1058-1064.
- (190) Liang, G., and *et al.* 2008. Synthesis and anti-bacterial properties of mono-carbonyl analogues of curcumin. **Chem. Pharm. Bull.** 56(2):162-167.
- (191) Mahady, G. B.; Pendland, S. L.; Yun, G.; and Lu, Z. Z. 2002. Turmeric (*Curcuma longa*) and curcumin inhibit the growth of *Helicobacter pylori*, a group 1 carcinogen. **Anticancer. Res.** 22(6C):4179-4181.

- (192) Han, C., and *et al.* 2006. Biochemical characterization and inhibitor discovery of shikimate dehydrogenase from *Helicobacter pylori*. **FEBS. J.** 273(20):4682-4692.
- (193) Mahady, G. B., and *et al.* 2005. *In vitro* susceptibility of *Helicobacter pylori* to botanical extracts used traditionally for the treatment of gastrointestinal disorders. **Phytother. Res.** 19(11):988-991.
- (194) Foryst-Ludwig, A.; Neumann, M.; Schneider-Brachert, W.; and Neumann, M. 2004. Curcumin block NF- κ B and the motogenic response in *Helicobacter pylori*-infected epithelial cells. **Biochem. Biophys. Res. Commun.** 316(4):1065-72.
- (195) Rudrappa, T., and Bais, H. P. 2008. Curcumin, a known phenolic from *Curcuma longa*, attenuates the virulence of *Pseudomonas aeruginosa* PAO1 in whole plant and animal pathogenicity models. **J. Agric. Food. Chem.** 56(6):1955-1962.
- (196) Costerton, J. W., and *et al.* 1987. Bacterial biofilms in nature and disease. **Annu. Rev. Microbiol.** 41:435-464.
- (197) Wilkins, M. R.; Williams, K. L.; Appel, R. D.; and Hochstrasser, D. F. 1997. **Proteome research: new frontiers in functional genomics.** New York: Springer.
- (198) Choe, L. H., and Le, K. H. 2000. A comparison of three commercially available isoelectric focusing units for proteome analysis: The multiphor, the IPGphor and the protean IEF cell. **Electrophoresis.** 21:993-1000.

- (199) Andrew, J. 1999. **2-D proteome analysis protocols**. New Jersey: Humana Press.
- (200) McDonough, J. L.; Neverova, I.; and Van Eyk, J. E. 2002. Proteomic analysis of human biopsy samples by single two-dimensional electrophoresis: Coomassie, silver, mass spectrometry, and Western blotting. **Proteomics**. 2:978-987.
- (201) Sparkman, O. D. 2006. **Mass spectrometry desk reference**. 2nd ed. Pittsburgh: Global View.
- (202) James, P.; Quadroni, M.; Carafoli, E.; and Gonnet, G. 1993. Protein identification by mass profile fingerprinting. **Biochem. Biophys. Res. Commun.** 195(1):58-64.
- (203) Henzel, W. J.; Billeci, T. M.; Stults, J. T.; Wong, S. C.; Grimley, C.; and Watanabe, C. 1993. Identifying proteins from two-dimensional gels by molecular mass searching of peptide fragments in protein sequence databases. **Proc. Natl. Acad. Sci. USA**. 90(11):5011-5015.
- (204) Mann, M.; Hejrup, P.; and Roepstorff, P. 1993. Use of mass spectrometric molecular weight information to identify proteins in sequence databases. **Biol. Mass. Spectrom.** 22(6):338-345.
- (205) Kalmokoff, M., and *et al.* 2006. Proteomic analysis of *Campylobacter jejuni* 11168 biofilms reveals a role for the motility complex in biofilm formation. **J. Bacteriol.** 188:4312-4320.
- (206) Soni, K., and *et al.* 2007. Proteomic analysis to identify the role of LuxS/AI-2 mediated protein expression in *Escherichia coli* O157:H7. **Foodborne. Pathog. Dis.** 4(4):463-471.

- (207) Park, J. W., and *et al.* 2006. Quantitative analysis of representative proteome components and clustering of *Helicobacter pylori* clinical strains. **Helicobacter.** 11(6):533-543.
- (208) Pereira, R. B., and *et al.* 2006. Comparative analysis of two-dimensional electrophoresis maps (2-DE) of *Helicobacter pylori* from Brazilian patients with chronic gastritis and duodenal ulcer: a preliminary report. **Rev. Inst. Med. Trop. S. Paulo.** 48(3):175-177.
- (209) Ge, R., and *et al.* 2007. A proteomic approach for the identification of bismuth-binding proteins in *Helicobacter pylori*. **J. Biol. Inorg. Chem.** 12:831-842.
- (210) Govorun, V. M., and *et al.* 2003. Comparative analysis of proteome maps of *Helicobacter pylori* clinical isolates. **Biochemistry.** 68:52-60.
- (211) Potera, C. 1999. Forging a link between biofilms and disease. **Science.** 283:1837,1839.
- (212) O'Toole, G. A.; Kaplan, H. B.; and Kolter, R. 2000. Biofilm formation as microbial development. **Annu. Rev. Microbiol.** 54: 49-79.
- (213) Wren, B. W.; Henderson, J.; and Ketley, J. M. 1994. A PCR-based strategy for the rapid construction of defined bacterial deletion mutants. **Biotechniques.** 16:994-996.
- (214) Dorrell, N.; Gyselman, V. G.; Foyne, S.; Li, S. R.; and Wren, B. W. 1996. Improved efficiency of inverse PCR mutagenesis. **Biotechniques.** 21:604-608.

- (215) Zeng, X.; He, L. H.; Yin, Y.; Zhang, M. J.; and Zhang, J. Z. 2005. Deletion of *cagA* gene of *Helicobacter pylori* PCR products. **World. J. Gastroenterol.** 11(21):3255-3259.
- (216) Weaver, J. C. 1995. Electroporation Theory: Concepts and Mechanisms, In J. A. Nickoloff (ed.), **Electroporation Protocols for Microorganisms**, pp.1-26. New Jersey: Humana Press.
- (217) Peek, R. M. 2009. *Helicobacter pylori* infection and disease: from humans to animal models. **Dis. Model. Mech.** 1:50-55.
- (218) Mitchell, D. J.; Huynh, H. Q.; Ceponis, P. J.; Jones, N. L.; and Sherman, P. M. 2004. *Helicobacter pylori* disrupts STAT1-mediated gamma interferon-induced signal transduction in epithelial cells. **Infect. Immun.** 72:537-545.
- (219) Brock, N. R.; Shao, J. Q.; and Apicella, M. A. 2009. Biofilm formation on human airway epithelia by encapsulated *Neisseria meningitidis* serogroup B. **Microbes. Infect.** 11:281-287.
- (220) Niehus, E., and *et al.* 2004. Genome-wide analysis of transcriptional hierarchy and feedback regulation in the flagellar system of *Helicobacter pylori*. **Mol. Microbiol.** 52(4):947-961.
- (221) Wosten, M. M.; Wagenaar, J. A.; and van Putten, J. P. 2004. The FlgS/FlgR two-component signal transduction system regulates the *fla* regulon in *Campylobacter jejuni*. **J. Biol. Chem.** 16:16214-16222.
- (222) Canals, R., and *et al.* 2006. Polar flagellum biogenesis in *Aeromonas hydrophila*. **J Bacteriol.** 188(2):542-55.

- (223) Macnab, R. M. 2003. How bacteria assemble flagella. **Annu. Rev. Microbiol.** 57:77-100.
- (224) Torres, J., and Backert, S. 2008. Pathogenesis of *Helicobacter pylori* infection. **Helicobacter.** 13(Suppl1):S13-17.
- (225) Ito, K.; Yamaoka, Y.; Ota, H. H.; and Graham, D. Y. 2008. Adherence, I internalization, and persistence of *Helicobacter pylori* in hepatocytes. **Dig. Dis. Sci.** 53:2541-2549.
- (226) Yahav, J.; Shmueli, H.; Niv, Y.; Bechor, J.; and Samra, Z. 2006. In vitro activity of levofloxacin against *Helicobacter pylori* isolates from patients after treatment failure. **Diag. Microbiol. Infect. Dis.** 55:81-83.
- (227) Houben, M. H.; van de Beek, D.; Hensen, E. F.; Craen, A. J.; Rauws, E. A.; and Tytgat, G. N. 1999. A systematic review of *Helicobacter pylori* eradication therapy-the impact of antimicrobial resistance on eradication rates. **Aliment. Pharmacol. Ther.** 13:1047-1055.
- (228) Levy, S. B. 2002. Factors impacting on the problem of antibiotic resistance. **J. Antimicrob. Chemother.** 49:25-30.
- (229) Tenke, P.; Riedl, C. R.; Jones, G. L.; Williams, G. J.; Stickler, D.; and Nagy, E. 2004. Bacterial biofilm formation on urologic devices and heparin coating as preventive strategy. **Int. J. Antimicrob. Agents.** 23(Suppl1):S67-74.
- (230) Limsuwan, S., and Voravuthikunchai, S. P. 2008. *Boesenbergia pandurata* (Roxb.) Schltr., *Eleutherine americana* Merr. and *Rhodomyrtus tomentosa* (Aiton)

- Hassk. as antibiofilm producing and antiquorum sensing in *Streptococcus pyogenes*. **FEMS. Immunol. Med. Microbiol.** 53:429-436.
- (231) Rasooli, I.; Shayegh, S.; Taghizadeh, M.; and Astaneh, S. D. 2008. Phytotherapeutic prevention of dental biofilm formation. **Phytother. Res.** 22:1162-1167.
- (232) Donlan, R. M. 2009. Preventing biofilms of clinically relevant organisms using bacteriophage. **Trends. Microbiol.** 17:66-72.
- (233) Limsong, J.; Benjavongkuichai, E.; and Kuvatanasuchati, J. 2004. Inhibitory effect of some herbal extracts on adherence of *Streptococcus mutants*. **J. Ethnopharmacol.** 92:281-289.
- (234) Duarte, S., and *et al* 2006. Inhibitory effects of cranberry polyphenols on formation and acidogenicity of *Streptococcus mutants* biofilms. **FEMS. Microbiol. Lett.** 57:50-56.
- (235) Cartagena, E.; Colom, O. A.; Neske, A.; Valdez, J. C.; and Bardon, A. 2007. Effects of plant lactones on the production of biofilm of *Pseudomonas aeruginosa*. **Chem. Pharm. Bull.** 55:22-25.
- (236) Kuzma, L.; Rozalski, M.; Walencka, E.; Rozalska, B.; and Wysokinska, H. 2007. Antimicrobial activity of diterpenoids from hairy roots of *Salvia sclarea* L.: salvipisone as a potential anti-biofilm agent active against antibiotic resistant Staphylococci. **Phytomedicine.** 14:31-35.

- (237) Negi, P. S.; Jayaprakasha, G. K.; Jagan, M. R. L.; and Sakariah, K. K. 1999. Antibacterial activity of turmeric oil: a byproduct from curcumin manufacture. **J. Agric. Food. Chem.** 47:4297-4300.
- (238) Filoche, S. K.; Soma, K.; and Sissons, C. H. 2005. Antimicrobial effects of essential oils in combination with chlorhexidine digluconate. **Oral. Microbiol. Immunol.** 20(4):221-225.
- (239) Adhvaryu, M. R.; Reddy, N. M.; and Vakharia, B. C. 2008. Prevention of hepatotoxicity due to anti tuberculosis treatment: a novel integrative approach. **World. J. Gastroenterol.** 14:4753-4762.
- (240) Paranhos, H. F. O., and Silva, C. H. L. 2004. Methods for the quantification of biofilm on complete dentures. **Braz. Oral. Res.** 18:215-223.
- (241) Wessler, S.; Muenzner, P.; Meyer, T. F.; and Naumann, M. 2005. The anti-inflammatory compound curcumin inhibits *Neisseria gonorrhoeae*-induced NF- κ B signaling, release of pro-inflammatory cytokines/chemokines and attenuates adhesion in late infection. **Biol. Chem.** 386:481-490.
- (242) Subhasitanont, P.; Srisomsap, C.; Chokchaichamnankit, D.; Ngiwsara, L.; Chiablaem, K.; and Svasti, J. 2007. Differential protein expression in human cholangiocarcinoma cell lines after treated with curcumin. **Proceeding of the Sixth Princess Chulabhorn International Science Congress.** 51.
- (243) Tavorpanich, C.; Tencomnao, T.; and Santiyanont, R. 2007. Effects of *Curcuma longa* extracts on the receptor for advanced glycation end products gene

expression of human cancer cells. **Proceeding of the Sixth Princess Chulabhorn International Science Congress.** 141.

- (244) Cvitkovitch, D. G.; Li, Y. H.; and Ellen, R. P. 2003. Quorum sensing and biofilm formation in Streptococcal infections. **J. Clin. Invest.** 112:1626-1632.
- (245) Lewis, K. 2005. Persister cells and the riddle of biofilm survival. **Biochemistry.** 70:267-274.
- (246) Ozcakir, O. 2007. Viable but non-culturable form of bacteria. **Mikrobiyol. Bul.** 41:477-484.
- (247) Piqueres, P.; Moreno, Y.; Alonso, J. L.; and Ferrus, M. A. 2006. A combination of direct viable count and fluorescent in situ hybridization for estimating *Helicobacter pylori* cell viability. **Res. Microbiol.** 157:345-349.
- (248) Kalchayanand, N.; Dunne, P.; Sikes, A.; and Ray, B. 2004. Viability loss and morphology change of foodborne pathogens following exposure to hydrostatic pressures in the presence and absence of bacteriocins. **Int. J. Food. Microbiol.** 91:91-98.
- (249) Lindsay, D., and von Holy, A. 1999. Different responses of planktonic and attached *Bacillus subtilis* and *Pseudomonas fluorescens* to sanitizer treatment. **J. Food. Prot.** 62:368-379.
- (250) DeQueiroz, G. A., and Day, D. F. 2007. Antimicrobial activity and effectiveness of a combination of sodium hypochlorite and hydrogen peroxide in killing and

- removing *Pseudomonas aeruginosa* biofilms from surfaces. **J. Appl. Microbiol.** 103:794-802.
- (251) Zambrano, M. M., and Kolter, R. 2005. Mycobacterial biofilms: a greasy way to hold it together. **Cell.** 123:762-764.
- (252) Shin, D. H.; Choi, Y. S.; and Cho, Y. H. 2008. Unusual properties of catalase A (KatA) of *Pseudomonas aeruginosa* PA14 are associated with its biofilm peroxide resistance. **J. Bacteriol.** 190:2663-2670.
- (253) Wen, Z. T.; Suntharaligham, P.; Cvitkovitch, D. G.; and Burne, R. A. 2005. Trigger factor in *Streptococcus mutants* is involved in stress tolerance competence development, and biofilm formation. **Infect. Immun.** 73:219-225.
- (254) Lazazzera, B. A. 2005. Lessons from DNA microarray analysis: the gene expression profile of biofilms. **Curr. Opin. Microbiol.** 8:222-227.
- (255) Kawamoto, J.; Kurihara, T.; Kitagawa, M; Kato, I.; and Esaki, N. 2007. Proteomic studies of an Antarctic cold-adapted bacterium, *Shewanella livingstonensis* Ac10, for global identification of cold-inducible proteins. **Extremophiles.** 11:819-826.
- (256) Ohnishi, K.; Ohto, Y.; Aizawa, S. I.; Macnab, R. M; and Iino, T. 1994. FlgD is a scaffolding protein needed for flagellar hook assembly in *Salmonella typhimurium*. **J. Bacteriol.** 176:2272-2281.

- (257) Austin, J. W.; Sanders, G.; Kay, W. W.; and Collinson, S. K. 1998. Thin aggregative fimbriae enhance *Salmonella enteritidis* biofilm formation. **FFEMS. Microbiol. Lett.** 612:295-301.
- (258) Bhattacharyya, S.; Go, M. F.; Dunn, B. E.; and Phadnis, S. H. 2001. Transcription and translation, In Hazell, S. L. (ed.), *Helicobacter pylori: physiology and genetic*, pp. 285-291. Washington DC: ASM Press.
- (259) Aoki, H.; Dekany, K.; Adams, S. L.; and Ganoza, M. C. 1997. The gene encoding the elongation factor P protein is essential for viability and is required for protein synthesis. **J. Biol. Chem.** 272:32254-32259.
- (260) Balasubramanian, S.; Kannan, T. R.; and Baseman, J. B. 2008. The surface-exposed carboxyl region of *Mycoplasma pneumoniae* elongation factor Tu interact with fibronectin. **Infect. Immun.** 76:3116-3123.
- (261) De Maio, A. 1999. Heat shock proteins: facts, thoughts, and dreams. **Shock.** 11: 1-12.
- (262) Wang, G.; Alamuri, P.; and Maier, R. J. 2006. The diverse antioxidant systems of *Helicobacter pylori*. **Mol. Microbiol.** 61:847-860.
- (263) Pesci, E., and Pickett, C. 1994. Genetic organization and enzymatic activity of a superoxide dismutase from the microaerophilic human pathogen, *Helicobacter pylori*. **Gene.** 143:111-116.
- (264) Seneviratne, C. J.; Wang, Y.; Jin, L.; Abiko, Y.; and Samaranyake, L. P. 2008. *Candida albicans* biofilm formation is associated with increased anti-oxidative capacities. **Proteomics.** 8:2936-2947.

- (265) Allegrucci, M., and *et al.* 2006. Phenotypic characterization of *Streptococcus pneumoniae* biofilm development. **J. Bacteriol.** 188:2325-2335.
- (266) Kelly, D. J.; Hughes, N. J.; and Poole, R. K. 2001. Microaerobic physiology: aerobic respiration, anaerobic respiration, and carbon dioxide metabolism, In Hazell S. L. (ed.), ***Helicobacter pylori: physiology and genetic***, pp. 113-124. Washington DC: ASM Press.
- (267) Cremades, N.; Bueno, M.; Neira, J. L.; Velazquez-Campoy, A.; and Sancho, J. 2008. Conformational stability of *Helicobacter pylori* flavodoxin fit to function at pH 5. **J. Biol. Chem.** 283:2883-2895.
- (268) Hanai, T.; Atsumi, S.; and Liao, J. C. 2007. Engineered synthetic pathway for isopropanol production in *Escherichia coli*. **Appl. Environ. Microbiol.** 73:7814-7818.
- (269) Reuse, H., and Skouloubris, S. 2001. Nitrogen metabolism, In Hazell S. L. (ed.), ***Helicobacter pylori: physiology and genetic***, pp. 125-133. Washington DC: ASM Press.
- (270) Eaton, K. A.; Brooks, C. L.; Morgan, D. R.; and Krakowka, S. 1991. Essential role of urease in pathogenesis of gastritis induced by *Helicobacter pylori* in gnotobiotic piglets. **Infect. Immun.** 59:2470-2475.
- (271) Stickler, D. J., and *et al.* 2006. Observations on the adherence of *Proteus mirabilis* onto polymer surfaces. **J. Appl. Microbiol.** 100:1028-1033.

- (272) Driffield, K.; Miller, K.; Bostock, J. M.; O'Neill, A. J.; and Chopra, I. 2008. Increased mutability of *Pseudomonas aeruginosa* in biofilms. **J. Antimicrob. Chemother.** 61:1053-1056.
- (273) Burt, S. A., and *et al.* 2007. Carvacrol induces heat shock protein 60 and inhibits synthesis of flagellin in *Escherichia coli* O157:H7. **Appl. Environ. Microbiol.** 73:4484-4490.
- (274) Teiten, M. H.; Reuter, S.; Schmucker, S.; Dicato, M.; and Diederich, M. 2009. Induction of heat shock response by curcumin in human leukemia cells. **Cancer. Lett.** 8:145-154.



ศูนย์วิทยทรัพยากร
จุฬาลงกรณ์มหาวิทยาลัย



APPENDIX

ศูนย์วิทยทรัพยากร
จุฬาลงกรณ์มหาวิทยาลัย

1. Preparation of antibiotic stock solution

1.1 Kanamycin stock solution (stock 50 mg ml⁻¹)

Kanamycin was prepared as a stock solution by dissolving in DW and the final concentration was set as 50 mg ml⁻¹. The stock solution was sterilized through a 0.45 µm filter and transferred into aliquot tubes. The stock solution was stored at -20 °C until used.

1.2 Ampicillin stock solution (stock 50 mg ml⁻¹)

Ampicillin was prepared as a stock solution by dissolving in DW and the final concentration was set as 50 mg ml⁻¹. The stock solution was sterilized through a 0.45 µm filter and transferred into aliquot tubes. The stock solution was stored at -20 °C until used.

1.3 Selective antibiotic stock solution for *H. pylori*

Selective antibiotic for *H. pylori* was consisted of 30 mg ml⁻¹ vancomycin, 15 mg ml⁻¹ trimethoprim, 1 mg ml⁻¹ polymyxin B, and 6 mg ml⁻¹ amphotericin B. All antibiotics were dissolved in 1 ml of DMSO, except for amphotericin B that dissolved in 29 ml of DW. The solutions were stirred until completely dissolved, and mixed together. The stock solution was sterilized through a 0.45 µm filter and transferred into aliquot tubes. The stock solution was stored at -20 °C until used.

2. Preparation of bacterial culture media

2.1 1% saponin

One g of saponin (Sigma) was added with 100 ml of DW. The medium was sterilized by autoclaving at 121 °C at 15 psi for 15 min.

2.2 Lysed horse blood

Thirty-five ml of horse blood was added with 3.5 ml of saponin. The blood was gently mixed until completely lysed.

2.3 Dent's selective agar (Dent's plate)

Forty g of blood agar base no. 2 was added with 930 ml of DW. The medium was sterilized by autoclaving at 121 °C at 15 psi for 15 min. Once the medium as cool as 50 - 60 °C, 4 ml of DENT supplement and 70 ml of lysed horse blood were added into the medium, and the medium was swirled gently. The medium was poured approximately 25 ml per plate and left until agar completely set. As for Dent's plates supplemented with 20 µg ml⁻¹ kanamycin, 400 µl of kanamycin stock solution was added into the medium together with DENT supplement.

2.4 LB agar

Five g of tryptone, 2.5 g of yeast extract, 2.5 g of NaCl, and 5 g of agar were added with 500 ml of DW. The medium was sterilized by autoclaving at 121 °C at 15 psi for 15 min. The medium was poured approximately 25 ml per plate and left until agar completely set.

2.5 LB broth

Five g of tryptone, 2.5 g of yeast extract, and 2.5 g of NaCl were added with 500 ml of DW. The medium was sterilized by autoclaving at 121 °C at 15 psi for 15 min.

2.6 Brain heart infusion (BHI) broth and BHI supplemented with 2% (w/v) β -cyclodextrin (BCD)

Eighteen and 0.5 g of BHI broth was added with 500 ml of DW. The medium was sterilized by autoclaving at 121 °C at 15 psi for 15 min. As for BHI supplemented with 2% BCD, 10 g of BCD was added into BHI before autoclaving.

2.7 Brain heart infusion agar

Thirty-seven g of BHI broth and 10 g of Bacto agar were added with 930 ml of DW. The medium was sterilized by autoclaving at 121 °C at 15 psi for 15 min. Once the medium as cool as 50 - 60 °C, 10 ml of selective antibiotic of *H. pylori*, as prepared as above, and 70 ml of sheep blood were added into the medium, and the medium was swirled gently. The medium was poured approximately 25 ml per plate and left until agar completely set.

2.8 Stock medium for *H. pylori*

Seventy-five ml of BHI broth was added with 10 ml fetal bovine serum and 15 ml glycerol. Stored in 1ml aliquots at 4 °C.

3. Preparation of molecular reagents

3.1 Ethylenediamine tetraacetic acid (0.5M EDTA)

$\text{Na}_2\text{EDTA}\cdot 2\text{H}_2\text{O}$, 136.10 g, was dissolved in 800 ml of DW using magnetic stirrer. The solution was adjusted to pH 8 by NaOH. The final volume was adjusted to 1,000 ml by DW and the solution was sterile by autoclaving.

3.2 1x TBE buffer (0.045M Tris-borate, 0.001M EDTA)

Tris base, 5.4 g, was added with 2.75 g of boric acid and 2 ml of EDTA. The final volume was adjusted to 1000 ml by DW and the solution was sterile by autoclaving.

3.3 Ethidium bromide

One-hundred μg of ethidium bromide was dissolved in 100 ml of DW using magnetic stirrer. Stored in closed container without sunlight exposure. Gloves must be on all the time when handling this carcinogen.

3.4 Tris-Hcl (1M, 1,000 ml)

Tris base, 121.14 g, was dissolved in 800 ml of DW. The solution was adjusted to pH 8 by HCl. The final volume was adjusted to 1,000 ml by DW and the solution was sterile by autoclaving.

3.5 0.7 and 1.5% agarose gel

Seven-hundred mg and 1.5 g of agarose was added with 100 ml of 1x TBE in order to prepare 0.7 and 1.5% agarose gel, respectively. Mix thoroughly and

heated by microwave until the gel completely dissolved. The gel was then added with $1 \mu\text{g ml}^{-1}$ ethidium bromide and poured into the mold. The gel was left until completely set.

4. Preparation of 2-D electrophoresis reagents

All the reagents used for 2-D gel electrophoresis purposes were prepared based on 2-D Electrophoresis using immobilized pH gradients Principal and Methods (Amersham Biosciences).

4.1 Rehydration stock solution with IPG buffer (8M urea, 2% CHAPS, 0.5% IPG buffer, 0.002% bromophenol blue, 25 ml)

Rehydration stock solution with IPG buffer was prepared in total volume of 25 ml. The solution was consisted of 12 g urea, 0.5 g CHAPS, 125 μl IPG buffer pH 3-10 NL, 50 μl bromophenol blue (1%; w/v), and DDW to 25 ml. Stored in 500 μl aliquots at -20°C . DTT, 1.4 mg per aliquot, was added just prior to use.

4.2 Bromophenol blue stock solution

Bromophenol blue stock solution was prepared in total volume of 10 ml. The solution was consisted of 100 mg bromophenol blue, 60 mg Tris-base, and DDW to 10 ml. Stored at room temperature.

4.3 SDS equilibration buffer stock solution (50 mM Tris-HCL, pH 8.8, 6 M urea, 30% glycerol, 2% SDS, bromophenol blue, 200 ml)

SDS equilibration buffer stock solution was prepared in total volume of 200 ml. The solution was consisted of 10 ml Tris-HCL, pH 8.8 (see 4x resolving gel buffer), 72.07 g urea, 69 ml glycerol (87%; v/v), 4 g SDS, 400 μ l bromophenol blue (1%; w/v), and DDW to 200 ml. Stored in 5 ml aliquots at -20°C . DTT, 50 mg, or IAA, 125 mg, per aliquot, was added just prior to use.

4.4 30% T, 2.6% C monomer stock solution (30% acrylamide, 0.8% N,N'-methylenebisacrylamide, 200 ml)

30% T, 2.6% C monomer stock solution was prepared in total volume of 200 ml. The solution was consisted of 60 g acrylamide, 1.6 g N,N'-methylenebisacrylamide, and DDW to 200 ml. The solution was filtered through a $0.45\ \mu\text{m}$ filter and stored at 4°C in the dark.

4.5 4x resolving gel buffer (1.5 M Tris-HCL, pH 8.8, 500 ml)

4x resolving gel buffer was prepared in total volume of 500 ml. The solution was consisted of 90.85 g Tris-base, 375 ml DDW. The solution was adjusted to pH 8.8 by HCl. Final volume was brought to 500 ml by DDW. The solution was filtered through a $0.45\ \mu\text{m}$ filter and stored at 4°C .

4.6 10% SDS

10% SDS was prepared in total volume of 50 ml. The solution was consisted of 5 g SDS and 50 ml DDW.

4.7 10% ammonium persulfate

10% ammonium persulfate was freshly prepared just prior to use. The solution was consisted of 50 mg ammonium persulfate and 500 μ l DDW.

4.8 10X SDS electrophoresis buffer (25 mM Tris-HCL, pH 8.3, 192 mM glycine, 0.1% SDS, 1000 ml)

10X SDS electrophoresis buffer was prepared in total volume of 1 L. The solution was consisted of 30.30 g Tris-base, 144 g glycine, 10 g SDS, and DDW to 1000 ml. The solution was stored at room temperature. Prior to use, the solution was 10-time diluted to bring a final concentration to 1x.

4.9 Agarose sealing solution

Agarose sealing solution was prepared in total volume of 50 ml. The solution was consisted of 50 ml SDS electrophoresis buffer, 0.25 g agarose, and 100 μ l bromophenol blue (1%; w/v). The solution was heat in a microwave oven until the agarose was completely dissolved. Stored in 2 ml aliquots at room temperature.

4.10 Fixative solution (10% CH₃COOH, 40% methanol, 1L)

One-hundred ml of CH₃COOH was added with 400 ml methanol and 500 ml DDW. The solution was mixed thoroughly.

4.11 Colloidal coomassie brilliant blue G-250 (400 ml)

Colloidal coomassie brilliant blue was freshly prepared just prior to use. Four-hundred mg of coomassie brilliant blue G-250 was dissolved in 100 ml methanol. Forty g of AmSO_4 and 4.8 ml of H_3PO_4 was dissolved in 295.2 ml DDW. These two solutions were mixed together.



ศูนย์วิทยทรัพยากร
จุฬาลงกรณ์มหาวิทยาลัย

5. Bovine serum albumin (BSA) standard curve construction

The standard curve of BSA was prepared using BSA solution at concentration of 10, 20, 30, 40, and 50 $\mu\text{g ml}^{-1}$. The method of Bradford was used following a manufacturer's instruction in the kit's manual (Bio-Rad Protein Assay; Bio-Rad). A standard curve was made between each BSA concentration and its corresponding absorbance value as shown in Table 20 and Figure 45. The concentration of protein in the unknown sample was determined by comparison to this standard curve.

| BSA ($\mu\text{g ml}^{-1}$) | 10 | 20 | 30 | 40 | 50 |
|-------------------------------|-------|-------|-------|-------|-------|
| A959 | 0.506 | 0.794 | 1.148 | 1.441 | 1.702 |

Table 22: The correlation between the final concentration at standard protein (BSA) and its corresponding absorbance value at 595 nm.

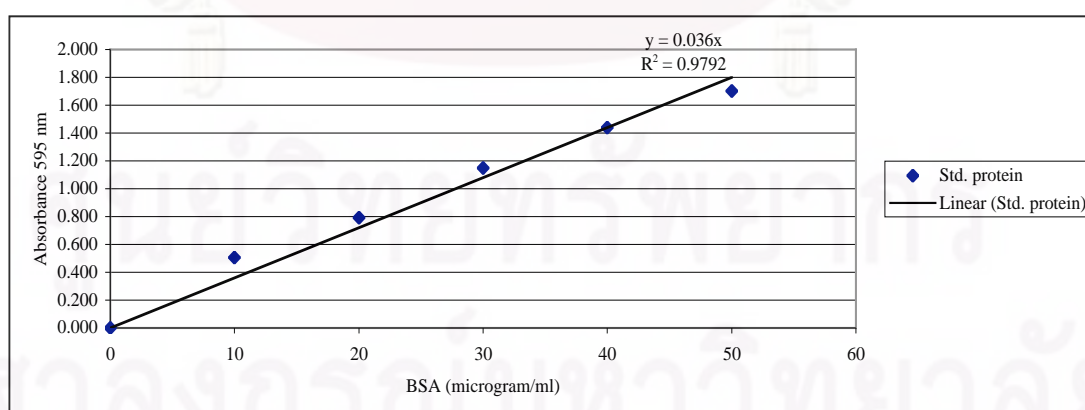


Figure 45: The correlation between final concentration ($\mu\text{g ml}^{-1}$) of standard BSA and their absorbance value at 595 nm.

6. International Oral Presentation

[O217] Roles of flagella and effect of curcumin against biofilm formation by *Helicobacter pylori*

P. Pattiyathanee, N. Dorrell. (Bangkok, TH; London, UK)

Objectives: The gastric pathogen *Helicobacter pylori* is shown to have alternate life style as a biofilm. In human infection, a presence of mature biofilm attached to cell surface has been shown and hypothesised that *H. pylori* infections resulting in gastric ulcers may be a manifestation of biofilm. Flagella have been considered to have a possible role during initial step of biofilm formation. Here we have investigated roles of three flagellar genes, including the *flaA* gene encoding flagellin protein, the *flgR* regulatory gene and the *fliQ* export apparatus gene, in the production of biofilm and control of adherence in *H. pylori*. The effect of curcumin against *H. pylori* biofilm formation and adherence to the human cancer cells has also been investigated.

Methods: Isogenic *flaA*, *flgR*, and *fliQ* mutants were constructed from *H. pylori* wild-type 26695 and N6 by inverse PCR mutagenesis. A minimum inhibitory concentration (MIC) of curcumin (diferuloylmethane) against *H. pylori* was determined using agar dilution technique. The ability to form biofilm in liquid culture and on glass surface, and adhere to the HEP-2 cells was examined in vitro in a presence of curcumin compared to the controls.

Results: Two different types of biofilm were observed in this study, including pellicle and attached biofilm. The wild-type *H. pylori* 26695 and N6 strains formed biofilm and adhered to HEP-2 cells more efficiently than the isogenic mutants, including *flaA* mutants; PA315 and NA2, *flgR* mutants; PR611 and NR, and *fliQ* mutants; PQ and NQ. These results indicate that these genes are involved in the biofilm formation and adhesion of *H. pylori*. Our results showed that curcumin not only inhibited bacterial growth, but also greatly decreased the number of biofilm formation and the ability to adhere to the HEP-2 cells.

Conclusion: We have demonstrated that *H. pylori* in monoculture can form biofilm. It attached to a glass surface and formed a pellicle at air-liquid interface. Flagellar components were found to be important for biofilm formation on abiotic glass surface, pellicle formation in liquid culture, and adherence to HEP-2 cells. Curcumin has been demonstrated an effect against to *H. pylori* biofilm and shown a significant inhibitory action on adherence of *H. pylori* to HEP-2 cells.

Session Info: Molecular approaches to biofilm biology

Session Type: Oral presentations

**European Congress of Clinical Microbiology and Infectious Disease
Barcelona, Spain
19-22 April 2008**

BIOGRAPHY

| | |
|------------------------------|---|
| Name | Panan Pattiyathanee |
| Date of birth | 16 October 1978 |
| Place of birth | Khon Kaen, Thailand |
| Institutions attended | |
| 1997-2000 | Department of Medical Technology, Faculty of Allied Health Sciences Chulalongkorn University |
| 2000-2002 | Department of Clinical Pathology Faculty of Medicine, Ramathibodi Hospital Mahidol University |
| 2004-2009 | Inter-department graduate school (Biomedical Sciences) Chulalongkorn University |
| Scholarship | Commission of Higher Education Ministry of Education. |

ศูนย์วิทยทรัพยากร
จุฬาลงกรณ์มหาวิทยาลัย